



HAL
open science

Inhibition of Transcription by Dactinomycin Reveals a New Characteristic of Immunogenic Cell Stress

Juliette Humeau

► **To cite this version:**

Juliette Humeau. Inhibition of Transcription by Dactinomycin Reveals a New Characteristic of Immunogenic Cell Stress. *Immunology*. Université Paris Saclay (COmUE), 2019. English. NNT : 2019SACLS492 . tel-02495351

HAL Id: tel-02495351

<https://theses.hal.science/tel-02495351>

Submitted on 2 Mar 2020

HAL is a multi-disciplinary open access archive for the deposit and dissemination of scientific research documents, whether they are published or not. The documents may come from teaching and research institutions in France or abroad, or from public or private research centers.

L'archive ouverte pluridisciplinaire **HAL**, est destinée au dépôt et à la diffusion de documents scientifiques de niveau recherche, publiés ou non, émanant des établissements d'enseignement et de recherche français ou étrangers, des laboratoires publics ou privés.

Inhibition of transcription by dactinomycin reveals a new characteristic of immunogenic cell stress

Thèse de doctorat de l'Université Paris-Saclay
Préparée à Gustave Roussy

École doctorale n°582 CBMS Cancérologie
Spécialité de doctorat : Aspects moléculaires et cellulaires de la biologie

Thèse présentée et soutenue à Paris, le 03 décembre 2019, par

Juliette Humeau

Composition du Jury :

François Ghiringhelli Pr, Centre Georges François Leclerc, Dijon (– UMRS866)	Rapporteur et président
Lubka Roumenina Dr, Centre de recherche des Cordeliers, Paris (– UMRS1138)	Rapporteur
Michaela Semeraro Dr, Hôpital Necker, Paris	Examineur
Sébastien Apcher Dr, Gustave Roussy, Villejuif (– UMRS1015)	Examineur
Guido Kroemer Pr, Centre de recherche des Cordeliers, Paris (– UMRS1138)	Directeur de thèse
Oliver Kepp Dr, Gustave Roussy, Villejuif (– UMRS1138)	Invité

Titre : L'inhibition de la transcription par la dactinomycine révèle une nouvelle caractéristique du stress cellulaire immunogène

Mots clés : cancer, mort cellulaire immunogène, dactinomycine, eIF2 α , transcription, traduction

Résumé : La chimiothérapie constitue encore le traitement de référence pour la majorité des cancers. Or certains agents chimiothérapeutiques sont capables de déclencher des signaux de stress *pre-mortem* permettant d'activer une réponse immunitaire antitumorale et confèrent ainsi une protection à long terme. A l'aide d'un modèle construit par intelligence artificielle, nous avons identifié, parmi une librairie comprenant 50 000 composés, des agents anti-cancéreux qui, d'après leurs propriétés physico-chimiques, pourraient induire une mort cellulaire immunogène (ICD, de l'anglais "immunogenic cell death"). Cet algorithme nous a permis d'identifier la dactinomycine, qui, en effet, active les mécanismes sous-jacents à l'activation des cellules dendritiques *in vitro* et a un effet anti-cancéreux dépendant du système

immunitaire *in vivo*. La dactinomycine, utilisée en clinique pour le traitement de sarcomes pédiatriques, est connue pour sa capacité à inhiber la transcription. Nous nous sommes donc demandé si d'autres inducteurs de l'ICD partageaient cette propriété. Différentes chimiothérapies immunogènes induisent en effet une inhibition de la synthèse d'ARN, qui est suivie d'une inhibition de la traduction et s'accompagne de l'activation des différentes voies de l'ICD. De plus, une étude rétrospective *in silico* révèle que les agents classés comme inhibiteurs de la synthèse d'ARN ou de protéines sont prédits comme étant immunogènes. Ces résultats montrent que l'inhibition de la transcription est un événement précurseur essentiel à l'activation d'une mort cellulaire immunogène.

Title: Inhibition of transcription by dactinomycin reveals a new characteristic of immunogenic cell stress

Keywords: cancer, immunogenic cell death, dactinomycin, eIF2 α , transcription, translation

Abstract: Chemotherapy still constitutes the standard treatment for most cancers. Yet, some chemotherapeutics are able to trigger *pre-mortem* stress signals which activate an antitumor immune response and thereby confer long term protection. We used an established model built on artificial intelligence to identify, among a library of 50,000 compounds, anticancer agents that, based on their physicochemical characteristics, were predicted to induce immunogenic cell death (ICD). This algorithm led us to the identification of dactinomycin, which indeed activates the mechanisms preceding dendritic cell activation *in vitro* and demonstrates immune-dependent

anticancer effects *in vivo*. Dactinomycin, mainly used to treat pediatric sarcomas, is known as able to inhibit transcription. We therefore investigated whether other ICD inducers would share this characteristic. Different immunogenic chemotherapeutics indeed inhibited RNA synthesis and secondarily translation, accompanied by an activation of ICD-related signaling. A retrospective *in silico* study revealed that agents annotated as inhibitors of RNA or protein synthesis are predicted as immunogenic. These results establish the inhibition of RNA synthesis as a major initial event for ICD induction.

Acknowledgements

To Lubka Roumenina and François Ghiringhelli, for being rapporteur of my thesis.

To Sebastien Apcher and Michaela Semeraro, for accepting to examine this work.

To Guido, for welcoming me into your lab during these four and a half years and for all the precious scientific inputs. Doing my PhD in this team have been a truly enriching experience, both scientifically and personally.

To Oliver for letting me into the team at Gustave Roussy and for your precious help for figures and manuscript preparation and submission.

To Laura S. for introducing me to the lab and teaching me fundamental biology techniques, always with patience.

To Allan for so many things: your contribution to this work, R teaching, your help with data analysis, your ideas, your trust, our passionate discussions regarding science and life in general and the happy mood you carry and spread into the team.

To Giulia for your calm, your tolerance, your kindness and your friendship, as well as for the trusted working partner you have become.

To Marion, for your kindness and your help with platform use and data analysis.

To Sabrina, for sharing the office, always in a pleasant and confident atmosphere, as well as for your energy in maintaining good lab organization.

To Lucillia, for initiating the different projects I have been working on and your encouragements.

To Ligia for your infinite goodwill, your scientific and personal advice, your support and trust; I'm keeping at the back of my mind a potential experience in Coimbra.

To Wei for the very nice and curious persons you are, for all scientific and personal exchanges.

To Sylvère, for contributing to improve our general knowledge every lunchtime and for all the interesting discussions.

To Jo, for the very kind person you are, always ready to help. For your advice in mice experimentation and immunology.

To Friedo, for your help with gene engineering and for your continuous good mood.

To Aitzi for patiently teaching me how to work with mice, always in a good atmosphere.

To Norma, for teaching me different techniques, for your very kind and wise advice on how to deal with my PhD, but also for your sincerity and friendship.

To Sarah and Flo, for your continuous presence and personal as well as scientific support, but especially for all the great moments spent together and our friendship that continues beyond the lab.

To Juliette P., for your kindness, your friendship and for always being there to help.

To Franci for the crazy and so engaging person you are, as well as for our scientific discussions.

To Lilly, for all the events you organized and the good moments spent together.

To Maria P. and Adriana for our ever so rewarding scientific questionings and discussions.

To Sylvie, Lynda, Gauthier, for your kindness, your fun, for all the positive energy you put into keeping this lab a cohesive place to work and for all the “apéro” you initiate. To you, as well as Mehdi, Norma, Sarah and Juliette P., for our political debates and the memorable weekends spent together in Switzerland, in Copenhagen and in Italy.

To the engineers at CRC who helped me with my work: Didier, for your help with cell sorting and your jokes, but also for the judicious advice; Yohann and Isabelle for your help with flow cytometry; Gauthier for your inputs in statistics.

To Maria C. for your remarkable goodwill and tolerance, as well as for your advice at the appropriate time.

To Chiara, for your energy and involvement in making the lab work well and helping anyone in need.

To Carlos for your infinite kindness and for supporting me at a time I needed it most.

To all the other current and past members of the team, Naoufal, Mojgan, Thierry, Aména, Lorenzo, Eri, Fede, Chema, Vale S., Vale I., Shaoyi, Flora, Fatima, Julie, Gerasimos, Adrien, Antoine, Pan, Hui, Margerie, Lorella, Fanny, Deborah, David, Alexis, Noémie, Peng, Liwei, Guo, Yan, Wu Qi, Ai-Ling, Shuai, Hui, Ale, Georgio, Laura M., Barbara, Heng, Pauline and Francesca I. that have contributed to make these years so special.

To Brigitte Cyrille and Léa Poisot for your patience and help with all the administrative tasks.

To Flo, Eri and Oliver, for proofreading this manuscript.

To Susanne Brix Pedersen, for your fascinating lecture in immunology which gave me an insight in oncoimmunology and inspired me to continue on this path.

To my grand-parents, uncles, aunts, cousins, friends as well as to Quentin’s family for your curiosity and support.

To Quentin for the day-to-day support, for your happy mood and jokes that make the difficulties fly out the window every evening.

To Eva and Marius for your support and all the great family time. To my parents for passing on to me the passion for learning and understanding, for providing guidance in crucial choices of my life and for your constant trust, support and love.

Preamble

Cancer is a leading cause of death worldwide, requiring to find out more efficient strategies of treatment. The objective of this project was initially to discover agents that induce an immunogenic cell death among clinically used chemotherapeutics. We found that the chemotherapeutic agent dactinomycin, well known to inhibit transcription, induces such mechanism. This finding revealed that the inhibition of RNA synthesis constitutes a new characteristic of immunogenic cell stress. In consequence, after a short general presentation of cancer, the second part of this introduction deals with anticancer immunity, including a detailed presentation of immunogenic cell death. The third part focuses on the mechanisms of transcription and translation in eukaryotic cells, followed by the anticancer mechanisms, the pharmacokinetics and clinical use of the chemotherapeutic dactinomycin. In agreement with the doctoral school, the chapters “Material and methods” and “Results” are extracted from the article “Immunogenic cancer cell stress involves inhibition of transcription, Humeau J., Sauvat A., Cerrato G., Loos F., Iannantuoni¹ F., Bezu L., Lévesque S., Paillet J., Pol J., Leduc M., Zitvogel L., De Thé H., Kepp O., Kroemer G.”, which is in the reviewing process for the scientific journal EMBO Molecular Medicine, with minor modifications and supplements.

Content

ACKNOWLEDGEMENTS.....	3
PREAMBLE.....	5
CONTENT.....	6
ABBREVIATIONS.....	8
INTRODUCTION.....	12
1. Cancer.....	12
1.1. Overview.....	12
1.2. Mechanisms of oncogenesis.....	12
2. Role of the immune system in antitumor therapy.....	15
2.1. From the discovery of tumor antigens to the development of immunotherapies ..	15
2.2. Mechanisms of antitumor immunity.....	17
2.3. Immunoediting accompanies cancer progression.....	18
2.4. Adjuvanticity through immunogenic cell death.....	20
2.4.1. Mechanisms of chemotherapeutics-driven immunogenic cell death.....	22
2.4.1.1. eIF2 α phosphorylation-dependent calreticulin exposure.....	23
2.4.1.2. Autophagy-mediated ATP secretion.....	28
2.4.1.3. HMGB1 release and TLR4 mimicry.....	31
2.4.1.4. Autocrine signaling of type I interferon.....	32
2.4.1.5. The ANXA1 FPR1 axis.....	33
2.4.2. Methods to assess immunogenic cell death.....	34
2.4.1. Immunogenic cell death inducers.....	36
3. The anticancer agents dactinomycin inhibits transcription.....	43
3.1. Transcription and translation in eukaryotic cells.....	44
3.1.1. Mechanisms of transcription.....	44
3.1.2. Mechanisms of translation.....	47
3.1.2.1. From mRNA to protein.....	47
3.1.2.2. ER stress inhibits cap-dependent translation.....	49
3.1.3. The inhibition of transcription and translation to prevent neoplastic cells proliferation.....	50
3.2. Dactinomycin intercalates into the DNA and inhibits transcription.....	51
3.3. Other anticancer mechanisms of dactinomycin.....	53
3.3.1. Dactinomycin is a topoisomerase inhibitor.....	53
3.3.2. Dactinomycin inhibits protein synthesis.....	54
3.3.3. Dactinomycin induces apoptosis.....	54

3.3.4.	Dactinomycin induces photosensitization	56
3.3.5.	Dactinomycin inhibits respiration and glycolysis	56
3.3.6.	The effect of dactinomycin on the immune system.....	57
3.4.	Pharmacokinetics of dactinomycin	57
3.5.	Dactinomycin in the clinic	60
3.5.1.	Cancers treated with dactinomycin-based chemotherapy	60
3.5.2.	Clinical trials involving dactinomycin	63
	AIM OF THE WORK	66
	MATERIAL AND METHODS.....	68
	RESULTS.....	80
	Identification of dactinomycin as a <i>bona fide</i> ICD inducer.....	80
	Immune-dependent anticancer effects of dactinomycin.	85
	Inhibition of transcription by a panel of ICD inducers.....	88
	Inhibition of transcription as an ICD hallmark.....	93
	SUPPLEMENTARY FIGURES AND TABLES.....	96
	DISCUSSION.....	110
	PERSPECTIVES	118
	COLLABORATIONS	121
	BIBLIOGRAPHY	123
	SUMMARY IN FRENCH.....	146

Abbreviations

5'UTR	5' untranslated region
ABC	Adenosine triphosphate binding cassette
ADCC	antibody-dependent cell mediated toxicity
ADP	adenosine triphosphate
ALK	anaplastic lymphoma kinase
AML	acute myeloid leukemia
AMP	adenosine monophosphate
ANXA1	annexin A1
ATF	activating transcription factor
ATG	autophagy related genes
ATP	adenosine triphosphate
ATRA	all-trans-retinoid acid
b-ZIP	basic leucine zipper
BAK	bcl-2-associated K
BAP31	B-cell receptor-associated protein 31
BAX	bcl-2-associated X
BDP	B-double-prime
BiP	binding immunoglobulin protein
BMDC	bone marrow derived cells
bp	base pair
BRE	transcription factor IIB recognition element
BRF	transcription factor IIB-related factor
CALR	calreticulin
CAR	chimeric antigen receptors
CCL	C-C motif chemokine ligand
CD	cluster of differentiation
CDDP	cis-diamminedichloridoplatinum(II) (also known as cisplatin)
CF	core factor
CPSF	cleavage and polyadenylation specificity factor
CSTF	cleavage stimulation factor
CTD	carboxy terminal domain
CTL	cytotoxic T cell
CTLA-4	cytotoxic T-lymphocyte-associated protein 4
CXCL	C-X-C motif chemokine ligand
CXCR	C-X-C chemokine receptor
DACT	dactinomycin
DAMP	damage-associated molecular pattern
DDIT3	DNA damage inducible transcript 3
DMBA	7,12-Dimethylbenz[a]anthracene
DNA	deoxyribonucleic acid
DC	dendritic cell
DPE	downstream core promoter elements
dsDNA	double-stranded deoxyribonucleic acid
eEF1a1	elongation factor 1-alpha 1
EGFR	epidermal growth factor receptor

eIF	eukaryotic initiation factor
eIF2AK	eukaryotic translation initiation factor 2-alpha kinase
ER	endoplasmic reticulum
ERAD	endoplasmic reticulum-associated protein degradation
EF-Tu	elongation factor thermo unstable
ERG	erythroblast transformation-specific related gene
ETV	ETS translocation variant
EWSR	Ewing's sarcoma breakpoint region
FDA	Food and Drug Administration
FLI1	friend leukemia integration 1
FPR	formyl peptide receptor
GDP	guanosine diphosphate
GFP	green fluorescent protein
GTP	guanosine triphosphate
HER-2	human epidermal growth factor receptor 2
HHV-8	human gammaherpesvirus 8
HIF	hypoxia inducible factor
HIV	human immunodeficiency virus
HMGB1	high-mobility group box 1
HPV	human papilloma virus
HSP	heat shock protein
IC ₅₀	half maximal inhibitory concentration
ICD	immunogenic cell death
ICB	immune checkpoint blockade
IFN	interferon
IFNAR	interferon- α/β receptor
IL	interleukin
Inr	initiator
<i>i.p.</i>	intraperitoneally
IRE1	inositol-requiring enzyme 1
ISRIB	integrated stress response inhibitor
<i>i.v.</i>	intravenously
kbp	kilobase pair
KRAS	V-Ki-ras2 Kirsten rat sarcoma viral oncogene kinase domain like
LAMP	lysosomal-associated membrane protein
LC3 (or MAP1LC3B)	microtubule-associated proteins 1A/1B light chain 3B
LRP1	low density lipoprotein receptor-related protein 1
MAMP	microbe-associated molecular pattern
MDSC	myeloid-derived suppressor cells
MetRNA _i ^{Met}	methionine charged initiator transfer ribonucleic acid
MHC	major histocompatibility complex
MIC	major histocompatibility class I polypeptide related sequence
miRNA	micro ribonucleic acid
MLKL	mixed lineage kinase domain like
mRNA	messenger ribonucleic acid
MTX	mitoxantrone
MX1	myxovirus 1
MYC	myelocytose

MYD88	myeloid differentiation primary response protein 88
NCI	National Cancer Institute
NK	natural killer
NKG2D	natural killer group 2 member D
NLRP3	NOD-like receptor family pyrin domain containing-3
NOD	nucleotide-binding oligomerization domain
NOR	nucleolar organizer region
NSCLC	non-small-cell lung carcinoma
OXA	oxaliplatin
(p)eIF2 α	(phosphorylated) eukaryotic initiation factor 2 α
P-TFEB	positive transcription elongation factor
P2RX7	purinergic receptor P2X7
P2RY2	purinergic receptor P2Y2
PABP	poly(A)-binding protein
PANX1	pannexin 1
PERK	PKR-like ER protein kinase
PIC	pre-initiation complex
PKR	protein kinase R
PD-1	programmed cell death 1
PD-L1	programmed cell death ligand 1
PDIA3	protein disulfide isomerase family A member 3 (also known as ERp57)
PDT	photodynamic therapy
PML-RAR α	promyelocytic leukemia gene-retinoic acid receptor alpha
PP1	protein phosphatase 1
PPP1R15A	protein phosphatase 1 regulatory subunit 15A (also known as GADD3 for growth arrest and DNA damage-inducible protein 4 protein phosphatase 1)
PRR	pattern recognition receptor
RB	retinoblastoma
rCALR	recombinant calreticulin
RAGE	receptor for advanced glycation end products
RIPK	receptor interacting serine threonine kinase
ROS	reactive oxygen species
RFP	red fluorescent protein
rRNA	ribosomal ribonucleic acid
RUSH	retention using selective hook
<i>s.c.</i>	subcutaneous
SERCA	sarco/endoplasmic reticulum Ca ²⁺ ATPase
siRNA	small interfering ribonucleic acid
shRNA	short hairpin ribonucleic acid
SIOP	International Society of Pediatric Oncology
SMAC	synthetic second mitochondria derived activator of caspase
SNAP23	synaptosomal-associated protein 23
SNARE	soluble N-ethylmaleimide-sensitive-factor attachment protein receptor
ssDNA	single-stranded deoxyribonucleic acid
STAT1	signal transducer and activator of transcription 1
TAA	tumor associated antigen
TAM	tumor associated macrophage
TF	transcription factor

P-TEFb	positive transcription elongation factor
TGF	tumor growth factor
Th	T helper
TILs	tumor infiltrating lymphocytes
TLR	toll-like receptor
TNF	tumor necrosis factor
TP53	tumor protein 53
TRAIL	TNF related apoptosis inducing ligand
Treg	regulatory T cell
tRNA	transfer ribonucleic acid
(u)ORF	(upstream) open reading frame
UAF	upstream activating factor
UPR	unfolded protein response
UVC	ultraviolet C
VAC	vincristine, dactinomycin, cyclophosphamide
VAD	vincristine, dactinomycin, doxorubicin
wt	wild-type
WT	Wilms tumor
XBP1(s)	(spliced) X box binding protein 1

Introduction

1. Cancer

1.1. Overview

Cancer (or neoplasm or malignant tumor) is a generic term applied to a large group of diseases which can affect any part of the organism. One characteristic defining cancer is the apparition of abnormal cells growing out of control and above their physiological limits. The invasion of other organs by cancer cells is called metastasis.

In 2018, 18 million new cases of cancers occurred worldwide with 9.5 million in men and 8.5 million in women. This same year, 9.6 million persons succumbed to cancer, which makes it the second cause of death after cardiovascular disease and accounts for one over six deaths in the world. In France, it has even become the first cause of death since 2017. The four most common types of neoplasms are lung cancer, female breast cancer, colorectal cancer and prostate cancer, while lung, liver, stomach and colorectal cancers account for the highest number of deaths in the world (CancerResearchUK, Retrieved 2019-08-01; WHO, Retrieved 2019-08-01). The number of cancers is expected to reach 23.6 million new cases in 2030 (NCI, Retrieved 2019-08-01).

Tumorigenesis is due to close interaction between genetic factors and exposition to external agents that can be classified into three categories: physical agents (e.g. ultraviolet, ionizing radiations), chemical agents (e.g. abestos, compounds of tobacco smoke, arsenic) and biological agents (e.g. viral, bacterial or parasite infections, food). Aging is another essential element in cancer apparition: the number of cancers increases a lot throughout life, which may be due to accumulation of exposition to risk factors together with repair mechanisms that lose efficiency with aging (WHO, Retrieved 2019-08-01).

1.2. Mechanisms of oncogenesis

Tumorigenesis is a multistep process which initiates in normal cells undergoing DNA damage that in turn is not (or improperly) repaired, thus affecting gene functions. Certain mutations are particularly involved in tumorigenesis such as loss-of-function of tumor suppressor genes, like *TP53* or *RB* and gain of function of proto-oncogenes, such as *KRAS* or *MYC*.

During tumor promotion, selective clonal expansion of initiated cells results in tissue hyperplasia. Eventually, some of these pre-neoplastic cells may enter the progression stage

where they undergo malignant transformation by accumulating further genetic modifications. This can lead to invasion of neighboring tissues and further migration to other organs where it forms metastasis (Abel & DiGiovanni, 2011). Each process of sequential accumulation of mutations is unique, which explains (part of) the diversity of this disease and the complexity in identifying reliable biomarkers and efficient treatment options. However, certain characteristics essential to cancer development are shared by most tumors, such as intrinsic physiological alterations including growth autonomy, insensitivity to inhibitory growth signals, ability to escape apoptosis, unlimited replicative potential, strong ability to induce angiogenesis and the metastatic invasion of distant tissues (**Figure 1**) (Hanahan & Weinberg, 2000).

Consequently, in addition to surgical removal of malignant tissues, the first anticancer therapies that were developed in the past century and are still widely used in clinics aim at destroying malignant cells by targeting their rapid uncontrolled proliferation. For this, several, mechanistically diverse, anticancer strategies were designed that can be broadly subdivided based on their main mode of action into: (i) alkylating agents which induce the formation of inter- or intra- DNA crosslinks interfering with DNA replication (e.g. cyclophosphamide, oxaliplatin), (ii) topoisomerase inhibitors which impair DNA unwinding during replication and/or transcription (e.g. anthracyclines, topotecan), (iii) antimetabolites which prevents from DNA or RNA synthesis (e.g. 5-fluorouracil), (iv) spindle poisons affecting the (de)polymerization of tubulin and the formation of mitotic spindle (e.g. taxols, vinca-alkaloids), (v) radiation therapies which induce DNA damages and consequent apoptotic cell death, (vi) cytotoxic antibiotics which display anticancer effects through various mechanisms, such as reactive oxygen species production (e.g. bleomycin) or DNA intercalation (e.g. dactinomycin). Of note, most chemotherapeutics belong to several categories. Targeted therapy, yet another strategy that emerged during the past 20 years, focuses on cancer specific alterations such as oncogenic signaling pathways (e.g. anaplastic lymphoma kinase (ALK) inhibition with crizotinib).

More recently, ample evidence showed that cancer is not a merely cell autonomous genetic disease, but also a process depending on the tumor micro-environment and thus new characteristics were added to the list of cancer hallmarks: modifications in the cell metabolism and the ability to escape from immunosurveillance, together with genome instability that further drives mutational alterations and the capacity to subvert proinflammatory signals for cancer development (**Figure 1**) (Hanahan & Weinberg, 2011). These discoveries offer additional opportunities for the development of treatment options, including the immunotherapies, which aim at the reactivation of intrinsic anticancer immunosurveillance.

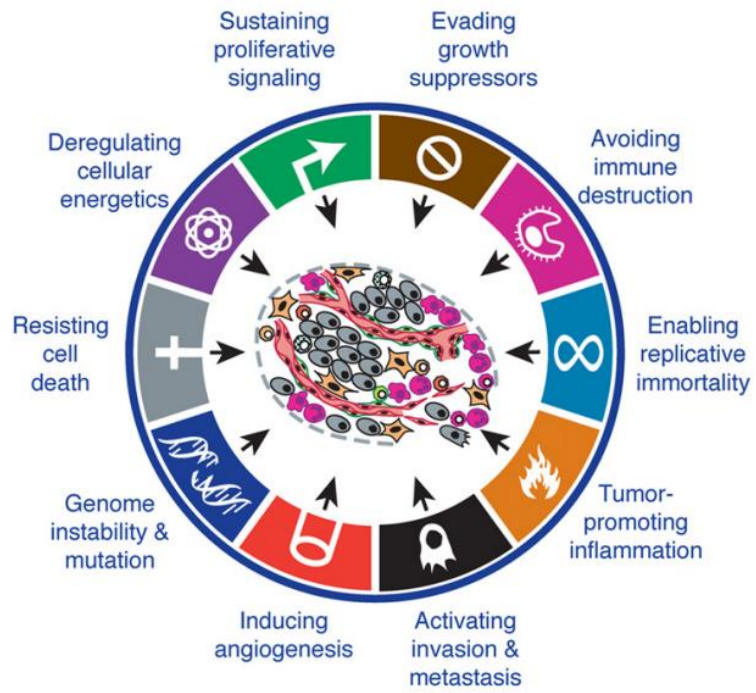


Figure 1. The hallmarks of cancer (Hanahan & Weinberg, 2011). Malignant cells share a set of common cell intrinsic and extrinsic distinctive features.

2. Role of the immune system in antitumor therapy

2.1. From the discovery of tumor antigens to the development of immunotherapies

In 1890, William B. Coley demonstrated that injection of dying bacterial cultures called Coley toxins could be beneficial for patients with soft tissue sarcoma, which was the first manifestation of the existence of an anticancer immune response. Fifty years later, it was shown that injection of irradiated sarcoma in syngeneic mice promoted immunity against a rechallenge with live sarcoma cells of the same kind (Burnet, 1957; Foley, 1953; Klein et al, 1960).

The specific recognition of tumors by the immune system suggests that cancer cells express characteristic antigens, usually proteins, peptides or polysaccharides, but also nucleic acids combined with proteins or polysaccharides, which are different from “self” antigens. Tumor associated antigens (TAAs) can indeed result from mutations that drive tumorigenesis, like alteration in the p53 transcription factor, or be viral antigens, such as E6 and E7 expressed by human papilloma virus (HPV), both giving rise to new peptides, therefore also called neoantigens, which constitute particularly interesting targets for immunotherapy due to their high tumor specificity. Nevertheless, “self” antigens presented by cancer cells can also be immunogenic if they are (i) over-expressed, with the example of human epidermal growth factor (HER2) in breast cancer, (ii) associated with differentiation, like melanocyte differentiated antigens, or (iii) expressed in an abnormal location, with the example of cancer/testis antigens, a group of proteins expressed by tumor cells, but not by normal tissues except germinal cells and trophoblasts (Scanlan et al, 2004; Schreiber et al, 2011). These TAAs are presented by the major histocompatibility complex (MHC) class I at the surface of tumor cells and can be recognized by the immune system. The first human TAA, the melanoma antigen 1 (MAGE-A1), was identified in 1991 (van der Bruggen et al, 1991). Since then, more than 400 antigens have been discovered (Wurz et al, 2016).

In 1994, it was shown that the immune system not only recognizes TAAs but also danger signals emitted by cells undergoing stress or abnormal differentiation (Matzinger, 2002). In spite of these elements, the role of the immune system against cancer has been long debated, in part due to the evidence that tumor cells could benefit from a proinflammatory environment, including proliferative and proangiogenic signaling (Balkwill & Mantovani, 2001; Karin et al, 2002).

In the early 2000's, the group of Robert Schreiber demonstrated that interferon (IFN) γ plays a crucial role in cancer immunosurveillance and that tumors coming from

immunodeficient mice are more immunogenic than tumors arising on immunocompetent mice, giving birth to the concept of immunoediting (Shankaran et al, 2001). These two fundamental findings led to a regain of interest for cancer immunotherapy. Today, immunotherapy comes in four main flavors including (i) monoclonal antibodies which target specific cancer antigens promoting complement fixation and antibody-dependent cell-mediated toxicity (ADCC), (ii) anticancer vaccines to boost adaptive anticancer immune responses with tumor specific antigens, (iii) chimeric antigen receptor (CAR) T cells which consists of autologous T cells of patients activated *in vitro* and (iv) immune checkpoint blockade (ICB) to target specific immune inhibitory signaling with monoclonal antibodies. Indeed, T lymphocytes express inhibitory receptors, such as programmed cell death 1 (PD-1) and cytotoxic T-lymphocyte-associated protein 4 (CTLA-4), and cancer cells may express ligands (like programmed cell death ligand 1, PD-L1) as a strategy to escape from immunosurveillance (**Figure 2**). This approach has largely demonstrated its antineoplastic efficacy first in melanoma and then in different other kinds of tumors (Lesokhin et al, 2015), with several ICBs currently on the market: a CTLA-4 targeting antibody ipilimumab (Yervoy), three PD-1 targeting antibodies, pembrolizumab (Keytruda), nivolumab (Opdivo) and cemiplimab (Libtayo), as well as three PD-L1 targeting antibodies, atezolizumab (Tecentriq), durvalumab (Imfinzi) and avelumab (Bavencio) (Cancer.org, Retrieved 2019-08-17; FDA, Retrieved 2019-08-17).

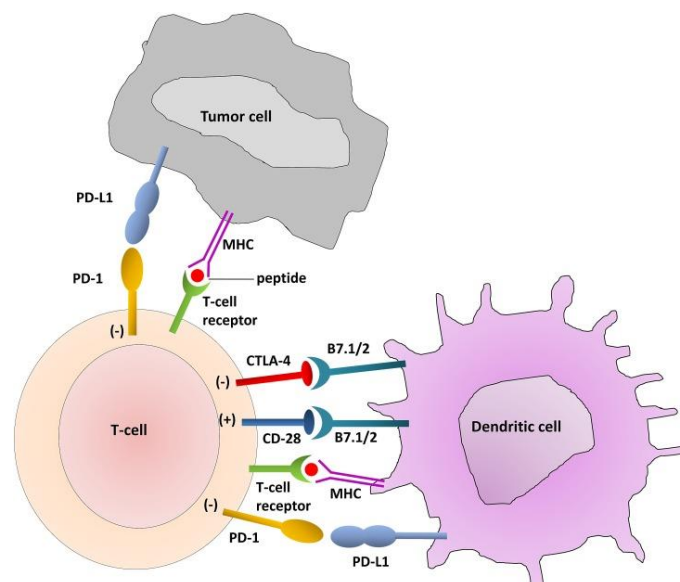


Figure 2. Activator and inhibitory T cell receptors and their ligands (Zaravinos, 2014). CTLA-4, cytotoxic T-lymphocyte-associated protein 4; MHC, major histocompatibility complex; PD-1, programmed cell death 1; PD-L1, programmed cell death ligand 1.

2.2. Mechanisms of antitumor immunity

The immune system is a biological defense system which protects the organism against infection. It consists of innate immune effectors, which elicit an immediate local response to pathogens in a rather nonspecific fashion, and the adaptive immune system, which takes longer to be activated but confers a specific reaction and durable protection against the initial insult. In the context of cancer, immunosurveillance is an extrinsic mechanism engaged after cell intrinsic mechanisms of control and elimination have failed.

During tumorigenesis, tumor cells require more important blood influx and stromal reorganization to pursue their expansion. This environment promotes proinflammatory cytokine release by tumor and stromal cells. Such cytokines include tumor necrosis factor (TNF)- α , transforming growth factor (TGF)- β , interleukin (IL)-1 β , IL-6 and IL-10, altogether leading to the recruitment of natural killer (NK) cells, NKT cells, $\gamma\delta$ T lymphocytes, macrophages and dendritic cells (DCs) on the site of the tumor (Matzinger, 2002; Smyth et al, 2001; Yamamoto et al, 2003). Recruited immune cells in turn secrete proinflammatory cytokines, like IL-12 and IFN- γ (Yamamoto et al, 2003). Tumor infiltrating NK cells bind to tumor cells via interaction between natural killer group 2 member D (NKG2D) and its ligands, MHC class I polypeptide-related sequence (MIC)-A and -B and mediate cytotoxic effect on neoplastic cells promoting tumor antigens release (Gajewski et al, 2013). Dying tumor cells and released antigens are ingested by DCs, which in addition sense damage-associated molecular patterns (DAMPs) via their pattern recognition receptor (PRRs). Altogether, these signals promote DCs maturation with the presentation of tumor antigens by MHC class II, cross-presentation by MHC class I, expression of the co-stimulatory molecules CD40, CD80 and CD86 and secretion of proinflammatory cytokines including IL-12, IL-6, TNF α , type I IFN (Albert et al, 1998; Banchereau & Steinman, 1998; Gardner & Ruffell, 2016). At the same time, DCs migrate to the draining lymph node where they activate naïve CD8⁺ T cells, promoting the clonal expansion of cytotoxic T lymphocytes (CTLs) as well naïve CD4⁺ T cells driving their differentiation in T helper (Th) 1 cells secreting IFN γ , IL-12, IL-6 and eventually in Th17 cells secreting IL-17 and IL-22 (Bailey et al, 2014) in the context of anticancer immune response. CTLs are recruited to the tumor site where they elicit cytotoxicity against cancer.

Altogether, CTLs, NK and NKT lymphocytes are considered as the main anticancer effectors as they induce apoptosis of their target cells through perforin, granzyme and granulysin secretion, as well as via the expression of TNF related apoptosis inducing ligand (TRAIL) (Mori et al, 1997; Takeda et al, 2001). Thanks to their ability to present antigens to

CD4⁺ and CD8⁺ T cells, DCs constitute the key mediator between innate and adaptive immune responses. In addition, $\gamma\delta$ T cells seem to have a rather antitumor effect even though their role and exact underlying mechanisms need to be further investigated (Fridman et al, 2017; Gajewski et al, 2013). In the context of cancer, macrophages can exert different roles. When activated by IFN γ , they display an M1 phenotype including the secretion of proinflammatory cytokines such as IL-2, IL-6, IL-1 β , IL-12, IL-23 and TNF α , altogether driving the anticancer response through a Th1 polarization. However, tumor-associated macrophages (TAMs), observed in most tumor infiltrates, rather display an M2 phenotype characterized by low MHCII expression and secretion of immunosuppressive cytokines such as IL-10 and TGF β . M2 macrophages also secrete cytokines and chemokines which promote angiogenesis and metastasis (Hao et al, 2012). In addition, this subtype of macrophages can recruit CD4⁺ FoxP3⁺ regulatory T cells (Treg) through the secretion of the C-C motif chemokine ligand 2 (CCL22) (Curiel et al, 2004). Tregs in turn promote tolerance by the secretion of inhibitory cytokines (e.g. TGF- β , IL-10) and the expression of the inhibitory ectoenzymes CD39 and CD73 among other suppressive mechanisms (Curiel et al, 2004; Fridman et al, 2017; Knochelmann et al, 2018). Like macrophages, neutrophils can have a dual role, proinflammatory under the N1 phenotype while protumoral when displaying as N2 phenotype.

2.3. Immunoediting accompanies cancer progression

Tumors develop despite the ability of the immune system to recognize and eliminate tumor cells. This paradox can be explained by tumor immunoediting, a process associated to the pressure exerted by the immune system during tumorigenesis.

Immunoediting, first described by the team of Robert Schreiber, occurs in three sequential steps: elimination, equilibrium and escape. In the elimination phase, long before a tumor gets clinically detectable, emerging cancer cells are under immunosurveillance by the innate and adaptive immune system, including in particular CTLs, NK cells and proinflammatory cytokines, as previously described. This might lead to complete tumor destruction. However, some cancer variants may survive and enter the “equilibrium” phase, in which tumor outgrowth is maintained in a state of dormancy by mediators belonging to the adaptive immune system. NK cells in particular are dispensable in this phase. Under the continuous pressure exerted by the immune system on genetically unstable cancer cells, tumors undergo transformation (or immunoediting), until resistant clones may emerge, which (i) are not recognized by the immune system due to antigen variation or a defect in antigen

presentation, (ii) are resistant to mechanisms of immune destruction and/or (iii) promote an immunosuppressive tumor micro-environment. In the escape phase, tumor proliferation cannot anymore be controlled by the immune system and a clinically detectable tumor forms (Dunn et al, 2004a; Dunn et al, 2004b; Schreiber et al, 2011) (**Figure 3**).

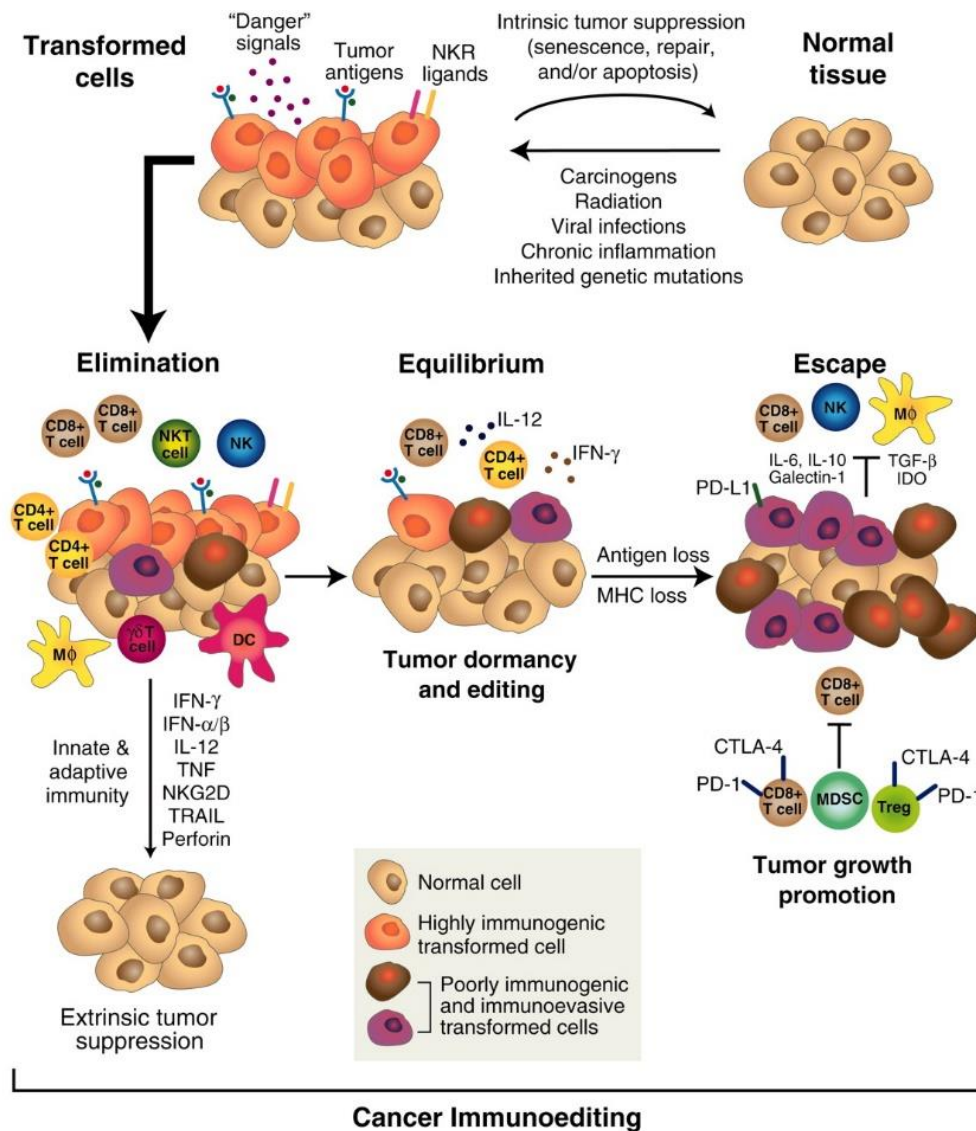


Figure 3. Cancer immunoediting (Schreiber et al, 2011). When tumor cells emerge, they are recognized and eliminated by the immune system, including in particular natural killer (NK), NKT cells, dendritic cells (DCs) primed CD8⁺ T cells, $\gamma\delta$ T cells, macrophages (M⁰) and CD4⁺ T cells, the pro-inflammatory cytokines interferon (IFN) γ , IFN α/β , interleukin (IL)-12, tumor necrosis factor (TNF), natural killer group 2 member D (NKG2D) and the cytotoxic enzymes TNF related apoptosis inducing ligand (TRAIL) and perforin; this constitutes the elimination phase. Under the pressure of these immune mediators, tumor will undergo transformation to resist to the immune attacks; this corresponds to the equilibrium phase, a state of functional dormancy in which proliferation is controlled by mediators of the adaptive immune response. This may last for a while, until variants arise which have acquired the capacity not to be recognized and/or eliminated by the immune system; this constitutes the escape phase. CTLA-4, cytotoxic T-lymphocyte-associated protein 4; IDO, indoleamine 2,3-dioxygenase; MDSC, myeloid-derived suppressor cells; MHC, major histocompatibility complex; NKR, natural killer receptor; PD-1, programmed cell death 1; PD-L1, programmed cell death ligand 1; Treg, regulatory T cell.

At this stage, the constitution of the tumor immune infiltrate indicates the outcome of the disease, with the presence of CTLs, tertiary lymphoid structures and M1 macrophages as good prognostic factors, whereas Tregs and M2 macrophages being worst prognosis factors (Fridman et al, 2017; Pages et al, 2018). It can be driven by the choice of anticancer therapy: ICB prevents from CTLs exhaustion, vaccination enhances tumor specific CD8⁺ T cells and immunogenic cell death inducers promote the emission of danger signals.

2.4. Adjuvanticity through immunogenic cell death

For a long time, cell death has been classified based on morphological features in a dichotomic manner. Apoptosis was described as a regulated, physiological and non-immunogenic type of cell death, whereas necrosis was considered as an uncontrolled pathological and proinflammatory mechanism. Since then, we learned that regulated cell death can exert morphological features of necrosis whereas apoptosis can trigger an immune response (Galluzzi et al, 2015a). The immunogenicity of cell death cannot be defined merely based on morphological traits, but need to be addressed with vaccination experiment which consists in the injection of dying cells into syngeneic host on their sequential rechallenge with live cells (Kepp et al, 2014). An absence of (or delayed) tumor growth in this model is an indication for anticancer vaccination efficacy and thus for the immunogenicity of cell death.

Immunogenic cell death (ICD) following pathogens infection constitutes an ancient mechanism of defense. Indeed, when cells are infected by viruses or intracellular bacteria, they sense microbe-associated molecular patterns (MAMPs) via their specific PRRs which trigger an intracellular and micro-environmental danger response and consequent activation of immune cells. In 2005, it has been demonstrated that anthracyclines can also drive a kind of cell death which induces an anticancer adaptive immune response (Casares et al, 2005). In the following years, many other chemotherapeutics, like oxaliplatin (OXA), as well as physical modalities, like irradiation, photodynamic therapy (PDT) or high hydrostatic pressure (Fucikova et al, 2014; Garg et al, 2012a; Obeid et al, 2007a), were shown to be able to trigger ICD. Similarly to their microbial counterparts, these anticancer agents induce *pre-mortem* stress mechanisms leading to the emission of DAMPs, recognized by PRRs expressed on DCs (**Figure 4**). Calreticulin (CALR), adenosine triphosphate (ATP) and high-mobility group box 1 (HMGB1) are DAMPs common to almost all instances of ICD discovered until now (Galluzzi et al, 2017). Type I IFN and annexin A1 (ANXA1), discovered in the context of chemotherapeutics-induced ICD, have been further added to the list (Sistigu et al, 2014; Vacchelli et al, 2015a), but their general

involvement in ICD remains to be investigated. Even though these five DAMPs may be general features of ICD, the pathways underlying their emission is particular to each form of ICD, as exemplified by autophagy, which is involved in anthracyclines-induced ICD but displays an immunosuppressive action in the context of hypericin-based PDT (Garg et al, 2013).

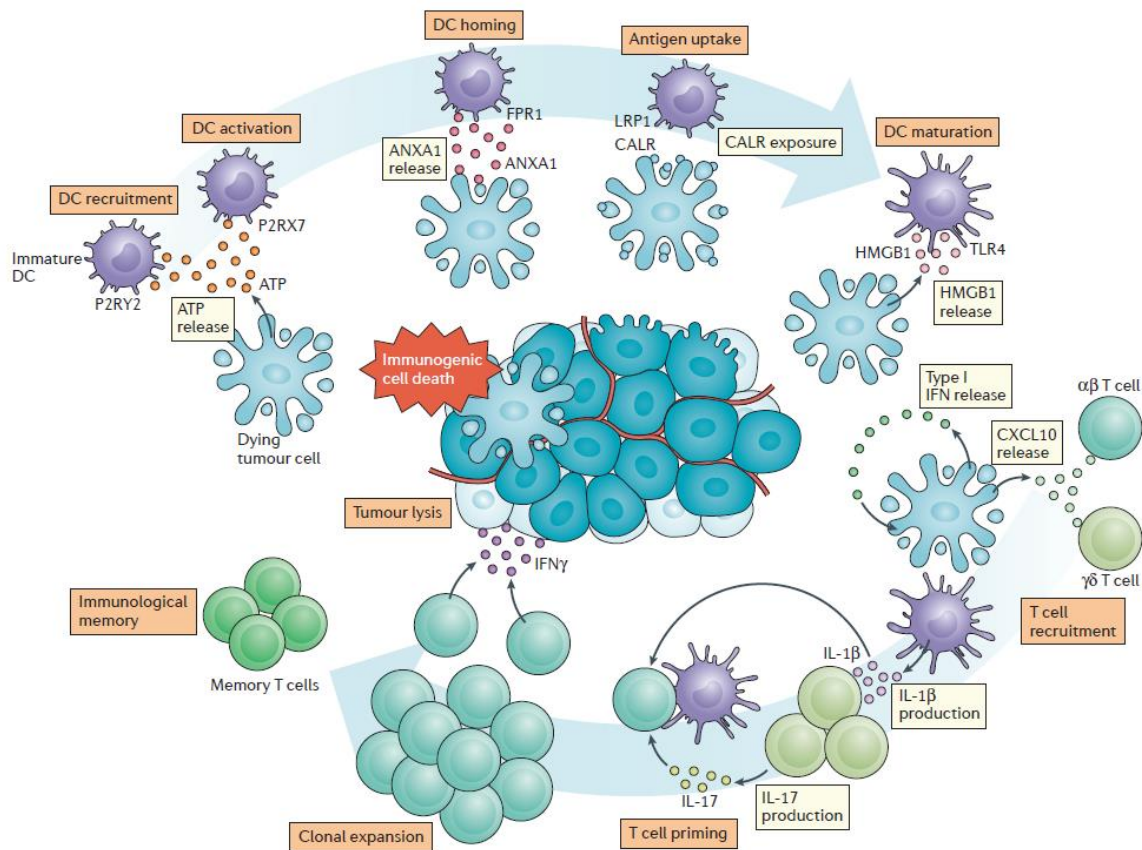


Figure 4 Activation of immunogenic cell death (Galluzzi et al, 2017). Chemotherapeutics induce calreticulin (CALR) exposure at the plasma membrane, as well as adenosine triphosphate (ATP), annexin A1 (ANXA1) and high-mobility box 1 (HMGB1) release from stressed and dying cancer cells, which are recognized by low density lipoprotein receptor related protein 1 (LRP1), purinergic receptors P2Y2 (P2RY2) and P2X7 (P2RX7), formyl peptide receptor 1 (FPR1) and toll-like receptor 4 (TLR4) expressed by dendritic cells (DCs) respectively. In addition, they induce the autocrine/paracrine secretion of type I interferon (IFN) leading to C-X-C motif chemokine ligand 10 (CXCL10) release. These mechanisms allow DCs recruitment, activation and maturation and elicit an adaptive immune response involving IL-17 producing $\gamma\delta$ T cells and type I IFN secreting $\alpha\beta$ T cells. In addition to the establishment of an immune memory, this has the potential to eliminate cancer cells through cytotoxic T lymphocytes (CTLs)-mediated cytotoxicity.

In the context of ICD, inflammatory DCs (CD11b⁺ CD11c⁺ Ly6C^{high}) sense the emission of DAMPs and in turn secrete proinflammatory cytokines and cross-present antigens to naïve T cells, most of which differentiate in IFN γ producing CD8⁺ T cells. IL-17 producing $\gamma\delta$ T cells are also activated and sustain the proliferation of CD8⁺ T cells (**Figure 4**) (Ma et al, 2013; Ma et al, 2011). In addition, neutrophils are recruited through the release of DAMPs, but also through the secretion of certain chemokines, such as C-X-C motif chemokine ligand (CXCL)1,

C-C motif chemokine ligand (CCL)2 and CXCL10, by dying cancer cells (Garg et al, 2017b). Altogether, these mechanisms participate in elimination of residual cancer cells.

Some signaling events in dying cells involving in particular RIPK1 and nuclear factor κ B (NF- κ B)-induced transcriptional programs have also been reported to be required for DCs cross-presentation and consequent CD8⁺ T cells activation, but the precise mechanism by which they activate DCs is not well understood (Giampazolias et al, 2017; Yatim et al, 2015).

Even though ICD was first described as an apoptotic kind of cell death (Casares et al, 2005), it has been recently reported that necroptosis, a form of regulated necrosis mediated by receptor-interacting serine-threonine kinase 1 (RIPK1), RIPK3 and mixed lineage kinase domain-like (MLKL), is also able to drive an anticancer immune response (Aaes et al, 2016; Yang et al, 2016). Necroptosis can be induced in cells engineered for *RIP3K3* to be inducible by doxycycline or by the combination of TNF- α with a synthetic second mitochondria derived activator of caspase (SMAC) mimetic and the caspase inhibitor z-VAD-FMK. Similarly to apoptotic ICD, it triggers the emission of DAMPs (CALR, ATP, HMGB1) that confer long term protection in mice against subsequent challenge with living cancer cells of the same type. Interestingly, anthracyclines and OXA's immunogenic properties are attributable to necroptosis in addition to apoptosis (Aaes et al, 2016; Yang et al, 2016).

The success of a specific anticancer immune response relies both on tumor antigenicity, which is related to its mutational load (Samstein et al, 2019), and on the choice of the therapy driving the antigenicity through DAMPs emission.

2.4.1. Mechanisms of chemotherapeutics-driven immunogenic cell death

Most ICD mechanisms discovered so far rely on the exposure of CALR, the secretion of ATP and the release of HMGB1, but the mechanisms underlying the emission of these DAMPs depend on the type of ICD. Moreover, more recently discovered hallmarks of ICD, *i.e.* type I IFN and ANXA1 release have been much less studied and we don't know yet if they are specific to chemotherapeutics-induced ICD or shared with other modalities. The present work aims at finding new ICD inducers among chemotherapeutics agents. Thus, here, we will present the mechanisms of chemotherapeutics-driven ICD (**Figure 5**), which have been most described so far.

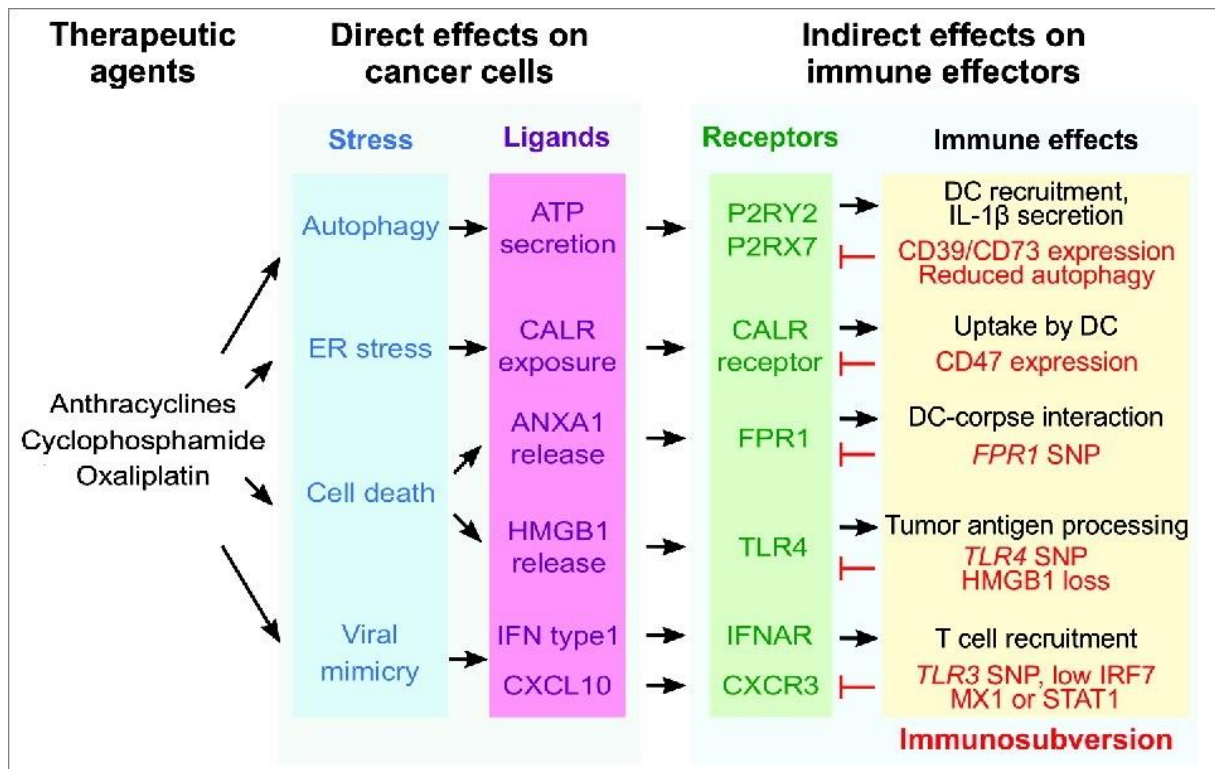


Figure 5. Mechanisms of immunogenic cell death induction by chemotherapeutics (modified from (Vacchelli et al, 2016b)). Immunogenic cell death agents trigger various pre-mortem stress pathways which activate the exposure and release of DAMPs recognized by dendritic cells (DCs) through particular receptors that exert different functions on immune cells. Cancer cells have developed certain strategies to avoid danger signaling. ANXA1, annexin A1; ATP, adenosine triphosphate; CALR, calreticulin; CXCL10, C-X-C motif chemokine ligand 10; CXCR3, C-X-C chemokine receptor 3; ER, endoplasmic reticulum; FPR1, formyl peptide receptor 1; HMGB1, high-mobility box 1; IFN, interferon; IFNAR, interferon- α/β receptor; IRF7, interferon regulatory factor 7, LRP1, low density lipoprotein receptor related protein 1; MX1, myxovirus 1; P2RY2, purinergic receptors P2Y2; P2RX7, purinergic receptors P2X7; STAT1, signal transducer and activator of transcription 1; TLR3/4, toll-like receptor3/4; SNP, single nucleotide polymorphism.

2.4.1.1. eIF2 α phosphorylation-dependent calreticulin exposure

Effect of CALR on the immune system

CALR, a 60 kDa chaperone, is the most abundant protein in the ER. It regulates calcium homeostasis and protein folding. When treated with ICD inducers, a fraction of CALR together with other ER chaperones, such as heat shock protein (HSP) 70 (also known as HSPA1A), HSP 90 (also known as HSP90AA1) and the protein disulfide isomerase family A member 3 (PDIA3, also known as ERp57), are externalized from the ER lumen to the plasma membrane of stressed and dying tumor cells (Fucikova et al, 2011; Gardai et al, 2005; Garg et al, 2012b; Obeid et al, 2007b; Panaretakis et al, 2008). These events occur before exposure of phosphatidylserine, meaning that it is not related to plasma membrane alterations accompanying apoptosis (Obeid et al, 2007b). At the surface of dying cells, CALR acts as an “eat-me” signal; it is recognized

by low density lipoprotein receptor related protein 1 (LRP1; also known as CD91) expressed by myeloid cells (mostly macrophages and DCs), unless the dying cells express simultaneously CD47, a “don’t eat-me” signal (Gardai et al, 2005; Garg et al, 2012b). Following, signaling through CD91 in DCs promote the activation of a Th1 or Th17 immune response according to the profile of danger signals (Pawaria & Binder, 2011). Accordingly, vaccination induced by anthracyclines-, OXA- or crizotinib-treated cells is abolished if dying cells are incubated with neutralizing CALR antibodies or if CALR is depleted with siRNAs (Liu et al, 2019b; Obeid et al, 2007b; Tesniere et al, 2010). In addition, PDT-driven ICD is reduced when LRP1 expression is down regulated with shRNAs (Garg et al, 2012b), bortezomib- and capsaicin-induced ICDs are abolished by LRP1 targeted monoclonal antibody or by silencing LRP1 with siRNA (Gilardini Montani et al, 2015) and mouse macrophages lacking LRP1 exhibit a reduced phagocytotic potential (Gardai et al, 2005; Lillis et al, 2008).

EIF2 α phosphorylation-dependent mechanism of CALR exposure

The canonical response to ER stress is called unfolded protein response (UPR) and involves three pathways, which are mediated by the transmembrane proteins eukaryotic translation initiation factor 2-alpha kinase 3 (eIF2AK3, also called PERK for protein kinase R (PKR)-like endoplasmic reticulum kinase), inositol-requiring enzyme 1 (IRE1 α) and the activating transcription factor (ATF) 6. In normal conditions, these proteins are maintained in an inactive state by the binding immunoglobulin protein (BiP) chaperone. During ER stress, BiP dissociates from them to bind the misfolded/unfolded proteins, resulting in the activation of the three arms of UPR. EIF2AK3 is a type I ER transmembrane kinase that contains a PEK-like catalytic domain in its cytosolic C-terminal region. When dissociated from BiP, EIF2AK3 oligomerizes, autophosphorylates and promotes phosphorylation of the serine 51 on eukaryotic initiation factor 2 α (eIF2 α). EIF2 α phosphorylation leads to messenger RNA (mRNA) translational attenuation by preventing cap-dependent ribosomal initiation complexes formation. In addition, phosphorylated eIF2 α selectively activates the translation of the mRNA encoding for ATF4. ATF4 is a basic leucine zipper (b-ZIP) transcription factor that induces growth arrest and upregulates genes coding for chaperones, antioxidants, XBP1 as well as DNA damage-inducible transcript 3 (DDIT3, also known as CHOP for CCAAT/enhancer-binding homologous protein). IRE1 is also a type I ER transmembrane endoribonuclease/kinase that has a kinase domain and an endoribonuclease domain in its cytosolic N-terminal luminal domain. IRE1 exists as two isoforms: IRE1 α and IRE1 β . IRE1 α is present in all cell types and has been widely studied. Upon ER stress conditions, it becomes active by dimerization and

autophosphorylation. Activated IRE1 α catalyzes the splicing of a 26 nucleotides intron from the X-box binding protein 1 (XBP1) mRNA. Spliced XBP1 encodes a b-ZIP transcription factor that upregulates UPR genes, including genes involved in ER-associated protein degradation (ERAD) as well as genes involved in protein folding. The third pathway involves ATF6, a type II ER transmembrane protein that has a transcriptional activation domain in its cytosolic region. ATF6 has two isoforms, ATF6 α and ATF6 β ; when dissociated from BiP, ATF6 α transits from the ER membrane to the Golgi where it is cleaved by the Golgi resident site 1 and 2 proteases (respectively S1P and S2P), leading to the generation of an activated b-ZIP factor. The N-terminal fragment of ATF6 α is transported to the nucleus where it activates UPR genes, like chaperones, XBP1 and BiP overexpression, which promote protein folding (**Figure 6-A**) (Kato & Nishitoh, 2015; Osowski & Urano, 2011).

Importantly, eIF2 α phosphorylation is induced by eIFAK3 during ER stress, but can also be activated by eIF2AK1 (also called HRI for heme regulated inhibitor) upon heme deprivation, eIF2AK2 (also named PKR for protein kinase R) in response to viral infection or eIF2AK4 (also called GCN2 for general control nonderepressible 2) in the context of nutrient deprivation.

In ICD induced by chemotherapeutics, CALR exposure is preceded by the phosphorylation of eIF2 α , which has been showed to be mediated by eIF2AK3 in the murine methylcholanthrene-induced fibrosarcoma MCA205, the human osteosarcoma U2OS and colon carcinoma CT26 (Bezu et al, 2018a; Obeid et al, 2007b; Panaretakis et al, 2009). However, it was recently demonstrated that in melanoma human cells, anthracyclines induce eIF2 α phosphorylation via the activation of other kinases: eIF2AK2 or eIF2AK4 (Giglio et al, 2018). Importantly, during ER stress elicited by chemotherapeutics, solely eIF2 α phosphorylation is involved, without the downstream expression of ATF4 and DDIT3 and without activation of the two other arms of ER stress, *i.e.* the translocation of ATF6 and the alternative splicing of XBP1 (**Figure 6-B**) (Bezu et al, 2018a). This split ER stress response was also observed for crizotinib-induced ICD in various cell lines (Liu et al, 2019b) and for anthracyclines-treated human melanoma cells (Giglio et al, 2018). In addition, following administration of the EGFR specific antibody cetuximab, ICD was abolished by overexpression of XBP1 (Pozzi et al, 2016).

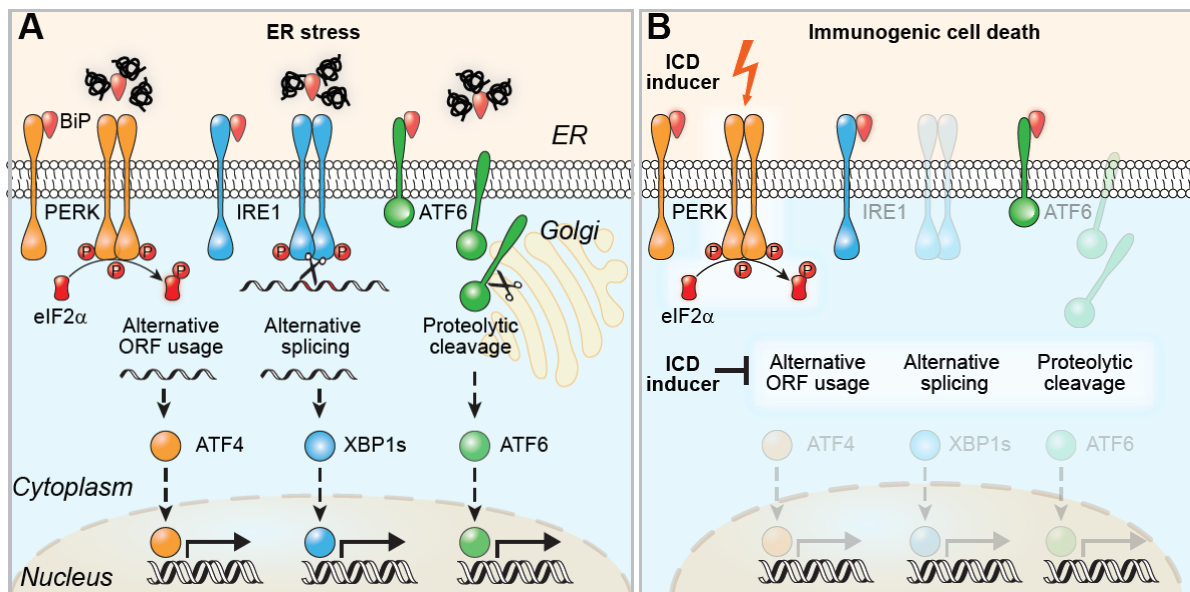


Figure 6. Split ER stress response involved in chemotherapeutics driven ICD (Bezu et al, 2018b). Canonical endoplasmic reticulum (ER) stress activates three pathways: (i) protein kinase R-like endoplasmic reticulum kinase (PERK)-mediated eukaryotic initiation factor 2 α (eIF2 α) phosphorylation leading to activating transcription factor (ATF) 4 translation due to particular open reading frame (ORF) arrangement, (ii) inositol-requiring enzyme 1 (IRE1) dimerization leading to X-box protein 1 alternative splicing (XBP1s) and (iii) ATF6 translocation to the Golgi where it undergoes proteolytic cleavage followed by translocation to the nucleus of the N-terminal part; all aiming at eliminating and/or repairing misfolded proteins (A). Immunogenic cell death (ICD) inducers mediate PERK-dependent eIF2 α phosphorylation but none of the other protein activation (B).

CALR needs to be engaged in a complex with PDIA3 to be able to translocate from the ER to the membrane (Liu et al, 2019a; Panaretakis et al, 2008). Following eIF2 α phosphorylation, B-cell receptor-associated protein 31 (BAP31) is proteolyzed in a caspase 8-dependent manner, leading to the activation of the pro-apoptotic Bcl-2-associated factors X et K (BAX and BAK) and the anterograde translocation of the CALR/PDIA3 complex from the ER lumen to the plasma membrane via the Golgi apparatus. CALR is finally secreted by soluble N-ethylmaleimide-sensitive-factor attachment protein receptor (SNARE)-dependent exocytosis (Panaretakis et al, 2009). Inhibition of any step of this pathway abolished CALR exposure. In addition, the inhibition of (i) eIF2AK3 phosphorylation with a siRNA, (ii) caspase 8 activation with a pharmacologic inhibitor (Z-VAD-fmk) or siRNA, (iii) BAX with a siRNA, (iv) the ER-Golgi traffic with brefeldin A or (iv) SNARE-dependent exocytosis with a synaptosomal-associated protein 23 (SNAP23) siRNA also abolished vaccination capacity of anthracyclines (Panaretakis et al, 2009). Of note, even though eIF2AK3-dependent CALR exposure is also required for the immunogenicity of cells treated with hypericin based PDT, this does not involve eIF2 α phosphorylation, caspase 8 and PDIA3 (Garg et al, 2012b).

Additionally, CALR exposure following anthracyclines chemotherapy is not only dictated by cell intrinsic pathways, but also relies on autocrine/paracrine signalization pathways

in stressed cancer cells, mediated by the CXCL8 (also known as IL-8) and its receptor CXCL2 (Sukkurwala et al, 2014b).

Eventually, it has been recently shown that CALR exposure also relies on ANXA1. Indeed, following treatment with anthracyclines, CALR exposure and the consequent tumor growth control is abolished in *Anxa1*^{-/-} cells, effect which is restored by supplementation with rCALR. The underlying mechanism remains to be elucidated, but it may be related to the involvement of ANXA1 in unconventional protein secretion pathways or in intracellular trafficking (Baracco et al, 2019).

Strategies to modulate CALR exposure

Chemotherapeutics like CDDP or mitomycin C, which induce all ICD hallmarks apart from CALR exposure, are not able to induce ICD (Casares et al, 2005; Tesniere et al, 2010), which could be compensated by the co-incubation with CALR recombinant protein (rCALR) prior to vaccination (Obeid et al, 2007b; Tesniere et al, 2010). In line with this, coating with rCALR enhances phagocytosis and vaccination with apoptotic melanoma cells (Dudek-Peric et al, 2015; Qin et al, 2011). CALR trafficking can also be targeted: α -integrins and PDIA3 interact with CALR in the ER and coordinate CALR translocation. Incubation of cells with 9EG7, a β 1 integrin activating antibody, reduces CALR exposure; conversely, knocking down integrins leads to enhanced CALR exposure, even though this strategy can obviously not be transferred to the clinics (Liu et al, 2019a). The immunogenicity of CDDP or mitomycin C could also be restored in combination with activators of ER stress like the inhibitor of sarco/endoplasmic reticulum Ca^{2+} ATPase (SERCA) thapsigargin, or the inhibitor of N-glycosylation tunicamycin (Martins et al, 2011). Similarly, pyridoxine, a precursor of the bioactive vitamin B6 as well as zinc supplementations were able to restore immunogenicity to CDDP-induced cell death (Aranda et al, 2014a; Aranda et al, 2015; Cirone et al, 2013).

Another strategy consists in the administration of inhibitors of the eIF2 α phosphatase complex formed by protein phosphatase 1 regulatory subunit 15A (PPP1R15A, also called growth arrest and DNA damage-inducible protein, GADD34) and protein phosphatase 1 (PP1), like calyculin A, tautomycin or salubrinal, which mediate eIF2 α phosphorylation-dependent CALR exposure (Kepp et al, 2009; Obeid et al, 2007b). All these approaches underline the relevance of eIF2 α phosphorylation for CALR exposure and may be promising, but only coating with recombinant CALR could circumvent any kind of deficiency including downregulation of CALR itself.

Clinical relevance of CALR exposure

In patients with non-Hodkin's lymphoma, vaccinated with DCs which were previously activated by co-culture with radiation-treated lymphoma cells, high amounts of CALR and HSP90 were correlated with improved clinical outcome (Zappasodi et al, 2010). Growth of monocytes from melanoma patients were shown to be slower when LRP1 expression was elevated (Stebbing et al, 2004). In lung and ovarian cancers, high CALR expression was associated with better clinical response to therapies with ICD inducers (Garg et al, 2015). In two independent cohorts of patients with non-small cell lung carcinoma (NSCLC), high level of CALR correlated with eIF2 α phosphorylation and with improved clinical outcome (Fucikova et al, 2016a). The analysis of acute myeloid leukemia (AML) from patients showed that (i) CALR expression and exposure are associated with increased relapse free survival and overall survival (Fucikova et al, 2016b), (ii) spontaneous CALR exposure correlates with the phosphorylation of eIF2 α , with a stronger T cell response and with improved disease outcome, regardless of the chemotherapeutics regimen (Wemeau et al, 2010) and (iii) CALR exposure is higher in daunorubicin-treated patients accompanied by elevated CD8⁺ T cells infiltration and improved disease outcome (Aurelius et al, 2019). Immunohistochemical analysis of NSCLC patients' tumors revealed that loss of CALR expression was a negative prognostic factor and that CALR expression was correlated to CTLs infiltration (Stoll et al, 2016). These clinical data emphasize the importance of the CALR-LRP1 axis for the outcome of cancer treatment and the reestablishment of immunosurveillance. Another element that emphasize this finding is the negative prognostic value of CD47 expression in AML (Majeti et al, 2009), in ovarian cancer (Wang et al, 2015a) and in esophageal carcinoma (Suzuki et al, 2012).

Interestingly, in a cohort of breast cancer patients treated with neoadjuvant chemotherapy, none of the ER stress induced transcription factors ATF4, ATF6 and XBP1 could reflect therapy outcome, whereas a metagene analysis showed that IFN γ T cells infiltration was implicated (Stoll et al, 2014). This strengthens recent findings showing a split ER stress response involving exclusively eIF2 α phosphorylation in the response to anthracyclines (Bezu et al, 2018a).

2.4.1.2. Autophagy-mediated ATP secretion

Effect of ATP on the immune system

ATP is the most abundant metabolite in the human body which provides energy for most

biochemical reactions. It is also an important messenger that can act via the ligation of purinergic receptors (Burnstock, 2007). In addition to its involvement in transmission of neurological signals, ATP can be released into the extracellular space by various stimuli including ICD inducers, where it exerts chemotactic and adjuvant effects, serving as a “find-me” signal for myeloid cells (Elliott et al, 2009). Extracellular ATP interacts with purinergic receptors P2Y2 (P2RY2) and P2X7 (P2RX7) expressed by antigen presenting cells (Elliott et al, 2009; Ghiringhelli et al, 2009; Kronlage et al, 2010). Accordingly, injection of ATP γ S, a non-hydrolysable analog of ATP, induces local recruitment of DCs via P2Y (Muller et al, 2010).

Besides its role as chemoattractant, ATP can influence the function of immune cells by triggering DCs maturation *in vivo* (Idzko et al, 2007). Moreover, intradermal injection of ATP γ S stimulates vaccination effects dependent on the expression of MHC class II molecules, CD80, CD86, IL-1 β and IL-12 by Langerhans cells (Granstein et al, 2005). Conversely, enzymatic degradation of ATP (by administration of apyrase, an ectonucleotidase) or the deletion of P2Y2 (by incubation with suramin, a P2Y antagonist, or by gene knockout) reduces phagocytosis of thymocytes by macrophages (Elliott et al, 2009).

Accordingly, ICD fails when ATP is neutralized with apyrase or with the membrane bound nucleosidase CD39, or if the receptors P2RY2 or P2RX7 are not expressed at the surface of antigen presenting cells of the host (Elliott et al, 2009; Ghiringhelli et al, 2009; Liu et al, 2019b; Ma et al, 2013; Michaud et al, 2011). ATP-induced purinergic signaling activates the NOD-like receptor family pyrin domain containing-3 (NLRP3) caspase-1 activation complex (the inflammasome) in DCs, leading to IL-1 β secretion (Ghiringhelli et al, 2009). IL-1 β promotes activation of IL-17 producing $\gamma\delta$ T cells and further recruitment of IFN γ producing by CD8⁺ T cells (Ma et al, 2011). Accordingly, mice deficient for P2RX7, caspase 1, NLRP3, IL-1 β , IL-1 receptor, IL-17 or IL-17 receptor fail to elicit an adaptive anticancer immune response after treatment with anthracyclines (Ghiringhelli et al, 2009; Ma et al, 2011).

Autophagy-dependent mechanism of ATP release

ATP released from dying tumor cells in the course of ICD depends on the autophagic machinery. Autophagy is a mechanism which entails the engulfment of cytoplasmic material within doubled membrane cytosolic organelles, called autophagosomes. Subsequently, autolysosomes form through the fusion of autophagosomes with lysosomes, which leads to the degradation of autophagosomes cargo by lysosomal hydrolases (Kroemer et al, 2010). Of note, microtubule-associated proteins 1A/1B light chain 3B called (MAP1LC3B, hereafter referred to as LC3) is

the most widely used marker of autophagosomes. Accordingly, in cancer cells treated with anthracyclines, reduced or absent expression of the autophagy related genes (ATG) *Atg5*, *Atg7*, *Atg10*, *Atg12*, *Beclin 1*, *Vsp34* or lysosomal-associated membrane protein (*LAMP*) 1 and 2, either by shRNAs or by genetic alterations, were unable to induce ATP release, T cell activation and subsequent vaccination (Michaud et al, 2011). Consistently, autophagy-deficient virus-infected fibroblasts were unable to induce cross-presentation (Uhl et al, 2009). During anthracycline-induced autophagy, ATP switches from lysosomes to autolysosome and is further secreted by a mechanism dependent on LAMP1 which translocates to the membrane in a caspase-dependent manner. ATP secretion also requires membrane blebbing and the opening of pannexin 1 (PANX1) channels, both mechanisms depending on caspases activation (Martins et al, 2014). Of note, autophagy not only is dispensable for ICD induced by hypericin-based PDT but its inactivation can enhance immune cells activation (Garg et al, 2013).

Modulation of ICD via the autophagy-ATP axis

CD39 (also known as ENTPD1 for ectonucleosidase triphosphate diphosphohydrolase 1), which converts ATP into adenosine triphosphate (ADP) and adenosine monophosphate (AMP) as well as CD73, which converts AMP into adenosine, can degrade ATP and inhibits the activation of an anticancer immune response mediated by CD8⁺ T cells and NK cells (Stagg et al, 2012; Sun et al, 2010). CD39 is expressed by Tregs and a subset a Th17 cells, both described as immunosuppressive and tumor promoting (Chalmin et al, 2012; Sun et al, 2010). Accordingly, mice lacking the CD73 encoding genes develop less induced cancers due to enhanced immunosurveillance (Stagg et al, 2012). Consistently, co-administration of ARL67156, a nucleosidase inhibitor can restore the ability of ATP to trigger an immune response (Michaud et al, 2011; Michaud et al, 2012).

Another strategy to elicit ATP release consists in inducing autophagic flux. Caloric restriction mimetics (CRMs) have been recently described as agents able to mimic the effect of starvation, *i.e.* they promote autophagy without inducing any toxicity, and are therefore particularly interesting for clinical applications (Pietrocola et al, 2016). When combined with the anthracycline mitoxantrone (MTX), CRMs are able to potentiate the anticancer effect by enhancing ATP release and subsequent activation of an autophagy-dependent anticancer immune response (Pietrocola et al, 2016).

Clinical relevance of ATP as a hallmark of ICD

In a cohort of patients with breast carcinoma treated with anthracyclines, a loss-of-function

variation of P2RX7 led to rapid metastatic disease development (Ghiringhelli et al, 2009). In two other independent cohorts of breast cancer patients treated with anthracyclines, LC3 correlated with autophagic flux and the combination of LC3 and HMGB1 constituted a good prognostic factor for metastasis free survival (Ladoire et al, 2015). Another immunohistochemical study in a cohort of breast cancer patients revealed that the absence of autophagy was correlated with poor disease outcome as well as with reduced CD8⁺CD68⁺ T cells and increased CD4⁺FoxP3⁺ T cells in the tumor infiltrate (Ladoire et al, 2016).

2.4.1.3. HMGB1 release and TLR4 mimicry

Effect of HMGB1 on the immune system

HMGB1 is the most abundant non-histone chromatin-binding protein, present in the nucleus of all cells. It can be actively secreted by myeloid cells in response to infection or released by cells undergoing necrosis and promotes strong inflammation (Scaffidi et al, 2002; Sims et al, 2010; Wang et al, 1999). In line with this, induction of necroptosis in melanoma leads to HMGB1 release, as well as expression of MHC class II and CD86 by DCs and macrophages, effects which were abolished in *Rage*^{-/-} and *Myd88*^{-/-} mice (which respectively lack receptor for advanced glycation end products and myeloid differentiation primary response protein 88).

In response to tissue damage, HMGB1 could also form a complex with CXCL12 leading to the recruitment of immune cells (Schiraldi et al, 2012). However, in the context of ICD, the only receptor of HMGB1 is the toll-like receptor (TLR) 4. Indeed, both *Tlr4*^{-/-} and *Myd88*^{-/-} mice cannot mount an efficient anticancer immune response in response to anthracyclines or OXA (Apetoh et al, 2007). This is reinforced by the fact that in co-culture experiments, neutralization or depletion of HMGB1 abolishes the cross-presentation, whereas administration of HMGB1 promotes inflammation (Apetoh et al, 2007). These findings reveal that the HMGB1-TLR4-MYD88 axis is required for ICD (Apetoh et al, 2007). However, the molecular mechanisms underlying HMGB1 release from the nucleus of cells undergoing ICD remains to be elucidated.

Modulation of ICD via the HMGB1 pathway

Dendrophilin, a highly potent and exclusive *Tlr4* agonist could both reestablish anticancer immune responses when HMGB1 expression is depleted by siRNA, and increase IFN γ production and consequent tumor growth reduction in several mice models when combined to anthracycline-based chemotherapy (Yamazaki et al, 2014). Besides, lots of ongoing clinical

trials employ TLR4 agonists, emphasizing their promising use as anticancer therapies (Aranda et al, 2014b; Vacchelli et al, 2013).

Clinical relevance of the importance of the HMGB1–TLR4 axis

Different loss-of-function polymorphisms in *TLR4* were associated with bad prognosis in different cohorts of patients: individuals with breast cancer undergoing anthracyclines-based chemotherapy had a more rapid post treatment relapse (Apetoh et al, 2007; Vacchelli et al, 2015a); subjects bearing head and neck squamous cell carcinoma treated with systemic chemotherapy had a reduced disease-free and overall survival (Bergmann et al, 2011) and colorectal cancer patients treated with OXA-based chemotherapy had a lower overall survival (Tesniere et al, 2010). *TLR4* loss-of-function was also a bad prognostic factor for melanoma patients treated with a DC-based vaccine (Tittarelli et al, 2012). Conversely, it has been shown that esophageal cancer patients bearing at least one mutated allele of *TLR4* exhibited an improved cancer-specific survival (Vacchelli et al, 2015b).

2.4.1.4. Autocrine signaling of type I interferon

The TLR3 – type I IFN – CXCL10 pathway

Type I IFN secretion serves as a mechanism of defense against pathogens. These cytokines can be secreted by any cell of the organism infected by virus or intracellular bacteria. Autocrine and paracrine type I IFN signaling protects surrounding cells from infection by binding the interferon- α/β receptor (IFNAR)1-IFNAR2 heterodimer, but also alerts the immune system of pathogens infection by promoting the activation of DCs, macrophages and NK cells. Accordingly, *Ifnar*^{-/-} mice are more sensitive to various viral infections (Goritzka et al, 2014; Robinson et al, 2012). Type I IFNs are also secreted by cells undergoing anthracycline- or radiation-mediated ICD, most likely due to the activation of TLR3 by RNA from dying cancer cells (Deng et al, 2014; Lim et al, 2014; Sistigu et al, 2014).

Type I IFN secretion induces autocrine signaling leading to CXCL10 secretion, promoting recruitment and activation of T cells (Sistigu et al, 2014). Accordingly, the efficacy of doxorubicin-based chemotherapy, which is reduced if cancer cells lack *Tlr3* or *Ifnar* or if IFNAR1 is neutralized by a specific antibody, can be restored by exogenous supply of recombinant type I IFN or CXCL10. Besides, the administration of a C-X-C chemokine receptor 3 (CXCR3, main receptor of CXCL10) neutralizing antibody abolishes the efficacy of doxorubicin, further supporting the importance of the TLR3 – type I IFN – CXCL10 – CXCR3

axis which may mediate chemotactic effect on T cells (Sistigu et al, 2014). Of note, the absence of IFNAR in the host has no influence on the vaccination efficacy of doxorubicin treated cells, which emphasizes the autocrine character of type I IFN signaling of dying tumor cells (Sistigu et al, 2014).

Activation of ICD by type I IFN release

Poly-ICLC, a TLR3 agonist combined with cetuximab, was shown to enhance immune cell activation in NSCLC (Ming Lim et al, 2013). Poly(A:U), another TLR3 agonist, could improve breast cancer patients' outcome in TLR3 positive individuals (Salaun et al, 2011). According to their present employment in numerous clinical trials, the use of TLR3 agonists in cancer therapy seems promising (Aranda et al, 2014b; Vacchelli et al, 2013). Eventually, this might suggest that oncolytic viruses, which stimulate type I IFN signaling, could be combined with chemotherapeutics to enhance ICD.

Clinical data related to the TLR3-dependent type I IFN release

Regarding the importance of this pathway in a cohort of breast cancer patients, a transcriptional signature centered on metagene myxovirus 1 (MX1) expression (a type I IFN related metagene), could predict the outcome of response to anthracyclines-based chemotherapy (Sistigu et al, 2014). In line with this notion, low levels of interferon regulatory factor 7 (IRF7), a transcription factor involved in type I IFN expression, were correlated with reduced metastasis free survival in a large cohort of breast carcinoma patients (Bidwell et al, 2012). In another cohort of mammary breast cancer patients, one third of the individuals had very low levels of signal transducer and activator of transcription 1 (STAT1), a transcription factor activated, among others, by IFN α 1 (Chan et al, 2012). In addition, TLR3 loss-of-function polymorphism was a sign of bad prognostic in a cohort of colorectal cancer patients (Castro et al, 2011) and of breast cancer patients (Chen et al, 2015; Vacchelli et al, 2015a).

2.4.1.5. The ANXA1 FPR1 axis

FPR1 activation by ANXA1

ANXA1 is expressed by immune cells as well as by many epithelial cells. It binds acidic phospholipids in a Ca²⁺-dependent manner and was initially described as a key factor in inflammatory responses through binding to formyl peptide receptor 2 (FPR2) (Perretti & D'Acquisto, 2009). In the context of ICD, it is the interaction between ANXA1 and another

receptor present at the surface of DCs, the formyl peptide receptor 1 (FPR1), that stands out as being essential for eliciting ICD. Indeed, anthracyclines and OXA fail to induce vaccination in *Anxa1*^{-/-} cancer cells and in *Fpr1*^{-/-} mice because DCs cannot initiate an adaptive immune response in these settings (Vacchelli et al, 2015a). This was confirmed in a carcinogen-induced breast cancer model in which the efficacy of chemotherapeutics was abolished when *Fpr1* receptors were blocked with the non-immunosuppressive antagonist cyclosporine H (Baracco et al, 2016). The detailed mechanisms underlying ANXA1 release in the context of ICD remain to be determined.

Clinical data

In line with the discovery of the aforementioned mechanism, a loss-of-function polymorphism in *FPR1* correlates with poor metastasis-free and overall survival in a cohort of breast carcinoma patients treated with anthracyclines-based chemotherapy and in a cohort of colorectal carcinoma patients treated with OXA-based chemotherapy (Vacchelli et al, 2015a). Of note, the presence of wild-type (wt) *FPR1* was only important in patients bearing wt *TLR3* and *TLR4*, suggesting that these three PRRs operate in a coordinated fashion to trigger an immune response (Vacchelli et al, 2016a; Vacchelli et al, 2015a).

2.4.2. Methods to assess immunogenic cell death

In anticancer therapy, all aforementioned ICD hallmarks, including the eIF2 α -dependent exposure of CALR, autophagy-mediated ATP release, the secretion of HMGB1 into the extracellular space, type I IFN responses as well as ANXA1 release, are essential for ICD induction and adaptive immune response mounting. However, the mere presence of the molecules cannot predict with an absolute certainty the immunogenicity of cell death, underlining the fact that other immunogenic pathways remain to be discovered (Galluzzi et al, 2017).

The current gold standard approach to evaluate immunogenic cell death relies on in vivo vaccination assay employing immunocompetent animals. The experiment consists in injection of murine cells treated *in vitro* with a cytotoxic agent into syngeneic mice, followed by rechallenge with living cells of the same type (one to two weeks later). The absence of tumors or delayed tumor growth indicates that an adaptive immune response has been elicited by the cells dying in response to the employed cytotoxicant (Humeau et al, 2019; Kepp et al, 2014). Of note, the standard ICD inducers MTX and doxorubicin vaccinate around 80 % mice from

CT26 colon carcinoma or MCA205 fibrosarcoma (Humeau et al, 2019; Kepp et al, 2014). In case of agents or combinations of drugs that enable the cure from transplanted cancers, the absence of proliferation of further injected cells of the same type also proves that immune memory has been elicited. The immunogenicity of such agents can be further confirmed by comparing their effect in immunocompetent versus immunodeficient mice. However, compounds that are endowed with immunostimulatory effect also exhibit decreased effectivity in immunodeficient mice, yet do not necessarily induce pre-mortem signals leading to the release of DAMPs from cancer cells, emphasizing the limitations of this technique to determine if an agent induces ICD. These methods are constrained by the restricted amount of available syngeneic models, as well as cost, time and ethical issues. As an alternative to vaccination, *in vitro* phagocytosis assay can be performed to assess the recruitment of DCs by dying tumor cells. Of note, this method does not test for the further activation of adaptive immune responses. Unfortunately, the aforementioned current available techniques do not enable to study ICD in human cells.

Regarding the growing importance of ICD for anticancer therapies, there is a need to discover new agents endowed with the capacity to elicit such process. We therefore investigated if we could predict *in silico* the immunogenic potential of drugs, based on their chemical and physical properties, such as molecular weight, number of hydrogen bonds donors/acceptors, polar surface area *etc.* Using machine learning approaches and taking into account that anthracyclines are strong ICD inducers, a model calculating an “ICD score” according to molecular properties was established (**Figure 7**) (Bezu et al, 2018a). This model was further applied to two independent chemical compound libraries, namely the US Drug Set of Food and Drug Administration (FDA)-approved drugs and the National Cancer Institute (NCI) mechanistic diversity set, returning the highest ICD scores for drugs previously shown as exhibiting hallmarks of ICD *in vitro* (Bezu et al, 2018a; Menger et al, 2012; Sukkurwala et al, 2014a). Hence, this algorithm is endowed with high accuracy and offers the opportunity to quickly predict new potential ICD inducers among huge libraries.

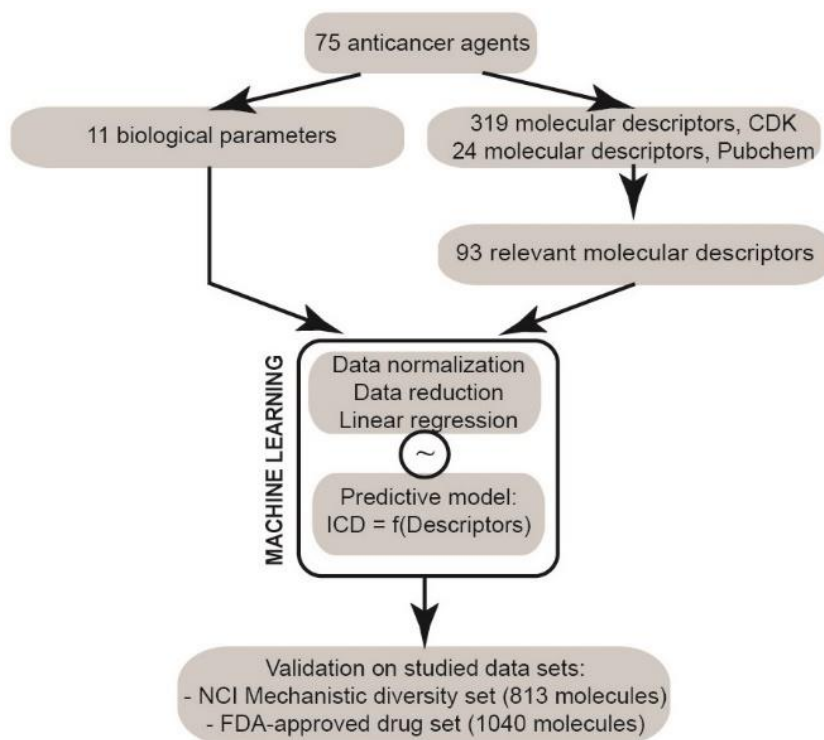


Figure 7. Construction of a model to predict ICD based on molecular descriptors (Bezu et al, 2018a). A screening of 75 anticancer agents was performed, for their ability to induce *in vitro* 11 biological parameters related to immunogenic cell death (ICD). Available molecular descriptors were obtained from PubChem or Github, accounting for 343 parameters in total which were further reduced to 93 independent descriptors by principal component analysis (PCA). Using a machine learning approach, we searched for a model which would fit a relationship between the relevant molecular descriptors and an ICD score (a linear combination of these 11 biological parameters), with the condition that anthracyclines display the highest ICD score. The selected model was able to fit the data with a high linear regression $R = 0.78$. The algorithm was further validated on two libraries previously screened for ICD. CDK, chemistry development kit; FDA, Food and Drug Administration; NCI, National Cancer Institute.

2.4.1. Immunogenic cell death inducers

The first anticancer agents discovered as intrinsically endowed with the ability to elicit a proinflammatory immune response in mice were doxorubicin, daunorubicin and idarubicin. Indeed, when dying cancer cells pre-treated with these agents are injected in mice, they induce long term protection against subsequent challenge with living cells of the same type, whereas cancer cells displaying the same extent of apoptosis following mitomycin C treatment or freeze thawing cycles are not able to do so (Casares et al, 2005). Yet another anthracycline MTX (Obeid et al, 2007a, Panaretakis et al, 2009), as well as the platinum derivative OXA (Ma et al, 2011; Obeid et al, 2007a; Panaretakis et al, 2009; Schiavoni et al, 2011), the alkylating agent cyclophosphamide (Chen et al, 2012; Ghiringhelli et al, 2009; Schiavoni et al, 2011), the proteasome inhibitor bortezomib (Chang et al, 2012; Cirone et al, 2012; Demaria et al, 2005; Spisek et al, 2007), the RNA polymerase II inhibitor lurbinedectin (Xie et al, 2019a), the cyclin-

dependent kinase inhibitor dinaciclib (Hossain et al, 2018), the topoisomerase inhibitor teniposide (Wang et al, 2019b), the bromodomain inhibitor JQ1 (Riganti et al, 2018; Wang et al, 2019a) and the antibiotics bleomycin (Bugaut et al, 2013), wogonin (Yang et al, 2012) and septacidin (Sukkurwala et al, 2014a) share the same properties. Some anticancer therapies involving physical signals such as radiotherapy (Apetoh et al, 2007; Ma et al, 2011; Obeid et al, 2007a), photodynamic therapy (Garg et al, 2012a; Gomes-da-Silva et al, 2018; Korbelik & Dougherty, 1999; Korbelik et al, 2007; Korbelik et al, 2011; Krosli et al, 1995), ultraviolet C (UVC) light (Obeid et al, 2007a; Panaretakis et al, 2009; Schiavoni et al, 2011; Yamamura et al, 2015), electrical pulses (Nuccitelli et al, 2015; Nuccitelli et al, 2017), high hydrostatic pressure (Fucikova et al, 2014; Urbanova et al, 2017), microwave thermal ablation (Yu et al, 2014) and photochemotherapy (Tatsuno et al, 2019; Ventura et al, 2018) have also shown to be immunogenic, as well as some targeted agents like targeting epidermal growth factor receptor (EGFR) antibody (Pozzi et al, 2016); (Garrido et al, 2011), certain oncolytic peptides (Zhou et al, 2016a), oncolytic viruses (Bommareddy et al, 2019; Koks et al, 2015; Zamarin et al, 2014) and certain specific bacterial toxins (Sun et al, 2015) (**Table 1**).

In most cases, chemotherapies that are non-immunogenic fail to induce CALR exposure, such as etoposide, mitomycin C or cisplatin (CDDP) (Martins et al, 2011; Obeid et al, 2007b). Their immunogenic potential can be restored by combination with agents targeting the endoplasmic reticulum (ER) and consequently activating CALR translocation, like the ER stress inducer thapsigargin or the eIF2 α phosphatase inhibitor salubrinal (Obeid et al, 2007b). Crizotinib (Liu et al, 2019b) and cardiac glycosides (Menger et al, 2012), even though eliciting all the hallmarks of ICD *in vitro*, were efficient ICD inducers only when combined with cytotoxic agents like CDDP or mitomycin C.

Many other agents trigger the ICD-pathognomonic eIF2 α phosphorylation (Bezu et al, 2018a), elicit the exposure and release of certain DAMPs (CALR, ATP, HMGB1, ANXA1), activate some immune cells (DCs, NK, NKT, CD8⁺ T cells), inhibit immunosuppressive cells (Tregs, MDSCs) and/or promote proinflammatory cytokines secretion (typically type I IFNs, IL1- β , IFN γ or IL-6) (**Table 1**). Even if this suggests an immunogenic potential, it is not sufficient to ensure that they *bona fide* induce ICD. Agents that induce a partial immune response may synergize to efficiently trigger an anticancer immune response, like (i) 5-Fluorouracil and cycloheximide, which together are very efficient in reducing the proliferation of the thymoma cell line EL-4, (effect abolished in *nu/nu* mice) (Vincent et al, 2010), (ii) gemcitabine and the hypoxia inducible factor-1 (HIF-1) inhibitor, which can induce vaccination

in pancreatic ductal adenocarcinoma (Zhao et al, 2015), (iii) PX-478 or temozolomide with oncolytic adenovirus, which together could induce long term protection against prostate cancer in mice, accompanied by an activation of CALR exposure as well as ATP and HMGB1 release (effect even amplified by addition of cycloheximide) (Liikanen et al, 2013). In addition, different studies have shown that the synergistic anticancer effect of radiation therapy and chemotherapy relies on an activation of the immune system (Golden et al, 2014; Rubner et al, 2014).

Underlying the potential impact in clinics of these immunogenic chemotherapies, several of them, *e.g* anthracyclines, OXA, bleomycin and cyclophosphamide, are engaged in clinical trials to investigate their immunological effects in patients (Garg et al, 2017a).

Drug	peIF2 α	DAMPs	Immune infiltrate	Vaccination / memory	Effect in ID system	References
ICD inducers						
Anthracyclines (daunorubicin, doxorubicin, epirubicin, idarubicin, mitoxantrone)	Yes	CALR, ATP, HMGB1, ANXA1	↑DCs, CD8 ⁺ , $\gamma\delta$ T 17, IL-1 β , IFN γ ↑IFN1 ↓Tregs, MDSCs	Yes	Abolished (<i>nu/nu</i> mice, CD8 ⁺ , IFN γ , IL-17 or IL-17R depletion)	(Ma et al, 2011; Michaud et al, 2011; Obeid et al, 2007b; Panaretakis et al, 2009; Vacchelli et al, 2015a)
Oxaliplatin	Yes	CALR, ATP, HMGB1	↑DCs, CD8 ⁺ , $\gamma\delta$ T 17, IL-1 β , IFN γ	Yes	Abolished (<i>nu/nu</i> mice, CD8 ⁺ , IFN γ , IL-17 or IL-17R depletion)	(Michaud et al, 2011; Panaretakis et al, 2009; Pietrocola et al, 2016; Tesniere et al, 2010)
Bortezomib	Yes	CALR	↑DCs, CD8 ⁺	Yes	Abolished (<i>nu/nu</i> , <i>Rag</i> ^{-/-} , CD8 ⁺ depletion)	(Cirone et al, 2012; Spisek et al, 2007)
Cyclophosphamide (and its active derivative mafosfamide)	n.d.	CALR, HMGB1, ATP	↑DCs, NK ^{**} , CD8 ⁺ , IFN γ , IL-17, NKT ↑IFN1 ↓MDSCs, Tregs	Yes	n.d.	(Chen et al, 2012; Ghiringhelli et al, 2009; Giampazolias et al, 2017; Schiavoni et al, 2011; Viaud et al, 2011)
Bleomycin	Yes	CALR, ATP, HMGB1	↑CD8 ⁺ , IFN γ ↑Tregs, TGF- β	Yes	Abolished (CD8 ⁺ , IFN γ depletion)	(Bugaut et al, 2013)
Lurbinectedin	Yes	CALR, ATP, HMGB1	↑ IFN1	Partial	Abolished (CD4 ⁺ and CD8 ⁺ depletion)	(Xie et al, 2019a)
Septacidin	n.d.	CALR, ATP, HMGB1	n.d.	Yes	Abolished (<i>nu/nu</i> mice)	(Sukkurwala et al, 2014a)
Wogonin	Yes	CALR, ATP, HMGB1, ANXA1	↑DCs, lymphocytes	Yes	n.d.	(Yang et al, 2012)
Teniposide	n.d.	CALR, HMGB1	↑DCs, CD8 ⁺ , IL-2, IFN γ ↑ IFN1	Yes	n.d.	(Wang et al, 2019)
Bromodomain inhibitor JQ1	Yes	CALR, ATP, HMGB1	↑DCs, CD8 ⁺ ↓MDSCs	Yes	Reduced (<i>nu/nu</i> mice)	(Bauzon et al, 2019; Riganti et al, 2018)
EGFR antibody cetuximab	n.d.	CALR, HMGB1	↑DCs, CD8 ⁺	Yes	n.d.	(Pozzi et al, 2016)
EGFR antibody 7A7	Yes	CALR	↑DCs, CD8 ⁺ , CD4 ⁺ , IFN γ	Yes	Abolished (CD8 ⁺ depletion)	(Garrido et al, 2011)
CDK inhibitor dinaciclib	n.d.	CALR, HMGB1, ATP	↑DCs, CD8 ⁺ , CD4 ⁺ , IFN γ	Yes	Abolished (<i>Rag</i> ^{-/-} mice)	(Hossain et al, 2018)
Oncolytic peptides DTT-205 and DTT-304	n.d.	CALR, HMGB1	↑IFN1	Yes	Abolished (CD8 ⁺ and CD4 ⁺ depletion)	(Zhou et al, 2018)
Oncolytic peptide LTX-315	No	CALR, ATP, HMGB1	↑DCs, macrophages, CD8 ⁺ , Th1 CD4 ⁺ , IL-1 β , IL-6 ↑ IFN1 ↓MDSCs, Tregs	Yes	n.d.	(Camilio et al, 2014; Eike et al, 2015; Yamazaki et al, 2016; Zhou et al, 2016a)
Oncolytic peptide LTX-401	ROS	CALR, ATP, HMGB1,	↑ CD3 ⁺ IFN γ ↑ IFN1	Yes	n.d.	(Eike et al, 2016; Mauseth et al, 2019; Xie et al, 2019b; Zhou et al, 2016b)

Radiotherapy	n.d.	CALR, HMGB1	↑DCs, CD8 ⁺ , γδ T 17, IFN _γ	Yes	Abolished (<i>nu/nu</i> mice)	(Apetoh et al, 2007; Ma et al, 2011; Obeid et al, 2007a)
Photofrin-based PDT	n.d.	CALR, HMGB1	↑monocytes, neutrophils, CD8 ⁺ , NK	Yes	Abolished (CD8 ⁺ depletion)	(Korbelik & Dougherty, 1999; Korbelik et al, 2007; Korbelik et al, 2011; Krosi et al, 1995)
Hypericin-based PDT	No (but PERK and ROS)	CALR, ATP	↑DCs, IL-1β	Yes	n.d.	(Garg et al, 2012a; Garg et al, 2012b)
Redaporfin-based PDT	Yes	CALR, ATP, HMGB1	n.d.	Partial	n.d.	(Gomes-da-Silva et al, 2018)
Microwave thermal ablation	n.d.	CALR, ATP, HMGB1	↑CD8 ⁺ , TNFα, IFN _γ	Yes	Abolished (CD8 ⁺ depletion)	(Yu et al, 2014)
8-methoxypsoralen photochemotherapy	n.d.	CALR, ATP, HMGB1	↑DCs, monocytes CD8 ⁺ , NK ↑IFN1	Yes	Abolished (CD8 ⁺ , CD4 ⁺ , spleen, NK depletion)	(Tatsuno et al, 2019; Ventura et al, 2018)
Electrical nanopulses	n.d.	CALR, ATP, HMGB1	↑CD8 ⁺	Partial	n.d.	(Nuccitelli et al, 2015; Nuccitelli et al, 2017)
UVC light	n.d.	CALR**, HMGB1**	↑DCs, CD8 ⁺ , IFN _γ	Yes	n.d.	(Obeid et al, 2007a; Panaretakis et al, 2009; Schiavoni et al, 2011; Yamamura et al, 2015)
Oncolytic virus T-VEC	n.d.	CALR, ATP, HMGB1	↑CD8 ⁺ T cells IL-1β, TNFα ↑IFN1	Yes	n.d.	(Bommareddy et al, 2019)
Newcastle disease virus	n.d.	CALR, HMGB1 No ATP	↑DCs, CD8 ⁺ , CD4 ⁺ , NK, NKT, IFN _γ ↓MDSCs	Yes	Abolished (<i>Rag2</i> ^{-/-} mice, CD8 ⁺ depletion)	(Koks et al, 2015; Zamarin et al, 2014)
Clostridium difficile toxin B	ROS	CALR, HMGB1, ATP	n.d.	Yes	n.d.	(Sun et al, 2015)
Cardiac glycosides (digitoxin and digoxin)*	n.d.	CALR, ATP, HMGB1	↑ CD8 ⁺ , CD4 ⁺ , γδT 17, IFN _γ	Yes (with CDDP or mitomycin C)	Abolished (<i>nu/nu</i> mice)	(Menger et al, 2012)
Crizotinib*	Yes	CALR, ATP, HMGB1	↑DCs, CD8 ⁺ , NKT, IL-17 ↑ IFN1 ↓Tregs	Yes (with CDDP or mitomycin C)	Abolished (<i>nu/nu</i> mice)	(Liu et al, 2019b)
Agents endowed with immunogenic properties						
Shikonin	n.d.	CALR, HMGB1**	↑DCs, CD8 ⁺ , Th1	Partial (DC vaccine)	n.d.	(Chen et al, 2012; Lin et al, 2015)
Melphalan	No	CALR**, HMGB1 No ATP	↑DCs, monocytes, CD8 ⁺ , CD4 ⁺ , IL-1β, IL-6, IL-8 ↓Tregs	Partial (enhanced with rCALR)	n.d.	(Dudek-Peric et al, 2015; Lu et al, 2015b)
Docetaxel	Yes	CALR	↑DCs, CD8 ⁺ , cytokines	n.d.	n.d.	(Chan & Yang, 2000; Kodumudi et al, 2010;

		No HMGB1, no ATP	↓MDSCs, Tregs			Senovilla et al, 2012; Tanaka et al, 2009a; Wang et al, 2015b)
Paclitaxel	Yes	CALR, HMGB1	↑DCs ↑sensitivity to CTLs ↓Tregs	n.d.	n.d.	(Alagkiozidis et al, 2011; Chan & Yang, 2000; Golden et al, 2014; Senovilla et al, 2012; Tanaka et al, 2009a)
Epothilone B	Yes	CALR	↑IL-1β, IL-12, IL-6 ↑IFN1	n.d.	n.d.	(Pellicciotta et al, 2011; Senovilla et al, 2012)
Vinblastine	Yes	CALR**, HMGB1**	↑DCs	n.d.	Reduced (SCID mice)	(Senovilla et al, 2012; Tanaka et al, 2009a; Tanaka et al, 2009b)
Vincristine	Yes	CALR, ATP, HMGB1	↑DCs	n.d.	n.d.	(Menger et al, 2012; Senovilla et al, 2012; Tanaka et al, 2009a)
Vinorelbine	Yes	CALR	↑DCs	n.d.	n.d.	(Menger et al, 2012; Senovilla et al, 2012; Tanaka et al, 2009a)
Capsaicin	n.d.	CALR, ATP	↑DCs	n.d.	Abolished (<i>nu/nu</i> mice)	(Beltran et al, 2007; D'Eliseo et al, 2013; Gilardini Montani et al, 2015)
5-Fluorouracil	n.d.	CALR**	↑CD8 ⁺ , IFNγ ↓MDSCs	n.d.	n.d.	(Vincent et al, 2010; Yamamura et al, 2015)
Gemcitabin	n.d.	CALR**, HMGB1**, ATP**	↑DCs, CD8 ⁺ , NK**, NKT, IFNγ, IL-17 ↓MDSCs, Tregs**	Partial	Abolished (<i>nu/nu</i> mice)	(Fucikova et al, 2011; Giampazolias et al, 2017; Suzuki et al, 2005; Vincent et al, 2010; Yamamura et al, 2015; Zhao et al, 2015)
Camptothecin	n.d.	CALR **	↑DCs	Partial	n.d.	(Obeid et al, 2007b; Tanaka et al, 2009a)
Carboplatin	n.d.	CALR**, HMGB1** No ATP	↑ DCs, CD8 ⁺ , CD4 ⁺ ,	n.d.	n.d.	(Golden et al, 2014)
Platinum-N-heterocyclic carbene complex	ROS	CALR, ATP, HMGB1	↑DCs	n.d.	n.d.	(Wong et al, 2015)
Vemurafenib	n.d.	CALR	↑DCs	n.d.	n.d.	(Martin et al, 2015)
Coxsackievirus B3	n.d.	CALR, ATP, HMGB1	↑DCs, granulocytes, macrophages, NK	Yes (but in <i>nu/nu</i> mice)	n.d.	(Miyamoto et al, 2012)
Measles virus	n.d.	HMGB1	↑DCs, IFNγ, IL-6, IL-8 ↑IFN1	n.d.	n.d.	(Donnelly et al, 2013)
Adenovirus	n.d.	CALR, HMGB1, ATP	↑DCs, IFNγ, IL-12, TNFα	n.d.	Abolished (<i>nu/nu</i> mice)	(Diaconu et al, 2012; Hemminki et al, 2015)
Vorinostat	n.d.	CALR, ATP, HMGB1	↑B cells, IFNγ	n.d.	Abolished (<i>Rag2γ^{c/-}, IFNγR^{-/-}, IFNγ^{-/-}</i> mice)	(Sonnemann et al, 2010; West et al, 2013)
High hydrostatic pressure	n.d.	CALR, ATP, HMGB1	↑DCs, CD8 ⁺ , IL-6, IL-12	n.d.	n.d.	(Fucikova et al, 2014; Urbanova et al, 2017)
Docosahexaenoic acid	n.d.	CALR, HMGB1	↑DCs	n.d.	n.d.	(D'Eliseo et al, 2017)
Pemetrexed	n.d.	CALR, HMGB1	↑CD8 ⁺	n.d.	n.d.	(Schaer et al, 2019)
CM-272	n.d.	CALR, HMGB1	↑CD8 ⁺ , NK, IFNγ	n.d.	n.d.	(Segovia et al, 2019)

			↑ IFN1			
CY-1-4 NP	n.d.	CALR, HMGB1	↑DCs ↓MDSCs	n.d.	n.d.	(Yang et al, 2019)
KP1339/IT-13	Yes	CALR, ATP, HMGB1	n.d.	n.d.	n.d.	(Wernitznig et al, 2019)
Maytansine-bearing antibody	Yes	CALR, ATP, HMGB1	n.d.	n.d.	n.d.	(Bauzon et al, 2019)
Disulfiram	Yes	CALR	n.d.	n.d.	n.d.	(Majera et al, 2019; You et al, 2019)

Table 1. List of ICD inducers. Immunogenic cell death (ICD) inducers are agents that vaccinate against subsequent injection of tumors of the same type (either by injection of treated dying tumor cells or following complete treatment of transplanted tumors). Agents which delay tumor growth are considered as inducing partial vaccination and are classified as ICD inducers only if they elicit damage-associated molecular pattern (DAMPs) associated with ICD. In the second part of the table are listed agents that activate immune cells and/or act in an immune-dependent fashion in addition to exert at least one hallmark of ICD. *Immunogenic but need to be combined to a cytotoxicant. **Not activated in all the investigated cell lines. ANXA1, annexin A1; ATP, adenosine triphosphate; CALR, calreticulin; CTLs, cytotoxic T lymphocytes; CY-1-4 NP, nano-encapsulated tryptanthrin derivative CY-1-4; DCs, dendritic cells; $\gamma\delta$ T 17, interleukin-17A-producing $\gamma\delta$ T cells; HMGB1, high mobility group box 1; ID, immunodeficient; IFN, interferon; IFN1, type I interferon; KP1339/IT-13, ruthenium complex sodiumtrans-[tetrachloridobis(1H-indazole)-ruthenate(III)]; MDSC, myeloid derived suppressor cells; peIF2 α , eukaryotic initiation factor 2 α phosphorylation; PDT, photodynamic therapy; rCALR, recombinant calreticulin; SCID, severe combined immunodeficiency; Th, helper T cells; Treg, regulatory T cells; T-VEC, talimogene laherparepvec; ROS, reactive oxygen species; n.d. not determined; UVC, ultraviolet C.

3. The anticancer agents dactinomycin inhibits transcription

Dactinomycin (DACT, also known as actinomycin D and called actinomycin C1 in the past) is a 1.26 kDa peptide belonging to the family of actinomycins (**Figure 8**), which are characterized by their two pentapeptide lactones linked to a phenoxazinone dicarboxylic acid and appear as clear yellow liquids. They are produced by different strains of *Streptomyces* bacteria and were first isolated by Selman Waksman and H. Boyd Woodruff in 1940 (Waksman & Woodruff, 1940), with more than 40 actinomycin reported today. The group of Waksman has demonstrated the antibacterial and anticancer effects of DACT, further confirmed by several studies on sarcoma cell lines (Gregory et al, 1956; Reilly et al, 1953). This led to the approval of DACT by the FDA in 1964, constituting the first antibiotic used as an anticancer agent. DACT is commercialized under the name Cosmegen and is mostly obtained by fermentation of *Streptomyces parvullus*, even if it was recently shown that *Streptomyces flavogriseus* also enables to obtain high yield of DACT (Wei et al, 2017). It is currently part of chemotherapeutics combinations for the treatment of pediatric sarcoma: Wilms' tumors, rhabdomyosarcoma, and Ewing's sarcoma, for trophoblastic neoplasia, as well as for some cases of advanced testicular cancers, and is still subject of numerous *in vitro*, *in vivo* and clinical studies. Its anticancer effect is thought to be due to intercalation between the DNA helix leading to transcription inhibition, even though other effects on cells have been enlightened. It is also widely used in laboratories for its ability to inhibit transcription.

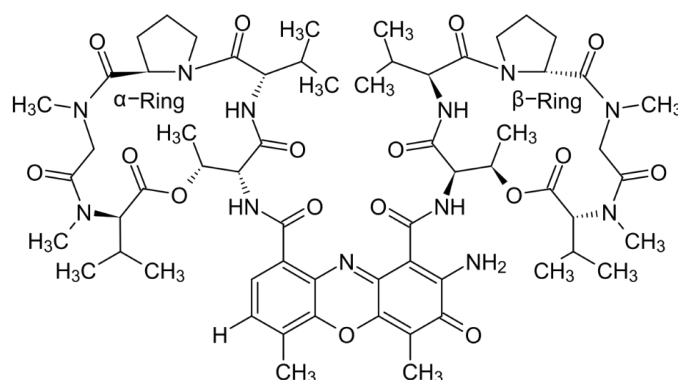


Figure 8. Chemical structure of DACT (Takusagawa et al, 1982). DACT is formed of two cyclic pentapeptide lactone groups (a and b rings), bound to a phenoxazine chromophore (4,6-dimethyl-2-amino-phenoxazinone-3-one-1,9-dicarboxylic acid).

3.1. Transcription and translation in eukaryotic cells

3.1.1. Mechanisms of transcription

Transcription is the synthesis of single stranded RNA from double stranded DNA (dsDNA) in the nucleus of cells, using the template (non-coding) strand. It generates a 5' to 3' pre-RNA molecule, similar to the coding strand apart from thymines which are replaced by uracils. Transcription is catalyzed by RNA polymerases (RNAP). There are three RNAP in the nucleus: RNAPI for 5.8S, 18S and 28S ribosomal RNA (rRNA) synthesis, RNAPII for mRNA and RNAPIII for transfer RNA (tRNA), 5S rRNA and other short RNAs transcription (**Table 2**), in addition to a mitochondrial-specific polymerase. All three nucleic polymerases contain ten common subunits forming the catalytic subunit core, two additional more distant subunits, as well as peripheral subunits for RNAPI and III. While RNAPII and III are located into the nucleoplasm, RNAPI operates within the nucleoli, which are located around tandem repeats of rDNA called nucleolus organizer regions (NOR). rRNA transcription occurs in fibrillar centers, then pre-rRNA is processed in dense fibrillar region involving the proteins fibrillarin and nucleolin and finally the 40S and 60S subunits of the pre-ribosome are assembled into granular components by nucleophosmin (**Figure 9**) (Pombo et al, 1999).

Name	Number of subunits	Molecular weight	Location	Abundance	Product	DACT specificity
RNA polymerase I	14	590 kDa	Nucleolus	50 to 75 %	Large rRNA subunits (28S, 18S, 5.8S)	High
RNA polymerase II	12	500 kDa	Nucleoplasm	5 to 10 %	mRNA, snRNAs, miRNAs	Medium
RNA polymerase III	17	700 kDa	Nucleoplasm	15 %	tRNA, 5S rRNA subunit, U6 snRNA and other short RNAs	Low

Table 2. Eukaryotic nucleic RNA polymerases. rRNA ribosomal RNA; mRNA messenger RNA; miRNA micro RNA; snRNA small nuclear RNA; tRNA transfer RNA.

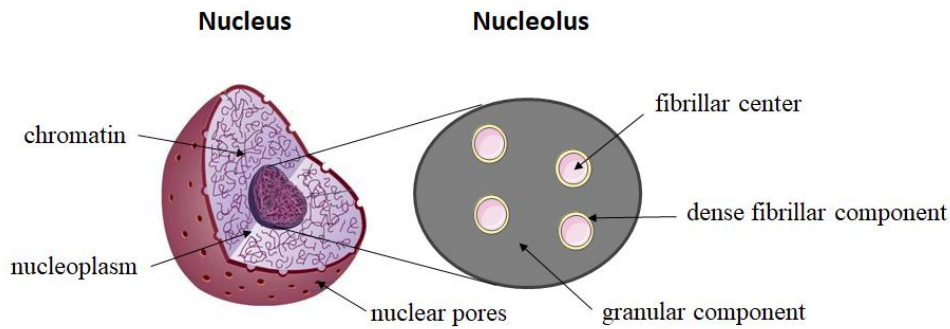


Figure 9. Structure and composition of the nucleus. The nucleus is a double-membraned organelle which contains the DNA and the nucleoli (one or several per nucleus, number which may vary during cell cycle). The nucleolus is the site for rRNA transcription, thanks to fibrillar centers surrounded by dense fibrillar components.

RNAPII serves the transcription of coding genes and has been widely studied since 2000. It is initiated at the core promoter, which typically includes the site of transcription initiation extended by around 35 supplementary downstream or upstream nucleotides. Several sequence motifs are typically found in core promoters such as the TATA box, initiator (Inr), TFIIB recognition element (BRE) and downstream core promoter elements (DPE). Importantly, none of these elements is found in all core promoters. These elements serve to recruit RNAPII as well as its general transcription factors: TFIIA, TFIIB, TFIID (including the core factor (CF) subunit), TFIIE, TFIIIF, and TFIIH. Once DNA is decondensed, helicase separates the two DNA strands, allowing fixation of RNA polymerase and transcription factors on the core promoter region. When the TATA box (located around 25 to 30 base pairs (bp) upstream transcription origin) is present in the core promoter, it forms a pre-initiation complex (PIC) by recruiting different elements in the following order: TFIID, TFIIB, RNAPII-TFIIIF complex, TFIIE and finally TFIIH. BRE serves to recruit TFIIB whereas Inr and DPE are mostly involved in TFIID recruitment (Butler & Kadonaga, 2002; Hahn, 2004). The initiation of RNAPI and III transcription has been only recently studied and is less well understood. The peripheral subunits of RNAPI and III share sequence similarity and location with general TF of RNAPII, with the heterodimer being homologous to TFIIIF and the heterotrimer being homologous to TFIIE, suggesting that during evolution, these polymerases have stably incorporated these enzymes. The PIC of RNAPI is composed of upstream activating factor (UAF), a TATA box binding protein (TBP), the trimeric CF comprising the TFIIB-like factor Rrn7 (TAFAB in human), Rrn6 and Rrn11, as well as Rrn3. The formation of the RNAPIII PIC begins with transcription factors binding to control sequences followed by TFIIB recruitment to the complex. TFIIB is made of a TBP, a TFIIB-related factor (BRF1 or BRF2) and a B-double-prime (BDP) 1 unit (Khatter et al, 2017).

Importantly, the majority of promoters contain CpG islands, regions containing high amounts of CG motifs, which are otherwise underrepresented in the genome due to methylation of the cytosine. In addition to the aforementioned most common motifs, other core promoter sequences have been found to contribute to transcription initiation and probably other remain to be discovered. Cis-regulator elements that are not part of the core promoter are also involved in RNAPII transcription control, such as proximal promoters which are located less than 250 bp far from the transcription start site, enhancers and silencers which can be positioned several kbp far from the start site as well as boundary/insulator elements, which aim at preventing enhancers and silencers to affect neighboring promoters (Butler & Kadonaga, 2002; Hahn, 2004).

Once the initiation complex is in place, abortive initiations may occur releasing short transcripts. Once a transcript reaches ten nucleotides, the polymerase breaks its interaction with the transcription factors, process which requires TFIIF-mediated hydrolysis of ATP, as well as the phosphorylation of a carboxy terminal domain (CTD), a specific domain of RNAPII. This promotes RNA polymerase positioning into the starting site of transcription where elongation begins, at a speed of 10 to 100 nucleotides per second. Addition of ribonucleotides requires, in addition to polymerase, different elongation factors including the positive transcription elongation factor (P-TEFb).

Termination differs for each three polymerases. For RNAPI transcription, several transcription termination sites are located into ribosomal intergenic spacer region. When RNAPI reaches the end of a gene, the 3'-end of the transcript is cut, creating a pre-rRNA molecule that is further processed into the mature 18S, 5.8S and 28S rRNAs. For RNAPII, the cleavage and polyadenylation specificity factor (CPSF) and the cleavage stimulation factor (CSTF) bind the polyadenylation signal AAUAA. This leads to recruitment of other proteins, which promote RNA cleavage and poly-A tail addition in 3', essential mechanism for mRNA stability (to prevent degradation by exonucleases). In addition, pre-mRNA undergoes two other steps of maturation: the addition of 7-methylguanosine cap in 5' which allows recognition by ribosomes for further translation, as well as introns removal by the spliceosome which can lead to varying mRNAs. Once this mature form of mRNA has been synthesized, it can translocate to the cytoplasm for translation. In contrary to both aforementioned termination mechanisms, RNAPIII transcription termination does not require any other transcription factors, but a stretch of thymines (poly-T). This termination signal induces RNAPIII backtrack to the closest RNA hairpin where it forms a "dead-end" complex. As a consequence, RNAPIII opens, leading to the disassembly of the elongation complex.

3.1.2. Mechanisms of translation

3.1.2.1. From mRNA to protein

Translation is the synthesis of a polypeptide from mRNA templates which can occur in the cytosol or across the membrane of the ER. Prior translation, each amino acid is attached by an ester bond at the 3' extremity of the corresponding tRNA by an enzyme called aminocacyl-tRNA synthetase using ATP. There are as many tRNAs and aminocacyl-tRNA synthetases as amino acids. Only selenocysteine differs because directly produced on its tRNA. Once mRNA enters the cytoplasm, it binds a ribosome, a complex made of proteins and rRNA. This organelle is composed of two subunits: 60S (large subunit) and 40S (small subunit) in eukaryotic cells and possess three notable sites: aminoacyl (A) site, peptidyl (P) site and exit (E) site.

Initiation of translation consists in the assembly of both ribosomal subunits with the initiation codon base paired with the anticodon of the methionine charged initiator tRNA (Met-tRNA_i^{Met}) in the P site of the ribosome. This process is catalyzed by eukaryotic initiation factors (eIF), which interact with the 5' cap and the 5' untranslated region (5'UTR) of mRNA molecules. Each eIF plays a particular role. EIF1, 1A and 3 associate with the 40S subunit, they stabilize the PIC and prevent from 60S subunit premature binding. EIF3 interacts with the eIF4F complex, a complex composed of eIF4A, an ATP-dependent RNA helicase that resolves certain secondary structures in the 5' region to prepare ribosome binding, eIF4E, a cap-binding protein which is considered as a rate limiting factor of translation, and eIF4G, a scaffold protein which binds the poly(A)-binding protein (PABP). PABP binds the poly(A) tail of mRNA transcript and is involved in mRNA movement during translation. EIF2 brings the Met-tRNA_i^{Met} to the P site of the 40S ribosome subunit. EIF2 is composed of three subunits, α , β and γ . EIF2 α can be phosphorylated on its serine 51 and thereby constitutes the regulatory subunit; the β subunit is responsible for the interaction with eIF2B as well as with mRNA and tRNA; the γ subunit can also interact with tRNA. EIF2B is a guanine nucleotide exchange factor that initiates translation through GDP hydrolysis by the GTPase activator protein eIF5; thereby it constitutes another translation initiation limiting step (**Figure 10**) (Jackson et al, 2010; Pavitt, 2005). Importantly, the transcription of certain mRNAs has a cap-independent initiation; the most described example of such mechanism is the internal ribosomal entry segment (IRES), in which the ribosome can traffic to the start site without scanning the whole 5'UTR (Lopez-Lastra et al, 2005). The different cap-independent translation initiation mechanisms seem to be strategies that have evolved to ensure the synthesis of proteins involved in cell repair under stress conditions.

Translation initiation starts by the formation of the ternary complex (eIF2-GTP-Met-tRNA_i^{Met}), which associates with the 40S subunit of the ribosome as well as with eIF1, eIF1A, eIF3 and likely eIF5, forming the 43S PIC, which is recruited to the 5' methylguanine cap. Together with eIF4F, they constitute the 48S complex, which scans the 5'UTR in the 5'→3' sense until it finds a start codon (AUG, corresponding to a methionine or eventually a CUG or UUG codons, which are viewed as methionine when initiating translation). This triggers eIF5-mediated conversion of eIF2-GDP into eIF2-GTP, dissociation of several factors from the 40S subunit and binding of the 60S subunit (**Figure 10**) (Jackson et al, 2010).

During elongation, each aminoacyl-tRNAs brings the corresponding amino acid, which involves elongation factor thermo unstable (EF-Tu) and elongation factor 1-alpha 1 (EF-1 α) proteins, that have previously bound to an aminoacyl-tRNA in the cytoplasm and accompany it at the entry of the A site. If the anti-codon of the tRNA is recognized by the mRNA, EF-Tu and eEF-1 α hydrolyze GTP to detach the aminoacyl-tRNA and push it into the A site. This leads to a rapprochement between nascent peptide chain (which is attached via a tRNA to the P site) and aminoacyl at the A site. The peptide chain is catalyzed by ribosome and transferred to the tRNA of the A site which liberates the tRNA of the P site. Then the EF-G and eEF-2 proteins push peptidyl-tRNA from A to P and the free tRNA from P to E where it is released from the ribosome. Elongations factors that hydrolyze GTP translocate the ribosome to the following codon along the mRNA subsequently receiving new aminoacyl-tRNAs. The polypeptide chain is synthesized from the N-terminal to the C-terminal extremity. Once the stop codon is reached (UAA, UGA or UAG), the ribosome detaches from both protein and mRNA. The two subunits of the ribosome are separated and can drive additional translation processes. mRNA can serve as a template for 10 to 20 other proteins translation before being degraded. Newly synthesized protein is released in the cytosols or in the ER where it will undergo post-translational modifications and can be stored for future vesicle transport and secretion.

The newly synthesized protein undergoes covalent modifications, usually mediated by enzymes to be functional. These modifications occur in the ER or in the Golgi apparatus. Of note, some structure modifications like acetylation, folding by chaperones occur during translation and are therefore called co-translation modifications. Phosphorylation is the most common modification. Post-translational modifications can be divided into three main classes: addition of functional groups (methylation, glycosylation which promote protein folding and increase stabilization, lipidation for proteins that aim to be part of membranes etc.), addition of peptide group (ubiquitination, sumoylation etc.), modification of the nature of amino acids or structural changes (formation of disulfide bridges formation between cysteine residues,

proteolytic cleavage etc.). Proteins which are intended to integrate into the plasma membrane or to be secreted, move from the ER to the Golgi apparatus to reach the plasma membrane.

3.1.2.2. ER stress inhibits cap-dependent translation

In eukaryotic cells, the ER is an organelle that serves protein assembly and folding, phospholipids synthesis as well as calcium homeostasis regulation. In response to the accumulation of misfolded/unfolded proteins in the ER lumen as well as in other contexts of stress including immunogenic cell stress (Paragraph 2.4.1.1), eIF2 α is phosphorylated (Figure 6), leading to the formation of a stable eIF2 α P-GDP-eIF2B complex preventing from the conversion of eIF2-GDP into its active form, eIF2-GTP. Cap-dependent initiation is thereby inhibited and allows the reduction of protein load in the ER lumen to protect cells from ER stress-mediated apoptosis (Figure 10).

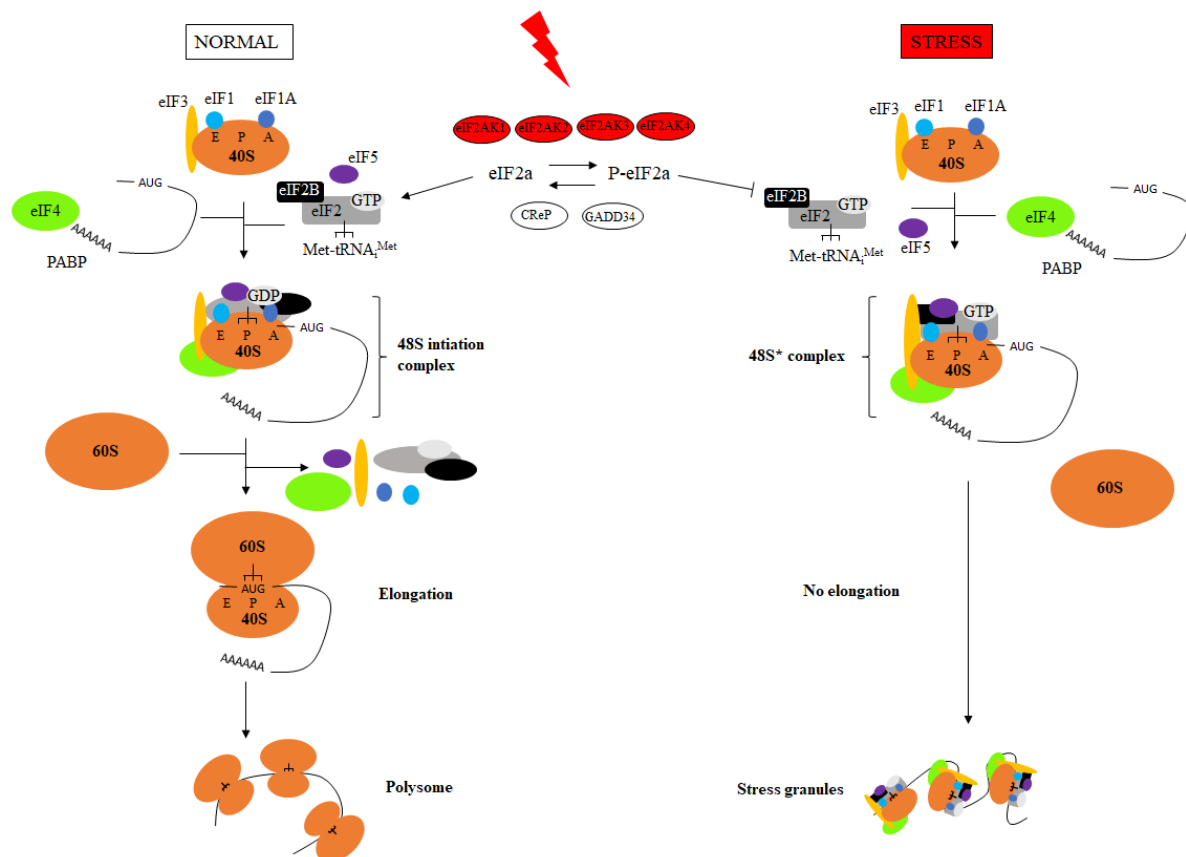


Figure 10. Translation initiation in physiological conditions and upon stress. Under normal conditions, different eukaryotic initiation factors (eIFs) assemble with the 5' untranslated region (5'UTR) region of the messenger RNA (mRNA) and the methionine charged initiator tRNA (Met-tRNA^{Met}) in the P site of the ribosome, forming the 48S initiation complex. After assembly with the 60S subunit, translation can start. Under stress conditions mediated by eIF2 α kinases (eIF2AK), the initiation complex is not functional and 48S* complex bound to mRNA form stress granules. CReP, constitutive repressor of eIF2 alpha phosphorylation; GADD34, growth arrest and DNA damage-inducible protein; GDP, guanine diphosphate; GTP, guanine triphosphate; PABP, poly(A)-binding protein.

Nevertheless, some mRNAs, such as ATF4, are translationally up-regulated in stress conditions, due to a particular configuration of upstream open reading frames (uORFs) in its 5'UTRs: a short uORF1 is followed by a long uORF2 overlapping ATF4 ORF. Thus, whereas high amounts of eIF2-GTP-Met-tRNA_i^{Met} under normal condition allows initiation set up on time for uORF2 after uORF1 translation and thereby prevents from ATF4 translation, low amounts of activated eIF2-GTP-Met-tRNA_i^{Met} during stress is not sufficient for binding the 40S subunit on time for uORF2 but is sufficient for initiating the next start codon, the one of ATF4. Importantly, the integrated stress response inhibitor (ISRIB) reverses the effect of eIF2 α phosphorylation by preventing eIF2B inhibition, without dissociating the subunits from the complex (Wortham & Proud, 2015).

3.1.3. The inhibition of transcription and translation to prevent neoplastic cells proliferation

The proliferation of cancer cells relies on the hyperactivation of oncogenes and the inactivation of tumor suppressor genes. Oncogenes encode growth factors, transcription factors, differentiation factors, surface membrane receptors or proteins involved in reception and transduction of growth signals. Many oncogenes have been discovered until now, such as the transcription factor c-myc which is mutated in nearly all cancers, the GTPase Ras which activate several metabolic pathways in most cancers or the transcription factor friend leukemia integration 1 transcription factor (FLI1) mutated in 80 % of Ewing's sarcoma. Consequently, altering the transcription of these specific genes constitute interesting anticancer strategies, with the successful example of all-trans-retinoid acid (ATRA) which binds promyelocytic leukemia gene-retinoic acid receptor alpha (PML-RAR α) oncogenic transcription factor responsible for acute promyelocytic leukaemia and is part of the first line therapy to treat this type of cancer (Lambert et al, 2018). Nevertheless, very few drugs targeting oncogenes have reached the clinics and this strategy suffers from the need to know the mutational status of each cancer (Bradner et al, 2017).

More generally, cancer cells require a high transcriptional and translational rate to sustain rapid proliferation. Besides, various oncogenes directly or indirectly upregulate transcription, like c-myc which activates RNAPI and III transcription, and many tumor suppressors inhibit transcription, such as pRB or p53. RNAPI transcription seems to be notably important in neoplastic cells. Indeed, rRNA level as well as abnormalities in morphology, quantity and size of nucleoli were shown to be particularly high in all kinds of investigated tumors (Drygin et al,

2010; White, 2008). It was also demonstrated that rRNA level constitutes a reliable prognostic factor in ovarian cancer and rhabdomyosarcoma (White, 2008; Williamson et al, 2006). Cancer cells are by consequence particularly sensitive to the inhibition of RNA synthesis, which appear to be an interesting target for anticancer treatment (Drygin et al, 2010). Even though most chemotherapeutic agents used in clinics for cancers were originally chosen and developed for their capacity to arrest cell cycle and induce apoptosis, it turns out that many of them, in parallel, affect transcription, such as irinotecan, dactinomycin and others.

3.2. Dactinomycin intercalates into the DNA and inhibits transcription

In the 1940's, DACT was isolated and its antibacterial and anticancer activity was discovered (Waksman & Woodruff, 1940). It was further shown that DACT inhibits RNA synthesis without affecting DNA replication in cancer cells (Goldberg, 1962; Reich et al, 1961). Moreover, it was demonstrated with bacterial material that DACT induces immediate arrest of RNA synthesis, followed by the inhibition of DNA synthesis but with a delay and a ten-fold reduced sensitivity (Hurwitz et al, 1962). Accordingly, DACT inhibits the proliferation of DNA viruses but not RNA viruses (Goldberg, 1962). Whereas addition of DNA material could partially enhance RNA synthesis, supplementation with any other material involved in the processes of transcription had no effect, meaning that DACT targets directly DNA (Hurwitz et al, 1962).

DACT behaves both as a DNA intercalator and as a minor groove binding agent. In opposite to most DNA intercalators that have a positive charge, DACT may compensate with a high dipole moment induced by non-symmetrical distribution of polar components. DACT was shown to specifically bind guanine residues belonging to a GpC step, displaying higher specificity to deoxyguanosine than any other nucleotide or nucleoside, and for dsDNA than single strand DNA (ssDNA) (Goldberg et al, 1962; Hurwitz et al, 1962; Reich, 1961). X-ray diffraction and molecular modelling studies have been used to characterize the complex formed by DACT and DNA. The phenoxazone chromophore inserts between the GpC step and hydrogen bonds are formed (i) between the amino group in position N2 of the guanine residue of the GpC step and the carboxyl oxygen of the threonine residue of DACT, (ii) between the ring nitrogen in position N3 of the guanine residue of the complementary strand and the amid group of the threonine residue of DACT, both interactions stabilizing the complex (**Figure 11**). The proline, sarcosine and methylamine residues of the pentapeptide establish hydrophobic interactions with the DNA minor groove leading to further stabilization. Due to the formation

of this very stable complex, DNA adopts a distorted structure, preventing from double helix unwinding and polymerase activity (Chinsky & Turpin, 1978; Kamitori & Takusagawa, 1992). The higher specificity of DACT for transcription inhibition rather than DNA replication inhibition may be explained by the difference of location of the polymerases in the DNA: DNA polymerase moves ahead into the major groove of DNA whereas RNA polymerase proceeds into the minor groove (Cavalieri & Nemchin, 1964). Besides, the distortion of DNA induced by DACT binding prevents another DACT molecule to intercalate closer than six bases away (Gellert et al, 1965; Muller & Crothers, 1968).

The observation that DACT does not bind with the same affinity to all guanine containing sequences suggests that the guanine environment is also important. Binding of DACT to DNA sequences have been intensively studied showing that DACT displays the highest affinity for d(TGCA), then d(CGCG), followed by d(AGCT) and finally d(GGCC) in self-complementary (Chen, 1988), but also non-self-complementary tetranucleotides (Chen, 1992), with a particularly strong affinity for the d(GAAGCTTC) sequence (Kamitori & Takusagawa, 1992). Surprisingly, DACT and the d(CXYGGCCY'X'G) sequence (with X' complementary nucleotide of X and Y' complementary nucleotide of Y) also formed a particularly stable complex despite a very slow association kinetics, properties explained by the involvement of hairpins structures in the formation of this complex (Chen et al, 2003). It was even later demonstrated that binding between DACT and some sequences lacking GpC can also occur, which is strongly sequence dependent (Chen et al, 2004) and that CTG triplets also exert an effect on DACT intercalation (Hou et al, 2002). In parallel, another team showed that DACT also displays affinity for ssDNA, especially for TAGT sites belonging to nucleotides longer than 14 bases (Wadkins et al, 1996). Altogether, these findings demonstrate that the specificity of DACT is highly sequence dependent and does not strictly requires d(GC) as previously believed. Importantly, the non-covalent binding of DACT to DNA is reversible but very slow, with a rate dependent on the DNA sequence involved (Ilan & Quastel, 1966; Muller & Crothers, 1968). In addition, even though transcription is restored after drug removal, abnormal transcription profiles are still observed after 48 h (Schluederberg et al, 1971).

The formation of this DACT-DNA complex interferes with all three eukaryotic RNA polymerases, yet with different sensitivity: class I transcription is inhibited with a half maximal inhibitory concentration (IC₅₀) going from 10 to 100 ng/mL, class II transcription is impaired with an IC₅₀ between 0.1 and 1 µg/mL and class III transcription inhibition occurs with an IC₅₀ from 1 µg/mL and up to 1µg/mL according to the cell lines (**Table 2**) (Bensaude, 2011; Fraschini et al, 2005; Kleeff et al, 2000). From a morphological point of view, low doses of

DACT lead to the dissociation of the fibrillar centers, dense fibrillar components and granular components of the nucleolus, which supports the specificity of DACT for rRNA synthesis inhibition (Boulon et al, 2010).

Of note, even though DACT induces a global decrease in RNA synthesis, it has the capacity to activate some pathways related to apoptosis, necrosis or inflammation, with an increase of the transcription of different caspases, *BIM*, *RIPK1*, genes belonging to the TNF/TNF receptors family and NF- κ B regulated genes (Liu et al, 2016).

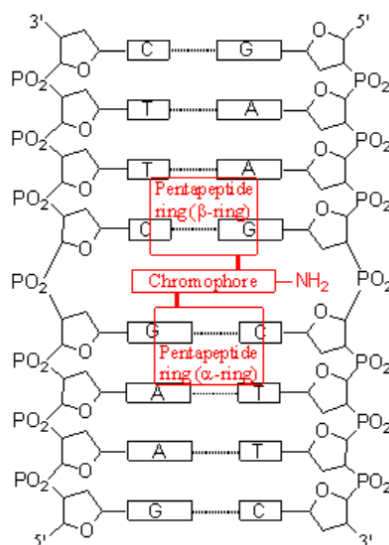


Figure 11. DACT intercalates into the minor groove of DNA (Kamitori & Takusagawa, 1993). The phenoxazone chromophore of DACT inserts between the GpC step and hydrogen bonds are formed between the pentapeptides of DACT and the neighbor guanine residues.

3.3. Other anticancer mechanisms of dactinomycin

3.3.1. Dactinomycin is a topoisomerase inhibitor

In addition to the effect on the activity of polymerases, the complex formed by DACT with DNA prevents the action of topoisomerases. DNA topoisomerases are nuclear enzymes that control the structure of the DNA by generating transitory breaks and further reparations in order to resolve topological problems such as underwinding or overwinding, arising during DNA replication, transcription and certain steps of the cell cycle such as chromatin condensation and chromosomes separation. They are divided into two classes: type I topoisomerases induce single strand breaks and type II topoisomerases induce ATP-dependent double strand breaks. Topoisomerase targeting antitumor drugs, such as DACT, stabilize the interaction between this enzyme and the DNA. The increase in cleavable complexes induces DNA damage leading to an arrest in G2 and if prolonged to apoptosis. DACT was first shown to induces cleavable

complexes with topoisomerases II (D'Arpa & Liu, 1989). It was further shown that it also affects topoisomerase I, which may be important for the high selectivity of DACT for rRNA transcription inhibition, since topoisomerase I is enriched into the nucleoli (D'Arpa & Liu, 1989; Trask & Muller, 1988). It was also demonstrated that no binding occurs at high concentrations of DACT, suggesting the following mechanism: at low concentration, DACT induces cleavable complexes with topoisomerases and abnormal DNA strand breaks. When drug concentration increases, the ratio of double to single strand breaks increases and finally at high concentration, the structure of DNA is modified in such an extent that topoisomerase binding is completely prevented (D'Arpa & Liu, 1989; Wassermann et al, 1990).

3.3.2. Dactinomycin inhibits protein synthesis

The rapid protein decrease, observed at the same time as mRNA synthesis inhibition following DACT treatment, first suggested that this drug also exerts direct effect on protein translation (Goldstein & Penman, 1973; Honig & Rabinovitz, 1965), emphasized by another study that has used cell fragmentation to show that DACT, at an elevated concentration of 5 mg/kg, inhibits protein synthesis independently of transcription inhibition (Revel et al, 1964). However, it was further demonstrated that proteins keep being synthesized in DACT-treated enucleated cells, meaning that the inhibition of translation by DACT is a consequence of the inhibition of transcription and not a direct effect of DACT (Cooper & Braverman, 1977). Numerous studies rather reinforce this view and all things considered, we can state that DACT induces an immediate and complete arrest of rRNA synthesis even at low doses, followed by the inhibition of mRNA synthesis, protein translation and finally DNA replication, with the course and amplitude of these events strongly depending on the dose and timing (Fraschini et al, 2005; Goldstein & Penman, 1973; Hurwitz et al, 1962; Martin et al, 1990b; Schluederberg et al, 1971).

3.3.3. Dactinomycin induces apoptosis

Quickly after DACT was isolated, its cytotoxic effect in tumor cells was already widely demonstrated (Gregory et al, 1956; Reilly et al, 1953), but it is only twenty years later that the kind of cell death induced was investigated and revealed that sarcoma transplanted tumors treated with DACT display phenotypic features of apoptosis (Searle et al, 1975). This has been further confirmed by numerous studies in various cell lines since (Cortes et al, 2016; Kam & Thompson, 2010; Takusagawa et al, 1982).

We can naturally wonder whether apoptosis is a consequence of transcription and/or

translation inhibition. DACT induces transcription inhibition within minutes following treatment, even at very low dose (around 50 ng/mL). At this same dose in HL-60 leukemic cells, DACT also induces apoptosis, but after a delay: first signs of apoptosis can be observed after 5 h and increase with time and/or concentration of drug (Martin et al, 1990a; Martin et al, 1990b). Of note, cycloheximide (the classical inhibitor of translation used in laboratory), even though inducing quicker and almost total translation inhibition as compared to DACT, induces apoptosis in a lower extent, suggesting that protein synthesis inhibition alone cannot explain the induction of apoptosis (Martin et al, 1990b). In the PANC-1 pancreatic cells, apoptosis via the JNK/SAP pathway was induced by DACT in a p53-dependent manner which may directly arise from DNA damage, leading to a higher susceptibility to TRAIL and TNF α (Kleeff et al, 2000). In ECV304 bladder carcinoma, apoptosis was induced at high dose (800 ng/mL) and could be increased by inhibition of the PI3K-PKB-caspase 8 pathway (which promotes cell survival) (Shim et al, 2004), consistent with the finding that inhibition of the PI3K-Akt pathway could enhance DACT-induced apoptosis in human hepatocyte-derived cells HL7702 (Li et al, 2006). Again at high dose (1 μ g/mL, 100 folds higher than the dose needed to inhibit rRNA synthesis), DACT induces apoptosis in HeLa cervix carcinoma (Fraschini et al, 2005). In T leukemic cells, DACT-triggered apoptosis was dependent on the activation of the potassium channel Kv1.3 in latter phases of the cascade (Bock et al, 2002) and can be mediated by the generation of ROS following DACT treatment (Kajiwarra et al, 2001). In osteosarcoma cells, DACT inhibits cell proliferation and induces apoptosis in a dose dependent manner. A potential mechanism linking apoptosis to transcription inhibition is proposed a more recent study: DACT inhibits, among others, cyclins A, D1, E mRNA synthesis, leading to cell cycle arrest and caspase 3 cleavage (Lu et al, 2015a). Another study revealed that, at low doses of DACT, despite the transcription of various genes is impaired, some apoptosis-related genes, like caspases or Bim, or the necroptosis associated gene RIPK2 exhibit a higher transcription level as compared to untreated cells (Liu et al, 2016). Importantly, apoptosis was also activated after DACT treatment in p53^{-/-} neuroblastoma cells (Cortes et al, 2016), in line with experiments performed in leukemia mouse models in which apoptosis was independent of the p53 status of the mice (Merkel et al, 2012) and in myeloid cells that were sensitive to DACT-induced apoptosis whatever p53 status (Li et al, 1998).

As a conclusion, apoptosis may be at least in part induced by the inhibition of transcription, without excluding that some other off-target effects of DACT are involved. The exact pathway leading to apoptosis remain to be elucidated but it appears clear that this kind of cell death is triggered by DACT in a large panel of cancer cell lines, suggesting that DACT is

efficient in other cancer types than sarcoma. In particular, the high sensitivity of neuroblastoma to DACT paves the way for treatment with low dose chemotherapy (and the reduced side effects that go with) (Cortes et al, 2016).

3.3.4. Dactinomycin induces photosensitization

The study of the photodynamic properties of DACT revealed that irradiation of DACT, especially when involved in a complex with ssDNA, induces electron transfer from nucleotides to photo-excited DACT, leading to the generation of active intermediates, first DACT radical anion and then superoxide radical anion, promoting the formation of a DNA base radical cation and DNA damage as a consequence. Among the four mononucleotides, deoxyguanosine mononucleotide is the most powerful electron donor, in agreement with previous finding showing that DACT preferentially binds to deoxyguanoside (Pan et al, 2001).

Moreover, after DACT treatment of HeLa cells, short irradiation leads to almost immediate cells death with a small proportion of the drug binding to hydrophobic proteins, inducing their photo-sensitization (Vekshin, 2011). Importantly, whereas nanomolar amount of DACT is sufficient to inhibit transcription, the generation of superoxide radicals requires much higher concentration (100 to 200 μM) (Avendaño, 2008; Pan et al, 2001). A recent study revealed another pathway through which DACT increases ROS accumulation: it inhibits CD133, a receptor present at the surface of chemotherapy resistant hepatocellular carcinoma, reducing the expression of the cystine/glutamate transporter xCT, which leads to lower glutathione amount, ROS accumulation and finally cell death (Song et al, 2019).

The anticancer activity of DACT could therefore be potentiated by light exposition. The elevation of ROS following DACT exposition may be an explanation for its synergistic effect with radiotherapy (D'Angio et al, 1965; Maddock et al, 1960). In addition, this may bring into consideration the use of DACT in photodynamic therapy or to induce DNA cleavage in a specific and controllable fashion (Pan et al, 2001).

3.3.5. Dactinomycin inhibits respiration and glycolysis

It was shown in leukemic lymphocytes that DACT inhibits transcription, translation, oxidative phosphorylation (respiration) and anaerobic glycolysis in addition to decrease ATP content in cells. Respiration and glycolysis impairment seem to be consequences of RNA synthesis inhibition (due to the timing of events and the impossibility to observe one without the other). Protein synthesis inhibition may be due to both RNA synthesis impairment and ATP decrease.

Of note, whereas puromycin also completely abolishes translation, it does not impair respiration, showing that other mechanisms than protein synthesis inhibition alone must explain blunt respiration (Laszlo et al, 1966). Long term exposure to DACT also inhibits glycolysis required for lymphocytes transformation (Rabinowitz et al, 1968). Moreover, DACT impairs oxidative phosphorylation in cancer cells in a caspase-dependent manner and lead to ATP decrease, although this last event may be explained by supplemental mechanisms (Tao et al, 2006). Of note, it was shown that DACT affects inorganic pyrophosphate exchange reaction with all nucleoside triphosphates (Goldberg et al, 1963), which may also affect intracellular ATP content.

3.3.6. The effect of dactinomycin on the immune system

Soon after DACT isolation, it was shown that DACT administered concomitantly to an antigen induces delayed production of antigen specific antibodies but does not affect their quantity, suggesting that (i) the inhibition of transcription retards but does not impair the efficacy of the immune response and (ii) DACT-treated cells do not stimulate strong B cell-mediated immune signaling (Wust et al, 1964). Since then, the effect of DACT on immune cells has been barely investigated. It has been shown that DACT-treated cells are more sensitive to NK and monocyte-derived cytotoxic factors (Uchida & Klein, 1985), with the fibrosarcoma cell line WEHI 164 being particularly sensitive to TNF-mediated monocyte killing (Austgulen et al, 1986; Bersani et al, 1986). In addition, it has been reported that DACT increases the expression of the early marker of activation CD69 in CD3⁺ T cells, resulting from the activation of intracellular stress pathways (Morgan et al, 1999). Conversely, some studies have revealed that DACT impairs proinflammatory cytokines secretion by macrophages (Kozmar et al, 2010; Perez et al, 2012).

3.4. Pharmacokinetics of dactinomycin

Administration route

For animal experimentation, DACT is usually administered intraperitoneally (*i.p.*) or intravenously (*i.v.*) Since the drug irritates tissues, *i.v.* route is recommended and used in clinics, with recent experimentation investigating the possibility to directly inject it in the limb for melanoma (Kam & Thompson, 2010).

Dosage

DACT was shown to be efficient to treat Ridgway osteosarcoma tumors transplanted in mice at concentrations above 0.4 mg/kg (as a single injection) and is lethal above 1 mg/kg (Schwartz et al, 1965; Schwartz et al, 1966). In patients, the doses vary according to the type of cancer, the combination regimen and the region in the world where the patients are treated. It should also be adapted to the age and weight of the patients (Walsh et al, 2016). Here are some ideas on the doses based on Cosmegen's prescription. To treat Wilms' tumor, childhood rhabdomyosarcoma and Ewing's sarcoma, DACT is combined with other chemotherapeutic agents and its dose should not exceed 15 µg/kg/day or 400 - 600 µg/m² body surface/day *i.v.* for five consecutive days. For testicular cancer, a dose of 1 mg/m² is administered *i.v.* the first day of treatment consisting of a combination regimen with cyclophosphamide, bleomycin, vinblastine, and cisplatin. For gestational trophoblastic neoplasia, 12 µg/kg/day is administered for five days as a single agent, or 500 µg *i.v.* at days 1 and 2 as part of a combination regimen with etoposide, methotrexate, folinic acid, vincristine, cyclophosphamide and cisplatin (Dohme-Chibret, 2004; FDA, 2008).

Metabolization

The drug is minimally metabolized; only one study has reported the presence of monolactone metabolites corresponding to 1 to 4 % of the initial *i.v.* dose (Galbraith & Mellett, 1975; Tattersall et al, 1975).

Distribution and effect on different tissues

Importantly, in spite of its high lipid solubility, DACT does not cross the blood brain barrier, maybe due to its elevated molecular weight, thus it is not present in the central nervous system (Galbraith & Mellett, 1975; Tattersall et al, 1975). DACT is rapidly distributed to nucleated cells of various tissues, with a maximum at 3 h and a quick decrease observed in plasma (Brothman et al, 1982; Veal et al, 2003). The team of Herbert S. Schwartz extensively studied DACT distribution and effects in mice tissues and showed that 30 minutes after *i.v.* injection, high amounts of drug are already present into the small intestine, liver, spleen and salivary gland of mice, followed by transient inhibition of transcription inhibition (Schwartz & Sodergren, 1968; Schwartz et al, 1965). Two models of tumors were shown to differently respond to DACT: while osteosarcoma was highly sensitive to DACT, a transplanted spindle cell carcinoma, which was not prone to DACT accumulation, kept proliferating after treatment

(Schwartz & Sodergren, 1968). It seems that toxicity induced by DACT in tissue is related to the time of exposure to the drug, but the nature of the tissue may also play a role. Indeed, osteosarcoma and intestine crypt cells, which have a high turnover meaning that they are highly dependent on transcription as compared to normal cells of most organs, turned out to be particularly sensitive to DACT (Kessel & Wodinsky, 1968; Schwartz et al, 1968). In addition, osteosarcoma cells undergo a significant RNA decrease following DACT administration (30 to 40 % in 24 h), that may be involved in their notable susceptibility to DACT (Schwartz & Sodergren, 1968). DACT was also reported as being toxic for lymph nodes and bone marrow in mice (Philips et al, 1960; Schwartz et al, 1968; Schwartz et al, 1965).

In patients, DACT was originally shown to be effective in sarcoma cells, with antitumor effects reported in other kinds of tumors since (Cortes et al, 2016; Kam & Thompson, 2010; Takusagawa et al, 1982). One severe adverse effect of chemotherapies including DACT is hepatotoxicity which can manifest through sinusoidal obstructive syndrome (SOS), also called veno-occlusive disease, a disorder that may be lethal due to blockage of the small blood vessels of the liver. It affects particularly young children; hence it constitutes a serious issue since DACT is most used for pediatric cancers. Indeed, SOS following DACT has been reported with an incidence of 2 to 13.5 % (Hill et al, 2014; Vidal; Walsh et al, 2016). DACT is also very irritating to tissues if extravasation occurs. Other classical side effects associated with chemotherapies have been reported like anemia, bone marrow suppression, neutropenia, alopecia, nausea, diarrhea, loss of appetite, renal disorders (FDA, 2008).

By studying the structure and interaction of DACT in the body, one can imagine to design less toxic and more specific analogues. Since the general toxicity, as well as (at least part of) the anticancerous effect of DACT, is a consequence of its DNA binding, the intercalating part of the molecule should not be further modified. Nevertheless, some chemical groups of the pentapeptide could be substituted in order to change the lipophilicity and water solubility which would possibly render the molecule more specific for certain kinds of tissues. Several such agents have been successfully designed for leukemia cells which are effective at concentrations 100 to 500-fold lower than the dose of DACT usually used (Takusagawa et al, 2001).

Excretion

DACT is excreted through bile, urine in faces in dogs (Dipaolo et al, 1957; Galbraith & Mellett, 1975). The first pharmacokinetics study in patients reported a plasma half-life of 36 h with 30 % DACT recovered in faces and urine after 9 days (Tattersall et al, 1975). A study on a large

cohort of children demonstrated that DACT clearance and volume of distribution stand around 5 L/h and 2 L respectively, with much lower values for high body weight (Hill et al, 2014). All in all, DACT, like anthracyclines, has a long half-life and poor excretion rate.

Some proteins, the ATP binding cassette (ABC), including ABCB1, ABCB2, ABCC1 and ABCC2, which are present in the membrane of various epithelial cells (in the intestine, liver, kidney, blood brain barrier, placenta etc.) to expel drugs and toxins, exert high affinity for DACT and have been shown to be involved in its efflux out of cells. Accordingly, overexpression of ABC proteins leads to decreased sensitivity to the drugs while *Abc*^{-/-} mice display higher plasma concentrations of DACT and require more time to eliminate it (Hill et al, 2013). The role of ABCB1 in DACT transport was confirmed in canine kidney cells (Walsh et al, 2016). However, when looking at the impact of ABCB1 polymorphism in a large cohort of patients, no significant effect on DACT-pharmacokinetics was noticed (Hill et al, 2014).

Mechanisms of resistance

Some cells, like mouse spindle cell carcinoma originally induced with 7,12-dimethylbenz[a]anthracene (DMBA), are insensitive to DACT (Schwartz & Sodergren, 1968). The mechanisms of resistance to DACT treatment has been studied in Chinese hamster ovarian cells, leukemia and HeLa cancer cells, showing variations in the membranes of resistant cells leading to lower permeability and consequent decrease in drug uptake, whereas no associated genetic variation was found (Biedler & Riehm, 1970; Bosmann & Kessel, 1970; Goldstein et al, 1966; Juliano & Ling, 1976; Kessel & Wodinsky, 1968). This variation in the composition and conformation of the membrane of resistant cells is due to the presence of glycosidase (Bosmann & Kessel, 1970) and of certain high molecular weight glycoproteins (Juliano & Ling, 1976). Both can alter hydrophobic regions of the plasma membrane and decrease permeability. In particular, the presence of p-glycoprotein (encoded by *ABCB1*) in the membrane of certain cells is involved in resistance to many chemotherapeutics including DACT because it limits their absorption and expulse them out of cells.

3.5. Dactinomycin in the clinic

3.5.1. Cancers treated with dactinomycin-based chemotherapy

DACT is currently used in clinics to treat certain form of sarcoma. It is employed in chemotherapy regimens like the VAC (vincristine, DACT, cyclophosphamide) or VAD (vincristine, DACT, doxorubicin) regimen and/or combined with radiation therapy, due to its

ability to enhance radio sensitivity in tumor cells. It is used both as a neoadjuvant to induce tumor shrinkage before surgery, but also after surgery to eliminate remaining cancer cells (Vidal, Retrieved 2019-08-08). Sarcoma arise from mesenchymal tissues (connective tissues) and are divided into two main categories: bone sarcoma and soft tissues sarcoma. As the name implied, bone sarcoma (including osteosarcoma, rhabdomyosarcoma, Ewing’s tumors etc.) are found in the bones or in the cartilage throughout the body, whereas soft tissue sarcoma often forms in the body muscles, joints, nerves, deep skin tissues, fat and blood vessels. Sarcoma are relatively rare tumors, accounting for only 1 % of adult cancers, but for no less than 15 % of children and teenagers’ cancers, with 12.7 % bone sarcoma and 87.3 % soft tissue sarcoma in total (**Figure 12**) (Blay & Ray-Coquard, 2017; Burningham et al, 2012). At early stages, sarcoma have a relatively good prognostic, but they become aggressive and metastatic in 40 to 50 % of the cases with a survival rate just over 12 months, underlying the need for new therapeutic strategies (Burgess & Tawbi, 2015; Savina et al, 2017). In addition, patients that have been treated with radiotherapy have a higher chance to develop a second sarcoma, probability which increases with the accumulation of radiation in the bones (Burningham et al, 2012).

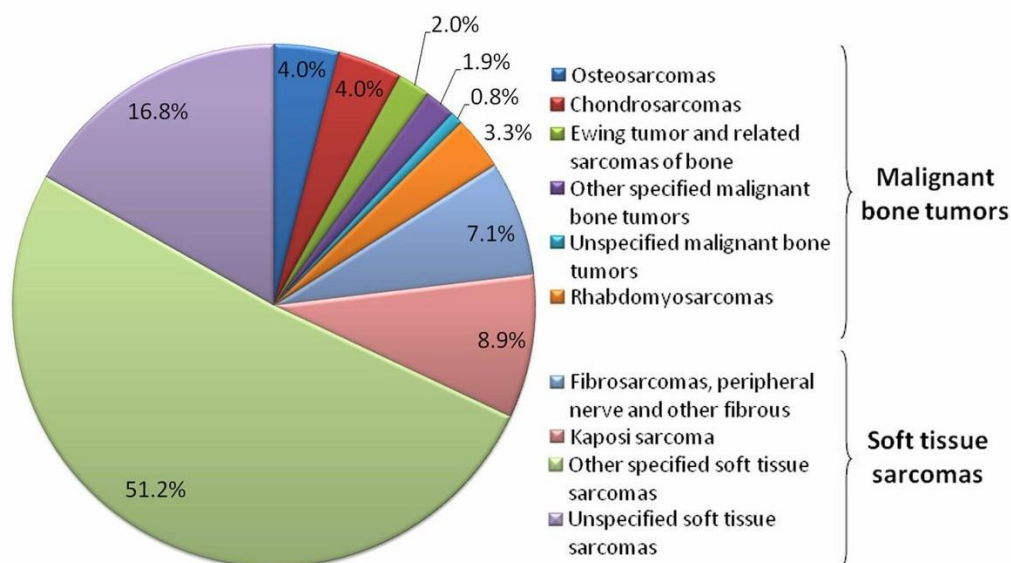


Figure 12. Prevalence of sarcoma in 2008 (Burningham et al, 2012). Sarcoma are divided into two main categories, bone sarcoma and soft tissue sarcoma, each of them divided in several subclasses.

DACT is recommended for the treatment of the following cancers:

Nephroblastoma, also called Wilms tumor is a kidney tumor that typically affects children under 15 (7.1 cases per million), rarely adults (0.2 cases per million). It represents more than 90 % of kidney cancers in children and 5 to 14 % of all cancers in children. Often due a limited number of mutations (in Wilms tumor (*WT1*), *WTX* or *CTNNB1* genes in one-

third of cases) in the embryonic tissue that gives rise to kidney, it manifests as an intra-abdominal mass. It is very responsive to treatments with a five-year survival rate around 90 %. The general protocol in Europe follows the International Society of Pediatric Oncology (SIOP) recommendations which consist in neoadjuvant and post-surgery chemotherapies combining DACT and vincristine, eventually supplemented with doxorubicin, etoposide, cyclophosphamide and/or radiation therapy (NCI, Retrieved 2019-08-08e).

Rhabdomyosarcoma is a tumor of striated skeletal muscles. It is an aggressive and metastatic form of sarcoma accounting for 3.5 % cancers among children, with 4.5 cases per million children. Although the cause is not known, different inherited diseases, like Li-Fraumeni syndrome, have been associated with rhabdomyosarcoma. This tumor can develop at any site but primarily occurs in the neck, head, genitourinary tract, genitals and extremities where it manifests as a lump or swelling that keeps enlarging. The five-years overall survival is around 70 % for children younger than 15 and of 50 % for teenagers between 15 and 19 years old. Treatments depend on the site of the tumor, but currently rely on surgery, radiation therapy and DACT- and vincristine-based chemotherapy (NCI, Retrieved 2019-08-08a).

Ewing's sarcoma arises from bone or soft tissue and are usually observed in legs, pelvis or chest wall. Whereas it touches only one person per million globally, it affects around 10 children between 10 and 19 years old per million, accounting for 2 % of pediatric cancers. The mechanisms of Ewing's sarcoma are well described: a translocation which fuses Ewing sarcoma breakpoint region 1 (*EWSR1*) gene on chromosome 22 to the *FLII* gene on chromosome 11 is found in more than 85 % of the cases, the *EWSR1* gene has also been reported to fuse with erythroblast transformation-specific related gene (*ERG*) in around 10 % of the cases and more rarely with ETS translocation variant (*ETV*) 1 or *ETV4*. These translocations lead to a continuous activation of the membrane receptor insulin-like growth factor-1 (IGF-1) responsible for cell proliferation and constitute key features for diagnosis of Ewing's sarcoma. Five-years survival is around 80 % for children under 15 and of 60 % for teenagers between 15 and 19. When this cancer is diagnosed, it has already spread to other parts of the body in 25 % of cases, therefore it requires highly aggressive treatments. They usually consist in neoadjuvant chemotherapy, followed by surgery and/or irradiation and by several other cycles of chemotherapy, based on combination of vincristine, DACT, doxorubicin, cyclophosphamide, ifosfamide and etoposide (NCI, Retrieved 2019-08-08b).

Gestational trophoblastic diseases are rare pregnancy-related tumors arising from trophoblastic tissue which forms the placenta. It includes the benign tumor hydatidiform moles as well as four malignant kinds of tumors: invasive mole, choriocarcinoma, placental site

trophoblastic tumors and epithelioid trophoblastic tumors. The incidence is very variable among countries with only 23 cases over 100,000 pregnancies reported in Paraguay whereas 1,299 cases per 100,000 were reported in Indonesia. The maternal age and the history of hydatidiform mole constitute the main risk factor, with vaginal bleeding and rapidly enlarging uterus as main symptoms. The prognosis for gestational trophoblastic diseases is very favorable, even when the disease has invaded other organs. Thus, only when the tumor is malignant and considered as high risk, it is treated with methotrexate- and DACT-based chemotherapy, eventually supplemented with etoposide, folinic acid, cyclophosphamide and vincristine (NCI, Retrieved 2019-08-08c).

Testicular carcinoma develops in the testicles of young- and middle-aged men, arising from germ cells in most of the cases. The five-year survival rate is above 90 % after treatment. Testicular cancers are divided in seminoma and nonseminoma, leading to different treatment strategies. Indeed, seminomas are more sensitive to radiation therapy and chemotherapy, in addition to be less prone to form metastasis, whereas nonseminomas often require surgery for cure. Thus, nonseminoma cancers are usually removed by surgery followed by radiation therapy and combination of chemotherapies including DACT at advanced stages of the disease (NCI, Retrieved 2019-08-08d).

3.5.2. Clinical trials involving dactinomycin

There are around fifty phase I, II, III, IV and pharmacokinetics clinical trials involving DACT. Most of them apply to childhood sarcoma (kidney cancer, rhabdomyosarcoma, Ewing's sarcoma) and gestational trophoblastic diseases, three in melanoma and a few in other types of cancers, like leukemia or germ cell tumors (**Table 3**). Its use for carcinomas is very little investigated in clinical trials. The effect of DACT is mostly evaluated in combination with other chemotherapies, as well as with radiation therapy. It is usually used *i.v.* but its administration by limb infusion for melanoma is investigated, in order to have a local and more specific effect of the chemotherapy (NCT00004250, NCT00004250, NCT01323517). One particularly interesting phase II clinical trial (NCT01323517) demonstrates that the combination between DACT and melphalan administered by limb infusions together with the systemic injection of the anti-CTLA-4 Ipilimumab could improve the response rate of patients. This was further investigated in mice, showing that this antitumor effect is accompanied by the elicitation of an immune response involving IFN γ , NK cells and perforin (Ariyan et al, 2018).

Indication	Phase	Status	Reference	Notes
Advanced melanoma of the extremity	II	Completed	NCT01323517	Combined with Ipilimumab and Melphalan Limb Infusion (for chemotherapies)
Gestational trophoblastic tumor	III	Completed	NCT00003702	Methotrexate compared to DACT Result: DACT more efficient
Various pediatric cancers (leukemia, sarcoma etc.)	NA	Completed	NCT00674193	Combined with vincristine Pharmacokinetics study
Gestational trophoblastic tumor	II	Completed	NCT00003688	Alone
Gestational trophoblastic tumor	III	Active, not recruiting	NCT01535053	Methotrexate compared to DACT
Rhabdomyosarcoma, nephroblastoma	IV	Unknown	NCT00491946	Combined with vincristine
Rhabdomyosarcoma	III	Unknown	NCT00075582	Benefit of radiation therapy to VAC regimen
Unspecified childhood solid tumor	NA	Unknown	NCT00900354	Alone Pharmacokinetics study
Stage IV nephroblastoma	III	Not yet recruiting	NCT03669783	Comparison between VCE and VAD
Rhabdomyosarcoma, soft tissue sarcoma	III	Completed	NCT00354835	Benefit of irinotecan and radiotherapy to VAC regimen
Sarcoma	II	Unknown	NCT00245089	Benefit of radiation therapy to VAC regimen
Nephroblastoma	III	Completed	NCT00352534	Benefit of radiation therapy to VAD regimen
Sarcoma	II	Unknown	NCT00245141	Benefit of radiation therapy to VAC regimen
Melanoma	I&II	Withdrawn	NCT01531244	Benefit of gene therapy to melphalan and DACT Isolated limb infusion
Rhabdomyosarcoma	III	Recruiting	NCT02567435	Alternance between VAC and VI with or without temsirolimus
Gestational trophoblastic disease	III	Active, not recruiting	NCT01823315	Methotrexate multidose compared to methotrexate and DACT
Gestational trophoblastic tumor	II&III	Recruiting	NCT03885388	Combined with methotrexate
Ewing's Sarcoma	II	Unknown	NCT00541411	Combined with vincristine, adriamycin, ifosfamide
Rhabdomyosarcoma, soft tissue sarcoma	III	Completed	NCT00003958	Comparison between VAC and vincristine, topotecan, cyclophosphamide
Melanoma, sarcoma	II	Completed	NCT00004250	Combined with melphalan Limb Infusion
Rhabdomyosarcoma	II	Recruiting	NCT01871766	Benefit of radiation therapy to VAC regimen
Sarcoma	III	Completed	NCT00354744	High dose chemotherapeutics combined with radiation
Nephroblastoma	IV	Not yet recruiting	NCT03892330	Benefit of anthracyclines to VAC regimen
Brain cancer, choroid plexus tumor	III	Suspended	NCT01014767	Different combinations chemotherapeutics
Sarcoma	III	Completed	NCT00002995	Benefit of radiation therapy to VAC regimen
Germ cell tumor	II	Recruiting	NCT01782339	Combined with paclitaxel, methotrexate, oxaliplatin, pegfilgrastim
Pleuropulmonary blastoma	NA	Active, not recruiting	NCT01464606	Comparison between VAC and IVADO
Kidney cancer	III	Unknown	NCT00003804	Combined with vincristine
Kidney cancer	III	Active, not recruiting	NCT00945009	Combined with vincristine and eventually doxorubicin
Ewing's sarcoma	III	Active, not recruiting	NCT02063022	Intensified chemotherapeutics treatment compared to classical one
Kidney cancer	III	Completed	NCT00002610	VAD regimen combined with radiation therapy and peripheral stem cell or bone marrow transplantation

Rhabdomyosarcoma, soft tissue sarcoma	II	Completed	NCT01055314	Cixutumumab IV, temozolomide combined with chemotherapeutics and radiation therapy
Childhood central nervous system tumor	II	Completed	NCT00084838	Benefit of radiation to chemotherapeutics combinations
Fibrosarcoma	II	Terminated	NCT00072280	Combination of different chemotherapeutics and surgery
Gestational trophoblastic disease	III	Recruiting	NCT02639650	Comparison between paclitaxel and cisplatin with EMA-CO
Renal cell cancer	II	Completed	NCT00335556	VAC regimen
Sarcoma	III	Unknown	NCT00020566	Different combinations based on VAI and VIDE
Rhabdomyosarcoma, soft tissue sarcoma	III	Terminated	NCT00162695	Combined with ifosfamide, oncovin, epirubicine, carboplatin, etoposide
Nephroblastoma	III	Completed	NCT00002611	Combined with filgrastim, pegfilgrastim, sargramostim, cyclophosphamide, irinotecan, vincristine, radiation therapy
Urothelial/bladder cancers	II	Recruiting	NCT02788201	COXEN algorithm used to determine the next best therapy from among 75 FDA approved agents
Nephroblastoma	III	Completed	NCT00379340	Different combinations of chemotherapeutics with radiation therapy
Sarcoma	II	Completed	NCT00003955	Benefit of radiation therapy to combination of chemotherapeutics
Sarcoma	III	Unknown	NCT00379457	Different combinations of chemotherapeutics with radiation therapy
Germ cell tumor, ovarian cancer	II	Completed	NCT00002489	Different combinations of chemotherapeutics
Nephroblastoma	III	Unknown	NCT00002516	Different combinations of chemotherapeutics with radiation therapy
Nephroblastoma	III	Unknown	NCT00047138	Different combinations of chemotherapeutics with radiation therapy
Ovarian cancer, sarcoma, small intestine cancer	II	Completed	NCT00025441	Different combinations of chemotherapeutics with radiation therapy and peripheral blood stem cell transplantation
Kidney cancer	II	Unknown	NCT00025103	Different combinations of chemotherapeutics with radiation therapy and peripheral blood stem cell transplantation
Childhood bone malignant fibrous histiocytoma, sarcoma	III	Completed	NCT00002898	Different combinations of chemotherapeutics with radiation therapy
Leukemia, lymphoma	III	Completed	NCT00002766	Different combinations of chemotherapeutics with radiation therapy
Many kinds of cancers	NA	Recruiting	NCT03382158	Different combinations with vincristine, cyclophosphamide, ifosfamide, doxorubicin
Upper tract urothelial carcinoma	II	Recruiting	NCT02969083	VAC regimen, combined with gemcitabine and cisplatin

Table 3. List of clinical trials involving DACT. EMA-CO etoposide, methoxetrate, DACT, cyclophosphamide, vincristine; IVADo ifosphamide, vincristine, DACT, doxorubicin; VAC vincristine, DACT, cyclophosphamide; VAD vincrisitne, DACT, doxorubicin; VAI vincristine, DACT, ifosfamide; VCE vincristine, carboplatin, etoposide; VI vincristine, irinotecan; VIDE vincristine, ifosfamide, doxorubicin, etoposide (clinicaltrials.gov, Retrieved 2019-08-10).

Aim of the work

1) Discovery of new ICD inducers

Based on the consideration, now widely demonstrated, that cancer progression does not merely depend on self-mutations but is also driven by its environment, a new question arose: may certain conventional therapies affect the immune system? It turns out that anthracycline-based chemotherapies, radiotherapy but also some targeted therapies are particularly efficient in inducing an anticancer immune response, allowing the elimination of cancer cells that were not killed through the direct cytotoxic effect of the treatment and conferring long term protection. This important finding should lead, besides the development of new molecules, to the investigation of the immunogenic potential of approved therapies in order to design, based on the existing options, new combination strategies which may increase antitumor efficacy while limiting adverse effects (Galluzzi et al, 2015b).

Using a machine learning approach, we recently built an algorithm, which can predict the capacity of agents, based on their physical and chemical properties, to induce ICD (Bezu et al, 2018a). With the leitmotiv to discover ICD inducers among anticancer agents that have already been submitted to clinical trials, we have used this informatic model to screen the National Cancer Institute (NCI) library. Agents that displayed a high theoretical ICD score were further investigated *in vitro* and *in vivo* in order to confirm their immunogenicity. Importantly, several ICD inducers, such as cyclophosphamide and crizotinib, synergize with subsequent immune checkpoint blockade (Liu et al, 2019b; Pfirschke et al, 2016), combination which may be interesting to explore with other identified ICD inducers.

2) Further elucidation of the mechanisms of ICD

Even though ever more details of the mechanisms underlying ICD are unraveled, with the most recent mechanistic discoveries being (i) the role of ANXA1, which is released in the course of ICD and activate DCs through interaction with FPR1 (Vacchelli et al, 2015a) in addition to be required for exposure of CALR at the plasma membrane (Baracco et al, 2019) and (ii) the split ER stress response induced by anthracyclines and OXA (Bezu et al, 2018a; Giglio et al, 2018), the mere combination of all known hallmarks is not sufficient to account for immune system activation and the rules governing ICD induction at the cellular and molecular levels are not fully understood yet (Galluzzi et al, 2017). Thus, it appears of the highest importance to keep investigating in that field in order to further facilitate the identification of novel and effective

anticancer treatments, as well as to design judicious treatment combination and to adapt the strategy of anticancer therapy to the profile of patients.

Material and methods

Cell lines. Human osteosarcoma U2OS cells stably expressing HMGB1-GFP together with H2B-RFP; CALR-GFP together with H2B-RFP; GFP-LC3; RFP-LC3; ATF4 reporter; XBP1 Δ DBD-venus, U2OS cells co-expressing ss-SBP-GFP and Str-KDEL or HT29 MX1-GFP (in which GFP is under the control of the MX1 promoter) were generated by our group in the past (Bezu et al, 2018a; Shen et al, 2012; Zhao et al, 2018; Zhou et al, 2016a). U2OS cells stably expressing GFP-ATF6 were obtained from Prof. Peter Walter (University of California, San Francisco, USA). U2OS cells stably expressing RFP-LC3 bearing a mutant non phosphorylatable version of eIF2 α (eIF2 α .S51A) were constructed using the CRISPR-Cas9 technology. We designed two complementary gRNAs (**Table S 1**) and inserted them into the pX458 vector (containing a tracrRNA and Cas9 fused with 2A-GFP) (Ran et al, 2013) following the manufacturer's protocol (New England Biolabs, Ipswich, Massachusetts, USA). We then used this plasmid together with a homology repair template that targets the serine in position 51 of eIF2 α for an exchange to alanine (**Figure S 1**), to transfect RFP-LC3 expressing U2OS cells with Lipofectamin 2000 (Thermo Fisher scientific, Waltham, MA, US) according to the manufacturer's protocol. Two days later, single cells were sorted by flow cytometry. DNA of clones which grew was extracted, amplified by PCR and analyzed for homozygous knock-in by sequencing (Eurofins Scientific, Luxembourg) (**Table S 1**). U2OS GFP-LC3 having one eIF2 α kinase knocked out (EIF2AK1^{-/-}, EIF2AK2^{-/-}, EIF2AK3^{-/-} and EIF2AK4^{-/-}) were constructed using a U6gRNA-Cas9-2A-RFP plasmid containing gRNAs (Sigma-Aldrich, St. Louis, MO, USA) (**Table S 1**) following the manufacturer's protocol. In short, U2OS GFP-LC3 cells were transfected and two days later, single cells were sorted by flow cytometry. Clones were validated by immunoblot with specific antibodies against human HRI, PKR, PERK and GCN2.

Cell Culture. Human osteosarcoma U2OS cells, mouse fibrosarcoma MCA205 cells, human colon adenocarcinoma HT29 cells and murine lung cancer TC-1 cells were cultured in Dulbecco's modified Eagle's medium (Thermo Fisher Scientific) and mouse fibrosarcoma WEHI 164 cells were cultured in Roswell Park Memorial Institute (RPMI) 1640 medium (ATCC), both supplemented with 10 % fetal bovine serum (Gibco by Life Technologies), 1 % non-essential amino acids (Thermo Fisher Scientific), 1 % HEPES (Thermo Fisher Scientific) in a humidified incubator with 5 % CO₂ at 37 °C. For U2OS cells co-expressing ss-SBP-GFP

and Str-KDEL, 0.25 mg/mL hygromycin and 0.5 mg/mL G418 were added to the culture medium. For U2OS co-expressing HMGB1-GFP and H2B-RFP, 5 µg/mL blasticidin and 0.5 mg/mL G418 were added to the culture medium. For U2OS MX1-GFP, culture medium was supplemented with 2 µg/mL puromycin. Cell culture plastics and consumables were purchased from Greiner Bio-One (Kremsmünster, Austria).

Antibodies. Rabbit polyclonal antibodies against CALR (ab2907), rabbit monoclonal phosphoepitope-specific antibody against phospho-eIF2 α (Ser51) (ab32157), rabbit polyclonal antibody against fibrillarin (ab5821), mouse monoclonal antibody against nucleolin (ab13541) and mouse monoclonal antibody against β -actin (ab49900) were purchased from Abcam (Cambridge, UK). Rabbit polyclonal antibody against HRI (sc-30143) and mouse monoclonal antibody against PKR (sc-6282) were purchased from Santa Cruz biotechnology (Dallas, TX, USA). Rabbit monoclonal antibody against PERK (#3192), rabbit polyclonal antibody against GCN2 (#3302) and rabbit polyclonal antibody against LC3B (#2775) came from Cell Signaling Technology (Danvers, MA, USA). Anti-PD-1 (BE0273) and a corresponding isotype, a rat IgG2a against trinitrophenol (BE0089), were purchased from BioXcell (West Lebanon, NH, USA). Anti-rabbit and anti-mouse AlexaFluor-488, -568 and -647 secondary antibodies came from Thermo Fisher scientific. Conjugated antibodies for flowcytometric analysis were purchased from BD Pharmingen (Franklin Lakes, NJ, USA), Biologend (San Diego, CA, USA) or Myltenyi Biotec (Bergisch Gladbach, Germany).

ICD prediction. The GI₅₀ (dose for which 50 % of cell growth is inhibited) for a panel of 52,578 compounds (identified via their NSC number) tested on 60 different cell lines was retrieved from the National Cancer Institute website (https://dtp.cancer.gov/databases_tools/bulk_data.htm). From these 52,578 compounds, 49,419 were found to possess a valid PubChem CID (Compound ID number) using the PubChem identifier exchange service (<https://pubchem.ncbi.nlm.nih.gov/idexchange/idexchange.cgi>). The related structure data file (sdf) for each CID was obtained from pubchem and the ICD prediction scores were calculated using the *ICDPred* R package available at <https://github.com/kroemerlab/ICDPred>. Mitoxantrone was used as a reference to select potential ICD inducers.

Compounds. A custom arrayed anticancer library was used (Bezu et al, 2018a). Bortezomib

(5043140001), cisplatin (C2210000); crizotinib (PZ0191); dactinomycin (A1410); daunorubicin (D0125000); docetaxel (01885); doxorubicin (D1515); epirubicin (E9406); flavopiridol (F30055); ISRIB (SML0843); β -lapachone (L2037); mitoxantrone (M6545); mycophenolate mofetil (SML0284); nonoxynol-9 (542334); paclitaxel (T7191); thapsigargin (T9033); tunicamycin (T7765); vinblastine sulfate (V1377); vincristine sulfate (V0400000) have been bought from Sigma-Aldrich. Dactolisib (BEZ235) (sc-364429) came from Santa Cruz. Oxaliplatin came from Accord Healthcare (Ahmedabad, India). Topotecan (609699), 7-hydroxystaurosporine (UCN-01) (72271), becatecarin (101524), 5-Fluorodeoxycytidine (B86) (515328) and RH-1 (394347) were kindly provided by the National Cancer Institute (NCI). Lurbinectedin (PM01183) came from PharmaMar (Madrid, Spain).

Fluorescence microscopy, image acquisition and analysis. One day before treatment, 2500 U2OS cells either wild-type or stably expressing ATF6-GFP, ATF4-GFP, XBP1 Δ DBD-venus or LC3-GFP were seeded in 384 well μ Clear imaging plates (Greiner BioOne) and let adhere. The next day, cells were treated 6, 12 and 24 h to assess ATP decrease, 6 h to look at eIF2 α phosphorylation (peIF2 α) and ATF6 or 12 h to assess ATF4 and spliced XBP1 (XBP1s) levels. Following, cells were fixed with 3.7 % formaldehyde (F8775, Sigma Aldrich) supplemented with 1 μ g/ml Hoechst 33342 for 1 h at room temperature. For ATF6, ATF4 and XBP1s, the fixative was exchanged to PBS and the plates were analyzed by automated microscopy. EIF2 α phosphorylation was assessed by immunostaining: to this aim, cells were treated and fixed as described above in the presence of Hoechst 33342. Then unspecific antibody interaction was blocked by 2 % BSA for 1 h at room temperature and followed by an incubation with primary antibody overnight at 4 °C. After several washing steps with PBS, cells were stained with AlexaFluor-568-coupled secondary antibody (Thermo Fisher scientific) for 2 h at room temperature and washed with PBS before acquisition. For the detection of ATP enriched vesicles, the cells were labeled after treatment with the fluorescent dye quinacrine as described before (Martins et al, 2011). Briefly, cells were incubated with 5 μ M quinacrine and 1 μ g/ml Hoechst 33342 in Krebs-Ringer solution (125 mM NaCl, 5 mM KCl, 1 mM MgSO₄, 0,7 mM KH₂PO₄, 2 mM CaCl₂, 6 mM glucose and 25 mM HEPES, pH 7.4) for 30 min at 37 °C. Thereafter, cells were rinsed with Krebs-Ringer and viable cells were microscopically examined. For automated fluorescence microscopy, a robot-assisted Molecular Devices IXM XL BioImager and a Molecular Devices IXM-C (Molecular Devices, Sunnyvale, CA, USA) equipped with either a SpectraX or an Aura II light source (Lumencor, Beaverton, OR, USA),

adequate excitation and emission filters (Semrock, Rochester, NY, USA) and a 16-bit monochromes sCMOS PCO.edge 5.5 camera (PCO Kelheim, Germany) or an Andor Zyla camera (Belfast, Northern Ireland) and a 20X PlanAPO objective (Nikon, Tokyo, Japan) were used to acquire a minimum of four view fields per well, followed by automated image processing with the custom module editor within the MetaXpress software (Molecular Devices). Image segmentation was performed using the MetaXpress software (Molecular Devices). The primary region of interest (ROI) was defined by a polygon mask around the nucleus allowing for the enumeration of cells, the detection of morphological alterations of the nucleus and nuclear fluorescence intensity. Secondary cytoplasmic ROIs were used for the quantification of quinacrine, peIF2 α , XBP1s ATF6 and LC3. After exclusion of cellular debris and dead cells from the data set, parameters of interest were normalized, statistically evaluated and graphically depicted by the freely available software R (<https://www.r-project.org>). Using R, images were extracted and pixel intensities scaled to be visible (in the same extent for all images of a given experiment). Scale bars represent 20 μm , except for microphotographs of tissue (**Fig. 3K, M**) where it represents 10 μm .

CALR translocation and HMGB1 release by video microscopy. One day before treatment, 2,500 U2OS cells stably co-expressing either CALR-GFP or HMGB1-GFP with H2B-RFP per well were seeded in 384 well μClear imaging plates (Greiner BioOne) and let adhere. The next day, cells were treated and CALR-GFP and HMGB1-GFP cells were observed by live cell microscopy as described before with a frequency of image acquisition at one image per hour for 12 and 24 h, respectively. The images were segmented and analyzed with R using the *EImage* and *flowcatchR* packages from the Bioconductor repository (<https://www.bioconductor.org>). H2B-RFP was used to segment nuclei; the obtained mask was either used to measure GFP intensity in the nuclear compartment (HMGB1-GFP), or as a seed to segment the cytoplasmic compartment (CALR-GFP). Then a top-hat filter was applied and the area of CALR-GFP^{high} regions was measured. HMGB1-GFP nuclear fluorescence intensity of single cells tracked over time was normalized to its value at first time point.

Determination of IC₆₀. U2OS wild-type cells were seeded at 8000 cells per well in 96 well μClear imaging plates (Greiner Bio-One) and let adhere for 24 h before treatment. Cells were treated with a large range of concentrations for 24 h and then stained by the addition of propidium iodide at a final concentration of 1 $\mu\text{g/mL}$ and Hoechst 33342 at 2 $\mu\text{g/mL}$ for 30

min. Plates were centrifuged in order to bring detached cells to the focal plane and following, images were acquired by automated microscopy using adequate filter sets as described above. The images were segmented with R by means of the *EImage* package. Nuclei were segmented based on Hoechst 33342 signal, then nuclear area and fluorescence intensities (in DAPI and Cy3) were measured. The assessed parameters were used to cluster cells as healthy (normalized, Hoechst^{low}, PI⁻), pyknotic (condensed, Hoechst^{high}, PI⁻), or dead (PI⁺). The number of healthy cells was then used to establish dose-response models, by fitting the data points with a 4-parameter log-logistic model. The model was then used to calculate the IC₆₀ (concentration for which 40 % of cell population is healthy) for each drug.

MX1 pathway activation. This technique was previously developed in our laboratory (Zhou et al, 2016a). U2OS or MCA205 wild-type cells were seeded at 8000 cells per well in 96 well μ Clear imagine plates (Greiner Bio-One) and let adhere for 24 h. Next, cells were treated for 6 h and medium was changed for the following 24 h. Afterwards, the supernatant of each condition was transferred on HT29 MX1-GFP plated at 4000 cells per well in 96 well μ Clear imagine plates two days before. As an additional control, HT29 MX1-GFP were treated with IFN α 1 (752802, Biolegend). 48 h later, the plates were fixed with 3.7 % formaldehyde supplemented with 1 μ g/ml Hoechst 33342 for 1 h at room temperature. The fixative was exchanged to PBS and the plates were analyzed by automated microscopy. The amount of GFP intensity in the whole cell was measured and the number of positive cells was calculated based on a threshold set between the distribution of the GFP-intensity in untreated cells and the one in IFN α 1-treated cells.

Protein immunoblot. Protein was extracted with RIPA buffer (#89900; Thermo Fisher Scientific) in the presence of phosphatase and protease inhibitors (#88669; Thermo Fisher Scientific) followed by sonication. Then protein content was measured by Bio-rad laboratory DC Protein Assay (#500-0113, #500-0114 and #500-0115) following the manufacturer's protocol. 20 μ g of protein was dissolved in Laemmli buffer (Thermo Fisher Scientific), denatured at 100 °C and separated by polyacrylamide gel electrophoresis (PAGE) using 4-12 % Bis-Tris pre-casted gels (Thermo Fisher Scientific) in MOPS buffer (Thermo Fisher Scientific). Following, proteins were transferred to EtOH-activated PVDF membranes (Merck Millipore IPVH00010) in transfer buffer (25 mM Tris; 190 mM glycine; 20 % methanol in H₂O) at 200 mA for 1.5 h. Membranes were washed in Tris-buffered saline with Tween20 buffer (TBST; 20 mM Tris, pH 7.5 150 mM NaCl 0.1 % Tween 20 in H₂O) and then blocked with 5 % BSA

in TBST for 1 h. Membranes were exposed to primary antibody diluted in 5 % BSA in TBST overnight at 4 °C. Following, membranes were washed 3 times with TBST and then were incubated with appropriate horseradish peroxidase-coupled secondary antibody (Southern Biotech, Birmingham, AL, USA) for 1 h at room temperature. Proteins were revealed with ECL (GE Healthcare, Chicago, IL, USA). Beta-actin was assessed to verify equal loading.

Assessment of CALR exposure by flow cytometry. U2OS wild-type cells were seeded at 8000 cells per well in 96-well plates. The cells were treated for 6 h and the drug was washed out. 24 h later, the cells were collected and ecto-CRT was detected by immunofluorescence staining. Cells were incubated for 30 min at 4 °C with primary rabbit monoclonal antibody against CALR (#ab2907, Abcam), then washed and further incubated with secondary AlexaFluor-488-coupled anti-rabbit antibody (#A11034, Thermo Fisher Scientific) for 30 min at 4 °C. Finally, 4', 6-diamidino-2 phenylindole dihydrochloride (DAPI, # D1306, Thermo Fisher Scientific) was added before flowcytometric analysis. Samples were analyzed using a CyAn ADP cytofluorometer (Beckman Coulter, Brea, CA, USA) coupled to a HyperCyt loader (Intellicyt, Albuquerque, NM, USA). Alternatively, after incubation with primary antibody, cells were stained with the LIVE/DEAD fixable dead cell stain (Thermo Fisher Scientific) and fixed with 3.7 % formaldehyde. After staining with the secondary antibody, they were acquired with a MacsQuant cytometer (Miltenyi Biotec).

Assessment of extracellular ATP. The ENLITEN ATP Bioluminescence Detection Kit (FF2000; Promega, Madison, MI, USA) was used for measurement of ATP in cell culture supernatants. Briefly, 8000 U2OS or MCA205 wild-type cells per well were seeded in 96 wells plates. The following day, the cells were treated and 24 h later, the supernatant was collected and centrifuged. The supernatant was transferred to a white bottom plate and the enzyme and substrate from the kit were added. ATP-dependent substrate conversion was measured by assessing luminescence at 560 nm in a SpectraMax I3 multi-mode plate reader (Molecular Devices).

Assessment of extracellular HMGB1. The ELISA kit (ST51011; IBL International GmbH, Hamburg, Germany) was for measuring HMGB1 released in the supernatant. Briefly, 8000 U2OS or MCA205 wild-type cells per well were seeded in 96 wells plates. The following day, the cells were treated and 24 h later, the supernatant was collected and centrifuged. ELISA was performed as described by the provider and absorbance at 450 nm was assessed with a

SpectraMax I3 multi-mode plate reader (Molecular Devices).

Assessment of BMDC-mediated phagocytosis. Bone marrow-derived dendritic cells (BMDC) were generated from femurs and tibias taken from C57BL/6 mice. Bone marrow was collected by flushing the bones with PBS and clusters were dissolved by pipetting. Red blood cells were lysed with red cell lysis buffer (0.01 M Tris, 0.83 % NH₄Cl in Milli-Q water). After washing and filtration through a 70 µm cell strainer, cells were seeded into 6 well plates at a density of 1.5 x 10⁶ viable cells in 2 mL of DC culture medium supplemented with 20 ng/mL recombinant mouse GM-CSF. At day 3, additional 1 mL of complete medium (RPMI 1640 medium supplemented with 10 % FBS, 100 U/mL penicillin, 1 M HEPES, 1X MEM Non-Essential Amino Acids Solutions, 50 µM 2-Mercaptoethanol) supplemented with 50 nM β-mercaptoethanol and 20 ng/mL GM-CSF were added to each well. At day 6, half of the supernatant was removed, centrifuged and added back to the original culture with the addition of 50 nM β-mercaptoethanol and 20 ng/mL GM-CSF. Non-adherent and loosely adherent BMDCs were harvested on day 7, counted, and 8 x 10⁵ mouse fibrosarcoma MCA205 cells were seeded in standard 25 cm² polystyrene flasks for cell culture. 24 h later, they were labelled with 0.5 µM CellTracker Orange (CMTMR) dye diluted in serum-free medium according to the manufacturer's protocol (ThermoFischer Scientific). Cells were then treated for 24 h. Following, MCA205 were co-cultured with BMDCs in 6-well plates at 37 °C, 5 % CO₂ at a 1:4 ratio (BMDC:MCA205). After 4 h, cells were detached with a cell lifter, BMDCs were stained with Pacific Blue CD11c anti-mouse antibody (BioLegend) diluted in 1 % BSA in PBS and incubated at 4 °C in the dark for 30 min. Cells were washed and fixed in 3.7 % formaldehyde in PBS prior to acquisition by flow cytometry (LSRII Fortessa, BD Biosciences). Phagocytosis efficiency was assessed by measuring the ratio of CMTMR⁺ CD11c⁺ cells among total amount of CD11c⁺ BMDCs, using FlowJo v10 software (TreeStar, Inc.).

***In vivo* experimentation.** Six- to eight-week-old female wild-type C57BL/6, Balb/c and *nu/nu* mice were purchased from Envigo (Huntingdon, UK) and were housed in the animal facility at the Gustave Roussy Cancer Center in a pathogen-free, temperature-controlled environment with 12 h day and night cycles and received water and food *ad libitum*. Animal experiments were conducted in compliance with the EU Directive 63/2010 and with protocols 2018071210276451_n2018_051_16095, 201903131451670_n2019_017_19749 or 2019072311495586_n2019_050_21586, and were approved by the Ethical Committee of the Gustave Roussy Cancer Center (CEEA IRCIV/IGR no. 26, registered at the French Ministry

of Research). For all mouse experiments, tumor length and width were assessed with a standard caliper 2 to 3 times a week and tumor areas were calculated using the formula of an ellipse: $L \times l \times 3.14 / 4$. The mice were sacrificed when tumors reached 1.8 cm² or depicted any signs of discomfort following the EU Directive 63/2010 and our Ethical Committee advice (or before, if required by the setting of the experiment). Tumor growth was analyzed with the help of the TumGrowth software package (Enot et al, 2018), freely available at <https://github.com/kroemerlab>.

***In vivo* xenograft experiments.** 5×10^6 U2OS CALR-RFP cells were subcutaneously (*s.c.*) injected into the flank of *nu/nu* mice. After 6 to 10 weeks, when tumors became palpable, 200 μ L of the agents diluted in PBS were administered intratumorally. Tumors were resected after 6 or 24 h of treatment, immediately fixed in 3.7 % formaldehyde overnight and then incubated in sucrose gradients. Tumors were sectioned into 5 μ M slices using a cryostat microtome. Two slices per tumor were stained with a phosphoepitope-specific eIF2 α antibody used at 1/500 in 2 % BSA overnight at 4 °C after blocking with 2 % BSA. Then slides were washed and incubated with AlexaFluor-647-coupled secondary antibody (Thermo Fisher scientific) for 2 h at room temperature and counterstained with Hoechst 33342. Images were acquired with an IXM-C confocal microscope (Molecular Devices) as described previously with a 10-fold magnification. Image segmentation was conducted with R. Nuclei were identified based on Hoechst 33342 staining and cytoplasmic regions were segmented based on CALR-RFP signal. The intensity of the Cy5 signal in the cytoplasmic region was measured to assess eIF2 α phosphorylation. For CALR translocation, the coefficient of variation of the RFP signal in the cytoplasmic region was calculated, which represents the standard deviation divided by the mean of the intensity of the signal.

Anticancer vaccination. For anticancer vaccination studies, we used standard protocol described before (Casares et al, 2005; Humeau et al, 2019). In brief, MCA205 cells were treated for 24 h to reach 50 to 70 % mortality, then 1×10^6 cells were resuspended in 200 μ L PBS and injected *s.c.* into the left flank of immunocompetent C57BL/6 animals. Two weeks later, 1×10^5 living MCA205 cells were injected *s.c.* in the other flank and tumor growth was monitored for the forthcoming weeks.

***In vivo* tumor treatment.** Established tumors were assessed for their response to DACT-based therapy. To this aim, MCA205 fibrosarcoma cancers were established subcutaneously (*s.c.*) in

C57BL/6 mice and in *nu/nu* mice by injection of 3×10^5 MCA205 cells. When tumors became palpable, 200 μ L of the chemotherapeutics (diluted in 10 % PEG 400, 10 % Tween 70, 4 % DMSO and 7 % NaCl) or the diluent alone were injected intraperitoneal (*i.p.*) and tumor growth was monitored for the forthcoming weeks. Alternatively, WEHI 164 tumors were established subcutaneously (*s.c.*) in Balb/c mice by injection of 3×10^5 MCA205 cells. When tumors became palpable, 200 μ L of the chemotherapeutics or the diluent alone were injected intraperitoneal (*i.p.*). Four days later, the treatment was repeated. To study the importance of the adaptive immune system, 100 μ g anti-CD4 (clone GK1.5, BioXcell) and 100 μ g anti-CD8a (clone 2.43, BioXcell) antibodies diluted in PBS were injected at days -1, 0 and 7 before and after the first chemotherapy.

Combination with immunotherapy. In order to boost the effect of the chemotherapeutics, the same treatments were combined sequential with immune checkpoint blockade. MCA205 fibrosarcoma cell cancers were established subcutaneously (*s.c.*) in C57BL/6 mice by injection of 1×10^5 MCA205 cells. When tumors became palpable, the chemotherapies were injected intraperitoneal (*i.p.*). At days 6, 10 and 14 after chemotherapy, 200 μ g/mouse of anti-PD-1 (Clone 29F.1A12, BioXcell) or its corresponding isotype (Clone LTF-2, BioXcell) prepared in 200 μ L PBS were injected *i.p.* Surviving animals that were tumor-free after treatments were tested for the generation of immunological memory by *s.c.* rechallenge with non-isogenic 1×10^5 TC-1 in the flank initially injected and isogenic 1×10^5 MCA205 cells injected in the contralateral flank. C57BL/6 naïve mice were used as control. Alternatively when used to treat WEHI 164 cells, 200 μ g/ mouse of anti-PD-1 were injected at days 8, 12 and 16 after the first chemotherapy. Tumor growth was monitored for the forthcoming weeks.

Immune infiltrate study. MCA205 fibrosarcoma cancers were established subcutaneously (*s.c.*) in C57BL/6 mice by injection of 2×10^5 MCA205 cells. When tumors became palpable, 200 μ L of the chemotherapeutics were injected *i.p.* with $n=10$ mice per group. Nine days later, tumors were harvested, weighed and then processed before phenotyping immune cells as described before (Levesque et al, 2019). In brief, tumors were dissociated mechanically with scissors, then enzymatically with the tumors dissociation kit (Miltenyi) and the gentle MACS Octo Dissociator (Miltenyi) following the manufacturer's protocol. Tumor cell homogenates were filtered through 70 μ m SmartStrainers (Miltenyi) and washed twice with PBS. Tumor cell homogenates, corresponding to 50 mg of the initial tumor sample, were stained with

LIVE/DEAD Fixable Yellow dye (Thermo Fisher Scientific) and then with anti-mouse CD16/CD32 (clone 2.4G2, Mouse BD Fc Block, BD Pharmingen) to block Fc receptors. To determine the production of cytokines by T lymphocytes, sample cells were stimulated for 5 h in serum-free CTL-Test PLUS Medium (ImmunoSpot) containing 20 ng/mL phorbol myristate acetate (PMA, Calbiochem), 1 µg/ml ionomycin (Sigma) and BD Brefeldin A (GolgiPlug, dilution 1:1000, BD Biosciences). Immune cells staining was performed with the set of fluorochrome-conjugated antibodies related to each panel with first, a staining of surface receptors and second, after incubation in eBioscience FoxP3/Transcription Factor Staining Buffer (Thermo Fisher Scientific) and permeabilization, a staining of intracellular receptors and cytokines:

- (Panel 1) “*T-cell panel*”: anti-CD3g,d,e APC (clone 17A2, Biolegend), anti-CD8a PE (clone 53-6.7, BD Pharmingen), anti-CD4 PerCP-Cy5.5 (clone RM4-5, Thermo Fisher Scientific) completed by an intranuclear staining with anti-FoxP3 FITC (clone FJK-16s, Thermo Fisher Scientific).
- (Panel 2) “*NK and cytokines panel*”: anti-CD45 BUV661 (clone 30F11, BD Pharmingen), anti-CD3g,d,e BV421 (clone 53-8.7, BD Pharmingen), anti-CD4 BUV496 (clone GK1.5, BD Pharmingen), anti-CD8a PE (clone 53-6.7, BD Pharmingen), anti-NK1.1 BV605 (clone PK136, BD Pharmingen), anti-TCRγδ BV711 (clone GL3, BD Pharmingen), completed by an intracellular staining with anti-IL17a APC-Cy7 (clone TC11-18H10, BD Pharmingen) to assess the Th17 response, anti-IFNγ APC (clone XMG1.2, BioLegend) for measuring the Th1/Tc1 response and anti-IL4 PerCP-Cy5.5 (clone 11B12, BD Pharmingen) characterizing a Th2 response.

Stained samples of panel 1 were run through a BD LSR II flow cytometer while samples of the panel 2 were run through a BD LSRFortessa flow cytometer. All samples were acquired using BD FACSDiva software (BD biosciences) and analyzed using FlowJo software (TreeStar, Inc.).

Evaluation of transcription by EU incorporation. This was performed by incorporation of a Click-iT chemistry-detectable 5-ethynyl uridine (EU) (C10327; Thermo Fisher Scientific) following the manufacturer’s advice. In short, 2500 cells per well were cultured in 384-well µClear imaging plates. The next day, cells were pre-treated for 1.5 h to 2.5 h, washed and treatment was pursued in the presence of 1 mM 5-ethynyl uridine (EU) for 1 h. Following, the cells were fixed with 3.7 % formaldehyde supplemented with 1 µg/ml Hoechst 33342 for 1 h and permeabilized with 0.1 % triton x-100 for 10 min. AlexaFluor-488-coupled azide was then added for 2 h. The intensity of the GFP signal (EU) in the nucleus was measured by microscopy

and the inhibition of transcription was calculated by ranging the GFP intensity in each condition between its value in untreated cells (0 % inhibition) and its value in cells that have not been incubated with EU (corresponding to 100 % inhibition).

Evaluation of transcription by colocalization of fibrillarin and nucleolin. 2500 cells per well were cultured in 384-well μ Clear imaging plates. The next day, cells were treated for 2.5 h. Following, cells were fixed with 3.7 % formaldehyde supplemented with 1 μ g/ml Hoechst 33342 for 1 h, permeabilized with 0.1 % triton x-100 for 10 min and blocked with 2 % BSA for 1 h. Cells were further incubated rabbit antibody against fibrillarin (ab5821) and mouse antibody against nucleolin (ab13541) overnight at 4 °C. After several PBS washing steps, anti-mouse AlexaFluor-488 and anti-rabbit AlexaFluor-647 (or -546 in mitoxantrone-treated cells to avoid interference of with drugs auto-fluorescence) coupled antibodies were added. Following several PBS washing steps, the DAPI, GFP and Cy5 (or Cy3) signals were acquired with a confocal microscope Molecular Devices IXM-C. The obtained images were analyzed using ColocalizR software (Sauvat et al, 2019) taking into consideration the SOC (Surface Overlap Coefficient) between the GFP and Cy5 (or Cy3) signals. Data were then ranged between 0 % inhibition (Ctr) and 100 % inhibition (corresponding to the well with lowest SOC among all dataset).

Translation study by AHA incorporation. Translation was measured by assessing the incorporation of L-azidohomoalanine (AHA) (C10289; Thermo Fisher Scientific), a labelled form of methionine by Click-iT chemistry following the manufacturer's advice. In short, 2000 cells per well were cultured in 384-well μ Clear imaging plates. The next day, cells were treated for 12 h. After several PBS washing steps, the cells were incubated 30 min in the presence of methionine-free medium. Then, they were treated 1.5 h in methionine-free medium in the presence of 25 μ M AHA. Following, the cells were fixed with 3.7 % formaldehyde supplemented with 1 μ g/ml Hoechst 33342 for 1 h, permeabilized with 0.1 % triton x-100 for 10 min and blocked with 2 % BSA for 1 h. Then, AlexaFluor-488-coupled azide was added for 2 h and the GFP intensity (AHA) was measured by microscopy. Translation inhibition was calculated by ranging the GFP intensity in each condition between its value in untreated cells (0 % inhibition) and its value in cells that have not been incubated with AHA (corresponding to 100 % inhibition).

Reversibility of proteins synthesis assessed by Rush. U2OS cells co-expressing ss-SBP-GFP

and Str-KDEL were seeded at 2500 cell per well in 384-well μ Clear imaging plates. The following day, cells were stained with 0.5 μ M CellTracker Orange (CMTMR) diluted in serum-free medium according to the manufacturer's protocol (ThermoFischer Scientific), then pretreated with 40 μ M biotin for 4 h and with the compounds to test for 2.5 h. After washout, cells were treated with 1 μ M avidin to assess reversibility of the inhibition of transcription (discontinuous treatments). As a positive control, treatments were pursued in the presence of avidin (continuous treatments). Images were then acquired every hour for 24 h. ROIs were defined based on CellTracker staining and GFP intensity was quantified. Values were normalized to the control at each time point and the percentage of inhibition and of reversibility were calculated. For this first parameter, the curve of continuous treatment was considered, with the maximum effect (100 % inhibition) obtained by the slope of avidin control curve; the percentage of inhibition was defined as the complementary ratio between these two slopes. For calculating the latter parameter, the maximum effect was defined as the measured area between biotin and avidin controls curves. Then a percentage of reversibility was computed by calculating the complementary ratio between the area separating the continuous and discontinuous treatment curves, normalized by the maximum effect.

Retrospective *in silico* analysis of different classes of inhibitors. Compound annotations were retrieved from the MeSH (Medical Subject Headings) database and drugs were clustered in function groups: protein synthesis inhibitors, DNA synthesis inhibitors, poly(ADP-ribose) polymerase (PARP) inhibitors and antimetabolites. Each of these clusters was analyzed for its enrichment in high ICD score by means of a Kolomogorov-Smirnov test against the entire compound population.

Statistical analyses. *In vitro*. Data are presented as means \pm SD if one representative experiment among at least three independent ones is depicted or means \pm SEM if we show the combination of at least three independent experiment. Statistical analyses were performed using R or Excel. Student's t-test were used to compare parametric data of different conditions to a control condition. Correlations were performed with R using a Pearson test. ***In vivo*.** Statistical analysis was performed with the TumGrowth software package (Enot et al, 2018) freely available at <https://github.com/kroemerlab>. A type II ANOVA test was used for tumor growth and a Log-Rank test for mice survival. For all tests, the statistical significance level was */#p<0.05, **/##p<0.01, ***/###p<0.001.

Results

Identification of dactinomycin as a *bona fide* ICD inducer.

We used an artificial intelligence machine learning approach (Bezu et al, 2018a) to predict the probability of inducing ICD of 50,000 distinct compounds tested for their anticancer effects on the NCI-60 panel of human tumor cell lines (Shoemaker, 2006) (**Figure 13A**), while plotting the ICD prediction score against their mean half maximal growth inhibitory concentration (IC_{50}), *i.e.* the dose that reduces cell proliferation by half (**Figure 13B**). The compounds that exhibited cytotoxicity and an ICD score higher than mitoxantrone (MTX), a standard ICD inducer (Ma et al, 2011; Obeid et al, 2007b), were considered as potential ICD inducers. Two compounds, among the ones that have entered clinical trials, stood out as drugs having a low IC_{50} and a high ICD score. Trabectedin is known for its capacity to selectively eliminate tumor-associated macrophages, which explains at least part of its anticancer activity (Germano et al, 2013). Dactinomycin (DACT, best known as actinomycin D, a product of *Streptomyces parvulus*), which is generally considered as a DNA intercalator that inhibits topoisomerases and RNA polymerases (Goldberg et al, 1962), is used for the treatment of childhood-associated sarcomas (Wilms, Ewing, rhabdomyosarcoma), gestational trophoblastic disease including hydatiform moles and choriocarcinomas (Khatua et al, 2004; Turan et al, 2006) and some types of testicular cancers (Early & Albert, 1976). We therefore evaluated DACT for its capacity to induce ICD.

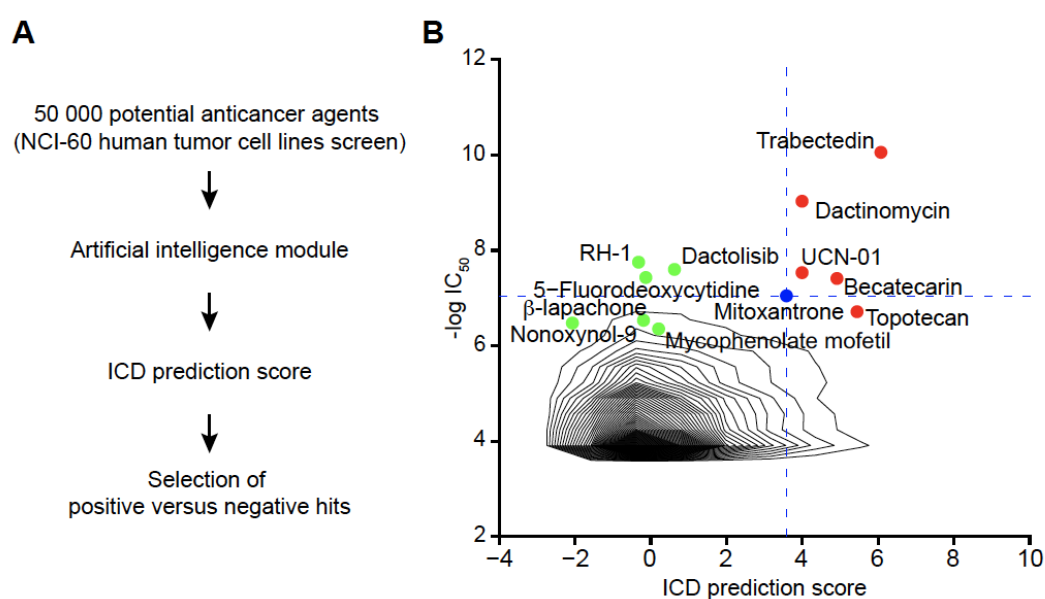


Figure 13. Prediction of immunogenic cell death (ICD). The 50,000 potential anti-cancer agents from the NCI-60 human tumor cell lines screen were analyzed with an artificial intelligence model that can predict immunogenic cell death (ICD) based on molecular descriptors. (A) The distribution of the drugs based on their IC_{50} and predicted ICD score is depicted as density plot. Based on the properties of the standard ICD inducer mitoxantrone (blue),

we selected negative (green) and positive (red) hits: agents that entered into clinical trials, having an $IC_{50} < 1 \mu M$ (and therefore $-\log(IC_{50}) > 6$) and whose predicted ICD score is higher than the ICD score of mitoxantrone are potential ICD inducers (positive hits). Some agents that entered into clinical trials, whose $IC_{50} > 1 \mu M$ and which have an ICD prediction score lower than 1 are negative hits (**B**).

When added to human osteosarcoma U2OS cells engineered to express a CALR-green fluorescent protein (GFP) fusion protein, DACT (used around the IC_{60} for these cells, *i.e.* at 0.5 and 1 μM , **Figure S 2**) caused peripheralization of the green fluorescence to the same extent as the positive control, MTX, as determined by videomicroscopy (**Figure 14A-C**). Accordingly, endogenous CALR became detectable on the plasma membrane surface of viable cells, as demonstrated by flow cytometry (**Figure 14K, L**). Videofluorescence microscopy revealed the decrease of HMGB1-GFP in the nuclei of DACT-treated cells (**Figure 14D-F**). The release of endogenous HMGB1 into the culture medium was confirmed by ELISA (**Figure 14M**). DACT also reduced the ATP-dependent quinacrine fluorescence staining of cells (**Figure 14G, H**) and induced ATP release into culture supernatants (**Figure 14N**). The supernatants of DACT-treated cells stimulated the expression of a type 1 interferon biosensor, a GFP placed under the control of the MX1 promoter (**Figure 14I, J**).

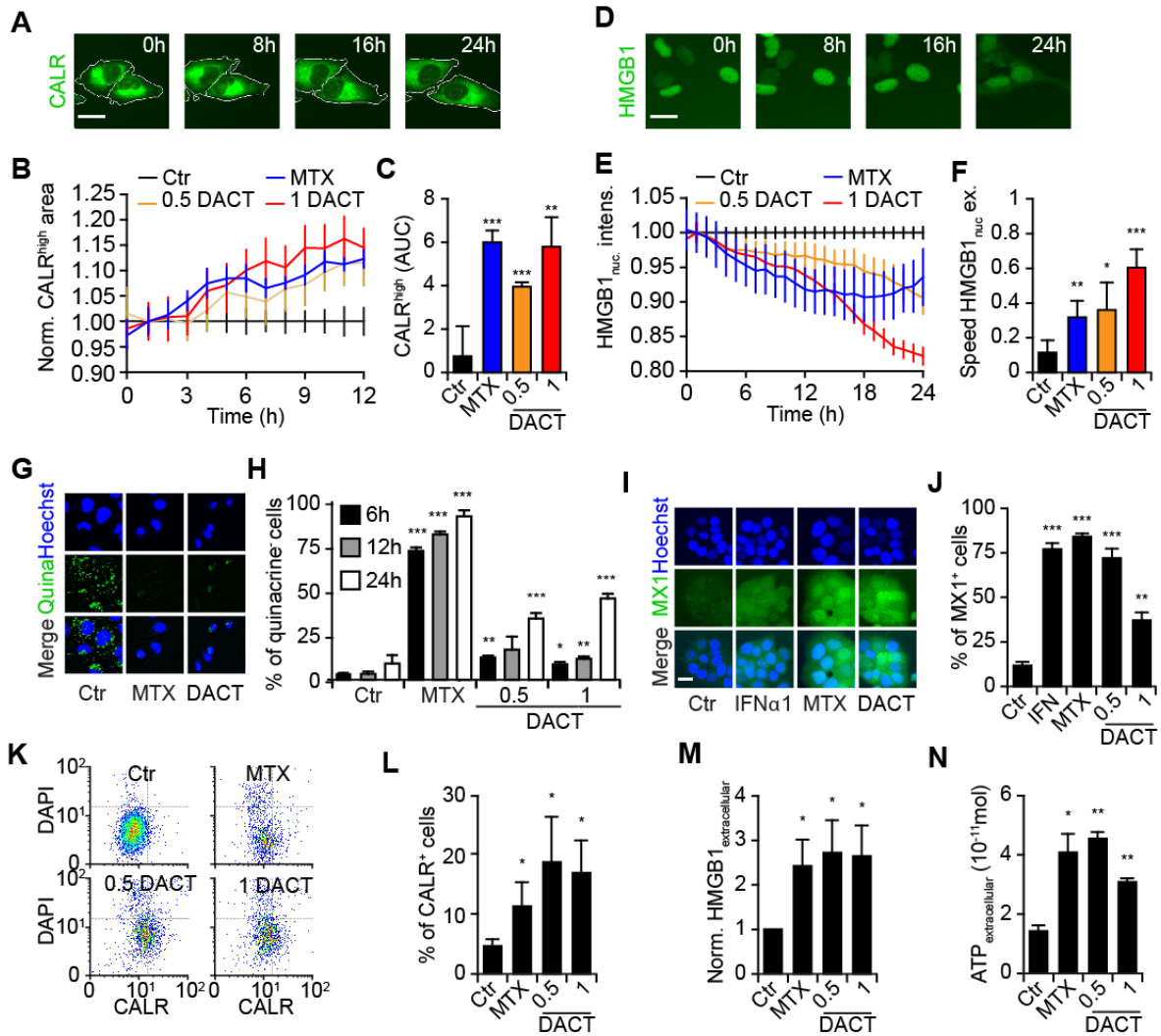


Figure 14. ICD hallmarks in human cancer cells. Human osteosarcoma U2OS cells were treated with dactinomycin (DACT) at 0.5 and 1 μM and mitoxantrone (MTX) at 4 μM was used as positive control for all experiments (A-N). Human osteosarcoma U2OS stably expressing CALR-GFP and H2B-RFP were treated as described above and images were acquired once per hour for 12 h (A). For one representative experiment among three, the mean ± SD of the average area of high CALR dots (normalized to the control at each timepoint) of quadruplicates is shown (B). Values are depicted as the area under the curve (AUC) ± SD of triplicates (C). Treated U2OS cells stably expressing HMGB1-GFP and H2B-RFP images were acquired every hour for 24 h (D). For one representative experiment among three, the mean ± SEM of the green fluorescence intensity in the nucleus (normalized to the control at each timepoint) of quadruplicates is depicted (E). For each cell, the speed of nuclear release (difference of HMGB1 nuclear green fluorescence intensity between two time points) was calculated. Values are depicted as the average speed of the nuclear release ± SD of quadruplicates (F). U2OS cells were treated for 6, 12 and 24 h and ATP was stained with quinacrine (G). The number of quinacrine negative cells was assessed based on the distribution of cellular green fluorescence intensity in MTX versus control conditions (H). U2OS were treated with MTX and DACT as described above for 6 h. Then medium was refreshed and 24 h later, type I interferon response was assessed by transferring the supernatant on HT29 MX1-GFP reporter cells lines cells for additional 48 h. Human type 1α interferon (IFNα1) was also added on the cells as another more direct positive control. The cells were acquired by fluorescence microscopy and the number of positive cells was assessed based on the distribution of cellular green fluorescence intensity in IFNα1 versus control conditions (I). The percentage of MX1 positive cells was calculated and the mean ± SEM of five independent experiment is depicted (J). U2OS were treated as mentioned previously for 6 h and then medium was refreshed. Twenty-four hours later, cells were collected and surface-exposed calreticulin (CALR) was stained with an antibody specific for CALR. DAPI was used as an exclusion dye and cells were acquired by flow cytometry (K). The percentage of CALR⁺ cells among viable (DAPI⁺) ones are depicted. The mean ± SEM of six independent experiments is depicted (L). U2OS cells were treated as described above for 24 h and the concentration of HMGB1 released in the supernatant was

quantified with an ELISA kit, then normalized to control. The mean \pm SEM of four independent experiments is shown (**M**). U2OS were treated as described above for 24 h. Concentration of secreted ATP in the supernatant was quantified with a luciferase-based bioluminescence kit. The mean \pm SD of quadruplicates of one representative among three experiments is depicted (**N**). All p-values shown significances of treatments compared to control (Ctr) were calculated with Student's t-test: *p<0.05 **p<0.01 ***p<0.001.

One of the pathognomonic features of ICD is a partial endoplasmic reticulum (ER) stress response that involves phosphorylation of eukaryotic initiation factor 2 α (eIF2 α) without activation of its downstream factor ATF4, and without the ATF6 and the IRE1/XBP1 arms of the unfolded protein response (Bezu et al, 2018a; Panaretakis et al, 2009; Pozzi et al, 2016). Accordingly, DACT caused eIF2 α phosphorylation (measured by immunofluorescence, **Figure 15A, B**), but no significant ATF4 activation (expressed as a GFP fusion protein, **Figure 15C, D**), and ATF6 translocation from the cytosol to the Golgi and to nuclei (detected as a GFP fusion protein, **Figure 15E, F**) and no expression of an XBP1 Δ DBD-venus fusion protein that is only in-frame for venus (a variant of GFP) when XBP1 has been spliced by IRE1 (**Figure 15G, H**). We knocked out each of the four eIF2 α kinases (EIF2AK1 to 4) in U2OS cells (**Figure S 3**) and determined their contribution to DACT-induced eIF2 α phosphorylation. As for other ICD inducers (such as anthracyclines and oxaliplatin) (Panaretakis et al, 2009), EIF2AK3 (also known as PERK) was responsible for DACT-stimulated eIF2 α phosphorylation (**Figure 15I, J**). Human U2OS osteosarcoma cells expressing a CALR-RFP fusion protein were implanted in immunodeficient mice to generate tumors that were then treated with DACT. DACT induced the rapid (6 h) phosphorylation of eIF2 α (**Figure 15K, L**) and the redistribution of CALR-RFP to the cell periphery within 24 h (**Figure 15M, N**). DACT also stimulated all ICD hallmarks (eIF2 α phosphorylation, CALR exposure, ATP and HMGB1 release, as well as induction of type 1 interferons) in another cell line, the murine methylcholanthrene-induced fibrosarcoma MCA205 (**Figure S 4**). Altogether, these results confirm the capacity of DACT to stimulate a signal transduction pathway that leads to immunogenic stress and death. Since ATP secretion relies on autophagic flux in the course of ICD induced by anthracyclines and OXA (Michaud et al, 2011), we investigated this pathway after DACT treatment. Surprisingly, DACT failed to induce LC3 dots-related autophagy, both in U2OS (**Figure S 5 A, B**) and in MCA205 (**Figure S 5C, D**).

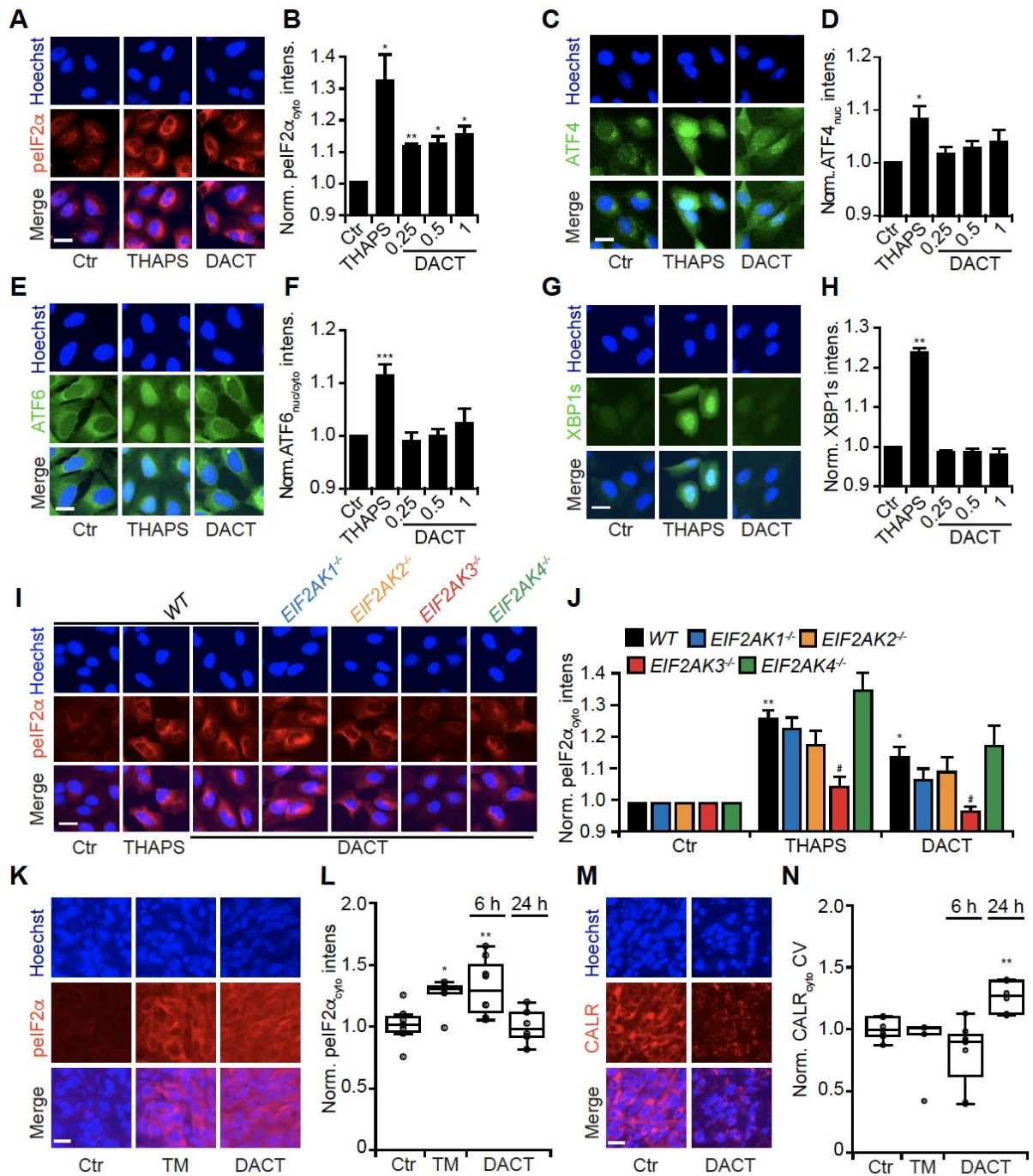


Figure 15. DACT induces a split ER stress response in U2OS. Human osteosarcoma cells were treated with different concentrations of dactinomycin (DACT) (0.25, 0.5 and 1 μM) for 6 h. Thapsigargin (THAPS) at 3 μM was used as a positive control. After fixation, cells were stained with a phosphoepitope-specific eIF2 α antibody (peIF2 α) followed by an AlexaFluor-647 secondary antibody, nuclei were counterstained with Hoechst 33342 and phosphorylation was assessed by fluorescence microscopy. Images were segmented, analyzed and the red cytoplasmic fluorescence intensity is shown (A, B). U2OS cells stably expressing ATF4-reporter were treated as described above for 12 h. The expression and nuclear translocation of ATF4 was assessed by fluorescence microscopy and the nuclear green fluorescence intensity is shown (C, D). U2OS stably expressing ATF6-GFP were treated as described above and nuclear translocation of ATF6 was represented as the ratio of nuclear versus cytoplasmic green fluorescence intensity (E, F). U2OS cells stably expressing venus in frame with alternatively spliced XBP1 (sXBP1) were treated as described above for 12 h. *De novo* expressed venus was measured intracellularly (G, H). U2OS wild-type and knock out for eIF2 α kinases 1, 2, 3 and 4 cells were treated with 3 μM THAPS, as a positive control for eIF2 α phosphorylation via EIF2AK3, or 1 μM DACT for 6 h. After fixation, cells were stained with a peIF2 α antibody followed by an AlexaFluor-647 secondary antibody, nuclei were counterstained with Hoechst 33342 and phosphorylation was assessed by fluorescence microscopy. Cytoplasmic

intensity is depicted (**I, J**). Images are shown for untreated cells (Ctr), THAPS and DACT at 1 μ M (**A, C, E, G, I**). For all bar charts, the mean \pm SEM of three to five independent experiments is shown and the p-value to the control was calculated with Student's t-test: *p<0.05 **p<0.01 ***p<0.001 (**B, D, F, H, J**). For peIF2 α quantification in the different cell lines, * show the statistics of each treatment to the control in the wild-type cells whereas # show the statistics comparing the kinases knock-out cells to the wild-type cells for a same treatment: #p<0.05 ##p<0.01 ###p<0.001 (**J**). U2OS CALR-RFP were injected subcutaneously (*s.c*) in the flank of *nu/nu* mice. Tumors were further injected with PBS (Ctr) (n=5), 0.5 mg/kg tunicamycin (TM) for 6 h (n=3) or 0.5 mg/kg DACT for 6 h (n=4) or 24 h (n=3). Tumor slices were cut and stained with a peIF2 α antibody followed by an AlexaFluor-647 secondary antibody and counterstained with Hoechst 33342. Two slices per tumor were imaged for their DAPI, RFP and Cy5 signals by the mean of a confocal microscope. Out-of-focused images were removed from the dataset leading to the following amount of slices per condition: 8 for Ctr, 5 for TM, 8 for DACT 6h and 6 for DACT 24h. PeIF2 α was quantified measuring Cy5 intensity in the cytoplasm (**K, L**) and CALR translocation by measuring the coefficient variation (CV) of the RFP signal in the cytoplasm (**M, N**). Representative images of peIF2 α are shown for Ctr, TM and DACT at 6 h (**K**) whereas images of CALR are shown for Ctr and DACT at 24 h (**M**). Both are depicted in boxplots with p-values calculated using Student's t-test: *p<0.05 **p<0.01 ***p<0.001 (**L, N**).

Immune-dependent anticancer effects of dactinomycin.

To further investigate the immunogenic properties of DACT, we treated cancer cells *in vitro* with this compound, labelled them with CellTracker 5-(and-6)-(((4-chloroethyl)benzoyl)amino) tetramethylrhodamine (CMTMR) and measured their engulfment by bone marrow-derived CD11c⁺ dendritic cells (BMDCs) (**Figure 16A**). DACT was able to stimulate phagocytosis by BMDCs (**Figure 16B, C**). Next, we determined the capacity of DACT to induce ICD in vaccination assays. For this, MCA205 cells were treated with the cytotoxicants *in vitro*, washed, and then injected subcutaneously (*s.c.*) in the absence of any adjuvant into immunocompetent C57BL/6 mice. These animals were then rechallenged two weeks later with live MCA205 cells injected into the opposite flank (**Figure 16D**). As compared to controls, mice vaccinated with DACT-treated cells exhibited a delay in tumor growth (**Figure 16E, F**).

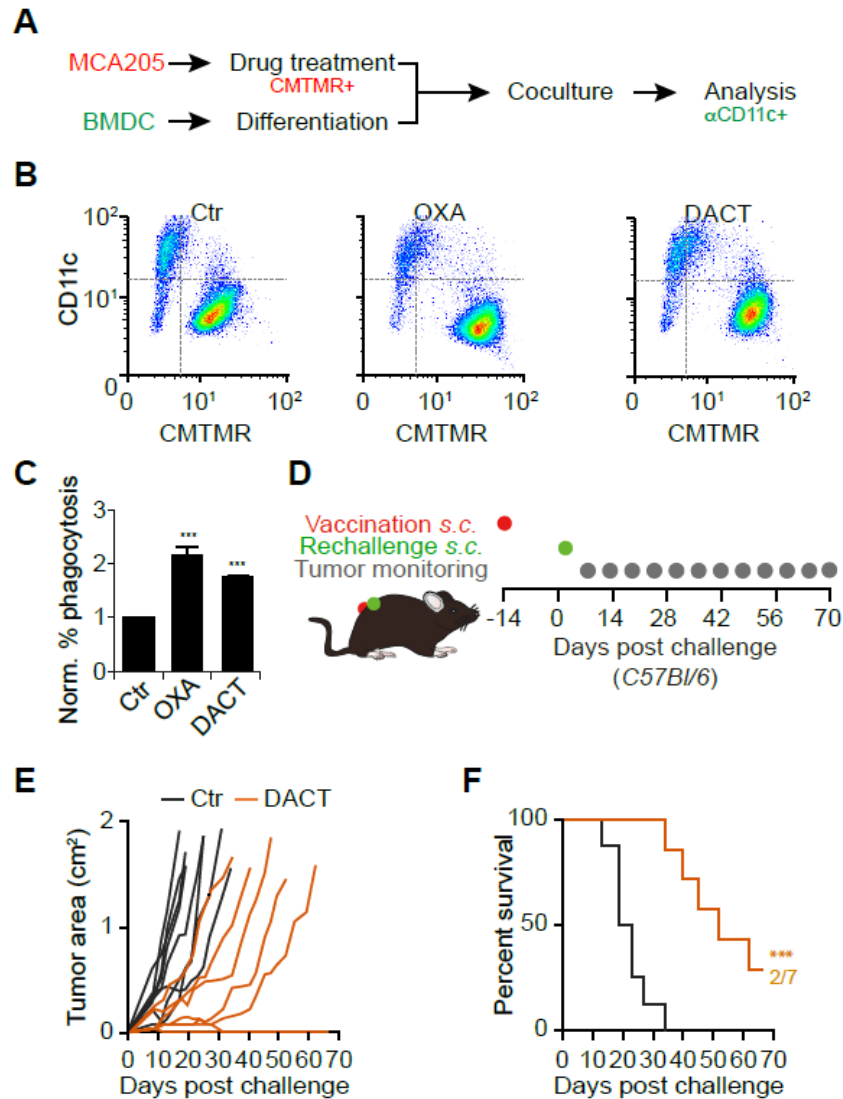


Figure 16. DACT-treated cells activate the immune system. Mouse fibrosarcoma MCA205 cells were stained with CellTracker orange (CMTMR) and treated for 24 h with 1 μ M dactinomycin (DACT) or 500 μ M oxaliplatin (OXA) as a positive control. Then, dying MCA205 were co-cultured with differentiated bone marrow derived dendritic cells (BMDCs) for 4 h. Cells were collected and dendritic cells were stained with CD11c specific antibody before analysis by flowcytometry (**A**, **B**). The percentage of CMTMR and CD11c double positive cells among all dendritic cells are depicted and normalized by the control (Ctr). The mean of three independent experiments \pm SD is depicted and the p-values were calculated using a Student's t-test (**C**). 1×10^6 mouse fibrosarcoma MCA205 cells were treated *in vitro* with 1 μ M DACT. Dying cells were harvested and injected subcutaneously (*s.c.*) into one flank of immunocompetent syngeneic C57BL/6 mice (n=8 mice) to assess vaccination efficacy. PBS was injected in the control group (Ctr) (**D**). Two weeks later, animals were rechallenged with 1×10^5 untreated MCA205 cells in the contralateral flank of the animals. Next, tumor size was measured regularly and tumor growth of DACT-vaccinated versus Ctr mice is depicted (**E**). Overall survival is depicted and p-values were calculated with a Log-Rank test (**F**). One representative experiment among three is shown (**E**, **F**). *indicates the p-value of the treatments versus Ctr (***p<0.001) (**C**, **F**).

Next, we administered DACT alone or in combination with the widely used and non-immunogenic chemotherapeutic cis-dichloro-diammine-platinum (cisplatin; CDDP) (Casares et al, 2005; Martins et al, 2011) and an anti-PD-1 antibody, to immunocompetent C57BL/6

mice bearing MCA205 (**Figure S 6A, K**). While DACT alone was not able to significantly reduce tumor growth, the combination of CDDP and DACT was efficient against established MCA205, reducing tumor growth and extending overall survival, when MCA205 fibrosarcomas were evolving in immunocompetent mice (**Figure S 6A-E**). However, this antineoplastic effect of CDDP plus DACT was lost when the cancer cells were growing in immunodeficient *nu/nu* mice that are athymic and hence lack mature T lymphocytes (**Figure S 6F-J**). Of note, DACT followed by PD-1 blockade delayed tumor growth (**Figure S 6L, N, O**) and the triple combination (CDDP+DACT+PD-1 blockade) allowed for the permanent cure of 3 out of 9 MCA205 cancers (**Figure S 6M, N, O**). When cured mice were re-inoculated with MCA205 cancers, no tumor growth was observed, although antigenically unrelated TC-1 non-small cell lung cancer readily formed macroscopic cancers in these animals (**Figure S 6P, Q**). Hence, in combination regimens, DACT can be used to stimulate a curative anticancer immune response that generates protective long-term memory.

In accordance with the hypothesis that DACT mediates immunostimulatory effects *in vivo*, the immune infiltrate of tumors from mice receiving systemic DACT exhibited an improved ratio of cytotoxic T lymphocytes over FoxP3⁺ regulatory cells as well as an increase in NK and NKT cells (**Figure S 7B-D**). Following a non-specific restimulation with phorbol myristate acetate (PMA) and ionomycin, an augmentation in IL17 producing CD4⁺, CD8⁺ and $\gamma\delta$ T cells was observed in the tumor infiltrate (**Figure S 7G-I**). In addition, DACT caused the secretion of IFN γ by CD8⁺ T cells, while the amount of IL4 produced by CD4⁺ T cells remained unchanged (**Figure S 7E, F**).

The immunostimulatory effect of DACT was recapitulated in WEHI 164 cells, yet another methylcholanthrene-induced fibrosarcoma, alone and in combination with anti-PD-1 checkpoint blockade (**Figure 17A**). In this model, DACT treatment alone sufficed to cure 5 out of 8 mice from transplanted fibrosarcoma (**Figure 17B, E, H**), an effect which was completely abolished when CD4⁺ and CD8⁺ T cells were depleted with specific antibodies (**Figure 17C, D, E**). DACT combined with anti-PD-1 checkpoint blockade led to the cure or disease control in all treated animals (**Figure 17F- H**).

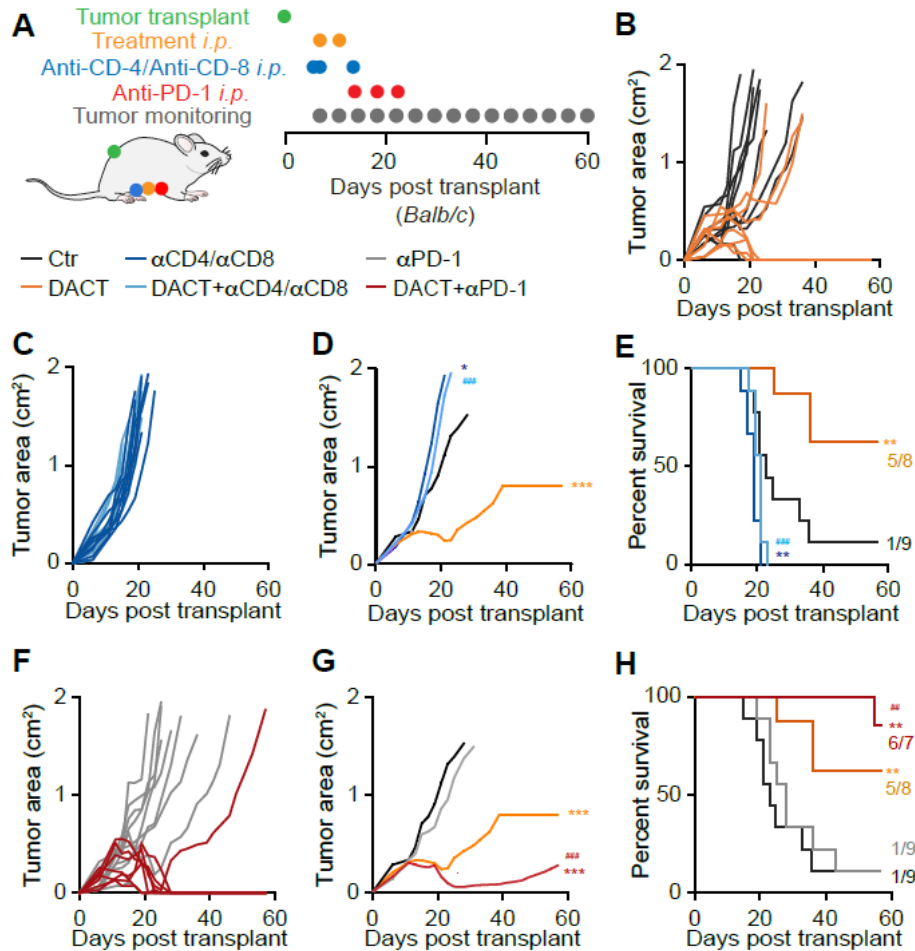


Figure 17. Immune-dependent effect of DACT on WEHI 164 tumors growth and sensitization to immunotherapy. 3 x 10⁵ mouse fibrosarcoma WEHI 164 cells were injected subcutaneously (*s.c.*) into the flank of immunocompetent syngeneic Balb/c mice with n mice per group (n=7 DACT + anti-PD-1, n=8 DACT, n=9 Ctr, anti-PD-1, anti-CD4/anti-CD8, DACT + anti-CD4/anti-CD8). When tumors became palpable, the mice were injected intraperitoneally (*i.p.*) with injectable solution (Ctr) or 0.5 mg/kg dactinomycin (DACT). A second injection of chemotherapy was performed four days later. Anti-CD4 and anti-CD8 were administered *i.p.* at days -1, 0 and 7 days before/after chemotherapy and anti-PD-1 at days 8, 12 and 16 (A). Tumor size was assessed regularly and tumor growth of DACT versus Ctr (B), DACT + anti-CD4/CD8 versus anti-CD-4/anti-CD-8 (C) and DACT + anti-PD-1 versus anti-PD-1 (F) are depicted. Mean tumor area for each group was calculated and significances were tested using a type II ANOVA test (D, G). Overall survival is depicted and p-values were calculated with a Log-Rank test (E, H). * indicates the p-value of each treatment versus Ctr (D, E, G, H) and # indicating p-values of the DACT + anti-CD-4/anti-CD-8 versus DACT alone (D, E) and of DACT + anti-PD-1 versus anti-PD-1 alone (G, H) (*/#p<0.05 **/##p<0.01 ***/### p<0.001).

Inhibition of transcription by a panel of ICD inducers.

DACT is known to suppress the transcription of DNA to RNA (Bensaude, 2011; Goldberg et al, 1962; Goldberg et al, 1963). Accordingly, DACT reduced the incorporation of the mRNA precursor 5-ethynyl uridine (EU) into cells, as revealed by means of click biochemistry yielding a fluorescent signal (Jao & Salic, 2008). Astonishingly, a series of other established ICD inducers also inhibited transcription, as documented for the anthracyclines daunorubicine,

doxorubicin, epirubicin and mitoxantrone (Casares et al, 2005; Obeid et al, 2007b), oxaliplatin (Tesniere et al, 2010) and crizotinib (Liu et al, 2019b). Bortezomib, which has been identified as an ICD inducer on myeloma cells (Garg et al, 2017a; Spisek et al, 2007), had a rather partial effect and only at high doses. Several microtubular inhibitors (docetaxel, paclitaxel, vinblastine and vincristine) which induce CALR exposure yet have not been reported to induce ICD *in vivo* (Alagkiozidis et al, 2011; Senovilla et al, 2012; Wang et al, 2015b) had no effect on transcription. Cisplatin, a drug that is not considered as an efficient ICD inducer (Casares et al, 2005), had partial effects (**Figure 18A, B**). An alternative method for measuring stalled transcription consists in determining the separation of fibrillarin (a nucleolar marker) and nucleolin (which spreads from the nucleolus to the entire nucleus when rRNA synthesis is inhibited) by immunofluorescence (Peltonen et al, 2014; Sauvats et al, 2019). The profile of inhibition obtained using this assay was very similar to that obtained with EU (**Figure 18C, D, G**). Inhibition of mRNA translation into proteins was also measured by monitoring the incorporation of the amino acid analogue L-azidohomoalanine (AHA) into cells (Wang et al, 2017). In this assay, all the tested agents caused an at least partial inhibition of protein synthesis. The magnitude of inhibition of translation correlated with that observed for transcription (**Figure 18E, F, H**).

Of note, this inhibition of translation was fully observable in cells homozygous for a non-phosphorylatable eIF2 α mutation (eIF2 α S51A) generated by CRISPR-Cas9-mediated knock-in or when the downstream effects of p-eIF2 α were abolished by integrated stress response inhibitor (ISRIB). As a positive control, the ER stress inducer thapsigargin, known to inhibit translation downstream eIF2 α phosphorylation (Sidrauski et al, 2013), did not induce the inhibition of translation in eIF2 α S51A mutants or in ISRIB-treated cells (**Figure 19A**). Hence, the ICD-induced inhibition of translation is likely secondary to the inhibition of transcription rather than a direct effect of EIF2AK3 on the translation-relevant factor eIF2 α .

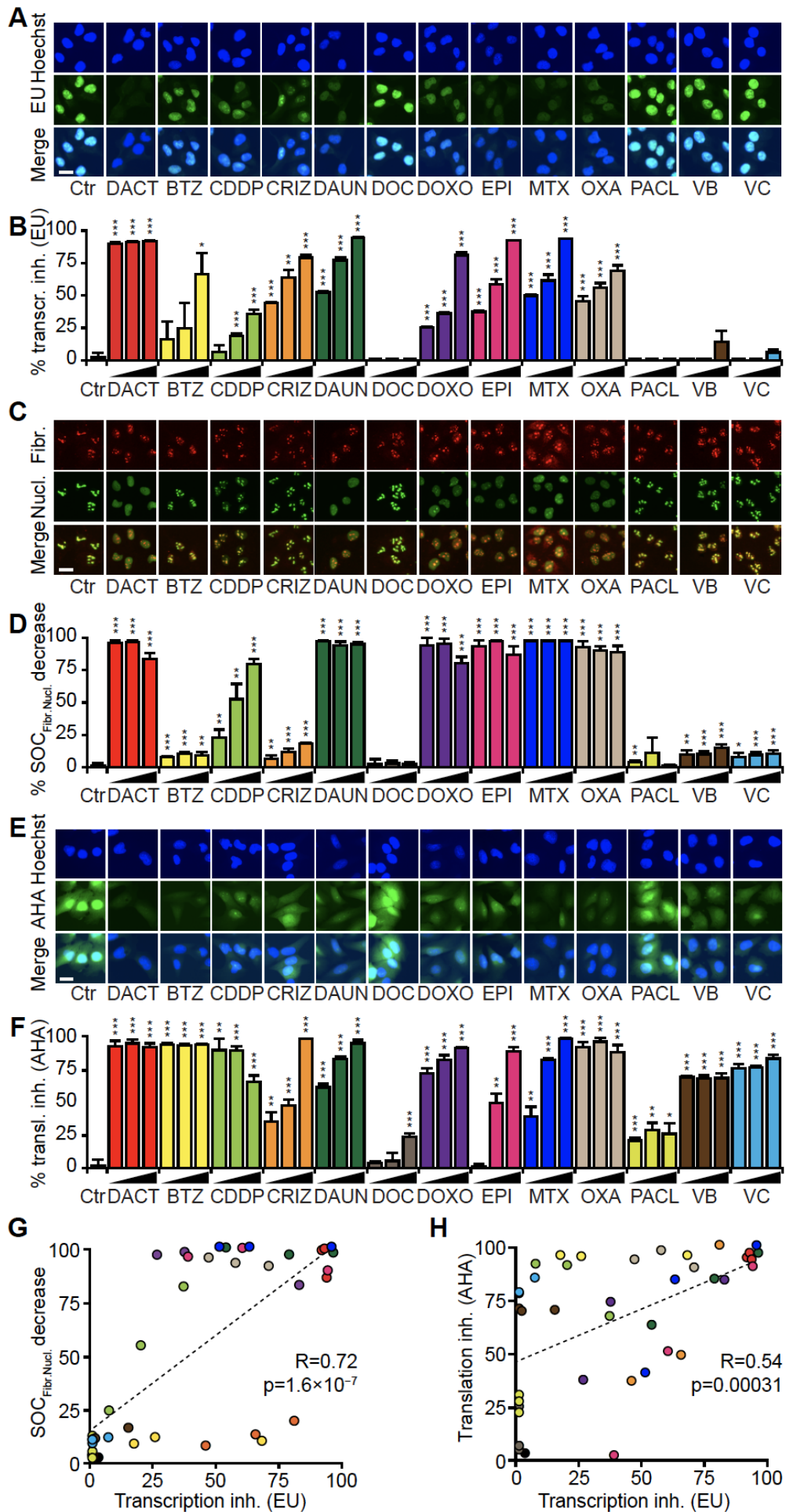


Figure 18. Inhibition of transcription and translation by ICD inducers. Human osteosarcoma U2OS cells were pre-treated with dactinomycin (DACT), bortezomib (BTZ), daunorubicin (DAUN), docetaxel (DOC), doxorubicin (DOXO), epirubicin (EPI), lurbinectedin (LURBI) mitoxantrone (MTX), paclitaxel (PACL), vinblastine (VB) and vincristine (VC) at 0.5, 1 and 5 μM ; with cisplatin (CDDP) at 75, 150 and 300 μM , with oxaliplatin (OXA) at 250, 500 and 1000 μM and with crizotinib (CRIZ) at 10, 20 and 40 μM for 1.5 to 2.5 h and followed by an additional hour of treatment in the presence of 100 mM 5-ethynyl uridine (EU). After fixation cells were permeabilized and EU was stained with an AlexaFluor-488-coupled azide. Representative images are shown (**A**). The EU intensity in the nucleus of each condition was ranked between the untreated control (Ctr, 0 % transcription inhibition) and the control that was not incubated with EU (corresponding to 100 % transcription inhibition) (**B**). Cells were treated for 2.5 h and then fixed and permeabilized. Following, cells were stained with a rabbit anti-fibrillarin antibody followed by a staining with an anti-rabbit AlexaFluor-647- or AlexaFluor-546-coupled secondary antibody as well as with a mouse anti-nucleolin antibody followed by a staining with an anti-mouse AlexaFluor-488-coupled secondary antibody. Then images were acquired and colocalization between both signals was assessed (**C**). The surface overlap coefficient (SOC) was calculated and ranked between the untreated control (Ctr) and the positive control (DACT) (**D**). Cells were pre-treated overnight with the aforementioned compounds in complete medium followed by washout and treatment pursued in methionine-free medium for 30 min. Following, the treatments were continued in methionine-free medium supplemented with 25 μM L-azidohomoalanine (AHA) for additional 1.5 h. AHA incorporation was detected after fixation, permeabilization and blocking by the addition of an AlexaFluor-488-coupled azide. Then images were acquired (**E**) and AHA intensity in the cells was ranked between the untreated control (Ctr, 0 % translation inhibition) and the untreated control without AHA (corresponding to 100 % translation inhibition). Cycloheximide at 50 μM was used as an additional control after pre-incubation and led to 100 % inhibition (data not shown) (**F**). Representative images of DACT 1 μM , BTZ 1 μM , CDDP 150 μM , CRIZ 20 μM , DAUN 0.5 μM , DOC 1 μM , DOXO 1 μM , EPI 1 μM , MTX 1 μM , OXA 500 μM , PACL 1 μM , VB 1 μM , VC 1 μM are shown (**A, C, E**). One representative experiment among three is shown \pm SD and p-values to the control were calculated with Student's t-test: * $p < 0.05$ ** $p < 0.01$ *** $p < 0.001$ (**B, D, F**). Correlation between the transcription measured by EU incorporation and measured by fibrillarin and nucleolin colocalization is depicted with Pearson correlation coefficient (R) and p-value (p) calculated with R (**G**). Same parameters are shown for correlation between transcription measured by EU incorporation and translation measured with AHA incorporation (**H**).

We also addressed the question as to whether ICD inducers must cause reversible or permanent inhibition of anabolic metabolism. For this, we designed a sort of run-on assay using the RUSH (retention using selective hooks) system (Zhao et al, 2018) in which an ER-targeted streptavidin protein retains GFP fused to a streptavidin-binding peptide (SBP) in the ER lumen. In the presence of biotin, the GFP signal is lost from the cells because most of the protein is released through the classical Golgi-dependent secretory pathway (Gomes-da-Silva et al, 2018; Zhao et al, 2018). However, upon washing (to remove biotin) and addition of avidin (to scavenge free biotin), neo-synthesized SBP-GFP is retained by streptavidin in the ER, leading to a progressive increase in fluorescence that directly measures protein synthesis (**Figure 19B**). Anthracyclines, oxaliplatin, crizotinib, DACT and lurbinectedin, which is known to inhibit transcription and has been recently described as an ICD inducer (Tumini et al, 2019; Xie et al, 2019a), largely prevented protein synthesis when continuously present in the system (**Figure 19C-F**). After its wash-out, cells could recover from crizotinib-mediated suppression of protein synthesis. In contrast, the wash-out of anthracyclines, DACT, oxaliplatin or lurbinectedin did not lead to the reestablishment of protein synthesis (**Figure 19C, E, G**). In sum, ICD-stimulatory anticancer drugs mediate inhibition protein synthesis, though with distinct degrees of reversibility.

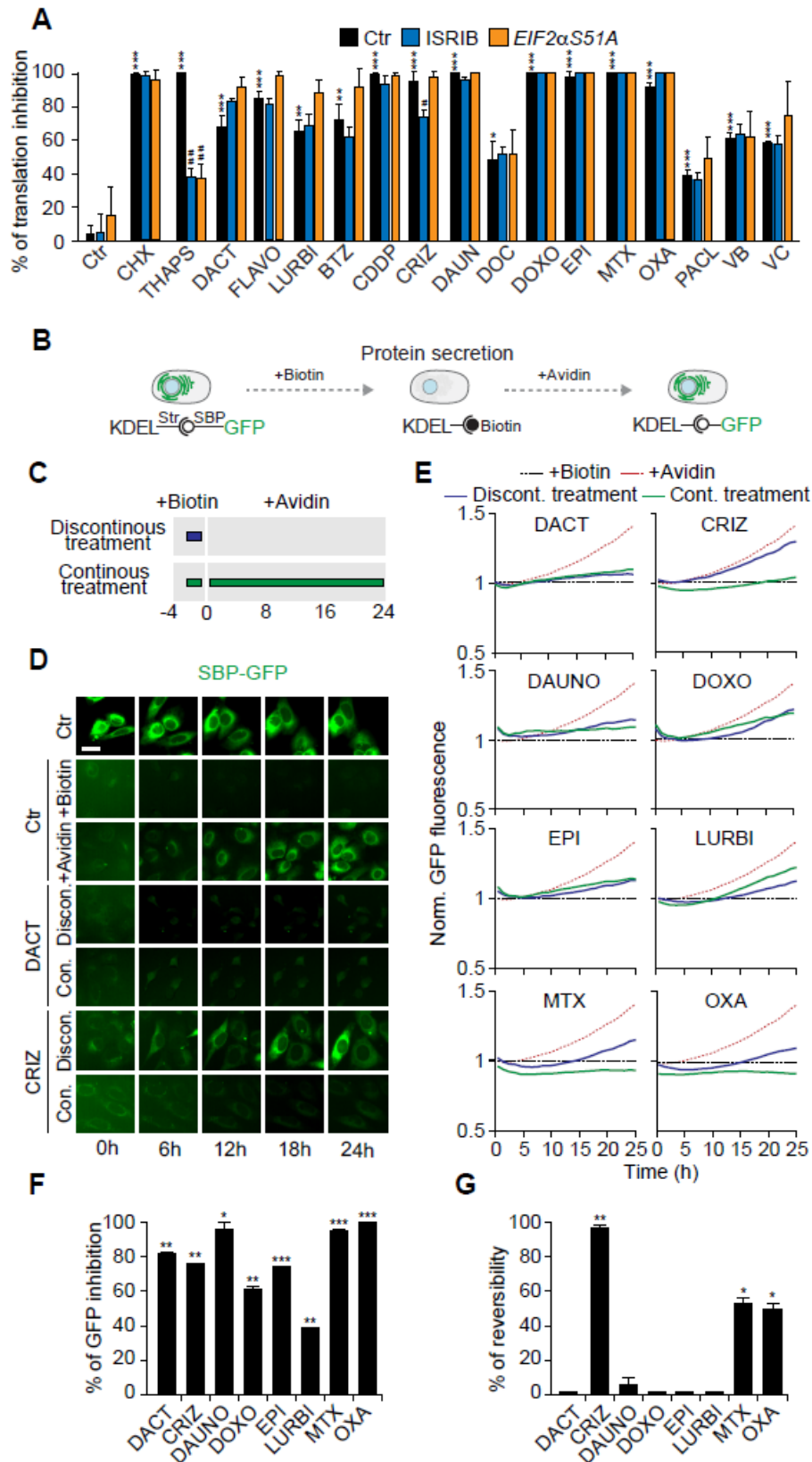


Figure 19. Mechanisms of inhibition of transcription and translation. U2OS wild-type, U2OS wild-type treated with 1 μ M ISRIB and U2OS eIF2 α S51A cells (three different clones) were used to assess if the inhibition of translation was dependent on eIF2 α phosphorylation. U2OS wild-type and the three U2OS eIF2 α S51A clones were pre-treated for 12 h with 3 μ M dactinomycin (DACT), 1 μ M flavopiridol (FLAVO), lurbnectedin (LURBI), 1 μ M bortezomib (BTZ), 150 μ M cisplatin (CDDP), 10 μ M crizotinib (CRIZ), 3 μ M daunorubicin

(DAUN), doxorubicin (DOXO), 5 μ M epirubicin (EPI), 3 μ M mitoxantrone (MTX), 500 μ M oxaliplatin (OXA), 3 μ M paclitaxel (PACL), 3 μ M vinblastine (VB) or 3 μ M vincristine (VC) or for 12 h (in the presence of ISRIB in the correspondent condition). Cells were further treated with the same drugs or with the controls, 50 μ M cycloheximide (CHX) or with 3 μ M thapsigargin (THAPS), for 30 min, in methionine-free medium, which was then supplemented with 50 μ M L-azidohomoalanine (AHA), a detectable analogue of methionine for an additional 1.5 h before fixation. Images were acquired by fluorescence microscopy and the percentage of translation inhibition is shown: fluorescent intensities were ranged between the untreated control (Ctr, 0 % inhibition) and a control that was not incubated with AHA (corresponding to 100 % inhibition). Results from one representative experiment among three is shown (mean \pm SD of quadruplicates) among three independent ones. The p-value of each treatment compared to the control in the wild-type cells was calculated using the Student's t-test: * $p < 0.05$ ** $p < 0.01$ *** $p < 0.001$. For one same treatment, the p-values in ISRIB-treated cells and eIF2 α S51A clones compared to the wild-type cells were calculated using the Student's t-test: # $p < 0.05$ ## $p < 0.01$ ### $p < 0.001$ (A). We used a Rush (retention using selective hooks) assay consisting of a GFP reporter coupled to a streptavidin binding peptide (SBP) that in the absence of biotin is retained by a streptavidin expressing hook in the endoplasmic reticulum, in order to evaluate the reversibility of transcription inhibition. Biotin has a high affinity to streptavidin and its addition leads to the release of the GFP reporter and its secretion via exocytosis. When biotin is removed and leftovers are sequestered by the addition of avidin, the GFP-reporter is retained inside the cells (B). Cells were pre-treated with 40 μ M biotin for 4 h and with 3 μ M doxorubicin (DOXO), 3 μ M daunorubicin (DAUN), 5 μ M epirubicin (EPI), 3 μ M mitoxantrone (MTX), 1 μ M bortezomib (BTZ), 1 μ M dactinomycin (DACT), 10 μ M crizotinib (CRIZ), 150 μ M cisplatin (CDDP) or 500 μ M oxaliplatin (OXA) for 2.5 h. After washout, cells were incubated with 1 μ M avidin to assess reversibility of the transcription inhibition (discontinuous treatment, blue line). As a positive control, cells were further treated in the presence of avidin (continuous treatment, green line). Other controls were performed: untreated control (Ctr), control with biotin pre-incubation only (+ Biotin), control with biotin pre-incubation followed by sequestration with avidin (+Avidin) (C). Then, images were acquired every hour for 24 h. Representative images of the different controls, as well as of CRIZ and DACT (continuous and discontinuous) treated cells are shown after background removal at each time point. (D). Green fluorescence intensity was normalized to biotin treated controls at each time point and kinetics is depicted (E). Protein inhibition is represented as slope of the continuous treatment, with the slope of the avidin condition corresponding to 0 % inhibition (F). Reversibility is depicted as the area between curves of continuous and discontinuous treatments, with the area between the curve of the control incubated with biotin the curve incubated with biotin and then avidin corresponding to 100 % reversibility (G).

Inhibition of transcription as an ICD hallmark.

In the next step, we addressed the question as to whether inhibition of RNA synthesis would be a general predictor of ICD. For this, we evaluated a homemade library of commonly used antineoplastic agents (Bezu et al, 2018a) for their capacity to inhibit RNA synthesis using the EU-based assay (Table S 2). We then correlated the level of transcriptional inhibition with the *in silico* ICD prediction score (Figure 20A), all major ICD hallmarks (Figure 20B-E) and their integration into the 'ICD score' (Bezu et al, 2018a) (Figure 20F). Note that vinca alkaloids affected the microscopical assessment of ICD parameters, due to their effect on microtubules, and behaved as outliers, as they failed to inhibit RNA synthesis, yet scored high in predicted ICD-related parameters. After their exclusion, all associations between RNA synthesis inhibition and ICD-related stress/death signals were significant, though with the highest Pearson coefficients for the correlation between, on one side, transcription inhibition and, on the other side HMGB1 release ($R=0.76$) or eIF2 α phosphorylation ($R=0.71$). Inhibition of transcription and translation were correlated (Figure 20G), and inhibition of translation correlated with most ICD hallmarks (Figure S 8, Table S 2).

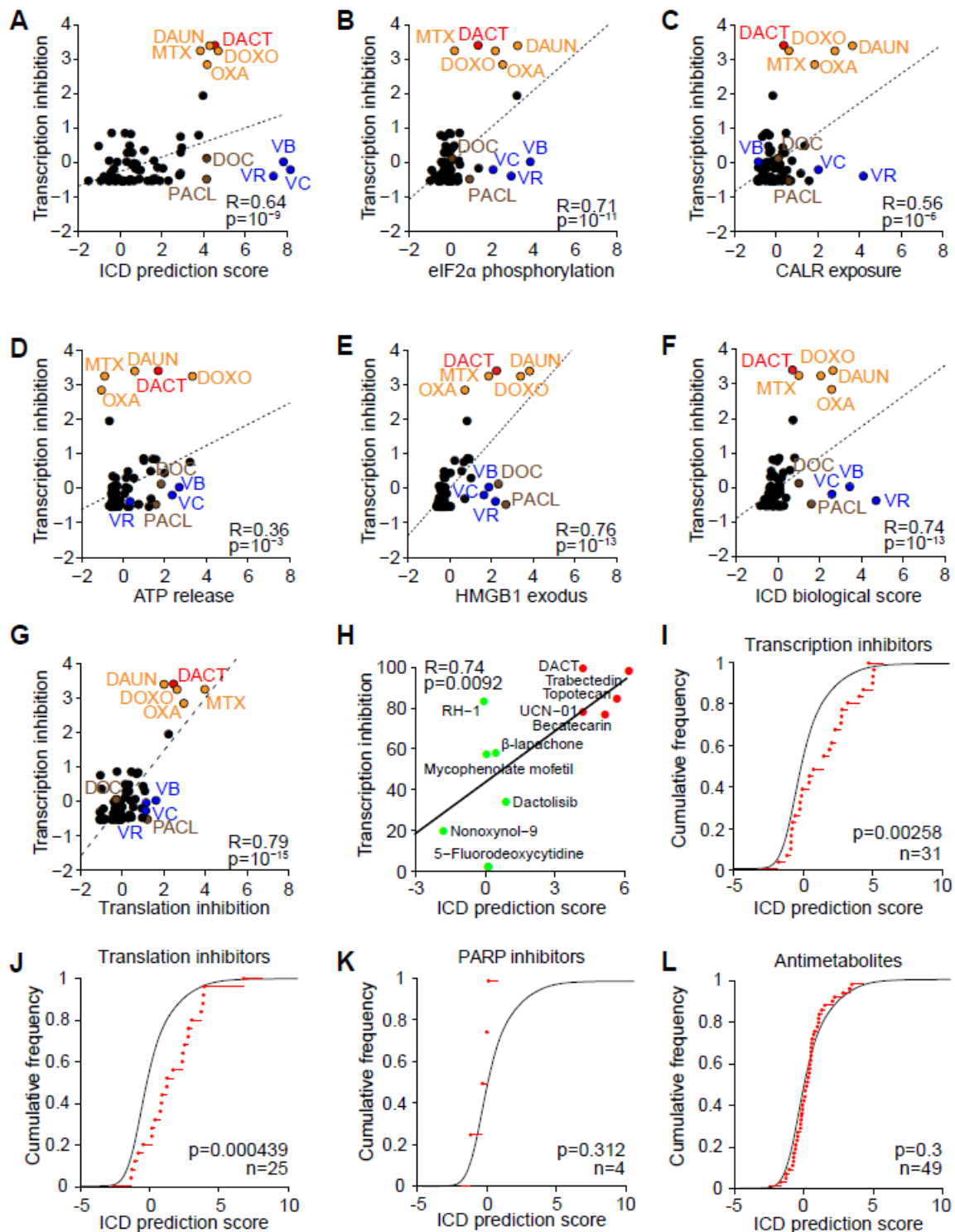


Figure 20. Validation of the inhibition of transcription as a hallmark of ICD at large scale. U2OS wild-type cells were treated with a custom made anti-cancer library previously described (Bezu et al, 2018a) at 3 μ M (A-G). For assessing transcription, cells were pre-treated for 1.5 h with the library followed by 1 h with the same drugs in which EU was added. For assessing translation, cells were pre-treated with the library for 12 h followed by 30 min in methionine free-medium, before addition of azidohomoalanine (AHA). Percentage of inhibition was calculated and transformed as z-scores. The correlations between transcription inhibition and ICD prediction score (A), peIF2 α expression (B), CALR exposure (C), ATP decrease (D), HMGB1 exodus (E), biological ICD score (F) previously measured and expressed as z-scores (except for ICD prediction score) (Bezu et al, 2018a), as well as

between transcription and translation inhibitions (**G**), were calculated with the Pearson method giving the correlation coefficient (R) and corresponding p-values (p). Known immunogenic drugs are indicated with colors: dactinomycin (DACT), mitoxantrone (MTX), doxorubicin (DOXO), daunorubicin (DAUN), oxaliplatin (OXA), docetaxel (DOC), paclitaxel (PACL), vinblastine (VB), vincristine (VC) and vinorelbine (VR) (A-G). The inhibition of transcription was assessed for the negative and positive ICD hits identified with the predictive algorithm (Fig. 1) U2OS cells were treated with the agents at concentrations corresponding to their IC₆₀: 1 μM dactinomycin (DACT), 50 μM topotecan, 1 μM becatecarin, 0.5 μM trabectedin, 5 μM UCN-01, 30 μM mycophenolate mofetil, 30 μM nonoxynol-9, 25 μM dactolisib, 2.5 μM β-lapachone, 5 μM 5-fluorodeoxycytidine and 2 μM RH-1 for 1.5 h followed by 1 h with EU. The percentage of transcription inhibition was calculated and the coefficient of correlation (R) and associated p-value (p) between the percentage of inhibition and the theoretical ICD score was calculated using the Pearson method (**H**). The 50,000 compounds of the NCI-60 library were annotated for different parameters including transcription and translation inhibition. The predicted ICD score was calculated with a previously described model built on artificial intelligence (Bezu et al, 2018a). Empirical cumulative frequency is plotted: in black for all compounds and in red for the compounds falling into the categories of interest which are transcription inhibitors (n=31) (**I**), translation inhibitors (n=25) (**J**), as well as two other random categories used as controls, PARP inhibitors (n=4) and antimetabolites (n=49) (**K**, **L**). The p-values calculated with a Kolmogorov-Smirnov test are indicated on each graph.

We also went back to the initial *in silico* screen (**Figure 13**) and compared the five compounds with the highest ICD prediction score having an IC₅₀ < 1 μM and that had been introduced into clinical assays (becatecarin, DACT, topotecan, trabectedin and UCN-01), as well as the six selected compounds with an ICD prediction score close to zero, always with an IC₅₀ < 1 μM and a clinical characterization (dactolisib, 5-fluorodeoxycytidine, β-lapachone, mycophenolate mofetil, nonoxynol-9 and RH-1). Consistently, if used at their IC₆₀ (**Figure S 2**) on U2OS cells, the five compounds with a high ICD prediction score were more efficient in suppressing RNA synthesis than the six compounds with a low ICD prediction score (**Figure 20H**, **Table S 3**).

We then subjected the 50,000 compounds library (Shoemaker, 2006) to data mining to identify agents that are annotated as inhibitors of transcription (n=31) or translation (n=25) or, as internal controls, as PARP inhibitors (n=4) or antimetabolites (n=45) (**Table S 4**). The calculated ICD prediction score was significantly higher than expected for transcription and translation inhibitors but not for PARP inhibitors and antimetabolites (**Figure 20I-L**, **Figure S 9**). This observation lends further support to the idea that the inhibition of transcription/translation is a major hallmark of ICD.

Supplementary figures and tables

eIF2 α S51A:

```

1  TTTTTCCTTT ATATAGTGAG TGGTAGCGTA TACAATGTTT GCTCACTTCG
51  GCAAAGAGTA GCTTTAGTTT TCTGATTAGT TATAATAGTG ATGCTTCCCA
101 TCATTTGATA TGCCTTAAAG TAGTATTTTA CTCTTGAGGT ATTCCTTTAA
151 TCCTTAGGTC TTGGAGTACT TTATAGATGG TCATTATTTT TTATGATTCC
201 TCTGAAACTA AAGGCAGAGA ATCACCCAAG CATTACAAAA ATGTTGAGCA
251 AAATAAAAAT TAAAGCTTGG TTCCTGAACA TTATCTGTTT TCTGGTACCA
301 CTTAAGAAGT TTCAAAGGAT GAGAAGACTA AGACTAATAA CTATTTTTTT
351 CTTCATCTTT TCTTTCAGTG GCAGGATGTG GAAATTGATT TTTTTTTTAT
401 TTTACCTTA ACTGAATACT TACTTAATTC TTTTGTTTAA ATTGCAGAAT
   Pro Gly Leu Ser Cys Arg Phe Tyr Gln His Lys Phe Pro Glu Val Glu
451 GCCGGGTCTA AGTTGTAGAT TTTATCAACA CAAATTTTCT GAGGTGGAAG
   Asp Val Val Met Val Asn Val Arg Ser Ile Ala Glu Met Gly Ala Tyr Val
501 ATGTAGTGAT GGTGAATGTC AGATCCATTG CTGAAATGGG GGCTTATGTC
   Ser Leu Leu Glu Tyr Asn Asn Ile Glu Gly Met Ile Leu Leu Ser Glu Leu
551 AGCTTGCTGG AATACAACAA CATTGAAGGC ATGATTCTTC TTAGTGAATT
   Ala Arg Arg Arg Ile Arg Ser Ile Asn Lys Leu Ile Arg Ile Gly Arg
601 AGCACCGAAGG CGTATCCGTT CTATCAACAA ACTCATCCGA ATTGGCAGGA
   Asn Glu Cys Val Val Val Ile Arg Val Asp Lys Glu Lys
651 ATGAGTGTGT GGTGTTCATT AGGGTGGACA AAGAAAAAGG TAAGTGAGAA
701 AAATATCTGT AATATAAATT TCAGATTTAA AATGGTTTAT TTAAAAATAC
751 ATTTTTTTGTA AATTGCAAGC TGCAGCTTAA AAAAAAAGC TCCTTTTATA
801 CTAAACCTT TTACATACAA AGTTGTTAGA AAAGGATGCC AATTAGCTAT
851 CTAAGCAAGA TCTCTTAATA GTAGTTTAAT TAGTACATCC TAGGATTTTA
901 TGGATCAGAT AACTTGAATT TTATTTCTAG TGTTTATCAG GATCTTGATA
951 ATTGACTCAT GGTAACCAAA CTTAGAGACA GGTAAGTCAG AGTACTAGTT
1001 CATTACATT GGTAGGCCTG AATATGTTGG ATGCCTTTTT CTTGATTTAA
1051 AGCTAAAATA GTAATGAGAT CACTGGGTAA GCATGAAAAT GGGGCAAATG
1101 GATTTTAGGG ATCTTTTATA TAAGCTTTGA AAAAGCAATA TACTATGCGT
1151 GTATATACAC ACCTGAAATC CAACATTGTA TATCTTGCTG GTAATTAGAA
1201 TGTTTCTCGA G

```

Figure S 1. Sequence for the eIF2 α knock-in mutation. To construct the eIF2 α non-phosphorylatable cell line (U2OS RFP-LC3 eIF2 α S51A), U2OS RFP-LC3 cells were co-transfected with a pX458 plasmid containing Cas9 and gRNAs to break the DNA at the appropriate site, together with a plasmid containing the DNA sequence of replacement given here. The objective is to replace serine in position 51 by an alanine, so to replace a TCC by a GCA on the gene sequence as marked in red. Moreover, to avoid further DNA breaks after insertion of the knock-in sequence, different other nucleotides were exchanged which do not modify the protein sequence. The corresponding amino acids of the coding sequence are indicated.

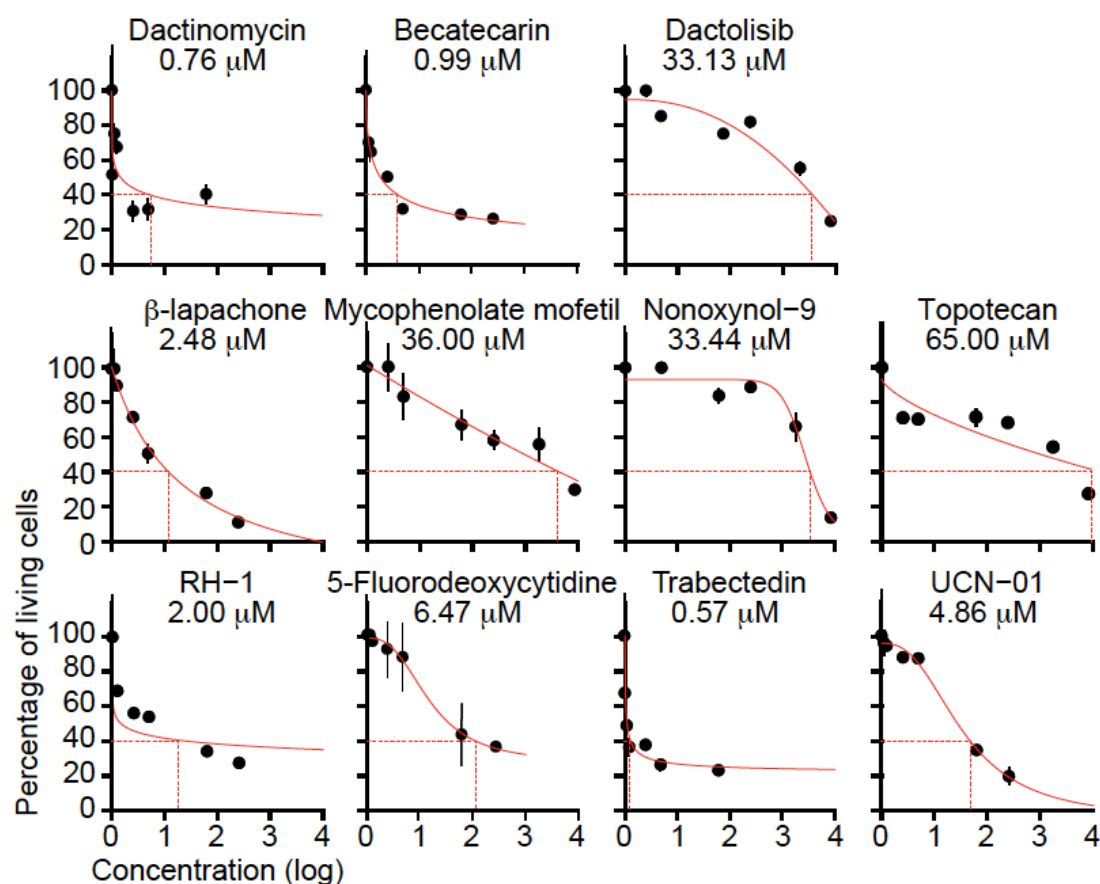


Figure S 2. IC₆₀ of predicted ICD inducers. To determine the IC₆₀ (concentration for which the agent leads to 40 % live cells after 24 h), we treated human osteosarcoma U2OS wild-type cells with a range of concentrations from 0.01 to 5 μM for dactinomycin and trabectedin; from 0.05 to 10 μM for becatecarin, RH-1, β-lapachone and 5-fluorodeoxycytidine; from 0.5 to 50 μM for dactolisib, UCN-01, topotecan and mycophenolate mofetil and from 1 to 100 μM for nonoxynol-9. Cells were further stained with Hoechst and PI. The mean ± SD of the percentage of living cells (normal-sized, Hoechst^{low}, PI) according to drug concentration represented after logarithmic-transformation ($\ln(\text{concentration}_{\mu\text{M}} + 1)$) for one representative experiment with quadruplicates is depicted. A log-logistic regression was performed allowing determination of the concentration leading to 40 % cells alive (IC₆₀). The indicated IC₆₀ are the mean of the IC₆₀ obtained in one to three independent experiments.

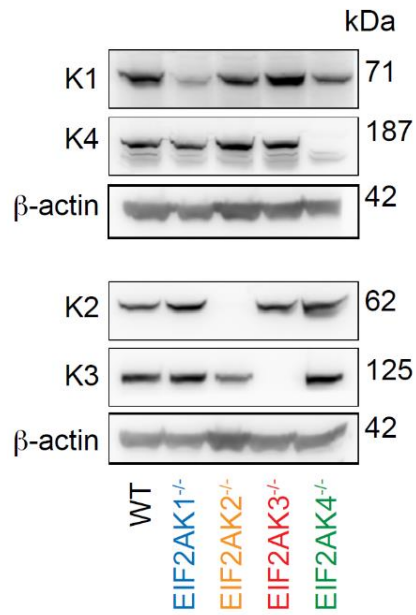


Figure S 3. Validation of the eIF2 α kinases knock out. U2OS cells were knocked out for each of the four eIF2 α kinases using the CRISPR-Cas9 technology. One knock-out clone was selected for each kinase and was further validated by immunoblot with HRI (K1) and GCN2 (K4) on one and PKR (K2) and PERK (K3) on a parallel blot. Both membranes were further probed with anti β -actin antibody as a loading control.

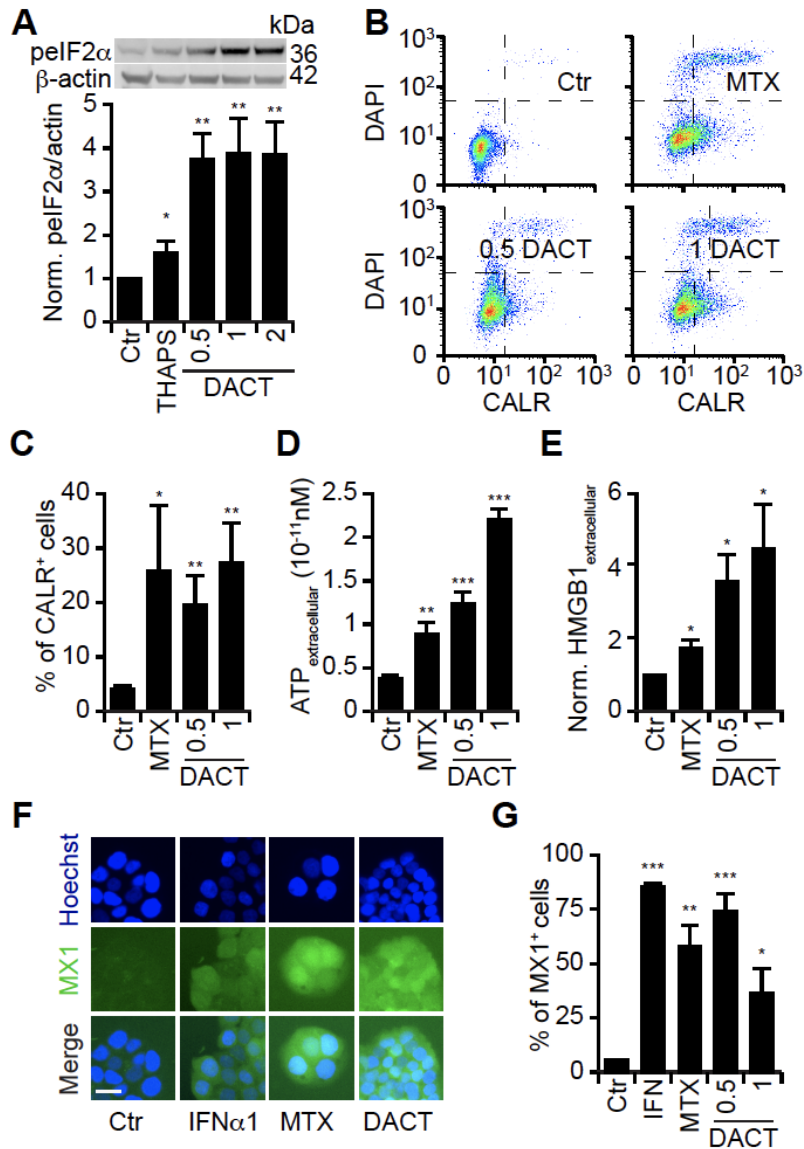


Figure S 4. Immunogenic cell death hallmarks in mouse cancer cells. Mouse fibrosarcoma MCA205 cells were treated with 0.5, 1 or 2 μ M dactinomycin (DACT) for 6 h. Thapsigargin (THAPS) at 3 μ M was used as a positive control. Cells were harvested and subjected to SDS-PAGE. The phosphorylation of eIF2 α was quantified by means of phosphoepitope-specific eIF2 α antibody. The graph represents pEIF2 α intensity normalized with β -actin intensity for each band (A). MCA205 cells were treated with dactinomycin (DACT) at a concentration of 0.5 and 1 μ M. Mitoxantrone (MTX) was used at 4 μ M as a positive control. Cells were treated with these for 6 h and then medium was refreshed. 24 h later, cells were collected and surface exposed calreticulin (CALR) was stained with an antibody specific for CALR. DAPI was used as an exclusion dye and cells were acquired by flow cytometry. The mean \pm SEM of the percentage of CALR⁺ cells among viable (DAPI⁺) ones in six independent experiments is depicted (B, C). MCA205 cells were treated as described above for 24 h. Concentration of secreted ATP in the supernatants was quantified with a luciferase-based bioluminescence kit. The mean \pm SD of one representative experiment among three is shown (D). MCA205 cells were treated as described above for 24 h and the concentration of HMGB1 in the supernatants was quantified with an ELISA kit. The mean \pm SEM of four independent experiments is depicted (E). MCA205 cells were treated as described above for 6 h. Then medium was changed and 24 h later, type I interferon response was assessed by transferring the supernatant on HT29 MX1-GFP reporter cells lines cells for additional 48 h. Some cells were incubated with interferon α 1 (IFN α 1) for 48 h as an additional control. Images were acquired by fluorescence microscopy; representative images of Ctr, IFN α 1, MTX and DACT 1 μ M are shown (F). The number of positive cells was assessed based on the distribution of cellular green fluorescence intensity in IFN α 1 versus control (Ctr) conditions. The mean \pm SEM of five independent experiments is depicted (G). P-values to the control were calculated with a Student's t-test: *p<0.05 **p<0.01 ***p<0.001 (A, C, D, E, G).

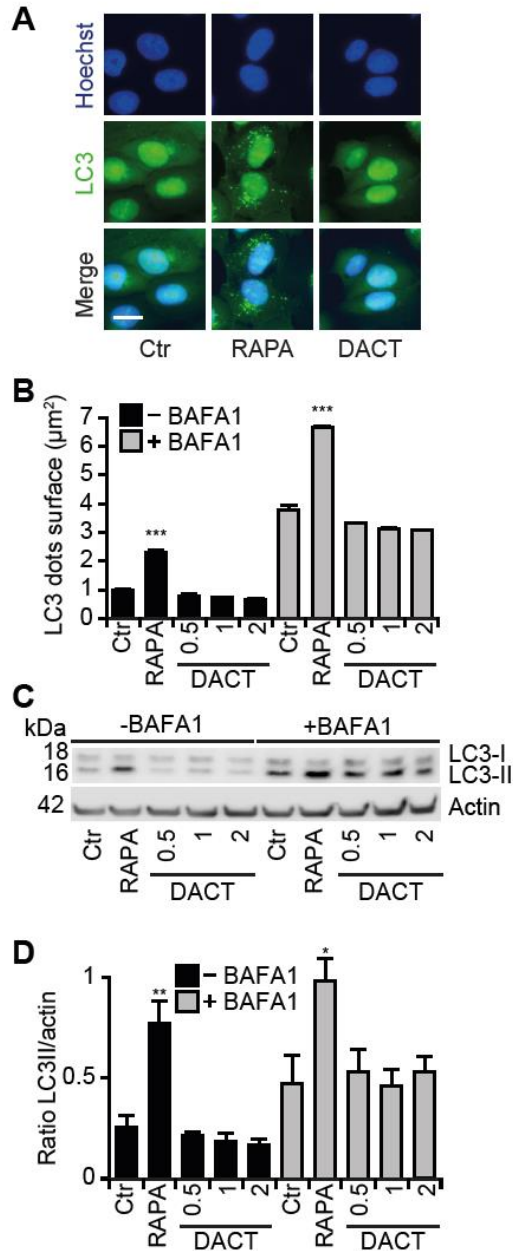


Figure S 5 DACT-induced ATP release does not require autophagy. U2OS LC3 GFP cells were treated with rapamycin (RAPA) or dactinomycin (DACT) at 0.5, 1 or 2 μM for 6 h. During the last 2 h of treatment, bafilomycin A1 (BAFA1) was added in the appropriate conditions. Images were acquired by fluorescence microscopy; representative images of Ctr, RAPA and DACT 1 μM are shown (A). LC3 dots were segmented and their total surface per cell normalized on the control are depicted. P-values to the respective Ctr were calculated with a Student's t-test: *** $p < 0.001$ (B). MCA205 fibrosarcoma were treated with RAPA or DACT at 0.5, 1 or 2 μM for 6 h. During the last 2 h of treatment, BAFA1 was added into the appropriate conditions. Cells were collected and subjected to immunoblotting (C). The amount of LC3II normalized by the loading control actin for each band is represented in the bar chart. P-values to the respective Ctr were calculated with a Student's t-test: * $p < 0.05$ ** $p < 0.001$ (D).

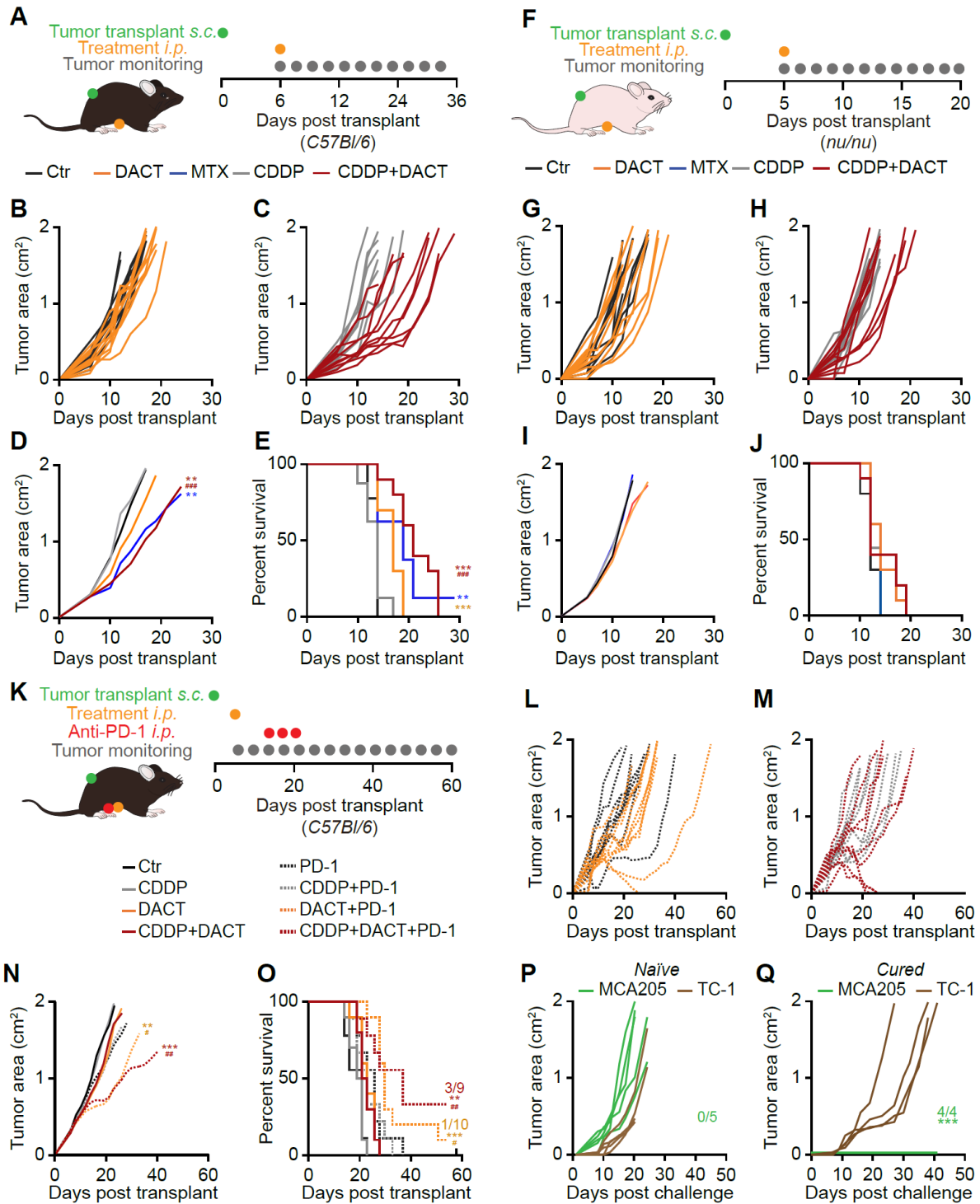


Figure S 6. DACT sensitizes MCA205 to CDDP in an immune-dependent manner and to immunotherapy. 3×10^5 mouse fibrosarcoma MCA205 cells were injected subcutaneously (*s.c.*) into the flank of immunocompetent syngeneic C57BL/6 mice with *n* mice per group ($n=8$ for MTX, $n=9$ for CDDP or $n=10$ for Ctr, DACT and CDDP + DACT) (A-E) or athymic immunodeficient *nu/nu* mice ($n=10$ per group) (F-J). When tumors became palpable, the mice were treated intraperitoneally (*i.p.*) with injectable solution (Ctr), 5.17 mg/kg mitoxantrone (MTX), 0.5 mg/kg cisplatin (CDDP), 0.5 mg/kg dactinomycin (DACT) or the combination of CDDP + DACT. Tumor size was assessed regularly and tumor growth of DACT versus controls Ctr (B, G) and DACT + CDDP versus CDDP alone (C, H) is depicted. Mean tumor area for each group was calculated and significances were tested using a type II ANOVA test (D, I). Overall survival is depicted and p-values were calculated with a Log-Rank test (E, J).

* indicates the p-value of each treatment versus Ctr control and # indicating p-values of the combination treatment versus CDDP alone (*/#p<0.05 **/##p<0.01 ***/### p<0.001) (**D**, **E**). 1×10^5 MCA205 cells were injected subcutaneously (*s.c.*) into the flank of immunocompetent syngeneic C57BL/6 mice (n=10 for Ctr, Ctr + anti-PD-1, CDDP + anti-PD-1 and CDDP + (DACT + anti-PD-1; n=9 for CDDP, DACT, DACT + anti-PD-1, CDDP + DACT) (**K**). When tumors became palpable, mice were treated intraperitoneally (*i.p.*) with injectable solution, 0.5 mg/kg CDDP, 0.5 mg/kg DACT or the combination of CDDP + DACT. At days 6, 10 and 14 after chemotherapy, mice were treated *i.p.* with 100 μ g anti-PD-1 per mouse or a corresponding isotype. Tumor size was assessed regularly and tumor growth of DACT + PD-1 versus PD-1 alone (**L**) and DACT + CDDP + PD-1 versus CDDP + PD-1 (**M**) is shown. Mean tumor area for each group was calculated and significances were determined using a type II ANOVA test (**N**). Overall survival is depicted and p-values were calculated with a Log-Rank test (**O**). * indicate the p-value of DACT + anti-PD-1 or CDDP + DACT + anti-PD-1 versus the respective conditions without anti-PD-1; # indicates the p-values of DACT + anti-PD-1 or CDDP + DACT+anti-PD-1 compared to the respective conditions without DACT (*/# p<0.05 **/## p<0.01 ***/### p<0.001) (**N**, **O**). The four surviving mice from this experiment were rechallenged with MCA205 and TC-1 cells injected in opposite flanks. Five naïve mice were co-injected as controls. Individual growth curves of both MCA205 and TC-1 tumors are depicted for cured (**P**) and naïve mice (**Q**). The tumor area formed by MCA205 growth in cured mice was compared to the one in naïve mice was calculated using a type II ANOVA test (**p<0.001) (**Q**).

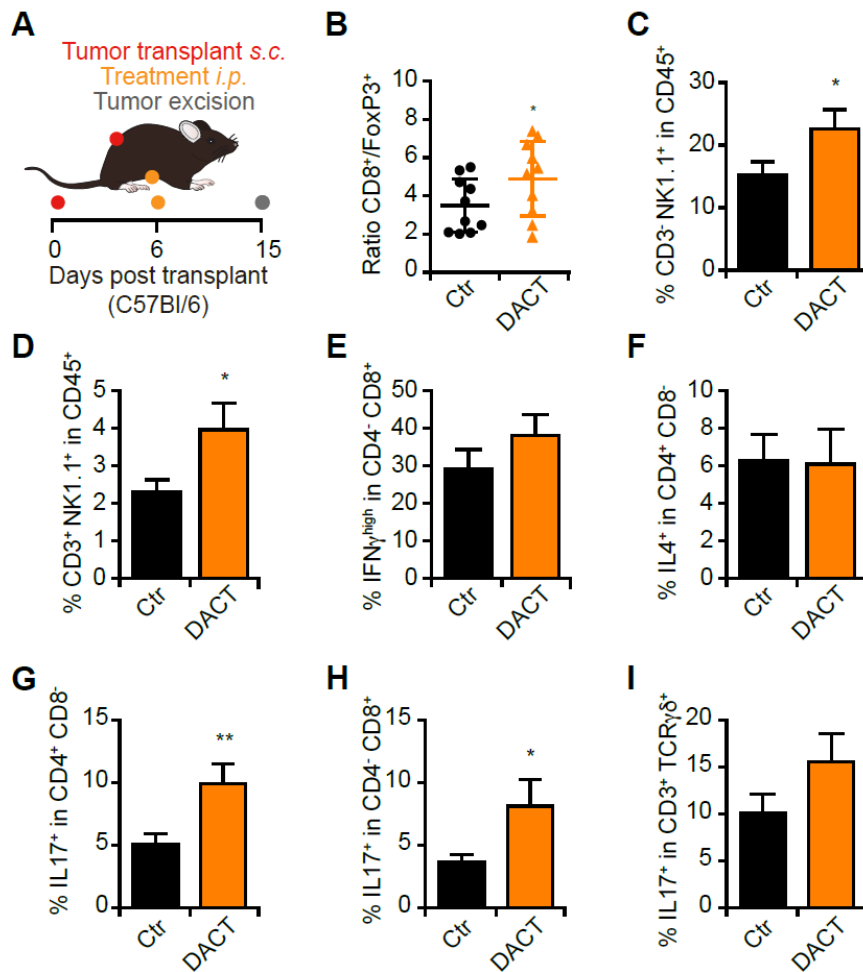


Figure S 7. T cell immune response induced by dactinomycin. 2×10^5 mouse fibrosarcoma MCA205 cells were injected subcutaneously (*s.c.*) into the flank of immunocompetent syngeneic C57BL/6 mice (n=10 per group). When tumors became palpable, injectable solution (Ctr) or 0.5 mg/kg dactinomycin (DACT) was administered intraperitoneally (*i.p.*). Nine days after chemotherapy, the mice were sacrificed, the tumors were collected and processed (A). 50 mg of tumors were used for each panel of staining, the “T-cell panel” with n=10 mice per group and the “NK cells and cytokines panel” with n=9 mice for Ctr group and n=8 mice for DACT group. The “T cell panel” included staining of CD4, CD8a and FoxP3 receptors. After staining with the corresponding antibodies, samples were run through a flow cytometer and analyzed with the FlowJo software. A boxplot of the ratio of the number of CD8a⁺ cells versus the number CD4⁺FoxP3⁺ cells in each tumor is depicted with each dot corresponding to one mouse (B). The “NK cells and cytokines panel” included CD45, CD3g,d,e, CD8a, CD4, NK1.1, TCR $\gamma\delta$, IL17a, IFN γ and IL4. The mean \pm SEM of the percentage of CD3g,d,e⁺NK1.1⁺ (C) and CD3g,d,e⁺NK1.1⁺ cells (D) among all CD45⁺ cells are depicted. The mean \pm SEM of the percentage of IFN γ ^{high} cells among CD4⁻CD8a⁺ T cells (E) and of IL4⁺ cells among CD4⁺CD8a⁻ T cells (F) is depicted. The mean \pm SEM of the percentage of IL17a⁺ positive cells among the CD4⁺CD8a⁻ T cells (G), among CD4⁻CD8a⁺ T cells (H) and among CD3⁺TCR $\gamma\delta$ ⁺ are shown (I). P-values to the Ctr group were calculated using a Student’s t-test: *p<0.05 **p<0.01 ***p<0.001 (B-I).

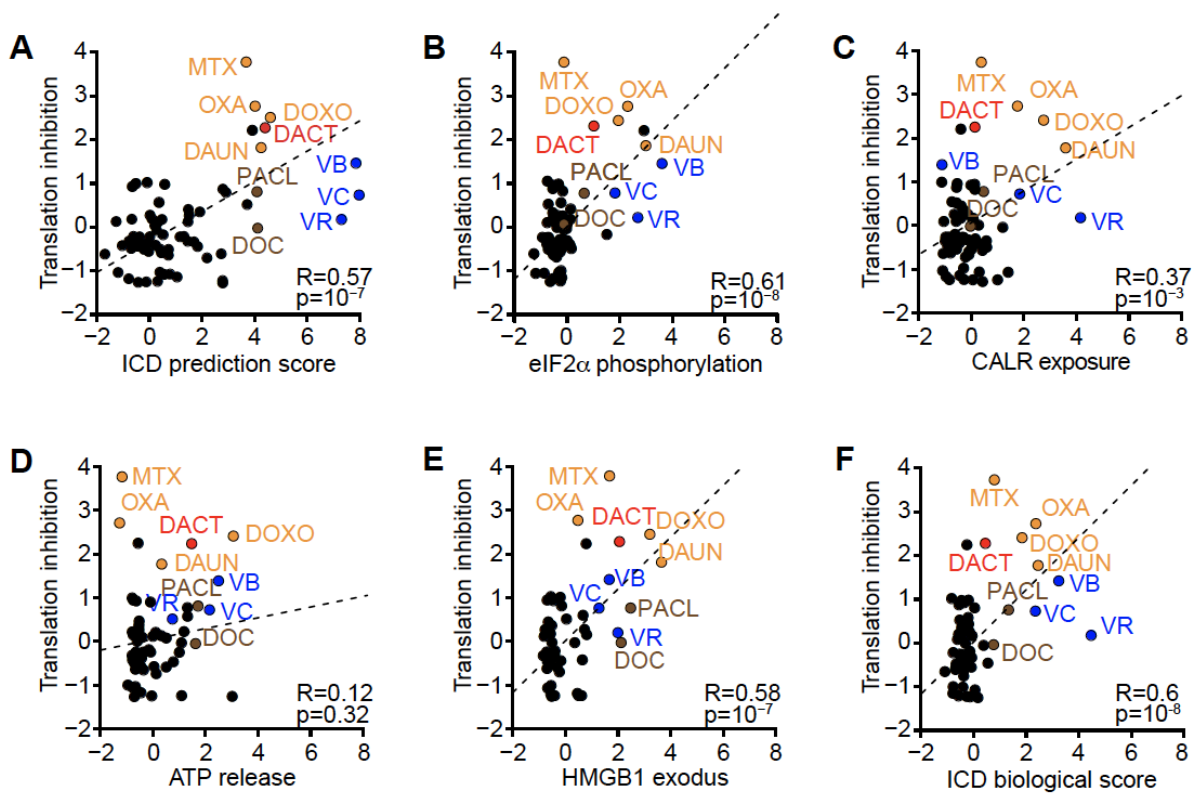


Figure S 8. Translation inhibition correlates with the hallmarks of ICD. U2OS wild-type cells were pre-treated for 12 h with a custom made anti-cancer library previously described (Bezu et al, 2018a) at 3 μ M followed by 30 min treatment in methionine free medium, before addition of azidohomoalanine (AHA). The percentages of inhibition of translation were transformed as z-scores. Correlation between translation inhibition and ICD prediction score (A), peIF2 α expression (B), CALR exposure (C), ATP decrease (D), HMGB1 decrease (E) and with biological calculated ICD score (F) previously measured and also expressed as z-scores (Bezu et al, 2018a), were calculated by the mean of the Pearson method resulting in a correlation coefficient (R) and corresponding p-value (p). Known immunogenic drugs are highlighted with colors: dactinomycin (DACT), mitoxantrone (MTX), doxorubicin (DOXO), daunorubicin (DAUN), oxaliplatin (OXA), docetaxel (DOC), paclitaxel (PACL), vinblastine (VB), vincristine (VC) and vinorelbine (VR) (A-F).

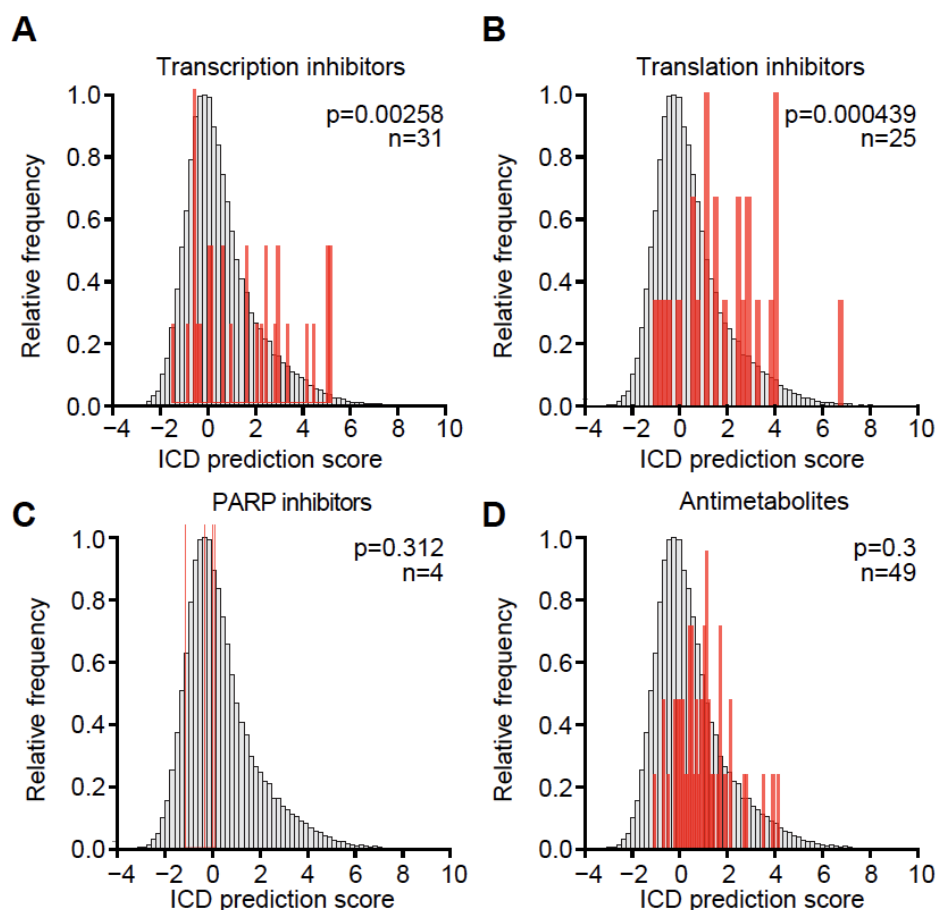


Figure S 9. Transcription and translation inhibitors are predicted as ICD inducers. The 50,000 compounds of the NCI-60 library were annotated for different parameters including transcription and translation inhibition. The predicted ICD score was calculated with a previously described model built by artificial intelligence (Bezu et al, 2018a). Data as in **Figure 20I-L** are depicted here as frequency normalized to the maximum frequency in relation to ICD scores. The distribution for all compounds is plotted in grey. In red, compounds falling into categories of interest are depicted which are transcription inhibitors ($n=31$) (**A**), translation inhibitors ($n=25$) (**B**) as well as two other random categories chosen as controls, PARP inhibitors ($n=4$) and antimetabolites ($n=49$) (**C**, **D**). The p-values (p) calculated with Kolmogorov-Smirnov test are indicated on each graph.

Cell line construction	Name	Sequence	Purpose	
eIF2 α S51A	474CRISPRoligo_Hh-chr14_S	CACCGTTCCTAGTGAATTATCCAGA	sgRNA to insert into a CRISPR-Cas9 vector (pX458) for eIF2 α knock-in	A
	475CRISPRoligo_Hh-chr14_AS	AAACTCTGGATAATTTCACTAAGAAC		
	478EIF2A_seqF	GTGGCAGGATGTGGAAATTGATT	primers to perform PCR to amplify eIF2 α mutated region before sending for sequencing	B
	479EIF2A_seqR	TCTCACTTACCTTTTCTTTGTCCAC (gtggacaagaaaaaggttaagtgaga)		
	482EIF2A_seq	AGAATGCCGGGTCTAAGTTGT	to sequence mutated eIF2 α region	C
eIF2AK1 ^{-/-}	K1 gRNA	TATTCGGGGTCCGGGCCTCGG	gRNAs in a U6gRNA-Cas9-2A-RFP (Sigma-Aldrich)	D
eIF2AK2 ^{-/-}	K2 gRNA	TTCAGGACCTCCACATGATAGG		
eIF2AK3 ^{-/-}	K3 gRNA	AGGTATATCTGTTTCTGCTCTGG		
eIF2AK4 ^{-/-}	K4 gRNA	GAACGGCTGCCATTCTACATGG		

Table S 1. DNA sequences for U2OS eIF2 α S51A and eIF2AK^{-/-} generation. To construct the eIF2 α non-phosphorylatable cell line (U2OS RFP-LC3 eIF2 α S51A), U2OS RFP-LC3 cells were co-transfected with a homology repair oligo coding for the knock-in mutation (**Table S 1**) together with a pX458 plasmid containing Cas9 and specific gRNAs whose sequences are given (**A**). After transfection, the DNA of cells that were able to proliferate was collected and amplified by PCR (**B**) before sending them for sequencing (**C**). To construct the eIF2 α kinases knock out cell lines (U2OS GFP-LC3 eIF2AK1^{-/-}, eIF2AK2^{-/-}, eIF2AK3^{-/-} and eIF2AK4^{-/-}), cells were transfected with all-in one plasmid from Sigma-Aldrich containing Cas9 and the indicated gRNAs (**D**).

DRUG	TRANSCRIPTION			TRANSLATION		
	MEAN	SD	PVAL	MEAN	SD	PVAL
CONTROL	0	0	1	1.605149831	1.927570339	1
ALLOPURINOL	0	0	1	18.05655325	3.541557537	0.005286126
ALTRETAMINE	3.394628788	3.799518783	0.261823223	16.68488961	2.682102288	0.002049494
AMINOLEVULINIC ACID	1.813436482	1.864756618	0.23414556	29.84314879	3.544350701	0.001050216
ANASTROZOLE	1.444939972	2.502709446	0.422649731	1.865462359	3.231075586	0.911613609
ARSENIC TRIOXIDE	1.070043951	1.099597567	0.233935876	26.80346906	1.482308012	8.91472E-05
AZACITIDINE	7.920171172	2.494067482	0.031500642	14.20493735	5.661146931	0.049117728
BENDAMUSTINE HCL	12.00498106	2.090029957	0.009952663	15.00957692	5.253004828	0.035177115
BUSULFAN	12.47561556	2.41820293	0.012293452	43.78590935	1.058510423	4.56118E-05
CAPECITABINE	0	0	1	19.77429635	4.760417133	0.012558631
CARBOPLATIN	0.467709585	0.422144676	0.194986553	4.586371037	7.943827658	0.586147718
CARMUSTINE	0	0	1	0.755182882	1.308015121	0.566095029
CELECOXIB	1.171403294	2.028930022	0.422649731	17.80154202	3.211330152	0.003617172
CHLORAMBUCIL	2.910934664	3.55261988	0.291649298	28.02751826	5.428095007	0.007821395
CISPLATIN	62.74371383	2.148502041	0.000390621	69.24183252	0.621762157	1.76495E-13
CLADRIBINE	25.96279064	1.120014994	0.000619755	23.93571675	11.88085839	0.079195962
CLOFARABINE	34.55271761	5.602076353	0.072667464	36.22798114	5.272629828	0.0036289
CRIZOTINIB	14.76889075	5.187006517	0.038742819	15.59663918	2.693351614	0.002701878
CYCLOPHOSPHAMIDE	4.499610478	7.774320499	0.421698675	19.93084032	2.365820661	0.000591848
CYTARABINE HCL	20.73766941	2.608142063	0.005231221	27.6106536	2.097560927	9.80684E-05
DACARBAZINE	0	0	1	3.440281102	5.958741661	0.654425878
DACTINOMYCIN	99.62125337	0.656008415	1.44539E-05	69.84188281	4.551413264	0.000323415
DAUNORUBICIN HCL	99.3333064	1.154747182	4.50436E-05	60.81296942	5.038817843	0.000775438
DECITABINE	0	0	1	16.81537417	2.300901429	0.01064565
DEXRAXOXONE	0	0	1	18.11229036	5.197964407	0.021039476
DOCEAXEL	16.48836423	1.60214901	0.003132457	24.10326014	4.033420801	0.00377287
DOXORUBICIN HCL	95.50723329	7.781700211	0.002205548	73.14931089	3.182070525	2.79714E-05
ESTRAMUSTINE DISODIUM PHOSPHATE	0	0	1	11.94125616	13.57659891	0.317381738
ETOPOSIDE	5.7160229	1.071770703	0.011517045	0	0	0.285966809
EVEROLIMUS	14.90929683	3.428301152	0.017172056	33.32936464	3.120480939	0.000357655
EXEMESTANE	0	0	1	20.18199456	6.012057364	0.024437286
FLOXURIDINE	0	0	1	44.42586651	4.453651923	0.001016022
FLUDARABINE	1.615507472	1.849193246	0.269408016	26.68512437	0.623201572	0.000818852
FLUOROURACIL	1.901903975	3.278963145	0.420865972	15.0983535	3.743427123	0.011625063
FULVESTRANT	9.353767625	1.866993709	0.013020985	31.65003912	4.673508988	0.003228844
GEFITINIB	2.124156428	0.94025238	0.05953897	13.88203602	2.040264568	0.001648783
GEMCITABINE HCL	34.94188763	0.439327387	5.269E-05	29.80055918	5.846009345	0.008569605
HYDROXYUREA	4.19369384	5.551862208	0.320905829	12.55182133	5.257453869	0.055310899
IFOSFAMIDE	0	0	1	44.96896635	3.287701996	0.000178025
IRINOTECAN HCL	21.06256936	4.411228451	0.014307896	42.5966317	4.204234863	0.000861376
LETROZOLE	0	0	1	4.608336701	4.278902939	0.354299644
LOMUSTINE CCNU	16.87070103	1.075880815	0.001352879	41.38445214	0.644994883	0.000251301
MEGESTROL ACETATE	0	0	1	10.72204661	3.44326966	0.025667211
MELPHALAN	0	0	1	13.73675395	1.655573604	0.001285376
MERCAPTOPYRINE	8.728407706	3.226917603	0.042665498	15.6537819	5.621650534	0.038017879
METHOTREXATE	0	0	1	16.820308	2.473104196	0.001408007
METHOXSALEN	0	0	1	18.13307272	0.440585974	0.003125476
MITOMYCIN C	24.42345134	0.750288425	0.000314424	40.8414439	3.863199483	0.000625938
MITOTANE	0	0	1	12.25593713	7.889554315	0.137514185
MTX	95.65615929	4.152949759	0.000627707	99.52451732	0.823560159	1.16722E-05
OXALIPLATIN	85.38965236	1.715333453	0.000134486	79.55505616	0.453250425	9.86278E-05
PACLITAXEL	1.307029829	0.989365492	0.149356376	40.17305978	3.220040013	0.00022815
PENTOSTATIN	20.66713103	1.342020176	0.001402562	24.77950488	3.811915288	0.002696279
PLICAMYCIN	33.71635081	0.905583966	0.00024038	34.71947447	6.843760203	0.009621205
PROCARBAZINE	6.523777728	2.87050246	0.055794443	43.3708838	0.982265238	6.30661E-05
RALOXIFENE HCL	1.320946527	2.287946498	0.422649731	13.0218436	6.788374403	0.09080936
RAPAMYCIN	21.61314613	1.798152667	0.002299302	34.28836652	0.959565105	0.000141207
RESVERATROL	35.13765962	3.264691338	0.002865152	16.16381587	2.523598632	0.001792194
SPERMIDINE	17.07618773	3.513559129	0.013820223	37.4743008	5.3107741	0.003416495
STREPTOZOCIN	0.319329662	0.553095199	0.422649731	18.16747278	6.106084748	0.032892381
SUNITINIB	7.788649054	3.898172898	0.074310636	3.318085263	5.74709226	0.665006066
TAMOXIFEN CITRATE	0	0	1	19.66405781	5.287812716	0.017918265
TEMOZOLOMIDE	12.95825277	1.792875738	0.00632053	13.29933595	5.201764417	0.046567263
TENIPOSIDE	32.60854724	1.639685564	0.00084176	0.452215425	0.783260093	0.416519206
THALIDOMIDE	14.1961107	5.602271905	0.048190455	28.95102654	0.330187911	0.001265674
THIOGUANINE	9.385434192	3.686233299	0.047766231	21.04919193	2.29447502	0.000418417
THIOTEPA	25.65590567	1.648052631	0.001372623	27.45165633	1.390650295	9.27133E-05
TRETINOIN	0	0	1	0	0	0.285966809
URACIL MUSTARD	13.91279766	5.386393682	0.046505087	19.96571396	7.905500931	0.049636433
VINBLASTINE SULFATE	14.09295987	2.227025694	0.008221351	53.1195346	2.758816413	3.093E-05
VINCRIStINE SULFATE	8.323878381	3.705053351	0.060144891	39.79601469	5.504874367	0.003351568
VINORELBINE TARTRATE	3.694465409	3.763683753	0.231197094	28.71256191	1.918008565	6.60352E-05
VORINOSTAT	0	0	1	0	0	0.285966809
ZOLENDRONIC ACID	9.712809586	2.620667786	0.023411778	18.81957153	0.674921727	0.001803471

Table S 2. Transcription and translation inhibition data for the drugs from a custom anticancer library. U2OS cells were treated with a home-made library of anticancer agents at 3 μ M for evaluating their ability to inhibit transcription (after 1.5 h treatment followed by 1 h in the presence of 5-ethynyl uridine (EU)) and translation (12 h treatment followed by 30 min in methionine-free medium and then 1.5 h in methionine-free medium supplemented with (L-azidohomoalanine (AHA)). The percentage of inhibition of transcription and translation was calculated and the mean of triplicates of one representative experiment is indicated as well as the standard deviation (SD) and the p-value (PVAL) which was calculated using a Student's t-test. These data were used to evaluate correlations with ICD parameters in **Figure 20** and **Figure S 8**.

CID	Name	Score	Transcription inhibition		
			Mean	SD	PVAL
515328	5-Fluorodeoxycytidine	-0.073944055	0	0	0.085102669
11977753	Dactolisib	0.681357703	14.04747238	0.065312273	0.000919228
3885	β -Lapachone	-0.159663085	20.95030652	13.50085812	0.305297648
5281078	Mycophenolate mofetil	0.239570191	44.84590908	2.499182983	0.001873086
72385	Nonoxynol-9	-2.034977072	8.451037648	2.110619699	0.076812698
394347	RH-1	-0.264524221	83.36458718	3.906836417	0.006344573
101524	Becatecarin	4.967787785	69.08411747	2.477979305	0.000656291
2019	Dactinomycin	4.02340177	100	0	1.76E-07
60699	Topotecan	5.498023981	76.69808547	1.087669761	9.13E-08
372978, 108150	Trabectedin	6.127930281	100	0	1.76E-07
72271	UCN-01	4.023450825	78.94456213	1.242796208	2.13E-07

Table S 3. Transcription inhibition for the positive and negative selected with the artificial intelligence module. Positive and negative agents were selected thanks to an algorithm that can predict ICD (Figure 13). They were tested for their ability to inhibit transcription: U2OS cells were treated with these agents around their IC₆₀: 1 μ M dactinomycin (DACT), 50 μ M topotecan, 1 μ M becatecarin, 0.5 μ M trabectedin, 5 μ M UCN-01, 30 μ M mycophenolate mofetil, 30 μ M nonoxynol-9, 25 μ M dactolisib, 2.5 μ M β -lapachone, 5 μ M 5-Fluorodeoxycytidine and 2 μ M RH-1 for 1.5 h followed by 1 h where treatment was pursued in the presence of EU. The percentage of inhibition of transcription were calculated as previously described.

Nucleic acid synthesis inhibitors			Protein synthesis inhibitors			Antimetabolites			PARP inhibitors		
CID	Name	Score	CID	Name	Score	CID	Name	Score	CID	Name	Score
126941	METHOTREXATE	1.569	6197	CX	-0.193	126941	METHOTREXATE	1.569	1645	M-AMINO BENZAMIDE	0.020
667490	MERCAPTOPURINE	-0.562	44115057	DACTINOMYCIN	4.023	2723601	THIOGUANINE	0.477	1853	6-PHENANTHRIDONE	-1.140
54695425	U-6591	4.316	439530	PUROMYCIN HYDROCHLORIDE	0.420	667490	MERCAPTOPURINE	-0.562	11960529	ABT-888	0.143
44415057	DACTINOMYCIN	4.023	5959	CAM	0.427	75420	4 APP	-0.571	23725625	OLAPARIB	-0.297
3187	C-6388	2.364	3084037	CACTINOMYCIN	4.060	24180949	SODIUM PHENYLACETATE	1.117			
6325719	PLICAMYCIN	3.231	92765	CRYPTOPLEURINE	1.097	39530	PUROMYCIN HYDROCHLORIDE	0.420			
5746	MITOMYCIN	2.803	6326719	PLICAMYCIN	3.231	9048	NSC 3074	2.909			
3657	HYDROXYUREA	2.768	6603320	EMETINE	4.087	676166	6-MPR	0.537			
3379405	THIAMIPRINE	0.571	54680694	AAT 4	3.888	222284	HARZOL	0.759			
2265	AZATHIOPRINE	-0.071	54712662	SANCYCLINE	6.885	71558	NICOTINIC ACID	2.127			
5905	IDOXURIDINE	0.028	5289124	U-15900	2.566	3385	FLUOROURACIL	-0.384			
656673	TOYOMYCIN	2.833	5287620	LUNATIN	-0.536	5790	FLOXURIDINE	-0.201			
72511	PHLEOMYCIN	5.068	447106	SPARSOMYCIN	1.483	3938248	TGS	1.170			
5289019	U 15167	4.988	122806	C 1228	2.593	236184	BDU	-0.190			
253602	ANISOMYCIN	-0.965	253602	ANISOMYCIN	-0.965	3379405	THIAMIPRINE	0.571			
3115	STALLINICIN	0.869	5354042	VERNAMYCIN A	0.649	2265	AZATHIOPRINE	-0.071			
20039	2',3'-DIDEOXYADENOSINE	-0.406	278679	CEPHALOTAXINE	1.009	5905	IDOXURIDINE	0.028			
4112	D-AMETHOPTERIN	1.569	285033	HOMOHARRINGTONINE	2.730	247955	B181008	1.025			
54608707	FOSFONET SODIUM	4.960	122731	STAPHYLOMYCIN S	1.132	5351180	CYTARABINE HYDROCHLORIDE	3.542			
284240	3'-FLUOROTHYIMIDINE	-0.676	99558	2-(AMINOETHYL)CYSTEINE MONOHYDROCHLORIDE	1.911	2796	CLOFBRATE	-1.265			
5476249	ZYGOSPORIN A	2.128	429598	BOUVARDIN	2.999	4912	PROBUCCOL	0.645			
528818	7-OMEN	5.048	429598	BOUVARDIN	2.999	25674	D-ETHIONINE	1.113			
47318	OLTIPIRAZ	-0.689	9553856	LEVOFURALTADONE	-1.044	20039	2',3'-DIDEOXYADENOSINE	-0.406			
3165	DRB	0.090	5459220	KRN5500	1.467	9444	AZACITIDINE	0.613			
6857732	LEVOMYCIN	2.364	400771	STENOROL	2.981	3366	FLUCYTOSINE	-0.165			
5718	2',3'-DIDEOXYCYTIDINE	-0.697	439647	TPCK	-0.769	4112	D-AMETHOPTERIN	1.569			
62999	CIPROFLOXACIN HYDROCHLORIDE	1.965				999	BENZENACETIC ACID	-1.024			
3229	1,8-NAPHTHYRIDINE-3-CARBOXYLIC ACID, 6-FLUORO-1,4-DIHYDRO-4-OXO-7-PIPERAZINYL	-0.058				16895	DECITABINE	0.114			
4463	BI-RG-587	-0.620				284240	3'-FLUOROTHYIMIDINE	-0.676			
5470819	CORYLIFOLIN	-1.538				25050	NSC-145668	3.374			
4583	OFLOXACIN	0.581				5386	FT 207	-1.256			
						5064	RIBAVIRIN	0.580			
						294641	ACIA	0.363			
						3034016	AATC	0.238			
						1651	3DADO	0.472			
						39981	NA	2.283			
						55710	ICN 4221	0.132			
						125219	D 19391	-0.768			
						457954	TIAZOFURIN	0.825			
						596	CYTARABINE	0.306			
						5694	WY-14,643	-0.459			
						30751	FLUDARABINE PHOSPHATE	1.344			
						21704	ARA-A	0.587			
						3599	MILTEFOSIN C	-0.707			
						5718	2',3'-DIDEOXYCYTIDINE	-0.697			
						5353599	(E)-5-(2-BROMOVINYL)-2'-DEOXYURIDINE	-0.097			
						53232	MEVACOR	-0.135			
						54454	SIMVASTATIN	-0.057			
						148177	D 21266	-1.659			

Table S 4. ICD scores of specific categories of agents. The 50,000 compounds of the NCI-60 library were annotated for different parameters including nucleic acid synthesis inhibition and protein synthesis inhibition. The predicted ICD score of agents from these categories (score) was calculated with a previously described artificial intelligence model. The name and compound ID number (CID) are indicated. Two other random categories were chosen as controls: PARP inhibitors and antimetabolites (n=49); their predicted ICD scores were also calculated with this artificial intelligence model.

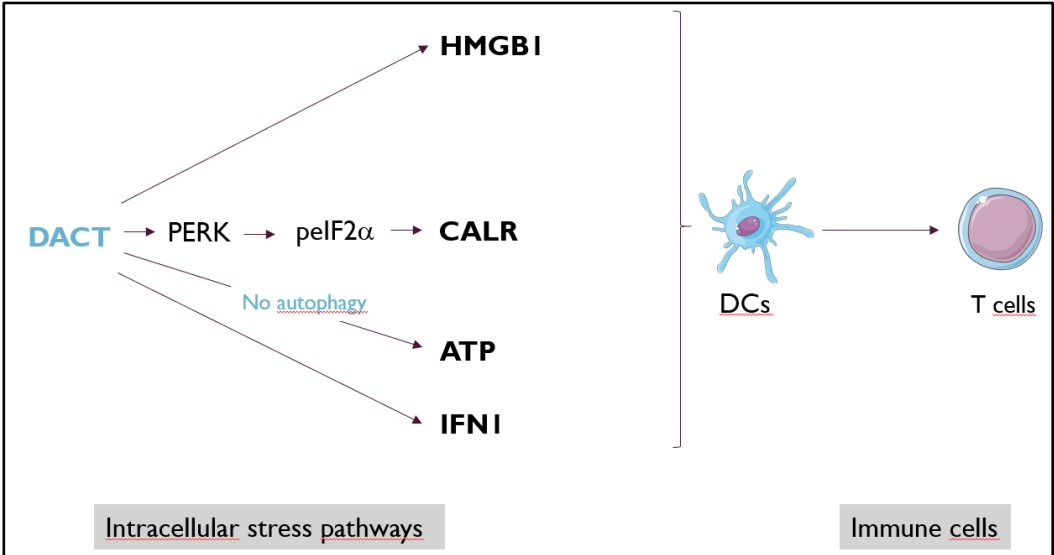
Discussion

DACT is an ICD inducer

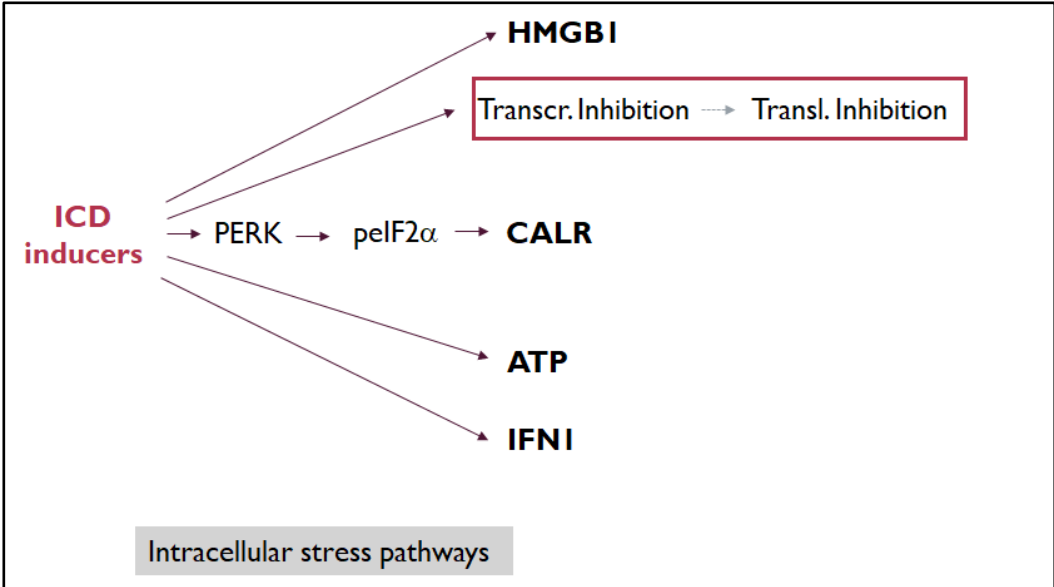
In the present work, we identified DACT as a new ICD inducer, using an *in silico* prediction model that was based on its physicochemical characteristics (the “ICD prediction score”). We then validated the capacity of DACT to induce surrogate hallmarks of ICD in cultured cells (CALR exposure as well as ATP, HMGB1 and type 1 IFN release), to kill cancer cells in a way that they undergo phagocytosis by DCs and to elicit an antitumor immune response in mice (**Figure 21A**). Until now, the effect of DACT on immune cells has been scarcely investigated. It has been demonstrated that DACT-treated cells are more sensitive to NK and to cytotoxic factors secreted by monocytes (Austgulen et al, 1986; Bersani et al, 1986; Uchida & Klein, 1985). It has been reported that DACT increases the expression of the early marker of activation CD69 in CD3⁺ T cells (Morgan et al, 1999), but conversely that DACT inhibits the secretion of pro-inflammatory cytokines by macrophages (Kozmar et al, 2010; Perez et al, 2012). Here, we have demonstrated that the anticancer effect of DACT is dependent on a T cell response. In addition, the analysis of the tumor immune infiltrate revealed that DACT induces an increase in CD8⁺ T cells and a decrease in Tregs resulting in a significant increase of the ratio CD8⁺/FoxP3⁺, which constitutes a reliable marker of positive outcome (Fridman et al, 2017; Ladoire et al, 2008; Semeraro et al, 2016; Stoll et al, 2014) and increases after treatment with ICD inducers (**Table 1**). Higher amounts of NK and NKT cells were also observed in the tumor infiltrate after DACT treatment, like with some other modalities of immunogenic inducers such as cyclophosphamide, crizotinib and photochemotherapy (Ghiringhelli et al, 2007; Liu et al, 2019b; Ventura et al, 2018) (**Table 1**). Moreover, the present work shows that DACT induces IL-17 secretion, in line with previous studies showing that a IL-17-mediated immune response is involved in ICD, elicited by $\gamma\delta$ T cells after anthracyclines treatment (Ma et al, 2011) and by CD4⁺ T cells after cyclophosphamide or crizotinib chemotherapy (Liu et al, 2019b; Viaud et al, 2011). To further confirm the role of IL-17 in DACT anticancer effect, we should investigate the efficacy of DACT in tumor growth when blocking IL-17. We also observed a non-significant increase in IFN γ secretion by CD8⁺ T cells in MCA205 tumors treated with DACT. This may be due to exhaustion of CD8⁺ T cells by cancer cells and may explain why the response of MCA205 to DACT alone is not so efficient. The immune infiltrate of WEHI 164 tumors which respond better to DACT may show a higher amount of IFN γ secretion. Finally, we showed that the anticancer effect of DACT can be potentiated by combination with PD-1 blockade, leading

to the cure of some mice from transplanted MCA205 and WEHI 164 fibrosarcoma. This is consistent with recent reports showing that ICD inducers synergize with ICBs due to a coordinate action on the adaptive immune system (Pfirschke et al, 2016; Serrano-Del Valle et al, 2019).

A. Mechanisms of DACT-mediated ICD



B. New characteristics of ICD



C. Hypothesis to be further explored

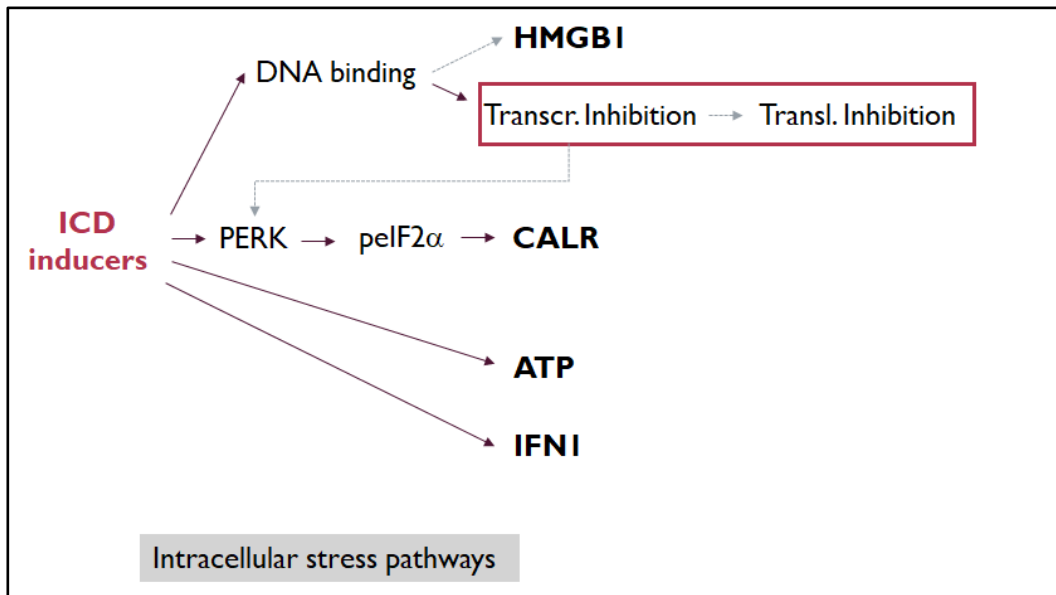


Figure 21. Conclusions of the study. Dactinomycin (DACT) induces the phosphorylation of eukaryotic initiation factor 2α (peIF2 α)-dependent exposure of calreticulin (CALR), high-mobility group box 1 (HMGB1) release, adenosine triphosphate (ATP) secretion and type 1 interferon (IFN1) release. The damage-associated molecular pattern (DAMPs) activate dendritic cells (DCs) which in turn inhibit FoxP3⁺ T cells and activate interleukin (IL)-17 producing CD4⁺ T cells, IL-17 and IFN γ producing T cells, natural killer (NK) and NK T cells. Unlike other immunogenic chemotherapeutics, the release of ATP is independent from autophagy (A). ICD inducers induce an inhibition of transcription followed by an inhibition of translation (B). The release of HMGB1 may occur concomitantly with transcription inhibition after the agents target DNA. In addition, the inhibition of transcription may participate in peIF2 α (C). The DAMPs involved in ICD are highlighted in bold; the particularities of DACT-induced ICD are written in blue; the new mechanistic findings related to immunogenic cell stress are surrounded in red and dashed grey arrows represent hypothetical links to be further explored.

Pre-mortem stress pathways activated by DACT

We have previously reported that a pathognomonic hallmark of ICD is the induction of eIF2 α phosphorylation, which most accurately predicts immunogenicity of therapeutic interventions *in vitro* and *in vivo* (Bezu et al, 2018a). EIF2 α phosphorylation induced by ICD-stimulatory chemotherapeutics is mediated by eIF2AK3 and correlates with CALR exposure, with increased tumor infiltration by activated DCs and T lymphocytes, as well as with favorable prognosis (Bezu et al, 2018a; Fucikova et al, 2016a; Fucikova et al, 2016b; Garg et al, 2012b; Giglio et al, 2018; Panaretakis et al, 2009). Although all ICD inducers discovered until now trigger eIF2 α phosphorylation, we recently demonstrated that anthracyclines- and OXA-induced cell death activate none of the other markers of ER stress (ATF4, ATF6 and XBP1s) in human osteosarcoma cells (Bezu et al, 2018a). Further studies with alternative ICD inducers, such as crizotinib or the EGFR targeting antibody cetuximab (Liu et al, 2019b; Pozzi et al, 2016), and within other cell lines, like human melanoma (Giglio et al, 2018), have emphasized this point. Consistently, in the present work, we observed that DACT triggers eIF2AK3-

mediated eIF2 α phosphorylation and subsequent CALR translocation and exposure *in vitro* and *in vivo*. Moreover, DACT did not enhance ATF4 expression, neither ATF6 translocation nor XBP1 splicing. It has been reported that ER stress is activated by the accumulation of ROS in ICD elicited by hypericin-based PDT (Garg et al, 2012a), bleomycin (Bugaut et al, 2013), anthracyclines and OXA (Panaretakis et al, 2009). At relatively high doses, it has been shown that DACT induces ROS production (Vekshin, 2011), which may at least in part be involved in the induction of the split ER stress response.

Surprisingly, as compared to anthracyclines-induced ICD, the mechanism underlying ATP release in the context of DACT-driven ICD seems not to be related to autophagy since no LC3 puncta were observed in MCA205 and U2OS treated cells (**Figure 21A**). In this sense, DACT-mediated ATP release resembles ICD induced by hypericin-based PDT (Garg et al, 2013). DACT has been shown to decrease intracellular ATP content (Laszlo et al, 1966; Tao et al, 2006) and to affect inorganic pyrophosphate exchange reaction with all nucleoside triphosphates due to its affinity for nucleotides (Goldberg et al, 1963). The release of ATP following DACT treatment may be related to these effects, yet this hypothesis requires further investigation.

Inhibition of transcription as a new characteristic of immunogenic cell stress

DACT is well-known as an inhibitor of transcription (and actually the standard reagent to block RNA synthesis in wet biology labs) and this effect appears to be important for its ICD-inducing activity. Indeed, we found that the inhibition of RNA synthesis was a common characteristic of multiple structurally different established ICD inducers (**Figure 21B**): the anthracyclines doxorubicin, daunorubicin, epirubicin and MTX which stabilize topoisomerase II, the platinum salt OXA which forms inter- and intra- strand DNA cross links with high affinity for guanine as well as in a lower extent the tyrosine kinase inhibitor crizotinib and the proteasome inhibitor bortezomib (**Figure 21B**). Lurbinectedin, another agent which binds into the minor groove of DNA and by consequence inhibits transcription, has recently been shown to induce ICD as well (Tumini et al, 2019; Xie et al, 2019a). Of note, OXA was more efficient in suppressing transcription than was CDDP, another platinum salt binding DNA, which is not endowed with strong ICD-inducing capabilities. Taxanes (docetaxel and paclitaxel) and vinca alkaloids (vinblastine and vincristine), which promote CALR exposure yet have not been reported to induce ICD *in vivo* (**Table 1**), do not inhibit transcription. Both classes of drugs are spindle poisons leading to arrest in cell division and apoptosis, but while taxanes stabilize GDP-bound tubulin in the microtubules preventing its depolymerization, vinca alkaloids inhibit tubulin

polymerization and further formation of microtubules. In addition, agents other than DACT that had an elevated ICD prediction score calculated *in silico* (UCN-01, trabectedin, becatecarin, topotecan) turned out to have a significantly higher capacity to suppress RNA synthesis than agents with low ICD prediction scores. Again, these agents widely differ in their chemical structure and mode of action. Topotecan and becatecarin bind to DNA and form a complex with topoisomerases I. Trabectedin binds into the minor groove of DNA with a high specificity for GC regions where it impairs the activity of both transcription factors and polymerases in addition to promote alkylation between guanine N2 residues (Tumini et al, 2019). UCN-01, also called 7-hydroxystaurosporine, is a cell-permeable staurosporine derived anticancer agent which inhibits various protein kinases, in a reversible and ATP-competitively fashion. It is endowed of high specificity for CDK2 and other CDKs. CDK2, which is involved in G1/S transition, induces RNA polymerase I transcription and certain other CDKs (7, 8 and 9 in particular) regulate RNA polymerase II transcription (Drygin et al, 2010; Roskoski, 2016); effects which may be related to the inhibition of transcription that we have observed following UCN-01 treatment. In sum, it appears that the inhibition of transcription (and downstream thereof translation) is a common characteristic of ICD inducers. This has been further confirmed with the *in silico* analysis of 50,000 agents of the NCI-60 library, that revealed a correlation between the “ICD score” and the inhibition of RNA and protein synthesis respectively.

NF- κ B transcriptional activity has been shown to be required for dying cancer cells to activate DCs cross-priming and CD8⁺ T cells (Giampazolias et al, 2017; Yatim et al, 2015). It may therefore look surprising that inhibition of transcription is associated with ICD. However, even though DACT inhibits global RNA synthesis, it also stimulates the transcription of specific genes related to apoptosis, necrosis and inflammation, with, among others, an activation of NF- κ B regulated genes (Liu et al, 2016). This may be also the case of other ICD inducers, although this should be investigated.

This work shows that anthracyclines, OXA and DACT induce close-to-irreversible inhibition of synthesis, whereas inhibition elicited by crizotinib, an immunogenic agent that has to be combined with CDDP for sufficient cytotoxicity in vaccination assay, is reversible. According to past studies, DACT binds to DNA and inhibits transcription in a reversible fashion (Ilan & Quastel, 1966). However, at the dose used in this study (IC₆₀ at 24 h in the U2OS osteosarcoma cells) and the time of treatment (2.5 h), which are relatively high, the inhibition of synthesis was not reversed and cell death occurred even after treatment removal. Thus, after such a dose and duration of treatment, DACT may have already triggered a number of DNA strand breaks and/or the inhibition of essential protein synthesis that cannot be reversed and

lead to apoptosis. Accordingly, it was demonstrated that anthracyclines and CDDP induce an irreversible cell death, which is not the case for crizotinib (Liu et al, 2019b). All in all, it seems that the reversibility of the inhibition of synthesis is linked to the reversibility of the cytotoxicity of the agents rather than their immunogenicity.

Relation between the inhibition of transcription and the other hallmarks of ICD

One question that is still unanswered is how transcription and translation inhibitions are related to other characteristics of ICD and to the emission of DAMPs. It appears as if eIF2 α phosphorylation is not required for stalling protein synthesis since cells that bear a non-phosphorylatable eIF2 α mutant, as well as cells treated with the integrated stress response inhibitor ISRIB, reduce protein synthesis in response to DACT and other ICD inducers to the same extent as their wild type counterparts. Translation inhibition may rather be a direct consequence of RNA synthesis inhibition, which should be further confirmed, for instance by investigating if translation is still inhibited in enucleated cells (cytoplasts). Another hypothesis could be that ICD inducers, by targeting DNA, induce DNA damage pathways which in turn activate ER stress and further CALR exposure (**Figure 21C**). However, it was shown that eIF2 α phosphorylation and CALR exposure were still activated by anthracyclines in cytoplasts, meaning that they at least in part originate from DNA-independent effects (Obeid et al, 2007b). ATP is mediated by cytoplasmic autophagy in most contexts of ICD and ANXA1 is located in the cytoplasmic side of the plasma membrane, thus it is unlikely that these pathways are related to the inhibition of transcription.

HMGB1 is a chromatin protein which binds into the minor groove of DNA, where it induces DNA bending and facilitates transcription factor recruitment (Bustin, 1999; Klass et al, 2003). It has been reported that DACT induces the dispersion of HMG-17, another protein of the high mobility group superfamily, through the nucleus (Bianchi & Beltrame, 2000). Similarly, we could imagine that DACT and other ICD inducers, by targeting DNA, induce both RNA synthesis inhibition and release of HMGB1 from the chromatin to the cytoplasm and finally into the extracellular space (**Figure 21C**). Interestingly, the release of HMGB1 is, among all the parameters tested, the one that has the highest correlation score with transcription inhibition ($R=0.76$), which supports this hypothesis.

ICD inducers in the context of non-oncogene addiction

In the present work, we have demonstrated that the antitumor effect of DACT relies on the

activation of the immune system. How to explain that, despite transcription inhibition, immune cells can proliferate following chemotherapy with DACT and more generally with other ICD inducers? Antineoplastic cytotoxicants seem to exert some degrees of “specificity” in the sense that they act more efficiently on cancer cells than on their normal counterparts including tumor-infiltrating leukocytes that participate to immunosurveillance. Sarcomas, which are routinely treated with some of the drugs characterized here (such as DACT and trabectedin) are highly sensitive to transcription inhibitors (Jaffe et al, 1976; Liebner, 2015; Manara et al, 2005; Tumini et al, 2019) and it is tempting to speculate that they may also be particularly prone to emit immunogenic signals in response to this kind of anticancer agent.

Only a particular vulnerability of cancer cells to transcriptional inhibitors may explain why agents that are expected to act on any cell type may elicit a therapeutically relevant stress response in cancer cells, without paralyzing vital functions in normal tissues including the immune system. The “non oncogene addiction” concept, in echo to the phenomenon of “oncogene addiction”, which describes the dependency of many tumors on the activation of a particular oncogene, explains the altered dependencies of cancer cells on certain (mutation-independent) pathways. Indeed, cancer cells display high level of various stress: DNA damage due to genomic instability, replication and mitotic stress induced by rapid proliferation, metabolic stress accompanying high glycolysis level, proteotoxic stress caused by frequent activation of heat shock response and oxidative stress due to generation of ROS in response to DNA damage; and are therefore more sensitive to supplemental stress than their healthy counterparts (**Figure 22**) (Luo et al, 2009; Nagel et al, 2016). To eliminate cancer cells, some strategies, consisting either in inhibiting stress reducing pathway or in applying additional stress, may therefore be efficient and relatively selective. This is actually the case of most chemotherapeutics, including DACT, which inhibit transcription, trigger DNA damage and promote ROS production in sarcoma and other cancers, inducing their destruction, whereas some other tissues exposed to DACT can recover. It may be that ICD-treated cancer cells are also more sensitive than their healthy counterpart to immune destruction for the same reason.

Even though the concept of “non-oncogene addiction” emerged during the last decade, Herbert S. Schwartz gave consistent explanations for the selectivity of DACT fifty years ago; whereas cancer cells are unstable and highly dependent on proliferative signals, hence very sensitive to DACT, some cells in normal tissues are in a phase of mitotic dormancy (G_0) so are not affected by altered transcription. These cells constitute a “stock” when neighbor cells are damaged (Schwartz et al, 1966). So even if various tissues, including immune cells, are affected during chemotherapy, some can recover. Accordingly, it was shown that DACT administered

concomitantly to an antigen induces delayed production of antigen specific antibodies but does not affect their quantity, meaning that the ability of the immune system to respond to antigen is not altered by DACT-induced inhibition of transcription (Wust et al, 1964).

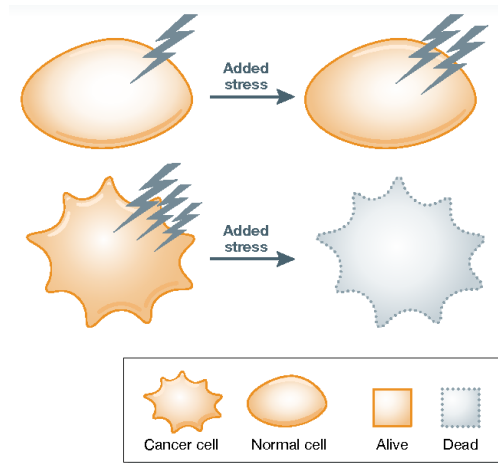


Figure 22. Non oncogene addiction (modified from (Nagel et al, 2016). While normal cells possess the ability to resist and adapt to various sources of stress, cancer cells, which already exhibit elevated level of intracellular stress and are highly dependent on external factors, are more sensitive to stress overload.

Perspectives

Identification of new ICD inducers

The ICD predicting artificial intelligence model has again demonstrated its potential. It enabled the identification of DACT which was further confirmed as an efficient ICD inducer, from a large group of compounds. Moreover, we could further discriminate positive and negative hits identified with this model based on their ability to inhibit transcription. To validate the additional predicted ICD inducers, *i.e.* trabectedin, UCN-01, becatecarin and topotecan, we aim at investigating their ability to induce phagocytosis and we plan to vaccinate mice with syngeneic cells treated with these compounds. Anyway, this algorithm has the potential to quickly screen huge libraries and pre-select potential ICD inducers. In the present study, we focused on agents that have already shown an anticancer effect and have been submitted to clinical trials, but we plan to go beyond that scope and screen various other libraries.

This work has shown that transcription inhibition is a feature shared by the well characterized ICD inducers MTX, daunorubicin, doxorubicin, epirubicin, OXA, bortezomib and crizotinib. Lurbinectedin has also been shown to inhibit transcription, which was confirmed here (Xie et al, 2019a). It would be interesting to investigate the effect of other confirmed ICD inducers, *i.e.* cyclophosphamide, bleomycin, septacidin, cardiac glycosides, vorinostat, wogonin, dinaciclib, teniposide, the bromodomain inhibitor JQ1, the EGFR targeting antibodies 7A7 and cetuximab, some oncolytic peptides, oncolytic viruses and different physical modalities, on RNA synthesis to further confirm this finding (**Table 1**). Of note, dinaciclib is an inhibitor of CDKs, which are involved in transcription regulation; this suggests that this agent may also inhibit RNA synthesis. This newly discovered characteristic may contribute to easily discriminate *in vitro* if new compounds may induce ICD.

Clinical use of DACT and combination with immunotherapies

The use of DACT is currently limited to some cases of pediatric sarcoma, gestational trophoblastic diseases and metastatic testicular carcinomas even though it has shown efficiency in pre-clinical studies performed in other kinds of cancers (Cortes et al, 2016; Kam & Thompson, 2010; Takusagawa et al, 1982). This work may lead to a regain of interest for this chemotherapeutic. Indeed, its ability to induce immunogenic cell death reveals that it is able to induce long term protection, which is a key element for efficient anticancer therapy.

The sequential combination of ICD inducers with ICBs has proven to be efficient in

various pre-clinical settings (Liu et al, 2019b; Luo et al, 2019; Pfirschke et al, 2016). This synergy is explained by their coordinate action on the immune system: ICD inducers promote the emission of DAMPs, mounting an adaptive anticancer immune response; once the tumor is highly infiltrated with CD8⁺ T cells, ICBs inhibit immunosuppressive mechanisms and prevent T-cells from extensive exhaustion. The potential of such combination is currently investigated in different clinical trials, with the example of the phase II clinical trial involving pembrolizumab and OXA for various neoplasms of the digestive organs (NCT03111732) or the phase II clinical trial combining nivolumab, ipilimumab, doxorubicin, vinblastine and dacarbazine for Hodgkin disease (NCT02181738). Here we show that DACT induces ICD and synergizes with PD-1 blockade therapy. This combination should be further investigated and may lead to new clinical opportunities for the treatment of cancers currently treated with chemotherapy regimen involving DACT. Of note, one clinical trial investigating the effect of DACT in combination with ipilimumab and melphalan for the treatment of melanoma has shown promising results (NCT01323517) (Ariyan et al, 2018).

The first kind of cancer successfully treated with ICB was melanoma, reported to be highly mutated (Hodi et al, 2010). As previously mentioned, DACT is mostly used in clinics to treat different pediatric sarcoma. Yet, sarcomas stand among low mutated tumors (Chalmers et al, 2017; Danaher et al, 2018) which by consequence are not expected to be highly sensitive to immunotherapy (Samstein et al, 2019). Recently, the immune contexture of sarcoma has been studied and revealed that sarcomas contain high levels of TILs and macrophages (D'Angelo et al, 2015; Majzner et al, 2017) and rather low PD-L1 expression (D'Angelo et al, 2015; Kim et al, 2016; Majzner et al, 2017). Nevertheless, PD-L1 expression in sarcomas and PD1 expression in TILs were shown to be negative prognostic factors in two cohorts of soft tissue sarcoma patients, paving the way for targeting the PD-1/PD-L1 axis in such tumors (Budczies et al, 2017; Kim et al, 2016; Kim et al, 2013) and the first clinical trials investigating the use of pembrolizumab for advanced sarcoma is ongoing (NCT02301039). Altogether, these elements suggest that the combination of ICD inducers and DACT constitute a promising therapeutic strategy for sarcoma which remain a large burden among children, but also for other kinds of cancers.

Combination with CRMs to induce autophagy-dependent ATP release

This work demonstrates that DACT, as compared to other immunogenic chemotherapeutics like MTX or OXA, is not able to induce autophagy-related LC3 aggregation (Martins et al, 2012). Despite this defective autophagy, it triggers ATP release from cancer cells by alternative

unknown mechanisms. The amount of extracellular ATP may be enhanced by combination of DACT with caloric restriction mimetics (CRMs), agents which activate autophagy without displaying any toxicity, like hydroxycitrate, spermidine or aspirin (Pietrocola et al, 2018; Pietrocola et al, 2016). Such combination might promote the recruitment and activation of DCs, thereby increase the anticancer immune response. Even more promising, it could be combined with PD-1 blockade antibodies and a CRM. It has indeed been shown that the triple combination of an ICD inducer, a CRM and ICB leads to complete tumor regression in mice (Levesque et al, 2019). The present *in vivo* work and the mechanistic study of the anticancer effect of DACT strongly suggest that this approach may be successful. In this setting, the dose of DACT required to be efficient may be reduced, as well as the associated adverse effects in patients.

Collaborations

In addition to this project, I have participated to other research work, protocol writing and reviews which led to the following publications:

Bezu, L., Chuang, A. W., **Humeau, J.**, Kroemer, G., & Kepp, O. (2019). Quantification of eIF2 α phosphorylation during immunogenic cell death. *Methods Enzymol*, 2019;629:53-69

Forveille, S., **Humeau, J.**, Sauvat, A., Bezu, L., Kroemer, G., & Kepp, O. (2019). Quinacrine-mediated detection of intracellular ATP. *Methods Enzymol*. 2019;629:103-113.

Xie, W., Forveille, S., Iribarren, K., Sauvat, A., Senovilla, L., Wang, Y., **Humeau, J.**, Perez-Lanzon, M., Zhou, H., Martínez-Leal, J.F., Kroemer, G., Kepp, O. (2019). Lurbinectedin synergizes with immune checkpoint blockade to generate anticancer immunity. *Oncoimmunology*, 1656502.

Humeau, J., Lévesque, S., Kroemer, G., Pol, J. G. (2019). Gold standard assessment of immunogenic cell death in oncological mouse models. *Methods in molecular biology* 1884: 297-315.

Bezu, L., Sauvat, A., **Humeau, J.**, Gomes-da-Silva, L. C., Iribarren, K., Forveille, S., Garcia, P., Zhao, L., Liu P., Zitvogel, L., Senovilla, L., Kepp, O., Kroemer, G. (2018). eIF2 α phosphorylation is pathognomonic for immunogenic cell death. *Cell Death & Differentiation*, 25(8), 1375.

Bezu, L., Sauvat, A., **Humeau, J.**, Leduc, M., Kepp, O., Kroemer, G. (2018). eIF2 α phosphorylation: A hallmark of immunogenic cell death. *Oncoimmunology*, 7(6), e1431089.

Bloy, N., Garcia, P., Laumont, C. M., Pitt, J. M., Sistigu, A., Stoll, G., Yamazaki, T., Bonneil, E., Buqué, A., **Humeau, J.**, Drijfhout, J.W., Meurice, G., Walter, S., Fritsche, J., Weinschenk, T., Rammensee, H.G., Melief, C., Thibault, P., Perreault, C., Pol, J., Zitvogel, L., Senovilla, L., Kroemer, G. (2017). Immunogenic stress and death of cancer cells: Contribution of antigenicity vs adjuvanticity to immunosurveillance. *Immunological reviews*, 280(1), 165-174.

Humeau, J., Bravo-San Pedro, J. M., Vitale, I., Nunez, L., Villalobos, C., Kroemer, G., Senovilla, L. (2018). Calcium signaling and cell cycle: progression or death. *Cell calcium*, 70, 3-15.

Pietrocola, F., Demont, Y., Castoldi, F., Enot, D., Durand, S., Semeraro, M., Baracco, E.E., Pol, J., Bravo-San Pedro, J.M., Bordenave, C., Levesque, S., **Humeau, J.**, Chery, A., Métivier, D., Madeo, F., Maiuri, M.C., Kroemer, G. (2017). Metabolic effects of fasting on human and mouse blood in vivo. *Autophagy*, 13(3), 567-578.

Senovilla, L., Demont, Y., **Humeau, J.**, Bloy, N., Kroemer, G. (2017). Image cytofluorometry for the quantification of ploidy and endoplasmic reticulum stress in cancer cells. *Cell Cycle Synchronization* (pp. 53-64).

Semeraro, M., Adam, J., Stoll, G., Louvet, E., Chaba, K., Poirier-Colame, V., Sauvat, A., Senovilla, L., Vacchelli, E., Bloy, N., **Humeau, J.**, Buque, A., Kepp, O., Zitvogel, L., Andre, F., Mathieu, M.C., Delaloge, S., Kroemer, G. (2016). The ratio of CD8+/FOXP3 T lymphocytes infiltrating breast tissues predicts the relapse of ductal carcinoma in situ. *Oncoimmunology*, 5(10), e1218106.

Bloy, N., Sauvat, A., Chaba, K., Buqué, A., **Humeau, J.**, Bravo-San Pedro, J. M., Bui, J., Kepp O., Kroemer, G., Senovilla, L. (2015). Morphometric analysis of immunoselection against hyperploid cancer cells. *Oncotarget*, 6(38), 41204.

Bibliography

- Aaes TL, Kaczmarek A, Delvaeye T, De Craene B, De Koker S, Heyndrickx L, Delrue I, Taminau J, Wiernicki B, De Groote P, Garg AD, Leybaert L, Grooten J, Bertrand MJ, Agostinis P, Bex G, Declercq W, Vandenaabeele P, Krysko DV (2016) Vaccination with Necroptotic Cancer Cells Induces Efficient Anti-tumor Immunity. *Cell reports* **15**: 274-287
- Abel EL, DiGiovanni J (2011) Multistage Carcinogenesis. *Penning T (eds) Chemical Carcinogenesis Current Cancer Research Humana Press*
- Alagkiozidis I, Facciabene A, Tsiatas M, Carpenito C, Benencia F, Adams S, Jonak Z, June CH, Powell DJ, Jr., Coukos G (2011) Time-dependent cytotoxic drugs selectively cooperate with IL-18 for cancer chemo-immunotherapy. *Journal of translational medicine* **9**: 77
- Albert ML, Sauter B, Bhardwaj N (1998) Dendritic cells acquire antigen from apoptotic cells and induce class I-restricted CTLs. *Nature* **392**: 86-89
- Apetoh L, Ghiringhelli F, Tesniere A, Obeid M, Ortiz C, Criollo A, Mignot G, Maiuri MC, Ullrich E, Saulnier P, Yang H, Amigorena S, Ryffel B, Barrat FJ, Saftig P, Levi F, Lidereau R, Nogues C, Mira JP, Chompret A, Joulin V, Clavel-Chapelon F, Bourhis J, Andre F, Delaloge S, Tursz T, Kroemer G, Zitvogel L (2007) Toll-like receptor 4-dependent contribution of the immune system to anticancer chemotherapy and radiotherapy. *Nature medicine* **13**: 1050-1059
- Aranda F, Bloy N, Galluzzi L, Kroemer G, Senovilla L (2014a) Vitamin B6 improves the immunogenicity of cisplatin-induced cell death. *Oncoimmunology* **3**: e955685
- Aranda F, Bloy N, Pesquet J, Petit B, Chaba K, Sauvat A, Kepp O, Khadra N, Enot D, Pfirschke C, Pittet M, Zitvogel L, Kroemer G, Senovilla L (2015) Immune-dependent antineoplastic effects of cisplatin plus pyridoxine in non-small-cell lung cancer. *Oncogene* **34**: 3053-3062
- Aranda F, Vacchelli E, Obrist F, Eggermont A, Galon J, Sautes-Fridman C, Cremer I, Henrik Ter Meulen J, Zitvogel L, Kroemer G, Galluzzi L (2014b) Trial Watch: Toll-like receptor agonists in oncological indications. *Oncoimmunology* **3**: e29179
- Ariyan CE, Brady MS, Siegelbaum RH, Hu J, Bello DM, Rand J, Fisher C, Lefkowitz RA, Panageas KS, Pulitzer M, Vignali M, Emerson R, Tipton C, Robins H, Merghoub T, Yuan J, Jungbluth A, Blando J, Sharma P, Rudensky AY, Wolchok JD, Allison JP (2018) Robust Antitumor Responses Result from Local Chemotherapy and CTLA-4 Blockade. *Cancer immunology research* **6**: 189-200
- Aurelius J, Mollgard L, Kiffin R, Ewald Sander F, Nilsson S, Bergh Thoren F, Hellstrand K, Martner A (2019) Anthracycline-based consolidation may determine outcome of post-consolidation immunotherapy in AML. *Leukemia & lymphoma*: 1-8
- Austgulen R, Espevik T, Hammerstrom J, Nissen-Meyer J (1986) Role of monocyte cytotoxic factor in cytolysis of actinomycin D-treated WEHI 164 cells mediated by freshly isolated human adherent mononuclear blood cells. *Cancer research* **46**: 4566-4570
- Avendaño CM, J.C. (2008) Anticancer Drugs Acting via Radical Species, Photosensitizers and Photodynamic Therapy of Cancer. *Medicinal Chemistry of Anticancer Drugs*
- Bailey SR, Nelson MH, Himes RA, Li Z, Mehrotra S, Paulos CM (2014) Th17 cells in cancer: the ultimate identity crisis. *Frontiers in immunology* **5**: 276
- Balkwill F, Mantovani A (2001) Inflammation and cancer: back to Virchow? *Lancet* **357**: 539-545
- Banchereau J, Steinman RM (1998) Dendritic cells and the control of immunity. *Nature* **392**: 245-252
- Baracco EE, Pietrocola F, Buque A, Bloy N, Senovilla L, Zitvogel L, Vacchelli E, Kroemer G (2016) Inhibition

of formyl peptide receptor 1 reduces the efficacy of anticancer chemotherapy against carcinogen-induced breast cancer. *Oncoimmunology* **5**: e1139275

Baracco EE, Stoll G, Van Endert P, Zitvogel L, Vacchelli E, Kroemer G (2019) Contribution of annexin A1 to anticancer immunosurveillance. *Oncoimmunology*

Bauzon M, Drake PM, Barfield RM, Cornali BM, Rupniewski I, Rabuka D (2019) Maytansine-bearing antibody-drug conjugates induce in vitro hallmarks of immunogenic cell death selectively in antigen-positive target cells. *Oncoimmunology* **8**: e1565859

Beltran J, Ghosh AK, Basu S (2007) Immunotherapy of tumors with neuroimmune ligand capsaicin. *Journal of immunology* **178**: 3260-3264

Bensaude O (2011) Inhibiting eukaryotic transcription: Which compound to choose? How to evaluate its activity? *Transcription* **2**: 103-108

Bergmann C, Bachmann HS, Bankfalvi A, Lotfi R, Putter C, Wild CA, Schuler PJ, Greve J, Hoffmann TK, Lang S, Scherag A, Lehnerdt GF (2011) Toll-like receptor 4 single-nucleotide polymorphisms Asp299Gly and Thr399Ile in head and neck squamous cell carcinomas. *Journal of translational medicine* **9**: 139

Bersani L, Colotta F, Mantovani A (1986) Involvement of tumour necrosis factor in monocyte-mediated rapid killing of actinomycin D-pretreated WEHI 164 sarcoma cells. *Immunology* **59**: 323-325

Bezu L, Sauvat A, Humeau J, Gomes-da-Silva LC, Iribarren K, Forveille S, Garcia P, Zhao L, Liu P, Zitvogel L, Senovilla L, Kepp O, Kroemer G (2018a) eIF2alpha phosphorylation is pathognomonic for immunogenic cell death. *Cell death and differentiation*

Bezu L, Sauvat A, Humeau J, Leduc M, Kepp O, Kroemer G (2018b) eIF2alpha phosphorylation: A hallmark of immunogenic cell death. *Oncoimmunology* **7**: e1431089

Bianchi ME, Beltrame M (2000) Upwardly mobile proteins. Workshop: the role of HMG proteins in chromatin structure, gene expression and neoplasia. *EMBO reports* **1**: 109-114

Bidwell BN, Slaney CY, Withana NP, Forster S, Cao Y, Loi S, Andrews D, Mikeska T, Mangan NE, Samarajiwa SA, de Weerd NA, Gould J, Argani P, Moller A, Smyth MJ, Anderson RL, Hertzog PJ, Parker BS (2012) Silencing of Irf7 pathways in breast cancer cells promotes bone metastasis through immune escape. *Nature medicine* **18**: 1224-1231

Biedler JL, Riehm H (1970) Cellular resistance to actinomycin D in Chinese hamster cells in vitro: cross-resistance, radioautographic, and cytogenetic studies. *Cancer research* **30**: 1174-1184

Blay JY, Ray-Coquard I (2017) Sarcoma in 2016: Evolving biological understanding and treatment of sarcomas. *Nature reviews Clinical oncology* **14**: 78-80

Bock J, Szabo I, Jekle A, Gulbins E (2002) Actinomycin D-induced apoptosis involves the potassium channel Kv1.3. *Biochemical and biophysical research communications* **295**: 526-531

Bommareddy PK, Zloza A, Rabkin SD, Kaufman HL (2019) Oncolytic virus immunotherapy induces immunogenic cell death and overcomes STING deficiency in melanoma. *Oncoimmunology* **8**: 1591875

Bosmann HB, Kessel D (1970) Altered glycosidase levels in drug-resistant mouse leukemias. *Molecular pharmacology* **6**: 345-349

Boulon S, Westman BJ, Hutten S, Boisvert FM, Lamond AI (2010) The nucleolus under stress. *Molecular cell* **40**: 216-227

Bradner JE, Hnisz D, Young RA (2017) Transcriptional Addiction in Cancer. *Cell* **168**: 629-643

Brothman AR, Davis TP, Duffy JJ, Lindell TJ (1982) Development of an antibody to actinomycin D and its application for the detection of serum levels by radioimmunoassay. *Cancer research* **42**: 1184-1187

- Budczies J, Mechtersheimer G, Denkert C, Klauschen F, Mughal SS, Chudasama P, Bockmayr M, Johrens K, Endris V, Lier A, Lasitschka F, Penzel R, Dietel M, Brors B, Groschel S, Glimm H, Schirmacher P, Renner M, Frohling S, Stenzinger A (2017) PD-L1 (CD274) copy number gain, expression, and immune cell infiltration as candidate predictors for response to immune checkpoint inhibitors in soft-tissue sarcoma. *Oncoimmunology* **6**: e1279777
- Bugaut H, Bruchard M, Berger H, Derangere V, Odoul L, Euvrard R, Ladoire S, Chalmin F, Vegran F, Rebe C, Apetoh L, Ghiringhelli F, Mignot G (2013) Bleomycin exerts ambivalent antitumor immune effect by triggering both immunogenic cell death and proliferation of regulatory T cells. *PloS one* **8**: e65181
- Burgess M, Tawbi H (2015) Immunotherapeutic approaches to sarcoma. *Current treatment options in oncology* **16**: 26
- Burnet M (1957) Cancer: a biological approach. III. Viruses associated with neoplastic conditions. IV. Practical applications. *British medical journal* **1**: 841-847
- Burningham Z, Hashibe M, Spector L, Schiffman JD (2012) The epidemiology of sarcoma. *Clinical sarcoma research* **2**: 14
- Burnstock G (2007) Physiology and pathophysiology of purinergic neurotransmission. *Physiological reviews* **87**: 659-797
- Bustin M (1999) Regulation of DNA-dependent activities by the functional motifs of the high-mobility-group chromosomal proteins. *Molecular and cellular biology* **19**: 5237-5246
- Butler JE, Kadonaga JT (2002) The RNA polymerase II core promoter: a key component in the regulation of gene expression. *Genes & development* **16**: 2583-2592
- Camilio KA, Rekdal O, Sveinbjornsson B (2014) LTX-315 (Oncopore): A short synthetic anticancer peptide and novel immunotherapeutic agent. *Oncoimmunology* **3**: e29181
- Cancer.org (Retrieved 2019-08-17) Immune checkpoint inhibitors.
- CancerResearchUK (Retrieved 2019-08-01)
- Casares N, Pequignot MO, Tesniere A, Ghiringhelli F, Roux S, Chaput N, Schmitt E, Hamai A, Hervas-Stubbs S, Obeid M, Coutant F, Metivier D, Pichard E, Aucouturier P, Pierron G, Garrido C, Zitvogel L, Kroemer G (2005) Caspase-dependent immunogenicity of doxorubicin-induced tumor cell death. *The Journal of experimental medicine* **202**: 1691-1701
- Castro FA, Forsti A, Buch S, Kalthoff H, Krauss C, Bauer M, Egberts J, Schniewind B, Broering DC, Schreiber S, Schmitt M, Hampe J, Hemminki K, Schafmayer C (2011) TLR-3 polymorphism is an independent prognostic marker for stage II colorectal cancer. *European journal of cancer* **47**: 1203-1210
- Cavalieri LF, Nemchin RG (1964) The Mode of Interaction of Actinomycin D with Deoxyribonucleic Acid. *Biochimica et biophysica acta* **87**: 641-652
- Chalmers ZR, Connelly CF, Fabrizio D, Gay L, Ali SM, Ennis R, Schrock A, Campbell B, Shlien A, Chmielecki J, Huang F, He Y, Sun J, Tabori U, Kennedy M, Lieber DS, Roels S, White J, Otto GA, Ross JS, Garraway L, Miller VA, Stephens PJ, Frampton GM (2017) Analysis of 100,000 human cancer genomes reveals the landscape of tumor mutational burden. *Genome medicine* **9**: 34
- Chalmin F, Mignot G, Bruchard M, Chevriaux A, Vegran F, Hichami A, Ladoire S, Derangere V, Vincent J, Masson D, Robson SC, Eberl G, Pallandre JR, Borg C, Ryffel B, Apetoh L, Rebe C, Ghiringhelli F (2012) Stat3 and Gfi-1 transcription factors control Th17 cell immunosuppressive activity via the regulation of ectonucleotidase expression. *Immunity* **36**: 362-373
- Chan OT, Yang LX (2000) The immunological effects of taxanes. *Cancer immunology, immunotherapy : CII* **49**: 181-185

Chan SR, Vermi W, Luo J, Lucini L, Rickert C, Fowler AM, Lonardi S, Arthur C, Young LJ, Levy DE, Welch MJ, Cardiff RD, Schreiber RD (2012) STAT1-deficient mice spontaneously develop estrogen receptor alpha-positive luminal mammary carcinomas. *Breast cancer research : BCR* **14**: R16

Chang CL, Hsu YT, Wu CC, Yang YC, Wang C, Wu TC, Hung CF (2012) Immune mechanism of the antitumor effects generated by bortezomib. *Journal of immunology* **189**: 3209-3220

Chen DN, Song CG, Yu KD, Jiang YZ, Ye FG, Shao ZM (2015) A Prospective Evaluation of the Association between a Single Nucleotide Polymorphism rs3775291 in Toll-Like Receptor 3 and Breast Cancer Relapse. *PloS one* **10**: e0133184

Chen FM (1988) Binding specificities of actinomycin D to self-complementary tetranucleotide sequences -XG₂CY. *Biochemistry* **27**: 6393-6397

Chen FM (1992) Binding specificities of actinomycin D to non-self-complementary -XG₂CY-tetranucleotide sequences. *Biochemistry* **31**: 6223-6228

Chen FM, Sha F, Chin KH, Chou SH (2003) Unique actinomycin D binding to self-complementary d(CXYGGCCY'X'G) sequences: duplex disruption and binding to a nominally base-paired hairpin. *Nucleic acids research* **31**: 4238-4246

Chen FM, Sha F, Chin KH, Chou SH (2004) The nature of actinomycin D binding to d(AACCAXYG) sequence motifs. *Nucleic acids research* **32**: 271-277

Chen HM, Wang PH, Chen SS, Wen CC, Chen YH, Yang WC, Yang NS (2012) Shikonin induces immunogenic cell death in tumor cells and enhances dendritic cell-based cancer vaccine. *Cancer immunology, immunotherapy : CII* **61**: 1989-2002

Chinsky L, Turpin PY (1978) Ultraviolet resonance Raman study of DNA and of its interaction with actinomycin D. *Nucleic acids research* **5**: 2969-2977

Cirone M, Di Renzo L, Lotti LV, Conte V, Trivedi P, Santarelli R, Gonnella R, Frati L, Faggioni A (2012) Primary effusion lymphoma cell death induced by bortezomib and AG 490 activates dendritic cells through CD91. *PloS one* **7**: e31732

Cirone M, Garufi A, Di Renzo L, Granato M, Faggioni A, D'Orazi G (2013) Zinc supplementation is required for the cytotoxic and immunogenic effects of chemotherapy in chemoresistant p53-functionally deficient cells. *Oncoimmunology* **2**: e26198

clinicaltrials.gov (Retrieved 2019-08-10)

Cooper HL, Braverman R (1977) The mechanism by which actinomycin D inhibits protein synthesis in animal cells. *Nature* **269**: 527-529

Cortes CL, Veiga SR, Almacellas E, Hernandez-Losa J, Ferreres JC, Kozma SC, Ambrosio S, Thomas G, Tauler A (2016) Effect of low doses of actinomycin D on neuroblastoma cell lines. *Molecular cancer* **15**: 1

Curiel TJ, Coukos G, Zou L, Alvarez X, Cheng P, Mottram P, Evdemon-Hogan M, Conejo-Garcia JR, Zhang L, Burow M, Zhu Y, Wei S, Kryczek I, Daniel B, Gordon A, Myers L, Lackner A, Disis ML, Knutson KL, Chen L, Zou W (2004) Specific recruitment of regulatory T cells in ovarian carcinoma fosters immune privilege and predicts reduced survival. *Nature medicine* **10**: 942-949

D'Angelo SP, Shoushtari AN, Agaram NP, Kuk D, Qin LX, Carvajal RD, Dickson MA, Gounder M, Keohan ML, Schwartz GK, Tap WD (2015) Prevalence of tumor-infiltrating lymphocytes and PD-L1 expression in the soft tissue sarcoma microenvironment. *Human pathology* **46**: 357-365

D'Angio GJ, Maddock CL, Farber S, Brown BL (1965) The enhanced response of the Ridgway osteogenic sarcoma to roentgen radiation combined with actinomycin D. *Cancer research* **25**: 1002-1007

- D'Arpa P, Liu LF (1989) Topoisomerase-targeting antitumor drugs. *Biochimica et biophysica acta* **989**: 163-177
- D'Eliseo D, Di Renzo L, Santoni A, Velotti F (2017) Docosahexaenoic acid (DHA) promotes immunogenic apoptosis in human multiple myeloma cells, induces autophagy and inhibits STAT3 in both tumor and dendritic cells. *Genes & cancer* **8**: 426-437
- D'Eliseo D, Manzi L, Velotti F (2013) Capsaicin as an inducer of damage-associated molecular patterns (DAMPs) of immunogenic cell death (ICD) in human bladder cancer cells. *Cell stress & chaperones* **18**: 801-808
- Danaher P, Warren S, Lu R, Samayoa J, Sullivan A, Pekker I, Wallden B, Marincola FM, Cesano A (2018) Pan-cancer adaptive immune resistance as defined by the Tumor Inflammation Signature (TIS): results from The Cancer Genome Atlas (TCGA). *Journal for immunotherapy of cancer* **6**: 63
- Demaria S, Santori FR, Ng B, Liebes L, Formenti SC, Vukmanovic S (2005) Select forms of tumor cell apoptosis induce dendritic cell maturation. *Journal of leukocyte biology* **77**: 361-368
- Deng L, Liang H, Xu M, Yang X, Burnette B, Arina A, Li XD, Mauceri H, Beckett M, Darga T, Huang X, Gajewski TF, Chen ZJ, Fu YX, Weichselbaum RR (2014) STING-Dependent Cytosolic DNA Sensing Promotes Radiation-Induced Type I Interferon-Dependent Antitumor Immunity in Immunogenic Tumors. *Immunity* **41**: 843-852
- Diaconu I, Cerullo V, Hirvonen ML, Escutenaire S, Ugolini M, Pesonen SK, Bramante S, Parviainen S, Kanerva A, Loskog AS, Eliopoulos AG, Pesonen S, Hemminki A (2012) Immune response is an important aspect of the antitumor effect produced by a CD40L-encoding oncolytic adenovirus. *Cancer research* **72**: 2327-2338
- Dipaolo JA, Moore GE, Niedbala TF (1957) Experimental studies with actinomycin D. *Cancer research* **17**: 1127-1134
- Dohme-Chibret MS (2004) Recommendations pour l'utilisation de Cosmegen en France.
- Donnelly OG, Errington-Mais F, Steele L, Hadac E, Jennings V, Scott K, Peach H, Phillips RM, Bond J, Pandha H, Harrington K, Vile R, Russell S, Selby P, Melcher AA (2013) Measles virus causes immunogenic cell death in human melanoma. *Gene therapy* **20**: 7-15
- Drygin D, Rice WG, Grummt I (2010) The RNA polymerase I transcription machinery: an emerging target for the treatment of cancer. *Annual review of pharmacology and toxicology* **50**: 131-156
- Dudek-Peric AM, Ferreira GB, Muchowicz A, Wouters J, Prada N, Martin S, Kiviluoto S, Winiarska M, Boon L, Mathieu C, van den Oord J, Stas M, Gougeon ML, Golab J, Garg AD, Agostinis P (2015) Antitumor immunity triggered by melphalan is potentiated by melanoma cell surface-associated calreticulin. *Cancer research* **75**: 1603-1614
- Dunn GP, Old LJ, Schreiber RD (2004a) The immunobiology of cancer immunosurveillance and immunoediting. *Immunity* **21**: 137-148
- Dunn GP, Old LJ, Schreiber RD (2004b) The three Es of cancer immunoediting. *Annual review of immunology* **22**: 329-360
- Eike LM, Mauseth B, Camilio KA, Rekdal O, Sveinbjornsson B (2016) The Cytolytic Amphipathic beta(2,2)-Amino Acid LTX-401 Induces DAMP Release in Melanoma Cells and Causes Complete Regression of B16 Melanoma. *PloS one* **11**: e0148980
- Eike LM, Yang N, Rekdal O, Sveinbjornsson B (2015) The oncolytic peptide LTX-315 induces cell death and DAMP release by mitochondria distortion in human melanoma cells. *Oncotarget* **6**: 34910-34923
- Elliott MR, Chekeni FB, Trampont PC, Lazarowski ER, Kadl A, Walk SF, Park D, Woodson RI, Ostankovich M, Sharma P, Lysiak JJ, Harden TK, Leitinger N, Ravichandran KS (2009) Nucleotides released by apoptotic cells act as a find-me signal to promote phagocytic clearance. *Nature* **461**: 282-286
- Enot DP, Vacchelli E, Jacquilot N, Zitvogel L, Kroemer G (2018) TumGrowth: An open-access web tool for the

statistical analysis of tumor growth curves. *Oncoimmunology* **7**: e1462431

FDA (2008) Cosmegen for injection.

FDA (Retrieved 2019-08-17) FDA approves avelumab plus axitinib renal cell carcinoma.

Foley EJ (1953) Antigenic properties of methylcholanthrene-induced tumors in mice of the strain of origin. *Cancer research* **13**: 835-837

Fraschini A, Bottone MG, Scovassi AI, Denegri M, Risueno MC, Testillano PS, Martin TE, Biggiogera M, Pellicciari C (2005) Changes in extranucleolar transcription during actinomycin D-induced apoptosis. *Histology and histopathology* **20**: 107-117

Fridman WH, Zitvogel L, Sautes-Fridman C, Kroemer G (2017) The immune contexture in cancer prognosis and treatment. *Nature reviews Clinical oncology* **14**: 717-734

Fucikova J, Becht E, Iribarren K, Goc J, Remark R, Damotte D, Alifano M, Devi P, Biton J, Germain C, Lupo A, Fridman WH, Dieu-Nosjean MC, Kroemer G, Sautes-Fridman C, Cremer I (2016a) Calreticulin Expression in Human Non-Small Cell Lung Cancers Correlates with Increased Accumulation of Antitumor Immune Cells and Favorable Prognosis. *Cancer research* **76**: 1746-1756

Fucikova J, Kralikova P, Fialova A, Brtnicky T, Rob L, Bartunkova J, Spisek R (2011) Human tumor cells killed by anthracyclines induce a tumor-specific immune response. *Cancer research* **71**: 4821-4833

Fucikova J, Moserova I, Truxova I, Hermanova I, Vancurova I, Partlova S, Fialova A, Sojka L, Cartron PF, Houska M, Rob L, Bartunkova J, Spisek R (2014) High hydrostatic pressure induces immunogenic cell death in human tumor cells. *International journal of cancer* **135**: 1165-1177

Fucikova J, Truxova I, Hensler M, Becht E, Kasikova L, Moserova I, Vosahlikova S, Klouckova J, Church SE, Cremer I, Kepp O, Kroemer G, Galluzzi L, Salek C, Spisek R (2016b) Calreticulin exposure by malignant blasts correlates with robust anticancer immunity and improved clinical outcome in AML patients. *Blood* **128**: 3113-3124

Gajewski TF, Schreiber H, Fu YX (2013) Innate and adaptive immune cells in the tumor microenvironment. *Nature immunology* **14**: 1014-1022

Galbraith WM, Mellett LB (1975) Tissue disposition of 3H-actinomycin D (NSC-3053) in the rat, monkey, and dog. *Cancer chemotherapy reports* **59**: 1601-1609

Galluzzi L, Bravo-San Pedro JM, Vitale I, Aaronson SA, Abrams JM, Adam D, Alnemri ES, Altucci L, Andrews D, Annicchiarico-Petruzzelli M, Baehrecke EH, Bazan NG, Bertrand MJ, Bianchi K, Blagosklonny MV, Blomgren K, Borner C, Bredesen DE, Brenner C, Campanella M, Candi E, Cecconi F, Chan FK, Chandel NS, Cheng EH, Chipuk JE, Cidlowski JA, Ciechanover A, Dawson TM, Dawson VL, De Laurenzi V, De Maria R, Debatin KM, Di Daniele N, Dixit VM, Dynlacht BD, El-Deiry WS, Fimia GM, Flavell RA, Fulda S, Garrido C, Gougeon ML, Green DR, Gronemeyer H, Hajnoczky G, Hardwick JM, Hengartner MO, Ichijo H, Joseph B, Jost PJ, Kaufmann T, Kepp O, Klionsky DJ, Knight RA, Kumar S, Lemasters JJ, Levine B, Linkermann A, Lipton SA, Lockshin RA, Lopez-Otin C, Lugli E, Madeo F, Malorni W, Marine JC, Martin SJ, Martinou JC, Medema JP, Meier P, Melino S, Mizushima N, Moll U, Munoz-Pinedo C, Nunez G, Oberst A, Panaretakis T, Penninger JM, Peter ME, Piacentini M, Pinton P, Prehn JH, Puthalakath H, Rabinovich GA, Ravichandran KS, Rizzuto R, Rodrigues CM, Rubinsztein DC, Rudel T, Shi Y, Simon HU, Stockwell BR, Szabadkai G, Tait SW, Tang HL, Tavernarakis N, Tsujimoto Y, Vanden Berghe T, Vandenabeele P, Villunger A, Wagner EF, Walczak H, White E, Wood WG, Yuan J, Zakeri Z, Zhivotovsky B, Melino G, Kroemer G (2015a) Essential versus accessory aspects of cell death: recommendations of the NCCD 2015. *Cell death and differentiation* **22**: 58-73

Galluzzi L, Buque A, Kepp O, Zitvogel L, Kroemer G (2015b) Immunological Effects of Conventional Chemotherapy and Targeted Anticancer Agents. *Cancer cell* **28**: 690-714

Galluzzi L, Buque A, Kepp O, Zitvogel L, Kroemer G (2017) Immunogenic cell death in cancer and infectious disease. *Nature reviews Immunology* **17**: 97-111

- Gardai SJ, McPhillips KA, Frasch SC, Janssen WJ, Starefeldt A, Murphy-Ullrich JE, Bratton DL, Oldenborg PA, Michalak M, Henson PM (2005) Cell-surface calreticulin initiates clearance of viable or apoptotic cells through trans-activation of LRP on the phagocyte. *Cell* **123**: 321-334
- Gardner A, Ruffell B (2016) Dendritic Cells and Cancer Immunity. *Trends in immunology* **37**: 855-865
- Garg AD, Dudek AM, Ferreira GB, Verfaillie T, Vandenabeele P, Krysko DV, Mathieu C, Agostinis P (2013) ROS-induced autophagy in cancer cells assists in evasion from determinants of immunogenic cell death. *Autophagy* **9**: 1292-1307
- Garg AD, Elsen S, Krysko DV, Vandenabeele P, de Witte P, Agostinis P (2015) Resistance to anticancer vaccination effect is controlled by a cancer cell-autonomous phenotype that disrupts immunogenic phagocytic removal. *Oncotarget* **6**: 26841-26860
- Garg AD, Krysko DV, Vandenabeele P, Agostinis P (2012a) Hypericin-based photodynamic therapy induces surface exposure of damage-associated molecular patterns like HSP70 and calreticulin. *Cancer immunology, immunotherapy : CII* **61**: 215-221
- Garg AD, Krysko DV, Verfaillie T, Kaczmarek A, Ferreira GB, Marysael T, Rubio N, Firczuk M, Mathieu C, Roebroek AJ, Annaert W, Golab J, de Witte P, Vandenabeele P, Agostinis P (2012b) A novel pathway combining calreticulin exposure and ATP secretion in immunogenic cancer cell death. *The EMBO journal* **31**: 1062-1079
- Garg AD, More S, Rufo N, Mece O, Sassano ML, Agostinis P, Zitvogel L, Kroemer G, Galluzzi L (2017a) Trial watch: Immunogenic cell death induction by anticancer chemotherapeutics. *Oncoimmunology* **6**: e1386829
- Garg AD, Vandenberk L, Fang S, Fasche T, Van Eygen S, Maes J, Van Woensel M, Koks C, Vanthillo N, Graf N, de Witte P, Van Gool S, Salven P, Agostinis P (2017b) Pathogen response-like recruitment and activation of neutrophils by sterile immunogenic dying cells drives neutrophil-mediated residual cell killing. *Cell death and differentiation* **24**: 832-843
- Garrido G, Rabasa A, Sanchez B, Lopez MV, Blanco R, Lopez A, Hernandez DR, Perez R, Fernandez LE (2011) Induction of immunogenic apoptosis by blockade of epidermal growth factor receptor activation with a specific antibody. *Journal of immunology* **187**: 4954-4966
- Gellert M, Smith CE, Neville D, Felsenfeld G (1965) Actinomycin Binding to DNA: Mechanism and Specificity. *Journal of molecular biology* **11**: 445-457
- Ghiringhelli F, Apetoh L, Tesniere A, Aymeric L, Ma Y, Ortiz C, Vermaelen K, Panaretakis T, Mignot G, Ullrich E, Perfettini JL, Schlemmer F, Tasmemir E, Uhl M, Genin P, Civas A, Ryffel B, Kanellopoulos J, Tschopp J, Andre F, Lidereau R, McLaughlin NM, Haynes NM, Smyth MJ, Kroemer G, Zitvogel L (2009) Activation of the NLRP3 inflammasome in dendritic cells induces IL-1beta-dependent adaptive immunity against tumors. *Nature medicine* **15**: 1170-1178
- Ghiringhelli F, Menard C, Puig PE, Ladoire S, Roux S, Martin F, Solary E, Le Cesne A, Zitvogel L, Chauffert B (2007) Metronomic cyclophosphamide regimen selectively depletes CD4+CD25+ regulatory T cells and restores T and NK effector functions in end stage cancer patients. *Cancer immunology, immunotherapy : CII* **56**: 641-648
- Giampazolias E, Zunino B, Dhayade S, Bock F, Cloix C, Cao K, Roca A, Lopez J, Ichim G, Proics E, Rubio-Patino C, Fort L, Yatim N, Woodham E, Orozco S, Taraborrelli L, Peltzer N, Lecis D, Machesky L, Walczak H, Albert ML, Milling S, Oberst A, Ricci JE, Ryan KM, Blyth K, Tait SWG (2017) Mitochondrial permeabilization engages NF-kappaB-dependent anti-tumour activity under caspase deficiency. *Nature cell biology* **19**: 1116-1129
- Giglio P, Gagliardi M, Tumino N, Antunes F, Smaili S, Cotella D, Santoro C, Bernardini R, Mattei M, Piacentini M, Corazzari M (2018) PKR and GCN2 stress kinases promote an ER stress-independent eIF2alpha phosphorylation responsible for calreticulin exposure in melanoma cells. *Oncoimmunology* **7**: e1466765
- Gilardini Montani MS, D'Eliseo D, Cirone M, Di Renzo L, Faggioni A, Santoni A, Velotti F (2015) Capsaicin-mediated apoptosis of human bladder cancer cells activates dendritic cells via CD91. *Nutrition* **31**: 578-581
- Goldberg IH, Rabinowitz M, Reich E (1962) Basis of actinomycin action. I. DNA binding and inhibition of RNA-

polymerase synthetic reactions by actinomycin. *Proceedings of the National Academy of Sciences of the United States of America* **48**: 2094-2101

Goldberg IH, Rabinowitz M, Reich E (1963) Basis of actinomycin action. II. Effect of actinomycin on the nucleoside triphosphate-inorganic pyrophosphate exchange. *Proceedings of the National Academy of Sciences of the United States of America* **49**: 226-229

Goldberg IHR, M. (1962) Actinomycin D Inhibition of Deoxyribonucleic Acid-Dependent Synthesis of Ribonucleic Acid. *Science* **136**: 315-316

Golden EB, Frances D, Pellicciotta I, Demaria S, Helen Barcellos-Hoff M, Formenti SC (2014) Radiation fosters dose-dependent and chemotherapy-induced immunogenic cell death. *Oncoimmunology* **3**: e28518

Goldstein ES, Penman S (1973) Regulation of protein synthesis in mammalian cells. V. Further studies on the effect of actinomycin D on translation control in HeLa cells. *Journal of molecular biology* **80**: 243-254

Goldstein MN, Hamm K, Amrod E (1966) Incorporation of tritiated actinomycin D into drug-sensitive and drug-resistant HeLa cells. *Science* **151**: 1555-1556

Gomes-da-Silva LC, Zhao L, Bezu L, Zhou H, Sauvat A, Liu P, Durand S, Leduc M, Souquere S, Loos F, Mondragon L, Sveinbjornsson B, Rekdal O, Boncompain G, Perez F, Arnaut LG, Kepp O, Kroemer G (2018) Photodynamic therapy with redaporfin targets the endoplasmic reticulum and Golgi apparatus. *The EMBO journal* **37**

Goritzka M, Durant LR, Pereira C, Salek-Ardakani S, Openshaw PJ, Johansson C (2014) Alpha/beta interferon receptor signaling amplifies early proinflammatory cytokine production in the lung during respiratory syncytial virus infection. *Journal of virology* **88**: 6128-6136

Granstein RD, Ding W, Huang J, Holzer A, Gallo RL, Di Nardo A, Wagner JA (2005) Augmentation of cutaneous immune responses by ATP gamma S: purinergic agonists define a novel class of immunologic adjuvants. *Journal of immunology* **174**: 7725-7731

Gregory FJ, Hata T, Pugh LH, Thielen R (1956) The effect of actinomycin D on experimental ascitic tumors in the mouse. *Cancer research* **16**: 985-987

Hahn S (2004) Structure and mechanism of the RNA polymerase II transcription machinery. *Nature structural & molecular biology* **11**: 394-403

Hanahan D, Weinberg RA (2000) The hallmarks of cancer. *Cell* **100**: 57-70

Hanahan D, Weinberg RA (2011) Hallmarks of cancer: the next generation. *Cell* **144**: 646-674

Hao NB, Lu MH, Fan YH, Cao YL, Zhang ZR, Yang SM (2012) Macrophages in tumor microenvironments and the progression of tumors. *Clinical & developmental immunology* **2012**: 948098

Hemminki O, Parviainen S, Juhila J, Turkki R, Linder N, Lundin J, Kankainen M, Ristimäki A, Koski A, Liikanen I, Oksanen M, Nettelbeck DM, Kairemo K, Partanen K, Joensuu T, Kanerva A, Hemminki A (2015) Immunological data from cancer patients treated with Ad5/3-E2F-Delta24-GMCSF suggests utility for tumor immunotherapy. *Oncotarget* **6**: 4467-4481

Hill CR, Cole M, Errington J, Malik G, Boddy AV, Veal GJ (2014) Characterisation of the clinical pharmacokinetics of actinomycin D and the influence of ABCB1 pharmacogenetic variation on actinomycin D disposition in children with cancer. *Clinical pharmacokinetics* **53**: 741-751

Hill CR, Jamieson D, Thomas HD, Brown CD, Boddy AV, Veal GJ (2013) Characterisation of the roles of ABCB1, ABCC1, ABCC2 and ABCG2 in the transport and pharmacokinetics of actinomycin D in vitro and in vivo. *Biochemical pharmacology* **85**: 29-37

Hodi FS, O'Day SJ, McDermott DF, Weber RW, Sosman JA, Haanen JB, Gonzalez R, Robert C, Schadendorf D, Hassel JC, Akerley W, van den Eertwegh AJ, Lutzky J, Lorigan P, Vaubel JM, Linette GP, Hogg D, Ottensmeier

- CH, Lebbe C, Peschel C, Quirt I, Clark JI, Wolchok JD, Weber JS, Tian J, Yellin MJ, Nichol GM, Hoos A, Urba WJ (2010) Improved survival with ipilimumab in patients with metastatic melanoma. *The New England journal of medicine* **363**: 711-723
- Honig GR, Rabinovitz M (1965) Actinomycin D: inhibition of protein synthesis unrelated to effect on template RNA synthesis. *Science* **149**: 1504-1506
- Hossain DMS, Javaid S, Cai M, Zhang C, Sawant A, Hinton M, Sathe M, Grein J, Blumenschein W, Pinheiro EM, Chackerian A (2018) Dinaciclib induces immunogenic cell death and enhances anti-PD1-mediated tumor suppression. *The Journal of clinical investigation* **128**: 644-654
- Hou MH, Robinson H, Gao YG, Wang AH (2002) Crystal structure of actinomycin D bound to the CTG triplet repeat sequences linked to neurological diseases. *Nucleic acids research* **30**: 4910-4917
- Humeau J, Levesque S, Kroemer G, Pol JG (2019) Gold Standard Assessment of Immunogenic Cell Death in Oncological Mouse Models. *Methods in molecular biology* **1884**: 297-315
- Hurwitz J, Furth JJ, Malamy M, Alexander M (1962) The role of deoxyribonucleic acid in ribonucleic acid synthesis. III. The inhibition of the enzymatic synthesis of ribonucleic acid and deoxyribonucleic acid by actinomycin D and proflavin. *Proceedings of the National Academy of Sciences of the United States of America* **48**: 1222-1230
- Idzko M, Hammad H, van Nimwegen M, Kool M, Willart MA, Muskens F, Hoogsteden HC, Luttmann W, Ferrari D, Di Virgilio F, Virchow JC, Jr., Lambrecht BN (2007) Extracellular ATP triggers and maintains asthmatic airway inflammation by activating dendritic cells. *Nature medicine* **13**: 913-919
- Ilan J, Quastel JH (1966) Effects of actinomycin D on nucleic acid metabolism and protein biosynthesis during metamorphosis of *Tenebrio molitor* L. *The Biochemical journal* **100**: 441-447
- Jackson RJ, Hellen CU, Pestova TV (2010) The mechanism of eukaryotic translation initiation and principles of its regulation. *Nature reviews Molecular cell biology* **11**: 113-127
- Jaffe N, Paed D, Traggis D, Salian S, Cassady JR (1976) Improved outlook for Ewing's sarcoma with combination chemotherapy (vincristine, actinomycin D and cyclophosphamide) and radiation therapy. *Cancer* **38**: 1925-1930
- Jao CY, Salic A (2008) Exploring RNA transcription and turnover in vivo by using click chemistry. *Proceedings of the National Academy of Sciences of the United States of America* **105**: 15779-15784
- Juliano RL, Ling V (1976) A surface glycoprotein modulating drug permeability in Chinese hamster ovary cell mutants. *Biochimica et biophysica acta* **455**: 152-162
- Kajiwara K, Ikeda K, Kuroi R, Hashimoto R, Tokumaru S, Kojo S (2001) Hydrogen peroxide and hydroxyl radical involvement in the activation of caspase-3 in chemically induced apoptosis of HL-60 cells. *Cellular and molecular life sciences : CMLS* **58**: 485-491
- Kam PC, Thompson JF (2010) Isolated limb infusion with melphalan and actinomycin D in melanoma patients: factors predictive of acute regional toxicity. *Expert opinion on drug metabolism & toxicology* **6**: 1039-1045
- Kamitori S, Takusagawa F (1992) Crystal structure of the 2:1 complex between d(GAAGCTTC) and the anticancer drug actinomycin D. *Journal of molecular biology* **225**: 445-456
- Kamitori S, Takusagawa F (1993) [DNA intercalation; x-ray crystallographic studies]. *Tanpakushitsu kakusan koso Protein, nucleic acid, enzyme* **38**: 957-970
- Karin M, Cao Y, Greten FR, Li ZW (2002) NF-kappaB in cancer: from innocent bystander to major culprit. *Nature reviews Cancer* **2**: 301-310
- Kato H, Nishitoh H (2015) Stress responses from the endoplasmic reticulum in cancer. *Frontiers in oncology* **5**: 93

Kepp O, Galluzzi L, Giordanetto F, Tesniere A, Vitale I, Martins I, Schlemmer F, Adjemian S, Zitvogel L, Kroemer G (2009) Disruption of the PP1/GADD34 complex induces calreticulin exposure. *Cell cycle* **8**: 3971-3977

Kepp O, Senovilla L, Vitale I, Vacchelli E, Adjemian S, Agostinis P, Apetoh L, Aranda F, Barnaba V, Bloy N, Bracci L, Breckpot K, Brough D, Buque A, Castro MG, Cirone M, Colombo MI, Cremer I, Demaria S, Dini L, Eliopoulos AG, Faggioni A, Formenti SC, Fucikova J, Gabriele L, Gaipf US, Galon J, Garg A, Ghiringhelli F, Giese NA, Guo ZS, Hemminki A, Herrmann M, Hodge JW, Holdenrieder S, Honeychurch J, Hu HM, Huang X, Illidge TM, Kono K, Korbelik M, Krysko DV, Loi S, Lowenstein PR, Lugli E, Ma Y, Madeo F, Manfredi AA, Martins I, Mavilio D, Menger L, Merendino N, Michaud M, Mignot G, Mossman KL, Multhoff G, Oehler R, Palombo F, Panaretakis T, Pol J, Proietti E, Ricci JE, Riganti C, Rovere-Querini P, Rubartelli A, Sistigu A, Smyth MJ, Sonnemann J, Spisek R, Stagg J, Sukkurwala AQ, Tartour E, Thorburn A, Thorne SH, Vandenabeele P, Velotti F, Workenhe ST, Yang H, Zong WX, Zitvogel L, Kroemer G, Galluzzi L (2014) Consensus guidelines for the detection of immunogenic cell death. *Oncoimmunology* **3**: e955691

Kessel D, Wodinsky I (1968) Uptake in vivo and in vitro of actinomycin D by mouse leukemias as factors in survival. *Biochemical pharmacology* **17**: 161-164

Khatter H, Vorlander MK, Muller CW (2017) RNA polymerase I and III: similar yet unique. *Current opinion in structural biology* **47**: 88-94

Kim C, Kim EK, Jung H, Chon HJ, Han JW, Shin KH, Hu H, Kim KS, Choi YD, Kim S, Lee YH, Suh JS, Ahn JB, Chung HC, Noh SH, Rha SY, Kim SH, Kim HS (2016) Prognostic implications of PD-L1 expression in patients with soft tissue sarcoma. *BMC cancer* **16**: 434

Kim JR, Moon YJ, Kwon KS, Bae JS, Wagle S, Kim KM, Park HS, Lee H, Moon WS, Chung MJ, Kang MJ, Jang KY (2013) Tumor infiltrating PD1-positive lymphocytes and the expression of PD-L1 predict poor prognosis of soft tissue sarcomas. *PloS one* **8**: e82870

Klass J, Murphy FVt, Fouts S, Serenil M, Changela A, Siple J, Churchill ME (2003) The role of intercalating residues in chromosomal high-mobility-group protein DNA binding, bending and specificity. *Nucleic acids research* **31**: 2852-2864

Kleeff J, Kornmann M, Sawhney H, Korc M (2000) Actinomycin D induces apoptosis and inhibits growth of pancreatic cancer cells. *International journal of cancer* **86**: 399-407

Klein G, Sjogren HO, Klein E, Hellstrom KE (1960) Demonstration of resistance against methylcholanthrene-induced sarcomas in the primary autochthonous host. *Cancer research* **20**: 1561-1572

Knochelmann HM, Dwyer CJ, Bailey SR, Amaya SM, Elston DM, Mazza-McCrann JM, Paulos CM (2018) When worlds collide: Th17 and Treg cells in cancer and autoimmunity. *Cellular & molecular immunology* **15**: 458-469

Kodumudi KN, Woan K, Gilvary DL, Sahakian E, Wei S, Djeu JY (2010) A novel chemoimmunomodulating property of docetaxel: suppression of myeloid-derived suppressor cells in tumor bearers. *Clinical cancer research : an official journal of the American Association for Cancer Research* **16**: 4583-4594

Koks CA, Garg AD, Ehrhardt M, Riva M, Vandenberk L, Boon L, De Vleeschouwer S, Agostinis P, Graf N, Van Gool SW (2015) Newcastle disease virotherapy induces long-term survival and tumor-specific immune memory in orthotopic glioma through the induction of immunogenic cell death. *International journal of cancer* **136**: E313-325

Korbelik M, Dougherty GJ (1999) Photodynamic therapy-mediated immune response against subcutaneous mouse tumors. *Cancer research* **59**: 1941-1946

Korbelik M, Stott B, Sun J (2007) Photodynamic therapy-generated vaccines: relevance of tumour cell death expression. *British journal of cancer* **97**: 1381-1387

Korbelik M, Zhang W, Merchant S (2011) Involvement of damage-associated molecular patterns in tumor response to photodynamic therapy: surface expression of calreticulin and high-mobility group box-1 release. *Cancer immunology, immunotherapy : CII* **60**: 1431-1437

- Kozmar A, Greenlee-Wacker MC, Bohlson SS (2010) Macrophage response to apoptotic cells varies with the apoptotic trigger and is not altered by a deficiency in LRP expression. *Journal of innate immunity* **2**: 248-259
- Kroemer G, Marino G, Levine B (2010) Autophagy and the integrated stress response. *Molecular cell* **40**: 280-293
- Kronlage M, Song J, Sorokin L, Isfort K, Schwerdtle T, Leipziger J, Robaye B, Conley PB, Kim HC, Sargin S, Schon P, Schwab A, Hanley PJ (2010) Autocrine purinergic receptor signaling is essential for macrophage chemotaxis. *Science signaling* **3**: ra55
- Krosi G, Korbelik M, Dougherty GJ (1995) Induction of immune cell infiltration into murine SCCVII tumour by photofrin-based photodynamic therapy. *British journal of cancer* **71**: 549-555
- Ladoire S, Arnould L, Apetoh L, Coudert B, Martin F, Chaffert B, Fumoleau P, Ghiringhelli F (2008) Pathologic complete response to neoadjuvant chemotherapy of breast carcinoma is associated with the disappearance of tumor-infiltrating foxp3+ regulatory T cells. *Clinical cancer research : an official journal of the American Association for Cancer Research* **14**: 2413-2420
- Ladoire S, Enot D, Andre F, Zitvogel L, Kroemer G (2016) Immunogenic cell death-related biomarkers: Impact on the survival of breast cancer patients after adjuvant chemotherapy. *Oncoimmunology* **5**: e1082706
- Ladoire S, Penault-Llorca F, Senovilla L, Dalban C, Enot D, Locher C, Prada N, Poirier-Colame V, Chaba K, Arnould L, Ghiringhelli F, Fumoleau P, Spielmann M, Delalogue S, Poillot ML, Arveux P, Goubar A, Andre F, Zitvogel L, Kroemer G (2015) Combined evaluation of LC3B puncta and HMGB1 expression predicts residual risk of relapse after adjuvant chemotherapy in breast cancer. *Autophagy* **11**: 1878-1890
- Lambert M, Jambon S, Depauw S, David-Cordonnier MH (2018) Targeting Transcription Factors for Cancer Treatment. *Molecules* **23**
- Laszlo J, Miller DS, McCarty KS, Hochstein P (1966) Actinomycin D: inhibition of respiration and glycolysis. *Science* **151**: 1007-1010
- Lesokhin AM, Callahan MK, Postow MA, Wolchok JD (2015) On being less tolerant: enhanced cancer immunosurveillance enabled by targeting checkpoints and agonists of T cell activation. *Science translational medicine* **7**: 280sr281
- Levesque S, Le Naour J, Pietrocola F, Paillet J, Kremer M, Castoldi F, Baracco EE, Wang Y, Vacchelli E, Stoll G, Jolly A, De la Grange P, Zitvogel L, Kroemer G, Pol J (2019) A synergistic triad of chemotherapy, immunecheckpoint inhibitors, and caloric restrictionmimetics eradicates tumors in mice. *Oncoimmunology*
- Li R, Sutphin PD, Schwartz D, Matas D, Almog N, Wolkowicz R, Goldfinger N, Pei H, Prokocimer M, Rotter V (1998) Mutant p53 protein expression interferes with p53-independent apoptotic pathways. *Oncogene* **16**: 3269-3277
- Li W, Cai S, Cai L, Li X (2006) Anti-apoptotic effect of hepatocyte growth factor from actinomycin D in hepatocyte-derived HL7702 cells is associated with activation of PI3K/Akt signaling. *Toxicology letters* **165**: 142-148
- Liebner DA (2015) The indications and efficacy of conventional chemotherapy in primary and recurrent sarcoma. *Journal of surgical oncology* **111**: 622-631
- Liikanen I, Ahtiainen L, Hirvinen ML, Bramante S, Cerullo V, Nokisalmi P, Hemminki O, Diaconu I, Pesonen S, Koski A, Kangasniemi L, Pesonen SK, Oksanen M, Laasonen L, Partanen K, Joensuu T, Zhao F, Kanerva A, Hemminki A (2013) Oncolytic adenovirus with temozolomide induces autophagy and antitumor immune responses in cancer patients. *Molecular therapy : the journal of the American Society of Gene Therapy* **21**: 1212-1223
- Lillis AP, Greenlee MC, Mikhailenko I, Pizzo SV, Tenner AJ, Strickland DK, Bohlson SS (2008) Murine low-density lipoprotein receptor-related protein 1 (LRP) is required for phagocytosis of targets bearing LRP ligands

- but is not required for C1q-triggered enhancement of phagocytosis. *Journal of immunology* **181**: 364-373
- Lim JY, Gerber SA, Murphy SP, Lord EM (2014) Type I interferons induced by radiation therapy mediate recruitment and effector function of CD8(+) T cells. *Cancer immunology, immunotherapy : CII* **63**: 259-271
- Lin TJ, Lin HT, Chang WT, Mitapalli SP, Hsiao PW, Yin SY, Yang NS (2015) Shikonin-enhanced cell immunogenicity of tumor vaccine is mediated by the differential effects of DAMP components. *Molecular cancer* **14**: 174
- Liu CC, Leclair P, Pedari F, Vieira H, Monajemi M, Sly LM, Reid GS, Lim CJ (2019a) Integrins and ERp57 Coordinate to Regulate Cell Surface Calreticulin in Immunogenic Cell Death. *Frontiers in oncology* **9**: 411
- Liu P, Zhao L, Pol J, Levesque S, Petrazzuolo A, Pfirschke C, Engblom C, Rickelt S, Yamazaki T, Iribarren K, Senovilla L, Bezu L, Vacchelli E, Sica V, Melis A, Martin T, Xia L, Yang H, Li Q, Chen J, Durand S, Arahamian F, Lefevre D, Broutin S, Paci A, Bongers A, Minard-Colin V, Tartour E, Zitvogel L, Apetoh L, Ma Y, Pittet MJ, Kepp O, Kroemer G (2019b) Crizotinib-induced immunogenic cell death in non-small cell lung cancer. *Nature communications* **10**: 1486
- Liu XF, Xiang L, Zhou Q, Carralot JP, Prunotto M, Niederfellner G, Pastan I (2016) Actinomycin D enhances killing of cancer cells by immunotoxin RG7787 through activation of the extrinsic pathway of apoptosis. *Proceedings of the National Academy of Sciences of the United States of America* **113**: 10666-10671
- Lopez-Lastra M, Rivas A, Barria MI (2005) Protein synthesis in eukaryotes: the growing biological relevance of cap-independent translation initiation. *Biological research* **38**: 121-146
- Lu DF, Wang YS, Li C, Wei GJ, Chen R, Dong DM, Yao M (2015a) Actinomycin D inhibits cell proliferations and promotes apoptosis in osteosarcoma cells. *International journal of clinical and experimental medicine* **8**: 1904-1911
- Lu X, Ding ZC, Cao Y, Liu C, Habettsion T, Yu M, Lemos H, Salman H, Xu H, Mellor AL, Zhou G (2015b) Alkylating agent melphalan augments the efficacy of adoptive immunotherapy using tumor-specific CD4+ T cells. *Journal of immunology* **194**: 2011-2021
- Luo J, Solimini NL, Elledge SJ (2009) Principles of cancer therapy: oncogene and non-oncogene addiction. *Cell* **136**: 823-837
- Luo Q, Zhang L, Luo C, Jiang M (2019) Emerging strategies in cancer therapy combining chemotherapy with immunotherapy. *Cancer letters* **454**: 191-203
- Ma Y, Adjemian S, Mattarollo SR, Yamazaki T, Aymeric L, Yang H, Portela Catani JP, Hannani D, Duret H, Steegh K, Martins I, Schlemmer F, Michaud M, Kepp O, Sukkurwala AQ, Menger L, Vacchelli E, Droin N, Galluzzi L, Krzysiek R, Gordon S, Taylor PR, Van Endert P, Solary E, Smyth MJ, Zitvogel L, Kroemer G (2013) Anticancer chemotherapy-induced intratumoral recruitment and differentiation of antigen-presenting cells. *Immunity* **38**: 729-741
- Ma Y, Aymeric L, Locher C, Mattarollo SR, Delahaye NF, Pereira P, Boucontet L, Apetoh L, Ghiringhelli F, Casares N, Lasarte JJ, Matsuzaki G, Ikuta K, Ryffel B, Benlagha K, Tesniere A, Ibrahim N, Dechanet-Merville J, Chaput N, Smyth MJ, Kroemer G, Zitvogel L (2011) Contribution of IL-17-producing gamma delta T cells to the efficacy of anticancer chemotherapy. *The Journal of experimental medicine* **208**: 491-503
- Maddock CL, D'Angio GJ, Farber S, Handler AH (1960) Biological studies of actinomycin D. *Annals of the New York Academy of Sciences* **89**: 386-398
- Majera D, Skrott Z, Bouchal J, Bartkova J, Simkova D, Gachechiladze M, Steigerova J, Kurfurstova D, Gursky J, Korinkova G, Cwiertka K, Hodny Z, Mistrik M, Bartek J (2019) Targeting genotoxic and proteotoxic stress-response pathways in human prostate cancer by clinically available PARP inhibitors, vorinostat and disulfiram. *The Prostate* **79**: 352-362
- Majeti R, Chao MP, Alizadeh AA, Pang WW, Jaiswal S, Gibbs KD, Jr., van Rooijen N, Weissman IL (2009) CD47 is an adverse prognostic factor and therapeutic antibody target on human acute myeloid leukemia stem cells.

Cell **138**: 286-299

Majzner RG, Simon JS, Grosso JF, Martinez D, Pawel BR, Santi M, Merchant MS, Georger B, Hezam I, Marty V, Vielh P, Daugaard M, Sorensen PH, Mackall CL, Maris JM (2017) Assessment of programmed death-ligand 1 expression and tumor-associated immune cells in pediatric cancer tissues. *Cancer* **123**: 3807-3815

Manara MC, Perdichizzi S, Serra M, Pierini R, Benini S, Hattinger CM, Astolfi A, Bagnati R, D'Incalci M, Picci P, Scotlandi K (2005) The molecular mechanisms responsible for resistance to ET-743 (Trabectedin; Yondelis) in the Ewing's sarcoma cell line, TC-71. *International journal of oncology* **27**: 1605-1616

Martin S, Dudek-Peric AM, Maes H, Garg AD, Gabrysiak M, Demirsoy S, Swinnen JV, Agostinis P (2015) Concurrent MEK and autophagy inhibition is required to restore cell death associated danger-signalling in Vemurafenib-resistant melanoma cells. *Biochemical pharmacology* **93**: 290-304

Martin SJ, Bonham AM, Cotter TG (1990a) The involvement of RNA and protein synthesis in programmed cell death (apoptosis) in human leukaemia HL-60 cells. *Biochemical Society transactions* **18**: 634-636

Martin SJ, Lennon SV, Bonham AM, Cotter TG (1990b) Induction of apoptosis (programmed cell death) in human leukemic HL-60 cells by inhibition of RNA or protein synthesis. *Journal of immunology* **145**: 1859-1867

Martins I, Kepp O, Schlemmer F, Adjemian S, Tailler M, Shen S, Michaud M, Menger L, Gdoura A, Tajeddine N, Tesniere A, Zitvogel L, Kroemer G (2011) Restoration of the immunogenicity of cisplatin-induced cancer cell death by endoplasmic reticulum stress. *Oncogene* **30**: 1147-1158

Martins I, Michaud M, Sukkurwala AQ, Adjemian S, Ma Y, Shen S, Kepp O, Menger L, Vacchelli E, Galluzzi L, Zitvogel L, Kroemer G (2012) Premortem autophagy determines the immunogenicity of chemotherapy-induced cancer cell death. *Autophagy* **8**: 413-415

Martins I, Wang Y, Michaud M, Ma Y, Sukkurwala AQ, Shen S, Kepp O, Metivier D, Galluzzi L, Perfettini JL, Zitvogel L, Kroemer G (2014) Molecular mechanisms of ATP secretion during immunogenic cell death. *Cell death and differentiation* **21**: 79-91

Matzinger P (2002) The danger model: a renewed sense of self. *Science* **296**: 301-305

Mauseth B, Camilio KA, Shi J, Hammarstrom CL, Rekdal O, Sveinbjornsson B, Line PD (2019) The Novel Oncolytic Compound LTX-401 Induces Antitumor Immune Responses in Experimental Hepatocellular Carcinoma. *Molecular therapy oncolytics* **14**: 139-148

Menger L, Vacchelli E, Adjemian S, Martins I, Ma Y, Shen S, Yamazaki T, Sukkurwala AQ, Michaud M, Mignot G, Schlemmer F, Sulpice E, Locher C, Gidrol X, Ghiringhelli F, Modjtahedi N, Galluzzi L, Andre F, Zitvogel L, Kepp O, Kroemer G (2012) Cardiac glycosides exert anticancer effects by inducing immunogenic cell death. *Science translational medicine* **4**: 143ra199

Merkel O, Wacht N, Sift E, Melchardt T, Hamacher F, Kocher T, Denk U, Hofbauer JP, Egle A, Scheideler M, Schleederer M, Steurer M, Kenner L, Greil R (2012) Actinomycin D induces p53-independent cell death and prolongs survival in high-risk chronic lymphocytic leukemia. *Leukemia* **26**: 2508-2516

Michaud M, Martins I, Sukkurwala AQ, Adjemian S, Ma Y, Pellegatti P, Shen S, Kepp O, Scoazec M, Mignot G, Rello-Varona S, Tailler M, Menger L, Vacchelli E, Galluzzi L, Ghiringhelli F, di Virgilio F, Zitvogel L, Kroemer G (2011) Autophagy-dependent anticancer immune responses induced by chemotherapeutic agents in mice. *Science* **334**: 1573-1577

Michaud M, Sukkurwala AQ, Martins I, Shen S, Zitvogel L, Kroemer G (2012) Subversion of the chemotherapy-induced anticancer immune response by the ecto-ATPase CD39. *Oncoimmunology* **1**: 393-395

Ming Lim C, Stephenson R, Salazar AM, Ferris RL (2013) TLR3 agonists improve the immunostimulatory potential of cetuximab against EGFR(+) head and neck cancer cells. *Oncoimmunology* **2**: e24677

Miyamoto S, Inoue H, Nakamura T, Yamada M, Sakamoto C, Urata Y, Okazaki T, Marumoto T, Takahashi A, Takayama K, Nakanishi Y, Shimizu H, Tani K (2012) Coxsackievirus B3 is an oncolytic virus with

- immunostimulatory properties that is active against lung adenocarcinoma. *Cancer research* **72**: 2609-2621
- Morgan CD, Greene JF, Jr., Measel JW, Jr. (1999) Induction of surface antigen CD69 expression in T-lymphocytes following exposure to actinomycin D. *International journal of immunopharmacology* **21**: 689-703
- Mori S, Jewett A, Murakami-Mori K, Cavalcanti M, Bonavida B (1997) The participation of the Fas-mediated cytotoxic pathway by natural killer cells is tumor-cell-dependent. *Cancer immunology, immunotherapy : CII* **44**: 282-290
- Muller T, Robaye B, Vieira RP, Ferrari D, Grimm M, Jakob T, Martin SF, Di Virgilio F, Boeynaems JM, Virchow JC, Idzko M (2010) The purinergic receptor P2Y2 receptor mediates chemotaxis of dendritic cells and eosinophils in allergic lung inflammation. *Allergy* **65**: 1545-1553
- Muller W, Crothers DM (1968) Studies of the binding of actinomycin and related compounds to DNA. *Journal of molecular biology* **35**: 251-290
- Nagel R, Semenova EA, Berns A (2016) Drugging the addict: non-oncogene addiction as a target for cancer therapy. *EMBO reports* **17**: 1516-1531
- NCI (Retrieved 2019-08-01) Statistics about cancers. *National Cancer Institute*
- NCI (Retrieved 2019-08-08a) Childhood Rhabdomyosarcoma Treatment (PQR) – Health Professional Version. *National Cancer Institute*
- NCI (Retrieved 2019-08-08b) Ewing Sarcoma Treatment (PQR) – Health Professional Version. *National Cancer Institute*
- NCI (Retrieved 2019-08-08c) Gestational Trophoblastic Disease Treatment (PDQ) – Health Professional Version. *National Cancer Institute*
- NCI (Retrieved 2019-08-08d) Testicular Cancer Treatment (PDQ) – Health Professional Version. *National Cancer Institute*
- NCI (Retrieved 2019-08-08e) Wilms Tumor and Other Childhood Kidney Tumors Treatment (PQR) – Health Professional Version. *National Cancer Institute*
- Nuccitelli R, Berridge JC, Mallon Z, Kreis M, Athos B, Nuccitelli P (2015) Nanoelectroablation of Murine Tumors Triggers a CD8-Dependent Inhibition of Secondary Tumor Growth. *PloS one* **10**: e0134364
- Nuccitelli R, McDaniel A, Anand S, Cha J, Mallon Z, Berridge JC, Uecker D (2017) Nano-Pulse Stimulation is a physical modality that can trigger immunogenic tumor cell death. *Journal for immunotherapy of cancer* **5**: 32
- Obeid M, Panaretakis T, Joza N, Tufi R, Tesniere A, van Endert P, Zitvogel L, Kroemer G (2007a) Calreticulin exposure is required for the immunogenicity of gamma-irradiation and UVC light-induced apoptosis. *Cell death and differentiation* **14**: 1848-1850
- Obeid M, Tesniere A, Ghiringhelli F, Fimia GM, Apetoh L, Perfettini JL, Castedo M, Mignot G, Panaretakis T, Casares N, Metivier D, Larochette N, van Endert P, Ciccocanti F, Piacentini M, Zitvogel L, Kroemer G (2007b) Calreticulin exposure dictates the immunogenicity of cancer cell death. *Nature medicine* **13**: 54-61
- Osłowski CM, Urano F (2011) Measuring ER stress and the unfolded protein response using mammalian tissue culture system. *Methods in enzymology* **490**: 71-92
- Pages F, Mlecnik B, Marliot F, Bindea G, Ou FS, Bifulco C, Lugli A, Zlobec I, Rau TT, Berger MD, Nagtegaal ID, Vink-Borger E, Hartmann A, Geppert C, Kolwelter J, Merkel S, Grutzmann R, Van den Eynde M, Jouret-Mourin A, Kartheuser A, Leonard D, Remue C, Wang JY, Bavi P, Roehrl MHA, Ohashi PS, Nguyen LT, Han S, MacGregor HL, Hafezi-Bakhtiari S, Wouters BG, Masucci GV, Andersson EK, Zavadova E, Vocka M, Spacek J, Petruzalka L, Konopasek B, Dunder P, Skalova H, Nemejcova K, Botti G, Tatangelo F, Delrio P, Ciliberto G, Maio M, Laghi L, Grizzi F, Fredriksen T, Buttard B, Angelova M, Vasaturo A, Maby P, Church SE, Angell HK, Lafontaine L, Bruni D, El Sissy C, Haicheur N, Kirilovsky A, Berger A, Lagorce C, Meyers JP, Paustian C, Feng

- Z, Ballesteros-Merino C, Dijkstra J, van de Water C, van Lent-van Vliet S, Knijn N, Musina AM, Scripcariu DV, Popivanova B, Xu M, Fujita T, Hazama S, Suzuki N, Nagano H, Okuno K, Torigoe T, Sato N, Furuhashi T, Takemasa I, Itoh K, Patel PS, Vora HH, Shah B, Patel JB, Rajvik KN, Pandya SJ, Shukla SN, Wang Y, Zhang G, Kawakami Y, Marincola FM, Ascierto PA, Sargent DJ, Fox BA, Galon J (2018) International validation of the consensus Immunoscore for the classification of colon cancer: a prognostic and accuracy study. *Lancet* **391**: 2128-2139
- Pan JX, Liu Y, Zhang SP, Tu TC, Yao SD, Lin NY (2001) Photodynamic action of actinomycin D: an EPR spin trapping study. *Biochimica et biophysica acta* **1527**: 1-3
- Panaretakis T, Joza N, Modjtahedi N, Tesniere A, Vitale I, Durchschlag M, Fimia GM, Kepp O, Piacentini M, Froehlich KU, van Endert P, Zitvogel L, Madeo F, Kroemer G (2008) The co-translocation of ERp57 and calreticulin determines the immunogenicity of cell death. *Cell death and differentiation* **15**: 1499-1509
- Panaretakis T, Kepp O, Brockmeier U, Tesniere A, Bjorklund AC, Chapman DC, Durchschlag M, Joza N, Pierron G, van Endert P, Yuan J, Zitvogel L, Madeo F, Williams DB, Kroemer G (2009) Mechanisms of pre-apoptotic calreticulin exposure in immunogenic cell death. *The EMBO journal* **28**: 578-590
- Pavitt GD (2005) eIF2B, a mediator of general and gene-specific translational control. *Biochemical Society transactions* **33**: 1487-1492
- Pawaria S, Binder RJ (2011) CD91-dependent programming of T-helper cell responses following heat shock protein immunization. *Nature communications* **2**: 521
- Pellicciotta I, Yang CP, Goldberg GL, Shahabi S (2011) Epothilone B enhances Class I HLA and HLA-A2 surface molecule expression in ovarian cancer cells. *Gynecologic oncology* **122**: 625-631
- Peltonen K, Colis L, Liu H, Trivedi R, Moubarek MS, Moore HM, Bai B, Rudek MA, Bieberich CJ, Laiho M (2014) A targeting modality for destruction of RNA polymerase I that possesses anticancer activity. *Cancer cell* **25**: 77-90
- Perez B, Paquette N, Paidassi H, Zhai B, White K, Skvirsky R, Lacy-Hulbert A, Stuart LM (2012) Apoptotic cells can deliver chemotherapeutics to engulfing macrophages and suppress inflammatory cytokine production. *The Journal of biological chemistry* **287**: 16029-16036
- Perretti M, D'Acquisto F (2009) Annexin A1 and glucocorticoids as effectors of the resolution of inflammation. *Nature reviews Immunology* **9**: 62-70
- Pfirschke C, Engblom C, Rickelt S, Cortez-Retamozo V, Garris C, Pucci F, Yamazaki T, Poirier-Colame V, Newton A, Redouane Y, Lin YJ, Wojtkiewicz G, Iwamoto Y, Mino-Kenudson M, Huynh TG, Hynes RO, Freeman GJ, Kroemer G, Zitvogel L, Weissleder R, Pittet MJ (2016) Immunogenic Chemotherapy Sensitizes Tumors to Checkpoint Blockade Therapy. *Immunity* **44**: 343-354
- Philips FS, Schwartz HS, Sternberg SS, Tan CT (1960) The toxicity of actinomycin D. *Annals of the New York Academy of Sciences* **89**: 348-360
- Pietrocola F, Castoldi F, Maiuri MC, Kroemer G (2018) Aspirin-another caloric-restriction mimetic. *Autophagy* **14**: 1162-1163
- Pietrocola F, Pol J, Vacchelli E, Rao S, Enot DP, Baracco EE, Levesque S, Castoldi F, Jacquelot N, Yamazaki T, Senovilla L, Marino G, Aranda F, Durand S, Sica V, Chery A, Lachkar S, Sigl V, Bloy N, Buque A, Falzoni S, Ryffel B, Apetoh L, Di Virgilio F, Madeo F, Maiuri MC, Zitvogel L, Levine B, Penninger JM, Kroemer G (2016) Caloric Restriction Mimetics Enhance Anticancer Immunosurveillance. *Cancer cell* **30**: 147-160
- Pombo A, Jackson DA, Hollinshead M, Wang Z, Roeder RG, Cook PR (1999) Regional specialization in human nuclei: visualization of discrete sites of transcription by RNA polymerase III. *The EMBO journal* **18**: 2241-2253
- Pozzi C, Cuomo A, Spadoni I, Magni E, Silvola A, Conte A, Sigismund S, Ravenda PS, Bonaldi T, Zampino MG, Cancelliere C, Di Fiore PP, Bardelli A, Penna G, Rescigno M (2016) The EGFR-specific antibody cetuximab combined with chemotherapy triggers immunogenic cell death. *Nature medicine* **22**: 624-631

- Qin Y, Han Y, Cao C, Ren Y, Li C, Wang Y (2011) Melanoma B16-F1 cells coated with fusion protein of mouse calreticulin and virus G-protein coupled receptor induced the antitumor immune response in Balb/C mice. *Cancer biology & therapy* **11**: 574-580
- Rabinowitz Y, Schimo I, Wilhite BA (1968) Metabolic responses to separated leucocytes to phytohaemagglutinin: effects of anaerobiasis, actinomycin D and puromycin. *British journal of haematology* **15**: 455-464
- Ran FA, Hsu PD, Wright J, Agarwala V, Scott DA, Zhang F (2013) Genome engineering using the CRISPR-Cas9 system. *Nature protocols* **8**: 2281-2308
- Reich E (1961) Actinomycin: Correlation of Structure and Function of Its Complexes with Purines and DNA. *Science* **143**: 684-689
- Reich E, Franklin RM, Shatkin AJ, Tatum EL (1961) Effect of actinomycin D on cellular nucleic acid synthesis and virus production. *Science* **134**: 556-557
- Reilly HC, Stock CC, Buckley SM, Clark DA (1953) The effect of antibiotics upon the growth of sarcoma 180 in vivo. *Cancer research* **13**: 684-687
- Revel M, Hiatt HH, Revel JP (1964) Actinomycin D: An Effect on Rat Liver Homogenates Unrelated to Its Action on Rna Synthesis. *Science* **146**: 1311-1313
- Riganti C, Lingua MF, Salaroglio IC, Falcomata C, Righi L, Morena D, Picca F, Oddo D, Kopecka J, Pradotto M, Libener R, Orecchia S, Bironzo P, Comunanza V, Bussolino F, Novello S, Scagliotti GV, Di Nicolantonio F, Taulli R (2018) Bromodomain inhibition exerts its therapeutic potential in malignant pleural mesothelioma by promoting immunogenic cell death and changing the tumor immune-environment. *Oncoimmunology* **7**: e1398874
- Robinson N, McComb S, Mulligan R, Dudani R, Krishnan L, Sad S (2012) Type I interferon induces necroptosis in macrophages during infection with Salmonella enterica serovar Typhimurium. *Nature immunology* **13**: 954-962
- Roskoski R, Jr. (2016) Cyclin-dependent protein kinase inhibitors including palbociclib as anticancer drugs. *Pharmacological research* **107**: 249-275
- Rubner Y, Muth C, Strnad A, Derer A, Sieber R, Buslei R, Frey B, Fietkau R, Gaipl US (2014) Fractionated radiotherapy is the main stimulus for the induction of cell death and of Hsp70 release of p53 mutated glioblastoma cell lines. *Radiation oncology* **9**: 89
- Salaun B, Zitvogel L, Asselin-Paturel C, Morel Y, Chemin K, Dubois C, Massacrier C, Conforti R, Chenard MP, Sabourin JC, Goubar A, Lebecque S, Pierres M, Rimoldi D, Romero P, Andre F (2011) TLR3 as a biomarker for the therapeutic efficacy of double-stranded RNA in breast cancer. *Cancer research* **71**: 1607-1614
- Samstein RM, Lee CH, Shoushtari AN, Hellmann MD, Shen R, Janjigian YY, Barron DA, Zehir A, Jordan EJ, Omuro A, Kaley TJ, Kendall SM, Motzer RJ, Hakimi AA, Voss MH, Russo P, Rosenberg J, Iyer G, Bochner BH, Bajorin DF, Al-Ahmadie HA, Chaft JE, Rudin CM, Riely GJ, Baxi S, Ho AL, Wong RJ, Pfister DG, Wolchok JD, Barker CA, Gutin PH, Brennan CW, Tabar V, Mellinghoff IK, DeAngelis LM, Ariyan CE, Lee N, Tap WD, Gounder MM, D'Angelo SP, Saltz L, Stadler ZK, Scher HI, Baselga J, Razavi P, Klebanoff CA, Yaeger R, Segal NH, Ku GY, DeMatteo RP, Ladanyi M, Rizvi NA, Berger MF, Riaz N, Solit DB, Chan TA, Morris LGT (2019) Tumor mutational load predicts survival after immunotherapy across multiple cancer types. *Nature genetics* **51**: 202-206
- Sauvat A, Leduc M, Muller K, Kepp O, Kroemer G (2019) ColocalizR: An open-source application for cell-based high-throughput colocalization analysis. *Computers in biology and medicine* **107**: 227-234
- Savina M, Le Cesne A, Blay JY, Ray-Coquard I, Mir O, Toulmonde M, Cousin S, Terrier P, Ranchere-Vince D, Meeus P, Stoeckle E, Honore C, Sargos P, Sunyach MP, Le Pechoux C, Giraud A, Bellera C, Le Loarer F, Italiano A (2017) Patterns of care and outcomes of patients with METAstatic soft tissue SARComa in a real-life setting: the METASARC observational study. *BMC medicine* **15**: 78
- Scaffidi P, Misteli T, Bianchi ME (2002) Release of chromatin protein HMGB1 by necrotic cells triggers

inflammation. *Nature* **418**: 191-195

Scanlan MJ, Simpson AJ, Old LJ (2004) The cancer/testis genes: review, standardization, and commentary. *Cancer immunity* **4**: 1

Schaer DA, Geeganage S, Amaladas N, Lu ZH, Rasmussen ER, Sonyi A, Chin D, Capen A, Li Y, Meyer CM, Jones BD, Huang X, Luo S, Carpenito C, Roth KD, Nikolayev A, Tan B, Brahmachary M, Chodavarapu K, Dorsey FC, Manro JR, Doman TN, Donoho GP, Surguladze D, Hall GE, Kalos M, Novosiadly RD (2019) The Folate Pathway Inhibitor Pemetrexed Pleiotropically Enhances Effects of Cancer Immunotherapy. *Clinical cancer research : an official journal of the American Association for Cancer Research*

Schiavoni G, Sistigu A, Valentini M, Mattei F, Sestili P, Spadaro F, Sanchez M, Lorenzi S, D'Urso MT, Belardelli F, Gabriele L, Proietti E, Bracci L (2011) Cyclophosphamide synergizes with type I interferons through systemic dendritic cell reactivation and induction of immunogenic tumor apoptosis. *Cancer research* **71**: 768-778

Schiraldi M, Raucci A, Munoz LM, Livoti E, Celona B, Venereau E, Apuzzo T, De Marchis F, Pedotti M, Bachi A, Thelen M, Varani L, Mellado M, Proudfoot A, Bianchi ME, Uguccioni M (2012) HMGB1 promotes recruitment of inflammatory cells to damaged tissues by forming a complex with CXCL12 and signaling via CXCR4. *The Journal of experimental medicine* **209**: 551-563

Schluederberg A, Hendel RC, Chavanich S (1971) Actinomycin D; renewed RNA synthesis after removal from mammalian cells. *Science* **172**: 577-579

Schreiber RD, Old LJ, Smyth MJ (2011) Cancer immunoediting: integrating immunity's roles in cancer suppression and promotion. *Science* **331**: 1565-1570

Schwartz HS, Sodergren JE (1968) Actinomycin D effects on nucleic acids during tumor regression. *Cancer research* **28**: 445-451

Schwartz HS, Sodergren JE, Ambaye RY (1968) Actinomycin D: drug concentrations and actions in mouse tissues and tumors. *Cancer research* **28**: 192-197

Schwartz HS, Sodergren JE, Garofalo M, Sternberg SS (1965) Actinomycin D. Effects on Nucleic Acid and Protein Metabolism in Intact and Regenerating Liver of Rats. *Cancer research* **25**: 307-317

Schwartz HS, Sodergren JE, Sternberg SS, Philips FS (1966) Actinomycin D: effects on Ridgway osteogenic sarcoma in mice. *Cancer research* **26**: 1873-1879

Searle J, Lawson TA, Abbott PJ, Harmon B, Kerr JF (1975) An electron-microscope study of the mode of cell death induced by cancer-chemotherapeutic agents in populations of proliferating normal and neoplastic cells. *The Journal of pathology* **116**: 129-138

Segovia C, San Jose-Eneriz E, Munera-Maravilla E, Martinez-Fernandez M, Garate L, Miranda E, Vilas-Zornoza A, Lodewijk I, Rubio C, Segrelles C, Valcarcel LV, Rabal O, Casares N, Bernardini A, Suarez-Cabrera C, Lopez-Calderon FF, Fortes P, Casado JA, Duenas M, Villacampa F, Lasarte JJ, Guerrero-Ramos F, de Velasco G, Oyarzabal J, Castellano D, Agirre X, Prosper F, Paramio JM (2019) Inhibition of a G9a/DNMT network triggers immune-mediated bladder cancer regression. *Nature medicine* **25**: 1073-1081

Semeraro M, Adam J, Stoll G, Louvet E, Chaba K, Poirier-Colame V, Sauvat A, Senovilla L, Vacchelli E, Bloy N, Humeau J, Buque A, Kepp O, Zitvogel L, Andre F, Mathieu MC, Delaloue S, Kroemer G (2016) The ratio of CD8+/FOXP3 T lymphocytes infiltrating breast tissues predicts the relapse of ductal carcinoma in situ. *Oncoimmunology* **5**: e1218106

Senovilla L, Vitale I, Martins I, Tailler M, Paillet C, Michaud M, Galluzzi L, Adjemian S, Kepp O, Niso-Santano M, Shen S, Marino G, Criollo A, Boileve A, Job B, Ladoire S, Ghiringhelli F, Sistigu A, Yamazaki T, Rello-Varona S, Locher C, Poirier-Colame V, Talbot M, Valent A, Berardinelli F, Antoccia A, Ciccocanti F, Fimia GM, Piacentini M, Fueyo A, Messina NL, Li M, Chan CJ, Sigl V, Pourcher G, Ruckenstein C, Carmona-Gutierrez D, Lazar V, Penninger JM, Madeo F, Lopez-Otin C, Smyth MJ, Zitvogel L, Castedo M, Kroemer G (2012) An immunosurveillance mechanism controls cancer cell ploidy. *Science* **337**: 1678-1684

- Serrano-Del Valle A, Anel A, Naval J, Marzo I (2019) Immunogenic Cell Death and Immunotherapy of Multiple Myeloma. *Frontiers in cell and developmental biology* **7**: 50
- Shankaran V, Ikeda H, Bruce AT, White JM, Swanson PE, Old LJ, Schreiber RD (2001) IFN γ and lymphocytes prevent primary tumour development and shape tumour immunogenicity. *Nature* **410**: 1107-1111
- Shen S, Niso-Santano M, Adjemian S, Takehara T, Malik SA, Minoux H, Souquere S, Marino G, Lachkar S, Senovilla L, Galluzzi L, Kepp O, Pierron G, Maiuri MC, Hikita H, Kroemer R, Kroemer G (2012) Cytoplasmic STAT3 represses autophagy by inhibiting PKR activity. *Molecular cell* **48**: 667-680
- Shim D, Kang HY, Jeon BW, Kang SS, Chang SI, Kim HY (2004) Protein kinase B inhibits apoptosis induced by actinomycin D in ECV304 cells through phosphorylation of caspase 8. *Archives of biochemistry and biophysics* **425**: 214-220
- Shoemaker RH (2006) The NCI60 human tumour cell line anticancer drug screen. *Nature reviews Cancer* **6**: 813-823
- Sidrauski C, Acosta-Alvear D, Khoutorsky A, Vedantham P, Hearn BR, Li H, Gamache K, Gallagher CM, Ang KK, Wilson C, Okreglak V, Ashkenazi A, Hann B, Nader K, Arkin MR, Renslo AR, Sonenberg N, Walter P (2013) Pharmacological brake-release of mRNA translation enhances cognitive memory. *eLife* **2**: e00498
- Sims GP, Rowe DC, Rietdijk ST, Herbst R, Coyle AJ (2010) HMGB1 and RAGE in inflammation and cancer. *Annual review of immunology* **28**: 367-388
- Sistigu A, Yamazaki T, Vacchelli E, Chaba K, Enot DP, Adam J, Vitale I, Goubar A, Baracco EE, Remedios C, Fend L, Hannani D, Aymeric L, Ma Y, Niso-Santano M, Kepp O, Schultze JL, Tuting T, Belardelli F, Bracci L, La Sorsa V, Ziccheddu G, Sestili P, Urbani F, Delorenzi M, Lacroix-Triki M, Quidville V, Conforti R, Spano JP, Pusztai L, Poirier-Colame V, Delalogue S, Penault-Llorca F, Ladoire S, Arnould L, Cyryta J, Dessoliers MC, Eggermont A, Bianchi ME, Pittet M, Engblom C, Pfirschke C, Preville X, Uze G, Schreiber RD, Chow MT, Smyth MJ, Proietti E, Andre F, Kroemer G, Zitvogel L (2014) Cancer cell-autonomous contribution of type I interferon signaling to the efficacy of chemotherapy. *Nature medicine* **20**: 1301-1309
- Smyth MJ, Godfrey DI, Trapani JA (2001) A fresh look at tumor immunosurveillance and immunotherapy. *Nature immunology* **2**: 293-299
- Song Y, Park IS, Kim J, Seo HR (2019) Actinomycin D inhibits the expression of the cystine/glutamate transporter xCT via attenuation of CD133 synthesis in CD133(+) HCC. *Chemico-biological interactions* **309**: 108713
- Sonnemann J, Gressmann S, Becker S, Wittig S, Schmutte M, Beck JF (2010) The histone deacetylase inhibitor vorinostat induces calreticulin exposure in childhood brain tumour cells in vitro. *Cancer chemotherapy and pharmacology* **66**: 611-616
- Spisek R, Charalambous A, Mazumder A, Vesole DH, Jagannath S, Dhodapkar MV (2007) Bortezomib enhances dendritic cell (DC)-mediated induction of immunity to human myeloma via exposure of cell surface heat shock protein 90 on dying tumor cells: therapeutic implications. *Blood* **109**: 4839-4845
- Stagg J, Beavis PA, Divisekera U, Liu MC, Moller A, Darcy PK, Smyth MJ (2012) CD73-deficient mice are resistant to carcinogenesis. *Cancer research* **72**: 2190-2196
- Stebbing J, Bower M, Gazzard B, Wildfire A, Pandha H, Dalglish A, Spicer J (2004) The common heat shock protein receptor CD91 is up-regulated on monocytes of advanced melanoma slow progressors. *Clinical and experimental immunology* **138**: 312-316
- Stoll G, Enot D, Mlecnik B, Galon J, Zitvogel L, Kroemer G (2014) Immune-related gene signatures predict the outcome of neoadjuvant chemotherapy. *Oncoimmunology* **3**: e27884
- Stoll G, Iribarren K, Michels J, Leary A, Zitvogel L, Cremer I, Kroemer G (2016) Calreticulin expression: Interaction with the immune infiltrate and impact on survival in patients with ovarian and non-small cell lung cancer. *Oncoimmunology* **5**: e1177692

- Sukkurwala AQ, Adjemian S, Senovilla L, Michaud M, Spaggiari S, Vacchelli E, Baracco EE, Galluzzi L, Zitvogel L, Kepp O, Kroemer G (2014a) Screening of novel immunogenic cell death inducers within the NCI Mechanistic Diversity Set. *Oncoimmunology* **3**: e28473
- Sukkurwala AQ, Martins I, Wang Y, Schlemmer F, Ruckstuhl C, Durchschlag M, Michaud M, Senovilla L, Sistigu A, Ma Y, Vacchelli E, Sulpice E, Gidrol X, Zitvogel L, Madoe F, Galluzzi L, Kepp O, Kroemer G (2014b) Immunogenic calreticulin exposure occurs through a phylogenetically conserved stress pathway involving the chemokine CXCL8. *Cell death and differentiation* **21**: 59-68
- Sun C, Wang H, Mao S, Liu J, Li S, Wang J (2015) Reactive oxygen species involved in CT26 immunogenic cell death induced by Clostridium difficile toxin B. *Immunology letters* **164**: 65-71
- Sun X, Wu Y, Gao W, Enyoji K, Csizmadia E, Muller CE, Murakami T, Robson SC (2010) CD39/ENTPD1 expression by CD4+Foxp3+ regulatory T cells promotes hepatic metastatic tumor growth in mice. *Gastroenterology* **139**: 1030-1040
- Suzuki E, Kapoor V, Jassar AS, Kaiser LR, Albelda SM (2005) Gemcitabine selectively eliminates splenic Gr-1+/CD11b+ myeloid suppressor cells in tumor-bearing animals and enhances antitumor immune activity. *Clinical cancer research : an official journal of the American Association for Cancer Research* **11**: 6713-6721
- Suzuki S, Yokobori T, Tanaka N, Sakai M, Sano A, Inose T, Sohda M, Nakajima M, Miyazaki T, Kato H, Kuwano H (2012) CD47 expression regulated by the miR-133a tumor suppressor is a novel prognostic marker in esophageal squamous cell carcinoma. *Oncology reports* **28**: 465-472
- Takeda K, Smyth MJ, Cretney E, Hayakawa Y, Yamaguchi N, Yagita H, Okumura K (2001) Involvement of tumor necrosis factor-related apoptosis-inducing ligand in NK cell-mediated and IFN-gamma-dependent suppression of subcutaneous tumor growth. *Cellular immunology* **214**: 194-200
- Takusagawa F, Carlson RG, Weaver RF (2001) Anti-leukemia selectivity in actinomycin analogues. *Bioorganic & medicinal chemistry* **9**: 719-725
- Takusagawa F, Dabrow M, Neidle S, Berman HM (1982) The structure of a pseudo intercalated complex between actinomycin and the DNA binding sequence d(GpC). *Nature* **296**: 466-469
- Tanaka H, Matsushima H, Mizumoto N, Takashima A (2009a) Classification of chemotherapeutic agents based on their differential in vitro effects on dendritic cells. *Cancer research* **69**: 6978-6986
- Tanaka H, Matsushima H, Nishibu A, Clausen BE, Takashima A (2009b) Dual therapeutic efficacy of vinblastine as a unique chemotherapeutic agent capable of inducing dendritic cell maturation. *Cancer research* **69**: 6987-6994
- Tao Z, Ahmad SS, Penefsky HS, Goodisman J, Souid AK (2006) Dactinomycin impairs cellular respiration and reduces accompanying ATP formation. *Molecular pharmaceutics* **3**: 762-772
- Tatsuno K, Yamazaki T, Hanlon D, Han P, Robinson E, Sobolev O, Yurter A, Rivera-Molina F, Arshad N, Edelson RL, Galluzzi L (2019) Extracorporeal photochemotherapy induces bona fide immunogenic cell death. *Cell death & disease* **10**: 578
- Tattersall MH, Sodergren JE, Dengupta SK, Trites DH, Modest EJ, Frei E, 3rd (1975) Pharmacokinetics of actinomycin D in patients with malignant melanoma. *Clinical pharmacology and therapeutics* **17**: 701-708
- Tesniere A, Schlemmer F, Boige V, Kepp O, Martins I, Ghiringhelli F, Aymeric L, Michaud M, Apetoh L, Barault L, Mendiboure J, Pignon JP, Jooste V, van Endert P, Ducreux M, Zitvogel L, Piard F, Kroemer G (2010) Immunogenic death of colon cancer cells treated with oxaliplatin. *Oncogene* **29**: 482-491
- Tittarelli A, Gonzalez FE, Pereda C, Mora G, Munoz L, Saffie C, Garcia T, Diaz D, Falcon C, Hermoso M, Lopez MN, Salazar-Onfray F (2012) Toll-like receptor 4 gene polymorphism influences dendritic cell in vitro function and clinical outcomes in vaccinated melanoma patients. *Cancer immunology, immunotherapy : CII* **61**: 2067-2077
- Trask DK, Muller MT (1988) Stabilization of type I topoisomerase-DNA covalent complexes by actinomycin D. *Proceedings of the National Academy of Sciences of the United States of America* **85**: 1417-1421

Tumini E, Herrera-Moyano E, San Martin-Alonso M, Barroso S, Galmarini CM, Aguilera A (2019) The Antitumor Drugs Trabectedin and Lurbinectedin Induce Transcription-Dependent Replication Stress and Genome Instability. *Molecular cancer research : MCR* **17**: 773-782

Uchida A, Klein E (1985) Natural cytotoxicity of human blood monocytes and natural killer cells and their cytotoxic factors: discriminating effects of actinomycin D. *International journal of cancer* **35**: 691-699

Uhl M, Kepp O, Jusforgues-Saklani H, Vicencio JM, Kroemer G, Albert ML (2009) Autophagy within the antigen donor cell facilitates efficient antigen cross-priming of virus-specific CD8+ T cells. *Cell death and differentiation* **16**: 991-1005

Urbanova L, Hradilova N, Moserova I, Vosahlikova S, Sadilkova L, Hensler M, Spisek R, Adkins I (2017) High hydrostatic pressure affects antigenic pool in tumor cells: Implication for dendritic cell-based cancer immunotherapy. *Immunology letters* **187**: 27-34

Vacchelli E, Eggermont A, Sautes-Fridman C, Galon J, Zitvogel L, Kroemer G, Galluzzi L (2013) Trial Watch: Toll-like receptor agonists for cancer therapy. *Oncoimmunology* **2**: e25238

Vacchelli E, Enot DP, Pietrocola F, Zitvogel L, Kroemer G (2016a) Impact of Pattern Recognition Receptors on the Prognosis of Breast Cancer Patients Undergoing Adjuvant Chemotherapy. *Cancer research* **76**: 3122-3126

Vacchelli E, Ma Y, Baracco EE, Sistigu A, Enot DP, Pietrocola F, Yang H, Adjemian S, Chaba K, Semeraro M, Signore M, De Ninno A, Lucarini V, Peschiaroli F, Businaro L, Gerardino A, Manic G, Ulas T, Gunther P, Schultze JL, Kepp O, Stoll G, Lefebvre C, Mulot C, Castoldi F, Rusakiewicz S, Ladoire S, Apetoh L, Bravo-San Pedro JM, Lucattelli M, Delarasse C, Boige V, Ducreux M, Delalogue S, Borg C, Andre F, Schiavoni G, Vitale I, Laurent-Puig P, Mattei F, Zitvogel L, Kroemer G (2015a) Chemotherapy-induced antitumor immunity requires formyl peptide receptor 1. *Science* **350**: 972-978

Vacchelli E, Ma Y, Baracco EE, Zitvogel L, Kroemer G (2016b) Yet another pattern recognition receptor involved in the chemotherapy-induced anticancer immune response: Formyl peptide receptor-1. *Oncoimmunology* **5**: e1118600

Vacchelli E, Semeraro M, Enot DP, Chaba K, Poirier Colame V, Dartigues P, Perier A, Villa I, Rusakiewicz S, Gronnier C, Goere D, Mariette C, Zitvogel L, Kroemer G (2015b) Negative prognostic impact of regulatory T cell infiltration in surgically resected esophageal cancer post-radiochemotherapy. *Oncotarget* **6**: 20840-20850

van der Bruggen P, Traversari C, Chomez P, Lurquin C, De Plaen E, Van den Eynde B, Knuth A, Boon T (1991) A gene encoding an antigen recognized by cytolytic T lymphocytes on a human melanoma. *Science* **254**: 1643-1647

Veal GJ, Errington J, Sludden J, Griffin MJ, Price L, Parry A, Hale J, Pearson AD, Boddy AV, Group UPW (2003) Determination of anti-cancer drug actinomycin D in human plasma by liquid chromatography-mass spectrometry. *Journal of chromatography B, Analytical technologies in the biomedical and life sciences* **795**: 237-243

Vekshin N (2011) Actinomycins like anti-cancer photo-sensitizers. *Journal of fluorescence* **21**: 1417-1420

Ventura A, Vassall A, Robinson E, Filler R, Hanlon D, Meeth K, Ezaldein H, Girardi M, Sobolev O, Bosenberg MW, Edelson RL (2018) Extracorporeal Photochemotherapy Drives Monocyte-to-Dendritic Cell Maturation to Induce Anticancer Immunity. *Cancer research* **78**: 4045-4058

Viaud S, Flament C, Zoubir M, Pautier P, LeCesne A, Ribrag V, Soria JC, Marty V, Vielh P, Robert C, Chaput N, Zitvogel L (2011) Cyclophosphamide induces differentiation of Th17 cells in cancer patients. *Cancer research* **71**: 661-665

Vidal (Retrieved 2019-08-08) Dactinomycin.

Vincent J, Mignot G, Chalmin F, Ladoire S, Bruchard M, Chevriaux A, Martin F, Apetoh L, Rebe C, Ghiringhelli F (2010) 5-Fluorouracil selectively kills tumor-associated myeloid-derived suppressor cells resulting in enhanced T cell-dependent antitumor immunity. *Cancer research* **70**: 3052-3061

- Wadkins RM, Jares-Erijman EA, Klement R, Rudiger A, Jovin TM (1996) Actinomycin D binding to single-stranded DNA: sequence specificity and hemi-intercalation model from fluorescence and 1H NMR spectroscopy. *Journal of molecular biology* **262**: 53-68
- Waksman SA, Woodruff HB (1940) The Soil as a Source of Microorganisms Antagonistic to Disease-Producing Bacteria. *Journal of bacteriology* **40**: 581-600
- Walsh C, Bonner JJ, Johnson TN, Neuhoff S, Ghazaly EA, Gribben JG, Boddy AV, Veal GJ (2016) Development of a physiologically based pharmacokinetic model of actinomycin D in children with cancer. *British journal of clinical pharmacology* **81**: 989-998
- Wang H, Bloom O, Zhang M, Vishnubhakat JM, Ombrellino M, Che J, Frazier A, Yang H, Ivanova S, Borovikova L, Manogue KR, Faist E, Abraham E, Andersson J, Andersson U, Molina PE, Abumrad NN, Sama A, Tracey KJ (1999) HMG-1 as a late mediator of endotoxin lethality in mice. *Science* **285**: 248-251
- Wang H, Tan M, Zhang S, Li X, Gao J, Zhang D, Hao Y, Gao S, Liu J, Lin B (2015a) Expression and significance of CD44, CD47 and c-met in ovarian clear cell carcinoma. *International journal of molecular sciences* **16**: 3391-3404
- Wang J, Zhang J, Lee YM, Ng S, Shi Y, Hua ZC, Lin Q, Shen HM (2017) Nonradioactive quantification of autophagic protein degradation with L-azidohomoalanine labeling. *Nature protocols* **12**: 279-288
- Wang W, Qin S, Zhao L (2015b) Docetaxel enhances CD3+ CD56+ cytokine-induced killer cells-mediated killing through inducing tumor cells phenotype modulation. *Biomedicine & pharmacotherapy = Biomedecine & pharmacotherapie* **69**: 18-23
- Wang Z, Chen J, Hu J, Zhang H, Xu F, He W, Wang X, Li M, Lu W, Zeng G, Zhou P, Huang P, Chen S, Li W, Xia LP, Xia X (2019) cGAS/STING axis mediates a topoisomerase II inhibitor-induced tumor immunogenicity. *The Journal of clinical investigation* **130**: 4850-4862
- Wassermann K, Markovits J, Jaxel C, Capranico G, Kohn KW, Pommier Y (1990) Effects of morpholinyl doxorubicins, doxorubicin, and actinomycin D on mammalian DNA topoisomerases I and II. *Molecular pharmacology* **38**: 38-45
- Wei Z, Xu C, Wang J, Lu F, Bie X, Lu Z (2017) Identification and characterization of *Streptomyces flavogriseus* NJ-4 as a novel producer of actinomycin D and holomycin. *PeerJ* **5**: e3601
- Wemeau M, Kepp O, Tesniere A, Panaretakis T, Flament C, De Botton S, Zitvogel L, Kroemer G, Chaput N (2010) Calreticulin exposure on malignant blasts predicts a cellular anticancer immune response in patients with acute myeloid leukemia. *Cell death & disease* **1**: e104
- Wernitznig D, Kiakos K, Del Favero G, Harrer N, Machat H, Osswald A, Jakupec MA, Wernitznig A, Sommergruber W, Keppler BK (2019) First-in-class ruthenium anticancer drug (KP1339/IT-139) induces an immunogenic cell death signature in colorectal spheroids in vitro. *Metallomics : integrated biometal science* **11**: 1044-1048
- West AC, Mattarollo SR, Shortt J, Cluse LA, Christiansen AJ, Smyth MJ, Johnstone RW (2013) An intact immune system is required for the anticancer activities of histone deacetylase inhibitors. *Cancer research* **73**: 7265-7276
- White RJ (2008) RNA polymerases I and III, non-coding RNAs and cancer. *Trends in genetics : TIG* **24**: 622-629
- WHO (Retrieved 2019-08-01)
- Williamson D, Lu YJ, Fang C, Pritchard-Jones K, Shipley J (2006) Nascent pre-rRNA overexpression correlates with an adverse prognosis in alveolar rhabdomyosarcoma. *Genes, chromosomes & cancer* **45**: 839-845
- Wong DY, Ong WW, Ang WH (2015) Induction of immunogenic cell death by chemotherapeutic platinum complexes. *Angewandte Chemie* **54**: 6483-6487

- Wortham NC, Proud CG (2015) eIF2B: recent structural and functional insights into a key regulator of translation. *Biochemical Society transactions* **43**: 1234-1240
- Wurz GT, Kao CJ, DeGregorio MW (2016) Novel cancer antigens for personalized immunotherapies: latest evidence and clinical potential. *Therapeutic advances in medical oncology* **8**: 4-31
- Wust CJ, Gall CL, Novelli DG (1964) Actinomycin D: Effect on the Immune Response. *Science* **143**: 1041-1043
- Xie W, Forveille S, Iribarren K, Sauvat A, Senovilla L, Wang Y, Humeau J, Perez-Lanzon M, Zhou H, Martínez-Leal JF, Kroemer G, Kepp O (2019a) Lurbinectedin synergizes with immune checkpoint blockade to generate anticancer immunity. *Oncoimmunology* **In press**
- Xie W, Mondragon L, Mauseth B, Wang Y, Pol J, Levesque S, Zhou H, Yamazaki T, Eksteen JJ, Zitvogel L, Sveinbjornsson B, Rekdal O, Kepp O, Kroemer G (2019b) Tumor lysis with LTX-401 creates anticancer immunity. *Oncoimmunology* **8**: 1594555
- Yamamoto T, Kimura T, Ueta E, Tatemoto Y, Osaki T (2003) Characteristic cytokine generation patterns in cancer cells and infiltrating lymphocytes in oral squamous cell carcinomas and the influence of chemoradiation combined with immunotherapy on these patterns. *Oncology* **64**: 407-415
- Yamamura Y, Tsuchikawa T, Miyauchi K, Takeuchi S, Wada M, Kuwatani T, Kyogoku N, Kuroda A, Maki T, Shichinohe T, Hirano S (2015) The key role of calreticulin in immunomodulation induced by chemotherapeutic agents. *International journal of clinical oncology* **20**: 386-394
- Yamazaki T, Hannani D, Poirier-Colame V, Ladoire S, Locher C, Sistigu A, Prada N, Adjemian S, Catani JP, Freudenberg M, Galanos C, Andre F, Kroemer G, Zitvogel L (2014) Defective immunogenic cell death of HMGB1-deficient tumors: compensatory therapy with TLR4 agonists. *Cell death and differentiation* **21**: 69-78
- Yamazaki T, Pitt JM, Vetizou M, Marabelle A, Flores C, Rekdal O, Kroemer G, Zitvogel L (2016) The oncolytic peptide LTX-315 overcomes resistance of cancers to immunotherapy with CTLA4 checkpoint blockade. *Cell death and differentiation* **23**: 1004-1015
- Yang C, He B, Zheng Q, Wang D, Qin M, Zhang H, Dai W, Zhang Q, Meng X, Wang X (2019) Nano-encapsulated tryptanthrin derivative for combined anticancer therapy via inhibiting indoleamine 2,3-dioxygenase and inducing immunogenic cell death. *Nanomedicine* **14**: 2423-2440
- Yang H, Ma Y, Chen G, Zhou H, Yamazaki T, Klein C, Pietrocola F, Vacchelli E, Souquere S, Sauvat A, Zitvogel L, Kepp O, Kroemer G (2016) Contribution of RIP3 and MLKL to immunogenic cell death signaling in cancer chemotherapy. *Oncoimmunology* **5**: e1149673
- Yang Y, Li XJ, Chen Z, Zhu XX, Wang J, Zhang LB, Qiang L, Ma YJ, Li ZY, Guo QL, You QD (2012) Wogonin induced calreticulin/annexin A1 exposure dictates the immunogenicity of cancer cells in a PERK/AKT dependent manner. *PLoS one* **7**: e50811
- Yatim N, Jusforgues-Saklani H, Orozco S, Schulz O, Barreira da Silva R, Reis e Sousa C, Green DR, Oberst A, Albert ML (2015) RIPK1 and NF-kappaB signaling in dying cells determines cross-priming of CD8(+) T cells. *Science* **350**: 328-334
- You SY, Rui W, Chen ST, Chen HC, Liu XW, Huang J, Chen HY (2019) Process of immunogenic cell death caused by disulfiram as the anti-colorectal cancer candidate. *Biochemical and biophysical research communications* **513**: 891-897
- Yu Z, Geng J, Zhang M, Zhou Y, Fan Q, Chen J (2014) Treatment of osteosarcoma with microwave thermal ablation to induce immunogenic cell death. *Oncotarget* **5**: 6526-6539
- Zamarin D, Holmgaard RB, Subudhi SK, Park JS, Mansour M, Palese P, Merghoub T, Wolchok JD, Allison JP (2014) Localized oncolytic virotherapy overcomes systemic tumor resistance to immune checkpoint blockade immunotherapy. *Science translational medicine* **6**: 226ra232
- Zappasodi R, Pupa SM, Ghedini GC, Bongarzone I, Magni M, Cabras AD, Colombo MP, Carlo-Stella C, Gianni

- AM, Di Nicola M (2010) Improved clinical outcome in indolent B-cell lymphoma patients vaccinated with autologous tumor cells experiencing immunogenic death. *Cancer research* **70**: 9062-9072
- Zaravinos A (2014) An updated overview of HPV-associated head and neck carcinomas. *Oncotarget* **5**: 3956-3969
- Zhao L, Liu P, Boncompain G, Loos F, Lachkar S, Bezu L, Chen G, Zhou H, Perez F, Kepp O, Kroemer G (2018) Identification of pharmacological inhibitors of conventional protein secretion. *Scientific reports* **8**: 14966
- Zhao T, Ren H, Jia L, Chen J, Xin W, Yan F, Li J, Wang X, Gao S, Qian D, Huang C, Hao J (2015) Inhibition of HIF-1alpha by PX-478 enhances the anti-tumor effect of gemcitabine by inducing immunogenic cell death in pancreatic ductal adenocarcinoma. *Oncotarget* **6**: 2250-2262
- Zhou H, Forveille S, Sauvat A, Yamazaki T, Senovilla L, Ma Y, Liu P, Yang H, Bezu L, Muller K, Zitvogel L, Rekdal O, Kepp O, Kroemer G (2016a) The oncolytic peptide LTX-315 triggers immunogenic cell death. *Cell death & disease* **7**: e2134
- Zhou H, Mondragon L, Xie W, Mauseth B, Leduc M, Sauvat A, Gomes-da-Silva LC, Forveille S, Iribarren K, Souquere S, Bezu L, Liu P, Zhao L, Zitvogel L, Sveinbjornsson B, Eksteen JJ, Rekdal O, Kepp O, Kroemer G (2018) Oncolysis with DTT-205 and DTT-304 generates immunological memory in cured animals. *Cell death & disease* **9**: 1086
- Zhou H, Sauvat A, Gomes-da-Silva LC, Durand S, Forveille S, Iribarren K, Yamazaki T, Souquere S, Bezu L, Muller K, Leduc M, Liu P, Zhao L, Marabelle A, Zitvogel L, Rekdal O, Kepp O, Kroemer G (2016b) The oncolytic compound LTX-401 targets the Golgi apparatus. *Cell death and differentiation* **23**: 2031-2041

Summary in French

Les cancers constituent la seconde cause de mortalité dans le monde avec 18 millions de nouveaux cas diagnostiqués en 2018. Bien que de nouvelles stratégies comme l'immunothérapie ou les thérapies ciblées voient le jour, la chimiothérapie constitue encore le traitement de référence pour la majorité des cancers. Or certains agents chimiothérapeutiques sont capables de déclencher des signaux de stress intracellulaires permettant d'activer une réponse immunitaire antitumorale et confèrent ainsi une protection à long terme. Cette mort cellulaire est dite immunogène (ICD, de l'anglais « immunogenic cell death ») ; elle requiert l'exposition à la membrane plasmique de calréticuline précédée de la phosphorylation d'eIF2 α , la sécrétion d'ATP dépendant d'une activation préalable de la machinerie autophagique, ainsi que le relargage d'HMGB1, d'interféron de type 1 et d'ANXA1. Plusieurs études ont montré l'efficacité de ces chimiothérapies immunogènes chez l'homme ainsi que leur potentiel clinique en combinaison avec des immunothérapies, d'où leur implication dans un grand nombre d'essais cliniques. Il est donc nécessaire de pouvoir identifier si d'autres agents, notamment parmi ceux déjà testés en clinique, sont capables d'induire de tels mécanismes.

A l'aide d'un modèle construit par intelligence artificielle, nous avons identifié, parmi une librairie comprenant 50 000 composés, des agents anti-cancéreux ayant été soumis à des essais cliniques qui, d'après leurs propriétés physico-chimiques, pourraient induire une mort cellulaire immunogène. Cet algorithme nous a permis d'identifier la dactinomycine (DACT), chimiothérapie utilisée notamment pour le traitement de sarcomes pédiatriques. Notre travail montre qu'en effet la DACT active une réponse partielle au stress du réticulum endoplasmique (RE) impliquant la phosphorylation d'eIF2 α et conduisant à une exposition de calréticuline à la membrane plasmique, une sécrétion d'ATP, un relargage d'HMGB1 et une activation de MX1 (lié à la voie interféron), ceci dans la lignée d'ostéosarcome humain U2OS et dans la lignée de fibrosarcome murin MCA205. Par conséquent, les cellules tumorales traitées avec de la DACT sont phagocytées par les cellules dendritiques et induisent une réponse immunitaire mémoire chez la souris, empêchant la croissance de cellules de même type injectées par la suite. Nous montrons ensuite que le traitement de MCA205 sous-cutanées par la combinaison de la DACT avec le cisplatine, chimiothérapie très utilisée en clinique et peu immunogène, permet de réduire la croissance tumorale, effet aboli dans les souris athymiques *nu/nu*. Lorsque la DACT et le cisplatine sont combinés avec des anticorps bloquant anti-PD1, l'effet est amélioré,

conduisant à la guérison de quelques souris. L'étude de l'infiltrat immunitaire révèle qu'en effet la DACT induit une augmentation du ratio CD8⁺/FoxP3⁺, du nombre de cellules NK et NKT, ainsi qu'une sécrétion d'IL-17 et d'IFN γ . Dans un autre modèle de fibrosarcome murin, les WEHI 164, la DACT seule est très efficace, de façon dépendante des lymphocytes T, et permet de retarder la croissance tumorale ou guérir toutes les souris en combinaison avec des anti-PD1. Ces résultats peuvent permettre d'améliorer les stratégies de traitement des sarcomes et autres types de tumeurs, notamment en combinant la DACT avec des anticorps bloquant anti-PD-1 ou avec d'autres thérapies activatrices du système immunitaire. Actuellement, seul un essai clinique étudie la combinaison de la DACT avec une immunothérapie et s'applique au traitement de mélanomes (NCT01323517).

La DACT est un intercalant de l'ADN qui entrave l'action des ARN polymérase et stabilise les topoisomérases et qui par conséquent inhibe la transcription. Nous nous sommes donc demandé si d'autres agents immunogènes partageaient cette propriété. Nous montrons qu'en effet les anthracyclines, l'oxaliplatine, ainsi que le crizotinib et le bortezomib dans une moindre mesure, inhibent la transcription, ce qui n'est pas le cas pour les inhibiteurs de microtubules qui induisent une externalisation à la membrane plasmique de la calréticuline mais n'ont pas été caractérisés comme *bona fide* inducteurs de l'ICD. Cette inhibition de la synthèse d'ARN s'ensuit d'une inhibition de la synthèse protéique et s'accompagne de l'activation des différentes voies de l'ICD. Notons que l'inhibition de la traduction est une conséquence de l'inhibition de la transcription et non de la phosphorylation d'eIF2 α et que le caractère réversible ou non de l'inhibition de la synthèse protéique ne semble pas être important pour l'ICD. De façon remarquable, d'autres inducteurs de l'ICD prédits par notre modèle informatique induisent une inhibition de la transcription plus importante que les agents prédits comme non inducteurs. De plus, une étude rétrospective *in silico* révèle que les agents classés comme inhibiteurs de la synthèse d'ARN ou de protéines sont prédits comme étant immunogènes. Ces résultats montrent que l'inhibition de la transcription est un événement précurseur de l'activation d'une mort cellulaire immunogène. La découverte de cette nouvelle caractéristique du stress cellulaire immunogène offre l'opportunité d'identifier de nouveaux agents activant une réponse immunitaire anti-cancéreuse.

Titre : L'inhibition de la transcription par la dactinomycine révèle une nouvelle caractéristique du stress cellulaire immunogène

Mots clés : cancer, mort cellulaire immunogène, dactinomycine, eIF2 α , transcription, traduction

Résumé : La chimiothérapie constitue encore le traitement de référence pour la majorité des cancers. Or certains agents chimiothérapeutiques sont capables de déclencher des signaux de stress *pre-mortem* permettant d'activer une réponse immunitaire antitumorale et confèrent ainsi une protection à long terme. A l'aide d'un modèle construit par intelligence artificielle, nous avons identifié, parmi une librairie comprenant 50 000 composés, des agents anti-cancéreux qui, d'après leurs propriétés physico-chimiques, pourraient induire une mort cellulaire immunogène (ICD, de l'anglais "immunogenic cell death"). Cet algorithme nous a permis d'identifier la dactinomycine, qui, en effet, active les mécanismes sous-jacents à l'activation des cellules dendritiques *in vitro* et a un effet anti-cancéreux dépendant du système

immunitaire *in vivo*. La dactinomycine, utilisée en clinique pour le traitement de sarcomes pédiatriques, est connue pour sa capacité à inhiber la transcription. Nous nous sommes donc demandé si d'autres inducteurs de l'ICD partageaient cette propriété. Différentes chimiothérapies immunogènes induisent en effet une inhibition de la synthèse d'ARN, qui est suivie d'une inhibition de la traduction et s'accompagne de l'activation des différentes voies de l'ICD. De plus, une étude rétrospective *in silico* révèle que les agents classés comme inhibiteurs de la synthèse d'ARN ou de protéines sont prédits comme étant immunogènes. Ces résultats montrent que l'inhibition de la transcription est un événement précurseur essentiel à l'activation d'une mort cellulaire immunogène.

Title: Inhibition of transcription by dactinomycin reveals a new characteristic of immunogenic cell stress

Keywords: cancer, immunogenic cell death, dactinomycin, eIF2 α , transcription, translation

Abstract: Chemotherapy still constitutes the standard treatment for most cancers. Yet, some chemotherapeutics are able to trigger *pre-mortem* stress signals which activate an antitumor immune response and thereby confer long term protection. We used an established model built on artificial intelligence to identify, among a library of 50,000 compounds, anticancer agents that, based on their physicochemical characteristics, were predicted to induce immunogenic cell death (ICD). This algorithm led us to the identification of dactinomycin, which indeed activates the mechanisms preceding dendritic cell activation *in vitro* and demonstrates immune-dependent

anticancer effects *in vivo*. Dactinomycin, mainly used to treat pediatric sarcomas, is known as able to inhibit transcription. We therefore investigated whether other ICD inducers would share this characteristic. Different immunogenic chemotherapeutics indeed inhibited RNA synthesis and secondarily translation, accompanied by an activation of ICD-related signaling. A retrospective *in silico* study revealed that agents annotated as inhibitors of RNA or protein synthesis are predicted as immunogenic. These results establish the inhibition of RNA synthesis as a major initial event for ICD induction.